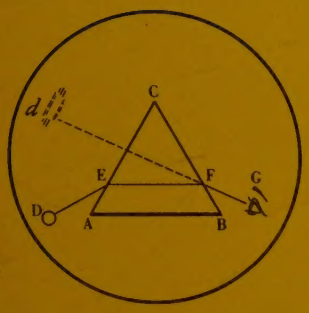

UNIVERSITY OF ILLINOIS
LIBRARY
JUN 12 1961
CHICAGO

optics and spectroscopy

volume x
number 2
february 1961

OPTICAL SOCIETY OF AMERICA

USSR ACADEMY OF SCIENCES

RUSSIAN EDITORIAL STAFF FOR
OPTIKA I SPEKTROSKOPIYA sponsored by
USSR ACADEMY OF SCIENCES

Editor: S. E. FRISH

Assistant Editor: P. P. FEOFILOV
Corresponding Secretary: L. S. SAZONOV

Associate Editors:

M. M. GUREVICH M. A. EL'IASHEVICH A. A. LEBEDEV V. P. LINNIK
S. L. MANDEL'SHTAM I. V. OBREIMOV V. K. PROKOF'EV
N. N. SOBOLEV A. N. TERENIN A. I. TUDOROVSKII

Translated from *OPTIKA I SPEKTROSKOPIYA* on the initiative of THE OPTICAL SOCIETY OF AMERICA, INC. with a grant-in-aid from THE NATIONAL SCIENCE FOUNDATION. *Optics and Spectroscopy* is a cover-to-cover translation of *Optika i Spektroskopiya* and no attempt is made to edit the material other than to correct obvious misprints. The views are those of the original authors and do not represent the Optical Society of America.

TRANSLATION EDITORIAL STAFF

Scientific Editors

CYRUS FELDMAN, *Oak Ridge National Laboratory*

CARL W. GARLAND, *Massachusetts Institute of Technology*

MATHEW G. GIBBONS, *Oakland, California*

Administrative Editor: PATRICIA R. WAKELING, *OSA*

Published monthly by the Optical Society of America, Inc. Executive office: 1155 Sixteenth Street, N.W., Washington, D.C. Subscriptions for one year to members of the Society: Associates $13.00; Regular members and Fellows $17.00. Subscriptions for non-members of the Society: One year U. S. and Possessions, $25.00; Foreign $28.00. Back numbers: $3.00 per copy. Subscriptions, changes of address and undeliverable copies should be referred to the Executive offices in Washington, D.C. The office of publication is 2500 South State Street, Ann Arbor, Michigan. Second class postage paid at Ann Arbor, Michigan.

Printed in the U.S.A. by Edwards Brothers, Inc., Ann Arbor, Michigan.

EFFECT OF FREE ROTATION IN MOLECULES ON THE NORMAL VIBRATION FREQUENCIES

B. L. Livshits (pp. 145-151)

Received 8 April 1960

The functional dependence of the vibrational operator $\hat{W}$[1] on the internal rotation coordinates of polyatomic molecules is established. In the first approximation of a perturbational method an expression is obtained for the frequency of a normal vibration as a function of an internal rotation coordinate.

It is well-known that the internal rotation coordinates Φ_2, ..., in the case of free rotation, can be disregarded in the solution for the eigenvalues (squares of the normal vibration frequencies) and the eigenvectors (normal vibration forms) of the vibrational operator for fixed values of the internal rotation coordinates, if the vibrational operator is given in the space of the natural (chemical) coordinates corresponding to the quasi-elastic forces in the molecule. This means that

$$\hat{W}(\Phi_1, \Phi_2, \ldots) = \hat{W}(0, 0, \ldots) + \Delta\hat{W}(\Phi_1, \Phi_2, \ldots) = \hat{W}_0 + \Delta\hat{W},$$

where $\hat{W}_0$ is the vibrational operator corresponding to a certain combination of the internal rotation coordinates taken as zero, and the operator $\hat{W}$ acts in the space of the nine independent internal coordinates of the molecule, inclusive of the internal rotation coordinates. The dependence of $\hat{W}$ on Φ_1, Φ_2, ... is due to the noninvariance with respect to changes in Φ_1, Φ_2, ... of four of the eleven[2] different types of matrix elements of the matrix $T^{-1} = \|t^{-1}_{ik}\|$. We will examine these noninvariant matrix elements, adhering to the designations adopted in ref. 2. In the derivation of the functional dependence of the elements of the matrix T^{-1} on the internal rotation coordinates we will make use of the following obvious identities

$$(\mathbf{f}_{ik}, \mathbf{e}_i) = 0, \tag{1}$$

$$(\mathbf{f}_{ik}[\mathbf{e}_i \times \mathbf{e}_k]) = 0, \tag{2}$$

where

$$\mathbf{e}_i^2 = \mathbf{f}_{ik}^2 = 1, \tag{3}$$

and also the well-known relation in vector algebra*

*for example, ref. 4.

$$\mathbf{r}(\Phi) = \mathbf{k}(\mathbf{kr})(1 - \cos\Phi) + \mathbf{r}\cos\Phi + \sin\Phi[\mathbf{k} \times \mathbf{r}], \tag{4}$$

where $\mathbf{r}(\Phi)$ is the vector into which the vector $\mathbf{r}$ transforms in a rotation by the angle Φ about the axis defined by the unit vector $\mathbf{k}$:

$$\mathbf{k}^2 = 1. \tag{5}$$

1. The first of the noninvariant types of matrix elements is the fifth type:

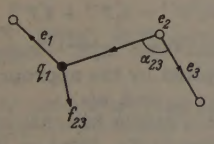

$$t^{-1}_{q_1, \alpha_{23}}(\Phi) = \varepsilon_0\sigma_2(\mathbf{e}_1\mathbf{f}_{23}). \tag{6}$$

It is seen from (6) that a rotation around the outer bonds with the unit vectors $\mathbf{e}_1$ and $\mathbf{e}_3$ does not change the mutual orientation of the vectors $\mathbf{e}_1$ and $\mathbf{f}_{23}$, thus leaving invariant matrix elements of the type $t^{-1}_{q1, \alpha_{23}}$.*

*The invariance relative to rotations about the outer bonds remains also valid for all the remaining types of matrix elements t^{-1}_{ik}; consequently, in the further discussion we will not consider rotations of this kind.

However, for rotations about $\mathbf{e}_2$ the mutual orientation of $\mathbf{e}_1$ and $\mathbf{f}_{23}$ changes and this leads to a change in $t^{-1}_{q, \alpha_{23}}$. To show this, let $\mathbf{e}_3$ and $\mathbf{e}_1$ rotate about $\mathbf{e}_2$ and let the angles of rotation be equal to Φ' and Φ'', respectively. Then, remembering that $\mathbf{f}_{23}$ always lies in the plane defined by $\mathbf{e}_2$ and $\mathbf{e}_3$, we obtain from Eqs. (1)-(4) and (6)

$$t^{-1}_{q_1, \alpha_{23}}(\Phi) = t^{-1}_{q_1, \alpha_{23}}(0)(\cos\Phi + a_1\sin\Phi), \tag{7}$$

where

$$t^{-1}_{q_1, \alpha_{23}}(0) = \varepsilon_0\sigma_2(\mathbf{e}_1(0)\mathbf{f}_{23}(0));$$

$\Phi = \Phi' - \Phi''$ is the value of the coordinate of the internal rotation for the rotations of $\mathbf{e}_1$ and $\mathbf{e}_3$;

$$a_1 = \frac{([\mathbf{e}_1(0) \times \mathbf{e}_2]\mathbf{f}_{23}(0))}{(\mathbf{e}_1(0)\mathbf{f}_{23}(0))}. \tag{8}$$

If for $\Phi = 0$ the vectors $\mathbf{e}_1$, $\mathbf{e}_2$, and $\mathbf{e}_3$ are coplanar, then $a_1 = 0$ and

$$t^{-1}_{q_1, \alpha_{23}}(\Phi) = t^{-1}_{q_1, \alpha_{23}}(0)\cos\Phi. \tag{9}$$

Formula (9) can be used for calculating the matrix elements of the fifth type.

When the various calculations are carried for the eighth, tenth, and eleventh types, we obtain the following results.

2.

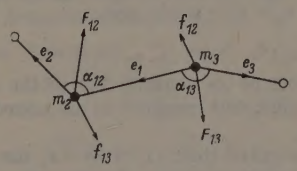

$$t^{-1}_{\alpha_{12}, \alpha_{13}}(\Phi) = t^{-1}_{\alpha_{12}, \alpha_{13}}(0)(\cos\Phi + a_2\sin\Phi), \tag{10}$$

where Φ is the coordinate of the internal rotation about $\mathbf{e}_1$;

$$t^{-1}_{\alpha_{12}, \alpha_{13}}(0) = -\varepsilon_1\sigma_1(\mathbf{f}_{13}(0)\mathbf{F}_{12}(0)) - \varepsilon_3\sigma_1(\mathbf{f}_{12}(0)\mathbf{F}_{13}(0));$$
$$a_2 = \{([\mathbf{e}_1 \times \mathbf{f}_{13}(0)]\mathbf{F}_{12}(0))\varepsilon_2\sigma_1(\mathbf{f}_{13}(0)\mathbf{F}_{12}(0)) + ([\mathbf{e}_1 \times \mathbf{F}_{13}(0)]\mathbf{f}_{12}(0))\varepsilon_3\sigma_1(\mathbf{f}_{12}(0)\mathbf{F}_{13}(0))\}: \tag{11}$$
$$:\{\varepsilon_2\sigma_1(\mathbf{f}_{13}(0)\mathbf{F}_{12}(0)) + \varepsilon_3\sigma_1(\mathbf{f}_{12}(0)\mathbf{F}_{13}(0))\},$$

where[2]

$$\mathbf{F}_{12} = \sigma_1\mathbf{f}_{12} + \sigma_2\mathbf{f}_{21}; \quad \mathbf{F}_{13} = \sigma_1\mathbf{f}_{13} + \sigma_3\mathbf{f}_{31}.$$

If for $\Phi = 0$ the vectors $\mathbf{e}_1$, $\mathbf{e}_2$, and $\mathbf{e}_3$ are coplanar, then $a_2 = 0$ and

$$t^{-1}_{\alpha_{12},\alpha_{13}}(\Phi) = t^{-1}_{\alpha_{12},\alpha_{13}}(0)\cos\Phi. \tag{12}$$

3.

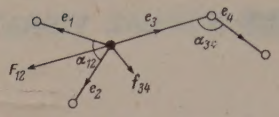

$$t^{-1}_{\alpha_{12},\alpha_{34}}(\Phi) = t^{-1}_{\alpha_{12},\alpha_{34}}(0)(\cos\Phi + a_3\sin\Phi), \tag{13}$$

where Φ is the coordinate of the internal rotation about $\mathbf{e}_3$;

$$t^{-1}_{\alpha_{12},\alpha_{34}}(0) = -\varepsilon_0\sigma_3(\mathbf{F}_{12}(0)\,\mathbf{f}_{34}(0))$$

and

$$a_3 = \frac{([\mathbf{e}_3\times\mathbf{F}_{12}(0)]\,\mathbf{f}_{34}(0))}{(\mathbf{F}_{12}(0)\,\mathbf{f}_{34}(0))}. \tag{14}$$

4.

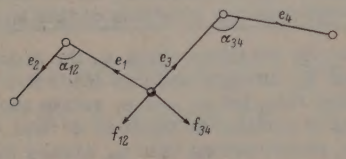

$$t^{-1}_{\alpha_{12},\alpha_{34}}(\Phi_r,\Phi_{r'}) = t^{-1}_{\alpha_{12},\alpha_{34}}(0,0)(\cos\Phi_r\cos\Phi_{r'} + a_4\sin\Phi_r\cos\Phi_{r'} + a_4'\sin\Phi_{r'}\cos\Phi_r + b\sin\Phi_r\sin\Phi_{r'}), \tag{15}$$

where Φ_r and $\Phi_{r'}$ are the coordinates of the internal rotation about the adjacent axes $\mathbf{e}_1$ and $\mathbf{e}_2$;

$$t^{-1}_{\alpha_{12},\alpha_{34}}(0,0) = \varepsilon_0\sigma_1\sigma_3(\mathbf{f}_{12}(0)\,\mathbf{f}_{34}(0));$$

$$a_4 = \frac{([\mathbf{e}_1(0)\times\mathbf{f}_{12}(0)]\,\mathbf{f}_{34}(0))}{(\mathbf{f}_{12}(0)\,\mathbf{f}_{34}(0))}; \tag{16}$$

$$a_4' = \frac{([\mathbf{e}_3(0)\times\mathbf{f}_{34}(0)]\,\mathbf{f}_{12}(0))}{(\mathbf{f}_{12}(0)\,\mathbf{f}_{34}(0))} \tag{17}$$

and

$$b = \frac{([\mathbf{e}_1(0)\times\mathbf{f}_{12}(0)]\,[\mathbf{e}_3(0)\times\mathbf{f}_{34}(0)])}{(\mathbf{f}_{12}(0)\,\mathbf{f}_{34}(0))} \tag{18}$$

if $\Phi_{r'} = 0$, Eq. (15) takes the simpler form

$$t^{-1}_{\alpha_{12},\alpha_{34}}(\Phi,\ 0) = t^{-1}_{\alpha_{12},\alpha_{34}}(0,\ 0)(\cos\Phi + a_4\sin\Phi), \tag{15a}$$

where $\Phi = \Phi_r$.

If for $\Phi_r = \Phi_{r'} = 0$ the vectors $\mathbf{e}_1$, $\mathbf{e}_2$, $\mathbf{e}_3$ and $\mathbf{e}_4'$ are coplanar, then $a_4 = a_4' = b = 0$ and

$$t^{-1}_{\alpha_{12},\alpha_{34}}(\Phi_r,\ \Phi_{r'}) = t^{-1}_{\alpha_{12},\alpha_{34}}(0,\ 0)\cos\Phi_r\cos\Phi_{r'}. \tag{19}$$

The elements of the matrix T^{-1} of the remaining types are invariant with respect to all coordinates of internal rotation.

It should be noted that: (1) if $\Phi = \pi$, the matrix elements in the first three cases change sign, according to Eqs. (7), (10), and (13); (2) if $\Phi_r = 0$ and $\Phi_{r'} = \pi$ or $\Phi_r = \pi$ and $\Phi_{r'} = 0$, the matrix elements of the eleventh type also change sign, according to Eq. (15); and (3) if $\Phi_r = \Phi_{r'} = \pi$, the matrix elements of the eleventh type do not change. It is useful to keep these facts in mind in setting up the matrix T^{-1} for the cis and trans configurations of the molecule.

We will rearrange formulas (7), (10), (13), and (15) separating out the term $t^{-1}(0)$. Then

$$t^{-1}_{q_1,\alpha_{23}}(\Phi) = t^{-1}_{q_1,\alpha_{23}}(0) + (\cos\Phi - 1)\,t^{-1}_{q_1,\alpha_{23}}(0) + \sin\Phi\cdot a_1 t^{-1}_{q_1,\alpha_{23}}(0), \tag{7'}$$

$$t^{-1}_{\alpha_{12},\alpha_{13}}(\Phi) = t^{-1}_{\alpha_{12},\alpha_{13}}(0) + (\cos\Phi - 1)\,t^{-1}_{\alpha_{12},\alpha_{13}}(0) + \sin\Phi\cdot a_2 t^{-1}_{\alpha_{12},\alpha_{13}}(0), \tag{10'}$$

$$t^{-1}_{\alpha_{12},\alpha_{34}}(\Phi) = t^{-1}_{\alpha_{12},\alpha_{34}}(0) + (\cos\Phi - 1)\,t^{-1}_{\alpha_{12},\alpha_{34}}(0) + \sin\Phi\cdot a_3 t^{-1}_{\alpha_{12},\alpha_{34}}(0) \tag{13'}$$

and

$$t^{-1}_{\alpha_{12},\alpha_{34}}(\Phi_r,\ \Phi_{r'}) = t^{-1}_{\alpha_{12},\alpha_{34}}(0,\ 0) + (\cos\Phi_r\cos\Phi_{r'} - 1)\,t^{-1}_{\alpha_{12},\alpha_{34}}(0,\ 0) + \sin\Phi_r\cos\Phi_{r'}\cdot a_4 t^{-1}_{\alpha_{12},\alpha_{34}}(0,\ 0) + \cos\Phi_r\sin\Phi_{r'}\cdot a_4' t^{-1}_{\alpha_{12},\alpha_{34}}(0,\ 0) + \sin\Phi_r\sin\Phi_{r'}\cdot b t^{-1}_{\alpha_{12},\alpha_{34}}(0,\ 0). \tag{15'}$$

From (7'), (10'), (13'), and (15') it follows that

$$T^{-1}(\Phi_1,\ \Phi_2,\ \ldots) = T^{-1}(0,\ 0,\ \ldots) + \sum_r \Delta_r' T^{-1}(\cos\Phi_r - 1) + \sum_{(r)} \Delta_r'' T^{-1}\sin\Phi_r + \sum_{(r)} \delta_r' T^{-1}(\cos\Phi_r - 1) + \sum_{(r,r')} \delta'_{r,r'} T^{-1}(\cos\Phi_r\cos\Phi_{r'} - 1) + \sum_{(r)} \delta_r'' T^{-1}\sin\Phi_r + \sum_{(r,r')} \delta''_{r,r'} T^{-1}\sin\Phi_r\cos\Phi_{r'} + \sum_{(r,r')} \delta'''_{r,r'} T^{-1}\sin\Phi_r\sin\Phi_{r'}, \tag{20}$$

where $T^{-1}(0, 0, \ldots)$ is the matrix T^{-1} for certain initial (zero) values of the internal rotation coordinates; $\Delta_r' T^{-1}$ is the matrix obtained from $T^{-1}(0, 0, \ldots)$ if in the latter the elements invariant with respect to Φ_r and the elements of the eleventh type are replaced by zeros; $\Delta_r'' T^{-1}$ is the matrix obtained in accordance with (7'), (10'), and (13') by multiplying the elements of $\Delta_r' T^{-1}$ by coefficients of the type a_1, a_2, and a_3, appropriate for the elements in question and determined from formulas (8), (11), and (14); $\delta_r' T^{-1}$ is a matrix in which only the elements of the eleventh type and depending on only one internal rotation coordinate Φ_r are different from zero; $\delta'_{r,r'} T^{-1}$ is a matrix in which only the elements of the eleventh type and depending on two adjacent internal rotation coordinates Φ_r and $\Phi_{r'}$ are different from zero; $\delta_r'' T^{-1}$ is the matrix obtained from the matrix $\delta_r' T^{-1}$ when in the latter, in accordance with Eq. (15'), the elements are multiplied by coefficients a_4 and a_4', appropriate for each, determined from formulas (16) and (17); $\delta''_{r,r'} T^{-1}$ is the matrix which can be obtained from $\delta'_{r,r'} T^{-1}$ when the elements of the latter are multiplied by the appropriate coefficients of the type a_4 and a_4'; $\delta'''_{r,r'} T^{-1}$ is a matrix also obtained from $\delta'_{r,r'} T^{-1}$ by multiplying its elements by coefficients of the type b, appropriate for each and determined from formula (18).

If there are no adjacent internal rotation axes in the molecule, $\delta'_{r,r'} T^{-1} = \delta''_{r,r'} T^{-1} = \delta'''_{r,r'} T^{-1} = 0$ and

$$T^{-1}(\Phi_1,\ \Phi_2,\ \ldots) = T^{-1}(0,\ 0,\ \ldots) + \sum_{(r)} \Delta_r^{\mathrm{I}} T^{-1}(\cos\Phi_2 - 1) + \sum_{(r)} \Delta_r^{\mathrm{II}} T^{-1}\sin\Phi_r, \tag{20a}$$

where

$$\Delta_r^{\mathrm{I}} T^{-1} = \Delta_r' T^{-1} + \delta_r' T^{-1}$$

is the matrix obtained from $T^{-1}(0, 0, \ldots)$ if in the latter all elements invariant with respect to Φ_r are replaced by zeros;

$$\Delta_r^{\mathrm{II}} T^{-1} = \Delta_2'' T^{-1} + \delta_r'' T^{-1}$$

is the matrix obtained from $\Delta_r^{\mathrm{I}} T^{-1}$ when the elements of the latter are multiplied by the appropriate coefficients of the type a_1, a_2, a_3, a_4, and a_4'.

A molecule with a single internal rotation coordinate is described according to Eq. (20a) by the matrix T^{-1} which is equal to

$$T^{-1}(\Phi) = T^{-1}(0) + \Delta^{\mathrm{I}} T^{-1}(\cos\Phi - 1) + \Delta^{\mathrm{II}} T^{-1}\sin\Phi. \tag{20b}$$

If there are redundant coordinates among the vibrational coordinates, then, since $T^{-1}(0)$, $\Delta^{\mathrm{I}} T^{-1}$, and $\Delta^{\mathrm{II}} T^{-1}$

occur additively in Eq. (20b), the matrices $\Delta^{I}T^{-1}$ and $\Delta^{II}T^{-1}$ transform in the same way as $T^{-1}(0)$, so that

$$T'^{-1}(\Phi) = T'^{-1}(0) + \Delta^{I}T'^{-1}(\cos\Phi - 1) + \Delta^{II}T'^{-1}\sin\Phi, \quad (21)$$

where the prime indicates the transformation which eliminates the redundant vibrational coordinates.

The vibration matrix $W(\Phi_1, \Phi_2, \ldots)$ is equal to

$$W(\Phi_1, \Phi_2, \ldots) = T'^{-1}(\Phi_1, \Phi_2, \ldots)\, U'(\Phi_1, \Phi_2, \ldots), \quad (22)$$

where $U'(\Phi_1, \Phi_2, \ldots)$ is the matrix of the force constants pertaining to the independent vibrational coordinates.

For free rotation it can be assumed that

$$U'(\Phi_1, \Phi_2, \ldots) = U'(0, 0, \ldots) = U'_0, \quad (23)$$

so that

$$W(\Phi_1, \Phi_2, \ldots) = T'^{-1}(\Phi_1, \Phi_2, \ldots)\, U'_0. \quad (24)$$

Substituting (20) in (24), we obtain

$$W(\Phi_1, \Phi_2, \ldots) = W(0, 0, \ldots) + \sum_{(r)} \Delta'_r W(\cos\Phi_r - 1) + \sum_{(r)} \Delta''_r W \sin\Phi_r + \sum_{(r)} \delta'_r W(\cos\Phi_r - 1) + \sum_{(r, r')} \delta'_{r, r'} W(\cos\Phi_r \cos\Phi_{r'} - 1) + \sum_{(r)} \delta''_r W \sin\Phi_r + \sum_{(r, r')} \delta''_{r, r'} W \sin\Phi_r \cos\Phi_{r'} + \sum_{(r, r')} \delta'''_{r, r'} \sin\Phi_r \sin\Phi_{r'}, \quad (25)$$

where

$$W(0, 0, \ldots) = W_0 = T'^{-1}(0, 0, \ldots)\, U'_0;$$

$$\Delta'_r W = \Delta'_r T'^{-1} U'_0;\ \Delta''_r W = \Delta''_r T'^{-1} U'_0;\ \delta'_r W = \delta'_r T'^{-1} U'_0;$$

$$\delta'_{r, r'} W = \delta'_{r, r'} T'^{-1} U'_0;\ \delta''_r W = \delta''_r T'^{-1} U'_0;$$

$$\delta''_{r, r'} W = \delta''_{r, r'} T'^{-1} U'_0;\ \delta'''_{r, r'} W = \delta'''_{r, r'} T'^{-1} U'_0. \quad (22a)$$

In the particular case of a single internal rotation coordinate we have, because of Eq. (20b),

$$\Delta W = W - W_0 = \Delta^{I}W(\cos\Phi - 1) + \Delta^{II}W\sin\Phi. \quad (25a)$$

The essential dependence of W on $\Phi_1, \Phi_2, \ldots$ shows that, when free rotation is present in the molecule, the solution for the eigenvalues and eigenvectors of the matrix W_0 can give only a rough approximation to the true frequency spectrum and normal vibration forms.

We will consider the case for which ΔW is a small perturbation, and, in the first approximation of the perturbation method for the operator of simple structure developed in ref. 3, we will solve the problem of the dependence of $\lambda(\Phi_1, \Phi_2, \ldots)$ for a nondegenerate vibration.

From Eq. (25) and formula (13) of ref. 3 we have

$$\lambda^{(i)}(\Phi_1, \Phi_2, \ldots) = \lambda^{(i)}(0, 0, \ldots) + \sum_{(r)} P_0^{(i)+} \Delta'_r W X_0^{(i)} (\cos\Phi_r - 1) + \sum_{(r)} P_0^{(i)+} \Delta''_r W X_0^{(i)} \sin\Phi_r + \sum_{(r)} P_0^{(i)+} \delta'_r W X_0^{(i)} (\cos\Phi_r - 1) + \sum_{(r, r')} P_0^{(i)+} \delta'_{r, r'} W X_0^{(i)} \times (\cos\Phi_r \cos\Phi_{r'} - 1) + \sum_{(r)} P_0^{(i)+} \delta''_r W X_0^{(i)} \sin\Phi_r + \sum_{(r, r')} P_0^{(i)+} \delta''_{r, r'} W X_0^{(i)} \sin\Phi_r \cos\Phi_{r'} + \sum_{(r, r')} P_0^{(i)+} \delta'''_{r, r'} W X_0^{(i)} \sin\Phi_r \sin\Phi_{r'}, * \quad (26)$$

*Since $P_0^{(1)}$ is real for the vibrational operator W we have $P_0^{(1)+} = \tilde{P}_0^{(1)}$, that is, the symbol (+) indicates the transposition of the column matrix $P_0^{(1)}$.

where $X_0^{(1)}$ are the eigenvectors of the operator W_0:

$$W_0 X_0^{(i)} = \lambda^{(i)}(0, 0, \ldots) X_0^{(i)},$$

and $P_0^{(1)}$ are the eigenvectors of the matrix W_0^{+} ($W_0^{+} = W$ because the matrix elements of W_0 are real):

$$\tilde{W}_0 P_0^{(i)} = \lambda^{(i)}(0, 0, \ldots) P_0^{i}.$$

In the case of a single internal rotation coordinate

$$\lambda^{(i)}(\Phi) = \lambda_0^{(i)} + P_0^{(i)+}\Delta^{I}W X_0^{(i)}(\cos\Phi - 1) + P_0^{(i)+}\Delta^{II}W X_0^{(i)}\sin\Phi \quad (26a)$$

or

$$\lambda^{(i)}(\Phi) = \lambda_0^{(i)} + A^{(i)}(\cos\Phi - 1) + B^{(i)}\sin\Phi, \quad (26a')$$

where

$$A^{(i)} = P_0^{(i)+}\Delta^{I}W X_0^{(i)},\ B^{(i)} = P_0^{(i)+}\Delta^{II}W X_0^{(i)}.$$

Hence,

$$\omega^{(i)}(\Phi) = \sqrt{\lambda^{(i)}(\Phi)} = \sqrt{\lambda_0^{(i)} + A^{(i)}(\cos\Phi - 1) + B^{(i)}\sin\Phi}$$

$$= \omega_0^{(i)}\sqrt{1 + \frac{A^{(i)}}{\lambda_0^{(i)}}(\cos\Phi - 1) + \frac{B^{(i)}}{\lambda_0^{(i)}}\sin\Phi}$$

$$\approx \omega_0^{(i)}\left[1 + \frac{A^{(i)}}{2\lambda_0^{(i)}}(\cos\Phi - 1) + \frac{B^{(i)}}{2\lambda_0^{(i)}}\sin\Phi\right], \quad (27)$$

$$a^{(i)} = \frac{A^{(i)}}{2\lambda_0^{(i)}} \ll 1,\quad b^{(i)} = \frac{B^{(i)}}{2\lambda_0^{(i)}} \ll 1. \quad (28)$$

Using the designations in (28) we can change (27) into the form

$$\omega^{(i)}(\Phi) = \omega_0^{(i)}[1 - a^{(i)} + \sqrt{a^{(i)2} + b^{(i)2}}\cos(\Phi - \psi^{(i)})],\ a^{(i)} \neq 0, \quad (27')$$

where

$$\tan\psi^{(i)} = \frac{b^{(i)}}{a^{(i)}} = \frac{B^{(i)}}{A^{(i)}}. \quad (29)$$

If the stationary distribution of the molecules over Φ is considered to be uniform, Eq. (27′) can be used to give a qualitative estimate of the effect of the free rotation on the shape of the infrared absorption line if it is assumed that the width $\Delta\omega^{(1)}(\Phi)$ of the line corresponding to each frequency in the range of the different normal frequencies, as determined by Eq. (27′), is much less than this interval, that is,

$$\Delta\omega^{(i)}(\Phi) \ll \omega^{(i)}_{\max}(\Phi_1) - \omega^{(i)}_{\min}(\Phi_2), \quad (30)$$

Here Φ_1 and Φ_2 are the values of the internal rotation coordinate corresponding to the maximum and the minimum normal frequency, respectively.

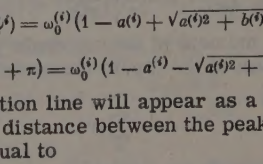

For this purpose we have made a graphical analysis of the dependence in Eq. (27′). From the diagram it is seen that a large fraction of the molecules will absorb in the neighborhood of the frequencies $\omega^{(1)}(\psi^{(1)})$ and $\omega^{(1)}(\psi^{(1)} + \pi)$:

$$\omega^{(i)}(\psi^{i}) = \omega_0^{(i)}(1 - a^{(i)} + \sqrt{a^{(i)2} + b^{(i)2}}), \quad (31)$$

$$\omega^{(i)}(\psi^{(i)} + \pi) = \omega_0^{(i)}(1 - a^{(i)} - \sqrt{a^{(i)2} + b^{(i)2}}), \quad (32)$$

Thus the absorption line will appear as a symmetrical doublet with the distance between the peaks, from Eqs. (31) and (32), equal to

$$\delta\omega^{(i)} = |\omega^{(i)}(\psi^{(i)}) - \omega^{(i)}(\psi^{(i)} + \pi)| = 2\omega_0^{(i)}\sqrt{a^{(i)2} + b^{(i)2}}, \quad (33)$$

or, taking Eq. (28) into account,

$$\delta\omega^{(i)} = \sqrt{A^{(i)2} + B^{(i)2}}\,\omega_0^{(i)-1}. \quad (34)$$

From (34) it follows that the effect of internal rotation should be observable for the low frequencies of the spectrum.

In conclusion I express my thanks to I. V. Obreimov for his interest in this research.

REFERENCES

1. L. S. Mayants, Trudy Fiz. Inst. Akad. Nauk SSSR **5**, 63 (1950).
2. M. A. El'yashevich, Zhur. Fiz. Khim. **15**, 847 (1941).
3. B. L. Livshits, Doklady Akad. Nauk SSSR **133**, 800 (1960), Soviet Phys.-Doklady **5**, 827 (1961).
4. G. Ya. Lyubarskii, "Teoriya grupp i ee primenenie v fizike" (Theory of Groups and Their Use in Physics Gosudarst. Tekh. Izd., Moscow, 1957.

THE THEORY OF THE INTENSITIES OF INFRARED SPECTRA OF POLYATOMIC MOLECULES IN THE ZERO AND FIRST APPROXIMATION OF THE GENERALIZED VALENCE-OPTICAL SCHEME

L. M. Sverdlov (pp. 152-156)

Received 8 April 1960

A generalized valence-optical scheme is given, which takes account of the presence of components of the dipole moment perpendicular to the direction of the bond. The generalized valence-optical scheme is formulated in the zero and first approximations. As an example, a calculation of the electro-optical parameters of the sulfur dioxide molecule is carried out.

1. In recent years there have been many investigations of the absolute integrated intensities of the infrared bands of polyatomic molecules. In connection with this, it has become particularly important to further develop the theory of intensities of infrared spectra, and to construct a rational theory relating the experimentally measured quantities with the electro-optical parameters of the molecule, since without a comparison with calculated values, the very rich experimental material on intensities will be of very little value. This is also very important in quantitative molecular spectral analysis, since only with the assistance of such a theory is it possible to understand the intensities of the vibrational spectra of polyatomic molecules, and, using the electro-optical parameters of bonds and the structural elements of simpler molecules, to calculate the intensities of infrared bands of complex compounds.

The semiclassical theory of the intensities of vibrational spectra, based on the valence-optical scheme, was first formulated by Vol'kenshtein[1] and then developed in the studies of Vol'kenshtein and El'yashevich.[2] The valence-optical scheme is based on the additivity of the dipole moments and polarizabilities of bonds, it being assumed that this additivity is also maintained while the molecule is vibrating.

The integrated intensity of an infrared band corresponding to the normal coordinate Q_l is defined by the square of the derivative of the dipole moment of the molecule with respect to the normal coordinate

$$I_l = \int k_\nu d\nu = \frac{\pi N_1}{3c}\left(\frac{\partial \mathbf{p}}{\partial Q_l}\right)^2 = \frac{\pi N_1}{3c}\left[\left(\frac{\partial p_\xi}{\partial Q_l}\right)^2 + \left(\frac{\partial p_\eta}{\partial Q_l}\right)^2 + \left(\frac{\partial p_\zeta}{\partial Q_l}\right)^2\right]. \quad (1)$$

The dipole moment of the molecule $\mathbf{p}$ is represented as the vector sum of the dipole moments of the separate bonds $\mu^{(n)}$

$$\mathbf{p} = \sum_n \mu^{(n)}. \quad (2)$$

It is assumed, in the valence optical scheme, that the direction of the dipole moment of a bond coincides with the direction of the bond itself (that is, with the line joining the two atomic nuclei which form the bond).

The components of the dipole moment with respect to the coordinate axes have the form

$$p_i = \sum_n \mu^{(n)} \cos(ni) \quad (i = \xi, \eta, \zeta). \quad (3$$

One can express the derivative $\partial p_i/\partial Q_l$ by means of the derivatives of the dipole moment with respect to the natural vibrational coordinates.

$$\frac{\partial p_i}{\partial Q_l} = \sum_{nt}\left[\frac{\partial \mu^{(n)}}{\partial q_t}\cos(ni) + \mu^{(n)}\frac{\partial \cos(ni)}{\partial q_t}\right]\frac{\partial q_t}{\partial Q_l} + \sum_{n\varkappa}\left[\mu^{(n)}\frac{\partial \cos(ni)}{\partial \gamma_\varkappa} + \frac{\partial \mu^{(n)}}{\partial \gamma_\varkappa}\cos(ni)\right]\frac{\partial \gamma_\varkappa}{\partial Q_l}. \quad (4$$

In the zero approximation of the valence-optical scheme it is assumed that the dipole moment of the bond $\mu^{(n)}$ is a function only of changes of the n-th bond, and the direction cosines are functions only of changes of the valence angles; i.e.,

$$\frac{\partial \mu^{(n)}}{\partial q_t} = 0 \ (t \neq n); \quad \frac{\partial \mu^{(n)}}{\partial \gamma_\varkappa} = 0; \quad \frac{\partial \cos(ni)}{\partial q_t} = 0, \quad (5$$

i.e., it is assumed that on a change of other bonds and angles the dipole moment of a given bond remains the same.

Until recently, all calculations of electro-optical parameters were made only in the zeroth approximation. However, the results obtained had no physical meaning, since the $\mu^{(n)}$ and $\partial\mu^{(n)}/\partial q_k$ values calculated from the integrated intensities of infrared bands corresponding to vibrations of different symmetry types had values which were not identical. We have calculated the intensities of infrared spectra and electro-optical parameters of a large number of molecules,[3,4] and have proved that in these calculations one can use only the first approximation of the valence-optical scheme, in which one takes account

of the interaction between different elements of the molecule:

$$\frac{\partial \mu^{(n)}}{\partial q_t} \neq 0 \quad (t \neq n); \quad \frac{\partial \mu^{(n)}}{\partial \gamma_s} \neq 0; \quad \frac{\partial \cos (ni)}{\partial q_t} \neq 0, \tag{6}$$

i.e., we do not represent a polyatomic molecule as a system consisting of N noninteracting bonds.

In these calculations we also assumed that the directions of the dipole moments of the bonds coincide with the directions of the bonds themselves. However, in the case of polyatomic molecules, when one considers the interactions of the bonds among themselves and with the valence angles, the direction of the dipole moment of the bond will, generally speaking, not coincide with the direction of the bond, but will form some angle with it. This follows from the fact that when we consider the interaction between the electron clouds of different bonds, the electron cloud of the bond studied will no longer possess axial symmetry. Quantum-mechanical calculations of dipole moments carried out in recent years confirm this conclusion.[5]

It is of interest to examine the electro-optical problem in this general case, taking account of the presence of components of the dipole moment which are perpendicular to the bonds (we will call this scheme the generalized valence-optical scheme).

2. The dipole moment of a bond $\mu^{(k)}$ can be resolved into three components along three mutually perpendicular directions, one of which coincides with the direction of the bond.

$$\mu^{(n)} = \sum_{m=1}^{3} \mu^{(nm)} = \mu_{\parallel}^{(n1)} + \mu_{\perp}^{(n2)} + \mu_{\perp}^{(n3)}$$

$$= \mu_{\parallel}^{(n1)} e^{(n)} + \mu_{\perp}^{(n2)} f^{(n)} + \mu_{\perp}^{(n3)} h^{(n)}. \tag{7}$$

$e^{(n)}$ is a unit vector directed along the bond and $f^{(n)}$ and $h^{(n)}$ are unit vectors perpendicular to the bond; $h^{(n)} = e^{(n)} \times f^{(n)}$. The dipole moment of the molecule is

$$p = \sum_n \mu^{(n)} = \sum_{nm} \mu^{(nm)} = \sum_n \mu_{\parallel}^{(n1)} + \sum_n \mu_{\perp}^{(n2)} + \sum_n \mu_{\perp}^{(n3)}, \tag{8}$$

$$p_i = \sum_{nm} \mu^{(nm)} \cos (nmi). \tag{9}$$

The derivative of the dipole moment with respect to the normal coordinate has the form

$$\frac{\partial p_i}{\partial Q_l} = \sum_k \frac{\partial p_i}{\partial S_k} L_{kl}$$

$$= \sum_k \left\{ \sum_{nmi} \left[\frac{\partial \mu^{(nm)}}{\partial q_i} \cos (nmi) + \mu^{(nm)} \frac{\partial \cos (nmi)}{\partial q_i} \right] \frac{\partial q_i}{\partial q_k^{(x)}} \right\} C_{kl}^{(x)}$$

$$+ \sum_k \left\{ \sum_{nms} \left[\mu^{(nm)} \frac{\partial \cos (nmi)}{\partial \gamma_s} + \frac{\partial \mu^{(nm)}}{\partial \gamma_s} \cos (nmi) \right] \frac{\partial \gamma_s}{\partial \gamma_k^{(x)}} \right\} D_{kl}^{(x)}. \tag{10}$$

where

$$S_k = \sum L_{kl} Q_l; \quad q_k^{(x)} = \sum_n C_{kl}^{(x)} Q_l; \quad \gamma_k^{(x)} = \sum_n D_{kl}^{(x)} Q_l. \tag{11}$$

Transforming to valence-optical coordinates $\beta_{mi}^{(n)}$ [denoting changes of the angles (nmi)] and φ_n, ψ_n (defining the bending of the n-th bond from its equilibrium position), we obtain

$$\frac{\partial p_i}{\partial Q_l} = \sum_n \left[\frac{\partial p_i}{\partial q_k^{(x)}} C_{kl}^{(x)} + \frac{\partial p_i}{\partial \varphi_k^{(x)}} E_{kl}^{(x)} + \frac{\partial p_i}{\partial \psi_k^{(x)}} F_{kl}^{(x)} \right], \tag{12}$$

where

$$\frac{\partial p}{\partial q_k^{(x)}} = \sum_{nmi} \left[\frac{\partial \mu^{(nm)}}{\partial q_i} \cos (nmi) - \mu^{(nm)} \sin (nmi) \frac{\partial \beta_{mi}^{(n)}}{\partial q_i} \right] \frac{\partial q_i}{\partial q_k^{(x)}}; \tag{13}$$

$$\frac{\partial p_i}{\partial \varphi_k^{(x)}} = -\sum_{nm} \mu^{(nm)} \sin (nmi) \frac{\partial \beta_{mi}^{(n)}}{\partial \varphi_k^{(x)}} + \sum_{km} \frac{\partial \mu^{(nm)}}{\partial \varphi_k^{(x)}} \cos (nmi); \tag{14}$$

$$\frac{\partial p_i}{\partial \psi_k^{(x)}} = -\sum_{nm} \mu^{(nm)} \sin (nmi) \frac{\partial \beta_{mi}^{(n)}}{\partial \psi_k^{(x)}} + \sum_{km} \frac{\partial \mu^{(nm)}}{\partial \psi_k^{(x)}} \cos (nmi); \tag{15}$$

$$\varphi_k^{(x)} = \sum_l E_{kl}^{(x)} Q_l; \quad \psi_k^{(x)} = \sum_l F_{kl}^{(x)} Q_l. \tag{16}$$

In formulas (13)-(15) all interactions are accounted for—this is the generalized valence-optical scheme in the first approximation. In this case, if

$$\frac{\partial \mu^{(nm)}}{\partial q_t} = 0 \quad (t \neq n); \quad \frac{\partial \mu^{(nm)}}{\partial \gamma_s} = 0; \quad \frac{\partial \cos (nmi)}{\partial q_t} = 0, \tag{17}$$

we obtain the generalized valence-optical scheme in the zeroth approximation. Formulas (13)-(15) then assume the form

$$\frac{\partial p_i}{\partial q_k^{(x)}} = \sum_{nm} \frac{\partial \mu^{(nm)}}{\partial q_k} \cos (nmi) \frac{\partial q_k}{\partial q_k^{(x)}}; \tag{18}$$

$$\frac{\partial p_i}{\partial \varphi_k^{(x)}} = -\sum_{nm} \mu^{(nm)} \sin (nmi) \frac{\partial \beta_{mi}^{(n)}}{\partial \varphi_k^{(x)}}; \tag{19}$$

$$\frac{\partial p_i}{\partial \psi_k^{(x)}} = -\sum_{nm} \mu^{(nm)} \sin (nmi) \frac{\partial \beta_{mi}^{(n)}}{\partial \psi_k^{(x)}}. \tag{20}$$

3. As an example, we will examine the triatomic nonlinear molecule XY_2 (refer to the Figure). From symmetry considerations it follows that the component of the

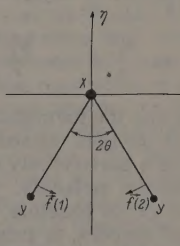

dipole moment of the XY bond perpendicular to the plane of the molecule is equal to zero. The dipole moment of the molecule is

$$p = 2 \cos \theta \cdot \mu_{\parallel}^{XY} + 2 \sin \theta \cdot \mu_{\perp}^{XY}. \tag{21}$$

We introduce the vibrational and valence-optical coordinates

$$\left.\begin{aligned} &\beta_{1\xi}^{(1)} = \varphi_1; \ \beta_{1\eta}^{(1)} = -\varphi_1; \ \beta_{2\xi}^{(1)} = \varphi_1; \ \beta_{2\eta}^{(1)} = \varphi_1; \\ &\beta_{1\xi}^{(2)} = -\varphi_2; \ \beta_{1\eta}^{(2)} = -\varphi_2; \ \beta_{2\xi}^{(2)} = -\varphi_2; \ \beta_{2\eta}^{(2)} = \varphi_2; \end{aligned}\right\} \tag{22}$$

$$\left.\begin{aligned} &q^{A_1} = \frac{1}{\sqrt{2}} (q_1 + q_2); \ \gamma^{A_1}; \ \varphi^{A_1} = \frac{1}{\sqrt{2}} (\varphi_1 + \varphi_2); \\ &q^{B_1} = \frac{1}{\sqrt{2}} (q_1 - q_2); \quad \varphi^{B_1} = \frac{1}{\sqrt{2}} (\varphi_1 - \varphi_2); \\ &q^{A_1} = \sum_{l=1}^{2} C_l^{A_1} Q_l; \ \gamma^{A_1} = \sum_{l=1}^{2} D_l^{A_1} Q_l; \ \varphi^{A_1} = \sum_{l=1}^{2} E_l^{A_1} Q_l; \\ &q^{B_1} = C_3^{B_1} Q_3; \ \varphi^{B_1} = E_3^{B_1} Q_3; \end{aligned}\right\} \tag{23}$$

$$E_l^{A_1} = \frac{1}{\sqrt{2}} D_l^{A_1}; \quad E_3^{B_1} = \frac{m_Y \sin 2\theta}{m_X + 2m_Y \sin^2 \theta} C_3^{B_1}. \tag{24}$$

Applying formulas (12)-(14), we obtain the following formulas for the $\partial p_i / \partial Q_1$ in the first approximation of the

generalized valence-optical scheme:

$$\frac{\partial p_\eta}{\partial Q_i^{A_1}} = \sqrt{2}\left\{-\left[\cos\theta\left(\frac{\partial \mu_\parallel^{(1)}}{\partial q_1}+\frac{\partial \mu_\parallel^{(2)}}{\partial q_1}\right)+\sin\theta\left(\frac{\partial \mu_\perp^{(1)}}{\partial q_1}+\frac{\partial \mu_\perp^{(2)}}{\partial q_1}\right)\right]\right.$$
$$\left.+\left[\left(\sin\theta\cdot\mu_\parallel^{(1)}-\cos\theta\cdot\mu_\perp^{(1)}\right)\left(\frac{\partial\varphi_1}{\partial q_1}+\frac{\partial\varphi_2}{\partial q_1}\right)\right]\right\} C_i^{A_1}$$
$$+\sqrt{2}\left\{\left[\sin\theta\cdot\frac{\mu_\parallel^{(1)}}{r}-\cos\theta\cdot\frac{\mu_\perp^{(1)}}{r}\right]-\left[\cos\theta\left(\frac{\partial \mu_\parallel^{(1)}}{\partial\varphi_1}+\frac{\partial \mu_\parallel^{(2)}}{\partial\varphi_1}\right)\frac{1}{r}\right.\right.$$
$$\left.\left.+\sin\theta\left(\frac{\partial \mu_\perp^{(1)}}{\partial\varphi_1}+\frac{\partial \mu_\perp^{(2)}}{\partial\varphi_1}\right)\frac{1}{r}\right]\right\} E_i^{A_1};\quad \frac{\partial p_\xi}{\partial Q_i^{A_1}}=\frac{\partial p_\zeta}{\partial Q_i^{A_1}}=0\quad (i=1,\ 2); \tag{25}$$

$$\frac{\partial p_\zeta}{\partial Q_3^{B_1}} = \sqrt{2}\left\{-\left[\sin\theta\left(\frac{\partial \mu_\parallel^{(1)}}{\partial q_1}-\frac{\partial \mu_\parallel^{(2)}}{\partial q_1}\right)-\cos\theta\left(\frac{\partial \mu_\perp^{(1)}}{\partial q_1}-\frac{\partial \mu_\perp^{(2)}}{\partial q_1}\right)\right]\right.$$
$$\left.-\left[\left(\cos\theta\cdot\mu_\parallel^{(1)}+\sin\theta\cdot\mu_\perp^{(1)}\right)\left(\frac{\partial\varphi_1}{\partial q_1}-\frac{\partial\varphi_2}{\partial q_1}\right)\right]\right\} C_3$$
$$+\left\{-\left[\cos\theta\cdot\frac{\mu_\parallel^{(1)}}{r}+\sin\theta\cdot\frac{\mu_\perp^{(1)}}{r}\right]-\left[\sin\theta\left(\frac{\partial \mu_\parallel^{(1)}}{\partial\varphi_1}-\frac{\partial \mu_\parallel^{(2)}}{\partial\varphi_1}\right)\frac{1}{r}\right.\right.$$
$$\left.\left.-\cos\theta\left(\frac{\partial \mu_\perp^{(1)}}{\partial\varphi_1}-\frac{\partial \mu_\perp^{(2)}}{\partial\varphi_1}\right)\frac{1}{r}\right]\right\} E_3;\quad \frac{\partial p_\eta}{\partial Q_3^{B_1}}=\frac{\partial p_\zeta}{\partial Q_3^{B_1}}=0. \tag{26}$$

In the zeroth approximation of the generalized valence-optical scheme, applying (18) and (19), we have

$$\left.\begin{aligned}\frac{\partial p_\eta}{\partial Q_i^{A_1}} &= \left\{-\sqrt{2}\left[\cos\theta\cdot\frac{\partial \mu_\parallel^{(1)}}{\partial q_1}+\sin\theta\cdot\frac{\partial \mu_\perp^{(1)}}{\partial q_1}\right]C_i^{A_1}+\right.\\ &\left.+\sqrt{2}\left[\sin\theta\cdot\frac{\mu_\parallel^{(1)}}{r}-\cos\theta\cdot\frac{\mu_\perp^{(1)}}{r}\right]E_i^{A_1}\right\};\\ \frac{\partial p_\xi}{\partial Q_2^{B_1}} &= \left\{-\sqrt{2}\left[\sin\theta\cdot\frac{\partial \mu_\parallel^{(1)}}{\partial q_1}-\cos\theta\cdot\frac{\partial \mu_\perp^{(1)}}{\partial q_1}\right]C_3-\right.\\ &\left.-\sqrt{2}\left[\cos\theta\cdot\frac{\mu_\parallel^{(1)}}{q_e}+\sin\theta\cdot\frac{\mu_\perp^{(1)}}{r}\right]E_3\right\}.\end{aligned}\right\} \tag{27}$$

It is easy to see that the formulas obtained for the first approximation of the generalized valence-optical scheme (25), (26) have a particularly complex form, even for the simplest triatomic molecule. This raises the question of whether it is not possible, in calculating the intensities of infrared spectra, to limit oneself to the zeroth approximation of the generalized valence-optical scheme, since in this case formulas (27) for the $\partial p_i/\partial Q_1$ acquire a comparatively simple form (simpler than the formulas of the first approximation of the valence-optical scheme—refer to ref. 4 where these formulas are given for the SO_2 molecule.

In order to answer this question, it is obviously ne essary to carry out specific calculations of the electro optical parameters of molecules of different classes i the zeroth approximation of the generalized valence-o scheme.

We present results of the calculation of the electr optical parameters of the sulfur dioxide molecule SO_2 (p = 1.59D). In this calculation, we used values for the coefficients C_1, E_1 and the derivatives of the dipole m ment with respect to the symmetry coordinates—$\partial p_\eta/\partial$ $\partial p_\eta/\partial\varphi^{A_1}$, $\partial p_\xi/\partial q^{B_1}$, given in ref. 4. For the combinati of signs $+\partial p_\eta/\partial Q_1^{A_1}+\partial p_\eta/\partial Q_2^{A_1}+\partial p_\xi/\partial Q_3^{B_1}$, which we chosen in ref. 4 we have, applying formulas (21) and (2

$$\left.\begin{aligned}&\mu_\parallel^{SO}=2.6222D;\ \mu_\perp^{SO}=-0.599D;\ \mu^{SO}=\sqrt{\mu_\parallel^2+\mu_\perp^2}=2.6898D;\\ &\frac{\partial \mu_\parallel^{(1)}}{\partial q_1}=-5.3487\ \frac{D}{\text{Å}};\quad \frac{\partial \mu_\perp^{(1)}}{\partial q_1}=0.1357\ \frac{D}{\text{Å}}.\end{aligned}\right\}$$

The angle between the direction of the dipole mom of the bond μ^{SO} and the direction of the SO bond is 12°

Thus the calculations show that in the case of tri- atomic molecules one can limit oneself to the zeroth a proximation of the generalized valence-optical scheme since the system of four parameters $\mu_\parallel^{(1)}$, $\mu_\perp^{(1)}$, $\partial\mu_\parallel^{(1)}/\partial q_1$ $\partial\mu_\perp^{(1)}/\partial q_1$ completely characterize the electro-optical v bration. The introduction of the perpendicular compo- nent of the dipole moment of the bond removed those d ficulties which arose in the zeroth approximation of th valence-optical scheme (different values of $\partial\mu^{(1)}/\partial q_1$ were obtained from the vibrational intensities of sym- metry types A_1 and B_1).

REFERENCES

1. M. V. Vol'kenshtein, Doklady Akad. Nauk SSSR **32**, (1941); Zhur. Eksptl. i Teoret. Fiz. **11**, 642 (1941); J. Phys. USSR **5**, 185 (1941).
2. M. V. Vol'kenshtein and M. A. El'yashevich, Doklad Akad. Nauk SSSR **41**, 380 (1943); Zhur. Eksptl. i Te Fiz. **15**, 124 (1945); J. Phys. USSR **9**, 101, 326 (194
3. L. M. Sverdlov, Opt. i Spektr. **4**, 697 (1958); Ibid. **6** 729 (1959); Ibid. **7**, 21, 600 (1959); Ibid. **8**, 183, 442 (1960), Optics and Spectroscopy **6**, 477 (1959); Ibid. **7**, 11 (1959); Ibid. **8**, 96, 316 (1960).
4. L. M. Sverdlov, Opt. i Spektr. **7**, 152 (1959), Optics and Spectroscopy **7**, 97 (1959).
5. W. Hamilton, J. Chem. Phys. **26**, 345 (1957); O. Burnell and C. Coulson, Trans. Faraday Soc. **53** 403 (1957).

TEMPERATURE DEPENDENCE OF THE VIBRATIONAL ABSORPTION BANDS OF CRYSTALLINE CHLOROFORM AND BROMOFORM

M. P. Lisitsa and Yu. P. Tsyashchenko (pp. 157-164)

Received 12 April 1960

We have studied quantitatively the changes in the intensities of the absorption bands which correspond to the fundamental vibrations ν_1, ν_4, and ν_5 of chloroform and bromoform during the liquid-to-crystal phase transition and in the crystalline state as the temperature is varied within the interval from −70 to −185°C. The data obtained are discussed and compared with the conclusions of A. S. Davydov's theory.

INTRODUCTION

In the greater part of the works which have appeared in recent years containing any information on the infrared absorption of molecular crystals, it is fundamentally the influence of the phase transitions on the number and spectral position of the absorption maxima which has been studied. Such data allow us to draw certain conclusions about the structure of the crystal cell and to establish the character of the action of the field surrounding the molecule on the dynamics of its intramolecular vibrations.[1-8] A series of works has been devoted to the control exerted by the temperature over the rotational isomers of complex molecules.[9-11]

During the gas-crystal and liquid-crystal phase transitions, there is observed* a shift of the vibrational bands, a marked narrowing of them, and sometimes a splitting[3,8] brought about both by the removal of degeneracy and by migration of the excitation energy. In the overwhelming majority of cases, the measurements have been carried out at two temperatures: room (gas, liquid) and −160 and −170°C (crystal), with nonequivalent absorbing layers, as a result of which there is no possibility of even a qualitative comparison of the intensities during phase transitions. The temperature variations of intensity have been practically unstudied. Quantitative data have been obtained only for the combination frequencies of crystalline CBr_4.[12] The remaining information is of a qualitative character and enables us to judge only concerning the direction of the temperature variation of the band intensities in crystalline benzene,[13] CH_3I,[3] and certain complex organic compounds.[14]

In the present work, we have undertaken quantitative investigations* of the course of the temperature dependence of the band intensities of the fundamental vibrations of crystalline chloroform and bromoform.

*We have in mind molecules which do not possess rotational isomerism.

*The measurements were performed on an IKS-6 spectrophotometer.

PROCEDURE AND EXPERIMENTAL ERRORS

Crystalline layers of a known thickness* have been obtained by freezing the liquids in a hermetically-sealed cell[18] placed in a cryostat.[17] The temperature was measured with an accuracy of 2-3° (to avoid glass formation near the crystallization points, it was lowered slowly). The layers obtained were polycrystalline, distinguished by pronounced scattering and a definite prevailing direction of growth. At thicknesses of ~250μ, the radiation scattered by the layer amounted to about 80% of the intensity of the incident illumination. In consequence of this, we did not study the bands of the combination frequencies and overtones. Allowance for the scattered light was made on the basis of the shift in the 100% transmission line of the liquid layer.[12]

All the measurements were performed with a single cell, in consequence of which an additional error is possible in the determination of the integrated absorption: an error due to failure to take account of the losses produced by reflections at the sample boundaries—the cell windows. Calculations show that, even with a 30% change in the refractive index of $CHCl_3$ and $CHBr_3$[15] as a result of crystallization, the coefficient of reflection from the above-mentioned phase boundaries does not exceed 2%; i.e., it has practcially no effect on the value of the measured integrated absorption. The band of the most intense vibration, ν_5, constitutes an exception; in the region of this band, this coefficient reaches 5%. However, if we admit the possibility of a breakdown of optical contact between the cell windows and the layer under study, as a result of flaking during crystallization, then the reflection coefficient increases markedly, reaching 10% on the average and 20% in the band of the ν_5 vibration. Neglect of reflections in such cases may bring about a pronounced error in the determination of the integrated absorption values. Inasmuch as the dispersion of crystalline $CHCl_3$ and $CHBr_3$ is unknown to us, and breakdown of optical contact between the layer and the cell windows was not always reliably established, the corresponding corrections were not introduced into the results of the measurements. Corrections for the increase in density which takes place on crystallization of the liquid and on further lowering of the temperature of the crystal were likewise not introduced, on account of the absence from the literature of the corresponding data for $CHCl_3$ and $CHBr_3$. By analogy with other molecular crystals,* however, one may suppose that they do not exceed a few percent and lie within the limits of random error of the experiment.

The integrated absorption values and band half-widths presented in the present work have been corrected

*The thickness of the cell in which the layer crystallized was determined either by the interference method or on the basis of the absorption of liquid $CHCl_3$ and $CHBr_3$, which is known[15,16] for ordinary conditions (it is assumed that the cell thickness does not change as the liquid crystallizes).

*For example, during the crystallization of benzene and naphthalene, the density of these substances changes by 2-3%;[19] the density of CHI_3 increases by 8% in the temperature interval from 17 to −188°C.[20]

Table 1. Influence of Temperature on the Position (ν), the Integrated Absorption (S), and the Half-Width (Γ) of the Fundamental Vibrational Bands of Crystalline Chloroform and Bromoform

$CHCl_3$													$CHBr_3$							
ν_1				ν_4				ν_5					ν_4				ν_5			
t (°C)	ν (cm^{-1})	Γ (cm^{-1})	S (cm^{-2})	t (°C)	ν (cm^{-1})	Γ (cm^{-1})	S (cm^{-2})	t (°C)	ν (cm^{-1})	Γ (cm^{-1})	S (cm^{-2})		t (°C)	ν (cm^{-1})	Γ (cm^{-1})	S (cm^{-2})	t (°C)	ν (cm^{-1})	Γ (cm^{-1})	S (cm^{-2})
Liquid													Liquid							
−58	3019	13.5	6060	−58	1212	9	24000	+18	760	23	210000		+18	1144.5	12	31000	+18	655.5	29	125000
Crystal													Crystal							
													0	1148	9	37000				
−70	3014	10	3200	−70	1220	3	5800 (2600	−70	750	4	42000		−70	1148.5	3	24000				
					1234.5	2	3200)		765		21000		−130	1149	2.5	20500	−130	653	15	120000
																		634.5		
−130	3013	8	2700	−130	1219.5	2	4600 (1900	−130	750	2.5	40800		−185	1150	1.5	18000	−185	653	15	117000
					1235	1	2700)		766		17500							634.5		
					1217.5															
−185	3012	7	2200	−185	1220	7	3900 (1500	−185	748	1.5	39000									
					1235		2400)		767		15500									

for the spectral slit width of the apparatus, computed according to ref. 21. The corrections were derived from refs. 22 and 23, with the assumption of a dispersion contour for the bands. For the ratios observed in our case between the band half-widths and the spectral slit widths, they do not essentially differ (~1-2%) from those calculated under the assumption of a Gaussian contour.[24,25] However, the band half-widths corrected for Gaussian and dispersion distribution do differ significantly one from another.[23,26] Therefore, the question of the real contours of the vibrational absorption bands of molecular crystals needs a special investigation. Corrections for the band wings were not taken into account.

On account of the incomplete allowance for light scattering, the absence of corrections for band wings, the failure to take reflection losses into account, and the neglect of the density change on crystallization and on cooling of the crystal, the error in the determination of the integrated absorption may reach 20-30%. The accuracy of the determination of the relative temperature changes in the band intensities depends principally on random errors and is therefore substantially higher (the error is roughly one-third as large).

EXPERIMENTAL RESULTS AND DISCUSSION

The experimental curves illustrating the influence of the liquid-crystal phase transition on the intensity a structure of the bands studied, and also the temperatur changes in them for the crystalline phase, are represented in Figs. 1-5. Information on the fundamental nu merical parameters of the bands is contained in Table

As follows from the figures, all the bands, with the exception of the ν_4 vibration of bromoform, are split into two or even three components in the crystal. It is true that, for the totally symmetric ν_1 vibration of $CHCl_3$, the splitting actually takes place in the case of the liquid phase also (Fig. 1). We have pointed out earlier[15] that the short-wavelength maximum of the doublet under consideration cannot be interpreted, but that it is hardly possible to assign it also to the vibration ν_1.

The intensity of the ν_1 vibration of chloroform diminishes by a factor of roughly two during the liquid-crystal transition. The band of the analogous bromofor vibration behaves in a most interesting manner. Where

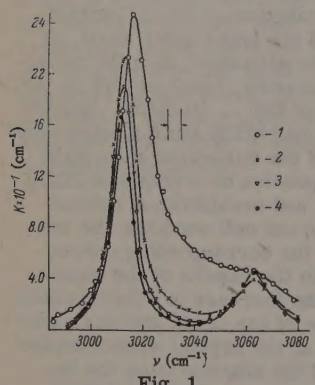

Fig. 1

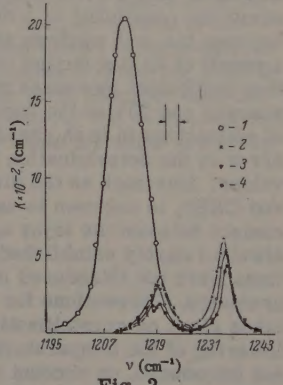

Fig. 2

Fig. 1. Absorption in the band of the ν_1 vibration of liquid (curve 1) and crystalline (curves 2-4) chloroform. Temperature (°C): curve 1—(−58); curve 2—(−70); curve 3—(−130); curve 4—(−185).

Fig. 2. Absorption in the band of the ν_4 vibration of liquid (curve 1) and crystalline (curves 2-4) chloroform at different temperatures. For the temperature values of curves 1-4, see legend of Fig. 1.

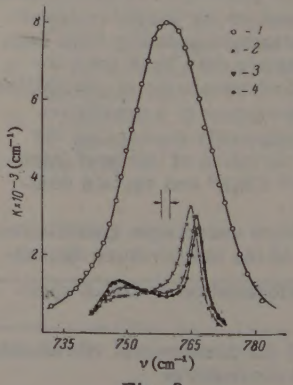

Fig. 3

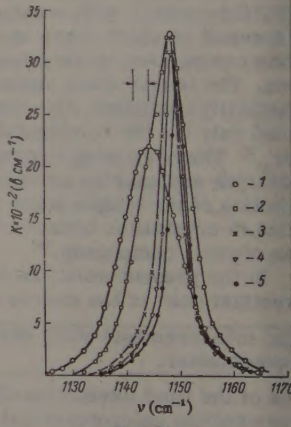

Fig. 4

Fig. 3. Absorption in the band of the ν_5 vibration of liquid (curve 1) and crystalline (curves 2-4) chloroform. Temperature (°C): curve 1—(+18); curve 2—(−70); curve 3—(−130); curve 4—(−185).

Fig. 4. Absorption in the band of the ν_4 vibration of liquid (curve 1) and crystalline (curves 2-5) bromoform. Temperature (°C): curve 1—(+18); curve 2—0; curve 3—(−70); curve 4—(−130); curve 5—(−185).

for the liquid phase its intensity exceeds by a factor of roughly three the intensity of the same band of chloroform. In the crystal this band could not be found at all, even when the layer thickness was increased. Such a "freezing out" of the fundamental frequencies has also been observed for other molecular crystals, for example benzene (vibrations ν_8, ν_9, and ν_{10}).[13] For crystals with a van der Waals type of bonding, in which the molecules retain their individuality, such a phenomenon may seem, at first glance, inexplicable. Nevertheless, it is not difficult to point out a possible cause for the disappearance of the bands, if we suppose that, when the liquid layer freezes, separate monocrystals are formed, in the overwhelming majority of which one of the directions of possible vibrational transitions is parallel to the incident ray (the dipole moment is perpendicular to the **E** vector) or makes a sufficiently small angle with the latter. Thus there arises a purely polarizational effect observed in ordinary light. The case under consideration testifies to the extremely complicated influence of the crystal structure on the intensity of the vibrational absorption bands. The disappearance of a maximum, or its weakening in comparison with the liquid phase, does not at all indicate that the same band might not appear almost as intense as in the liquid phase at a different orientation of the crystalline layer.

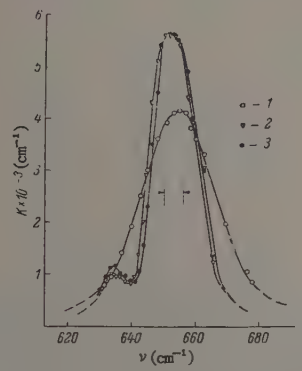

Fig. 5. Absorption in the band of the ν_5 vibration of liquid (curve 1) and crystalline (curves 2, 3) bromoform. Temperature (°C): curve 1—(+18); curve 2—(−130); curve 3—(−185).

For the absorption bands considered in the present work, only two causes can be indicated as bringing about their splitting on undergoing the liquid-crystal phase transition, namely: (a) Bethe-type splitting,[27] caused by the removal of degeneracy, and (b) Davydov-type splitting,[28] caused by the resonance interaction of the molecules in the crystal.

In ref. 27, only the question of the magnitude of the splitting of the atomic (ionic) terms under the influence of the crystal field is discussed. For concrete cases (crystals with an ionic bond type), the magnitude of this splitting is computed. It contains no information on the intensity ratio of the components thus produced or on the magnitude of the splitting in the case of the intramolecular vibrations of crystals with a van der Waals bond type. Bethe's theory also does not foresee the disappearance of individual bands on going from the isolated molecule to the crystal, and completely ignores the question of the temperature dependence of the intensities. All this indicates that the experimental material which we have obtained cannot be treated from the point of view of the theory expounded in ref. 27. It is true that, purely formally, the splitting of the bands corresponding to the doubly degenerate vibrations may be associated with the removal of the degeneracy; however, it does not appear possible to argue this conclusion seriously. It is therefore appropriate to turn to A. S. Davydov's theory, which was worked out especially for molecular crystals and which touches on all the aspects of interest to us. According to this theory, for a crystal with two molecules in the unit cell, there will generally correspond to each of the intramolecular vibrations two bands, the positions of the maxima of which are determined from the relationships

$$\left.\begin{aligned}\nu_1 &= \frac{1}{hc}\left[\Delta E + D + \sum_n (M'_{n1} + M''_{n1})\right],\\ \nu_2 &= \frac{1}{hc}\left[\Delta E + D + \sum_n (M'_{n1} - M''_{n1})\right],\end{aligned}\right\} \quad (1)$$

where ΔE is the excitation energy of the isolated molecule, D is the change (calculated for the equilibrium positions) in the energy of interaction between the molecules of the crystal after transition of one of them to the excited state, M'_{n1} and M''_{n1} are the matrix elements for the transfer of the excitation from a given molecule to molecules oriented identically and differently with respect to it, and n takes account of the orientation of both the cell and the single molecule (determined for a given M).

With the help of (1), it is easy to obtain the magnitude of the splitting,

$$\Delta\nu = \frac{2}{hc}\sum_n M''_{n1}. \quad (2)$$

$\Delta\nu$ being known, it is not difficult to establish the value of the matrix element M''_{n1}, namely,

$$\sum_n M''_{n1} = 3.07 \cdot 10^{-5}\Delta\nu \text{ (ev)}. \quad (3)$$

In accordance with the theory, splitting of a band into two components is not always to be expected. Furthermore, at a certain orientation of the molecules (the directions of the vibrational transitions coincide), it may disappear altogether. It is just this case which is realized for the ν_1 bromoform vibration considered above. Since in the case of $CHCl_3$ and $CHBr_3$ this vibration corresponds to a change in the dipole moment directed along the C_3 axis of the molecule, the considerations presented above enable us to conclude that, there being two molecules in the unit cell of crystalline bromoform, their symmetry axes must be practically parallel (the C—H bonds may then be disposed either parallel or antiparallel). The assumption we have expressed is apparently more realistic than the acceptance of the presence of one molecule per cell, since, according to the structural-analysis data,[29] the cell of the compound CHI_3, which is of the same type, contains two molecules.

Let us now pause to consider the magnitude of the splitting determined according to formula (2). Since the matrix element M''_{n1} depends on the dipole moments and their change as a result of quantum transitions, then $\Delta\nu$ is also a function of them. Actually, as the polarity and dipole moment values of $CHCl_3$ vibrations diminish in the regular sequence ν_5, ν_4, and ν_1,[16] the magnitude of the splitting also diminishes, amounting at the lowest temperature to 19, 16.3, and 0 cm^{-1} respectively. Analogously, in $CHBr_3$ only the most polar vibration ν_5 is split. The absence of splitting for the ν_4 bromoform vibration, the dipole moment of which in the liquid phase is equal to the dipole moment of the identical vibration of $CHCl_3$, is apparently explained by a different structure for the crystal cell. As a result of this, the bands

of one and the same vibration may, in different crystals, correspond to the excitation of excitons of different type: free in one crystal, localized in the other. However, the formation of excitons of a single type, namely free, is also entirely admissible. If we admit this, the directions of the transitions for the ν_4 vibration of the molecules situated in the $CHBr_3$ cell must be parallel or antiparallel, while being furthermore perpendicular* to the C_3 symmetry axes. We note that the perpendicularity just mentioned exists for crystalline chloroform also.

*The latter is all the more justified since we are speaking of a C—H bond deformation vibration, which possesses a high degree of specificity.

With the help of (3), the values of $\sum_n M''_{n1}$ presented in Table 2 have been obtained. Generally speaking, these data testify to a certain increase in the matrix elements for excitation transfer, as the temperature is lowered. Assuming that the theory gives a qualitatively correct result for temperatures that are not especially high, we may arrive at the conclusion that the migration of energy within the crystal is intensified as the temperature is lowered. This conclusion is entirely understandable, since a lowering of the temperature leads, first, to a contraction of the crystal lattice and, secondly, to a reduction in its vibrations. Both causes contribute to a strengthening of the inductive bonding between molecules, and along with this to the transfer of excitation.

Table 2. Values of the Matrix Elements $\sum_n M''_{n1}$ for Various Vibrations and Temperatures

$\sum_n M''_{n1} \cdot 10^4$ (ev) / t (°C)	$CHCl_3$		$CHBr_3$
	ν_4	ν_5	ν_5
−70	8.9	9.2	—
−130	9.5	10.0	11.4
−185	10.0	11.7	11.4

The majority of the absorption bands investigated by us belong to doubly degenerate vibrations and, as has already been noted, may be split into two components in the crystal. We have assigned the splittings considered above to the Davydov type, although more convincing conclusions on this matter may be obtained only after the establishment of the structure of the crystal cell and the carrying out of extensive polarization studies. Nevertheless, we can apparently point also to a splitting associated with degeneracy. It is small and is observed only at the lowest temperature for the ν_4 chloroform vibration (Fig. 2). It is characteristic that only the long-wavelength component of the doublet is split.

The question of the intensity ratio of the components in Davydov splitting is very important. When there are two molecules in the crystal cell, it is determined by the formula

$$\frac{I_{\nu_1}}{I_{\nu_2}} = \operatorname{cotan}^2 \frac{\varphi}{2}, \qquad (4)$$

where φ is the angle between the directions of the same vibrational transition of differently oriented molecules, as projected on a section of the crystal cell in the plane of which the **E** vector lies. Strictly speaking, formula (4) can connect the intensities I_{ν_1} and I_{ν_2} with the angle φ only at 0°K. However, it enables us to draw certain qualitative conclusions for higher temperatures as well.

The intensity ratio found from experiment for the components of the band of the ν_4 chloroform vibration equals 1.23, 1.42, and 1.60 respectively for the temperatures −70, −130, and −185°C. At the same time, the angle φ runs through the values 84°, 80°, and 77°; i.e. it diminishes as the temperature is lowered. If the give substance has certain crystal modifications which exist in different temperature regions, then the angle φ may actually change; however, in this case structural chang in the absorption spectrum must also be observed. Sin this has not been established in our case, the lack of co stancy in the ratio I_{ν_1}/I_{ν_2} is probably brought about by different effect of temperature on the matrix elements the transitions in the two different exciton zones. This question was not studied in detail by Davydov, although certain qualitative results are contained in his theory.[2] If we take account, to a first approximation, of the connection between excitons and phonons, then the transiti probability at temperature T is determined by the expression

$$W = \sum_i \int_2 |(\mu f | w | 0)_{qi}|^2 \, hq^2 \frac{dq}{\partial \nu} \cdot \frac{e^{h\nu_{qi}/kT}}{e^{h\nu_{qi}/kT} - 1} d\Omega,$$

where $(\mu f | w | 0)_{qi}$ is the matrix element of the transiti from the normal state of the crystal to the μ-th excito zone of the f-th excited state, with the simultaneous ex citation of phonons of polarization i; $d\Omega$ is the element of solid angle which characterizes the direction of the wave vector q of the phonon. Elevation of the tempera ture is accompanied by an increase in the exponential factor. The author[28] supposes that the matrix element $(\mu f | w | 0)_{qi}$ depends on the temperature in an analogous way (it seems to us that this conclusion requires the posing of special investigations). Thus the intensities the absorption bands of crystals must also increase wi temperature. Actually, the data presented in Table 1 o the integrated absorption, S, fully confirm this consequence of the theory. However, analysis of the curves Figs. 3 and 5 for the long-wavelength components show the reverse temperature dependence, although the over all intensity, which is basically determined by the mor intense short-wavelength component, does increase wi temperature. This indicates that the present-day state the theory cannot pretend to explain all aspects of the temperature dependence. Such a conclusion is confirm in particular, by the analysis of the data existing in the literature. Thus it has been shown in ref. 13 that the i tensity of the ν_{19} vibration of crystalline benzene, for example, diminishes in the ratio 1:0.88:0.64 on passing through the temperature points −12, −65, and −170°C respectively. A still greater fall in intensity has been tablished[3] for CH_3I. However, in the case of n-eicosan 4-eicosanone, 1,4,5,8-tetrahydroxyanthraquinone, and glycine,[14] an increase in absorption as the temperature is lowered has been qualitatively observed.* An analog

*It should be noted that, for complex compounds which show different isomeric forms, the temperature depen ence which is of interest to us may be masked to a con siderable extent by other phenomena.

dependence has been quantitatively obtained for CBr_4 i ref. 12.

REFERENCES

1. D. F. Hornig, Discuss. Faraday Soc., No. 9, 115 (1
2. G. Carpenter and R. Halford, J. Chem. Phys. 15, 9 (1947).
3. J. L. Mador and R. S. Quinn, J. Chem. Phys. 20, 1 (1952).
4. W. Freitag and E. Nixon, J. Chem. Phys. 24, 109 (1956).

5. R. Kagarise, J. Chem. Phys. 24, 200 (1956).
6. F. Reding and D. F. Hornig, J. Chem. Phys. 27, 1024 (1957).
7. D. Dows, J. Chem. Phys. 26, 745 (1957).
8. D. Dows, J. Chem. Phys. 29, 484 (1958).
9. J. Brown and N. Sheppard, Discuss. Faraday Soc., No. 9, 144 (1950).
10. V. A. Pozdyshev, Yu. A. Pentin, and V. M. Tatevskii, Opt. i Spektr. 3, 211 (1957).
11. Kh. Kesler, B. A. Pentin, D. G. Treshchova, and V. M. Tatevskii, Opt. i Spektr. 7, 302 (1959), Optics and Spectroscopy 7, 195 (1959).
12. M. P. Lisitsa, V. N. Malinko, and I. N. Khalimonova, Opt. i Spektr. 7, 638 (1959), Optics and Spectroscopy 7, 386 (1959).
13. R. Mair and D. Hornig, J. Chem. Phys. 17, 1236 (1949).
14. A. Walsh and J. Willis, J. Chem. Phys. 18, 552 (1950).
15. M. P. Lisitsa and Yu. P. Tsyashchenko, Opt. i Spektr. 6, 605 (1960), Optics and Spectroscopy 6, 396 (1959).
16. N. E. Gaponova, M. P. Lisitsa, and Yu. P. Tsyashchenko, Opt. i Spektr. 8, 465 (1960), Optics and Spectroscopy 8, 245 (1960).
17. M. P. Lisitsa and Yu. P. Tsyashchenko, Opt. i Spektr. 9, 438 (1960), Optics and Spectroscopy 9, 229 (1960).
18. M. P. Lisitsa and Yu. P. Tsyashchenko, Opt. i Spektr. 9, 188 (1960), Optics and Spectroscopy 9, 99 (1960).
19. J. Timmermans, Physico-Chemical Constants of Pure Organic Compounds. (Elsevier) Van Nostrand, New York, 1950.
20. Tekhnicheskaya entsiklopediya. Spravochnik fiz., khim. i tekhnol. velichin (Technical Encyclopedia. Handbook of Physical, Chemical, and Technological Quantities) 5, 186 (1935).
21. A. N. Aleksandrov and V. A. Nikitin, Uspekhi Fiz. Nauk 56, 3 (1955).
22. D. A Ramsay, J. Am. Chem. Soc. 74, 72 (1952).
23. V. N. Smirnov, Vestnik Moskov. Gosudarst. Univ., Ser. Mat., Fiz., Astron. No. 1, 61 (1959).
24. I. B. Willis, Australian J. Sci. Research, Ser. A 4, 172 (1951).
25. V. N. Smirnov and P. A. Bazhulin, Opt. i Spektr. 7, 193 (1959), Optics and Spectroscopy 7, 123 (1959).
26. H. Kostkowsky and A. Bass, J. Opt. Soc. Am. 46, 1060 (1956).
27. H. Bethe, Ann. Physik 3, 113 (1929).
28. A. S. Davydov, "Teoriya pogloshcheniya sveta v molekulyarnykh kristallakh (Theory of Light Absorption in Molecular Crystals)." Izd. Akad. Nauk Ukr. SSR, Kiev, 1951.
29. A. I. Kitaigorodskii, "Organicheskaya kristallokhimiya" (Organic Crystal Chemistry). Izd. Akad. Nauk SSSR, Moscow, 1955.

BAND-SPLITTING IN THE SPECTRA OF CUBIC CRYSTALS SUBJECTED TO ORIENTED DEFORMATION

A. A. Kaplyanskii (pp. 165-172)

Received 20 April 1960

An investigation is made of the amount of splitting of the spectral bands associated with anisotropic centers in cubic crystals subjected to deformation along certain crystallographic directions. It is shown that the amount of splitting is determined by two or three independent parameters which characterize the interaction of the centers with the lattice. The possibility of a similar splitting in the exciton and band state spectra of crystals subjected to oriented deformation is discussed.

INTRODUCTION

In previous publications,[1,2] we showed that in the case of anisotropic centers in cubic crystals, in principle there should occur a polarized splitting of bands in the spectra of samples subjected to uniform elastic uniaxial compression or tension. The cause of this splitting resides in the different displacements of energy levels of centers which (being oriented in the lattice along certain equivalent crystallographic directions) are oriented in various ways with respect to the compression axis. As was shown in ref. 1, an investigation of the number and polarization states of the components of the splitting which result when the crystal is deformed along symmetry axes of various orders can yield information about the symmetry of the centers and their orientation in the lattice, and also about the multipole nature of optical transitions in these centers. The existence of this phenomenon was demonstrated experimentally for several materials (luminescing color centers in LiF, the rare earth ions RE^{3+} in CaF_2), for which the orientation and multipole nature of the transitions for a number of spectral lines was determined from observations of the splitting.

In refs. 1 and 2 attention was directed mostly to the question of the number and polarization of the splitting components, while the magnitude of the splitting was taken to be arbitrary. The magnitude of the splitting constitutes a question of considerable interest, however. A theoretical calculation of the absolute magnitude of the splitting, which reduces to a calculation of the shift of the energy levels of the anisotropic centers in an elastically deformed lattice, requires detailed assumptions concerning the physical structure of the centers, their levels, and their wave functions; also about the interaction between the centers and the lattice; about the nature of the localized deformation in the vicinity of the center, etc.; i.e., it requires a knowledge of characteristics of the centers which is usually unavailable.

Thus a theoretical calculation of the absolute magnitude of the splitting of bands in the spectra of localized centers in uniaxially stressed crystals poses a very difficult problem. Nevertheless, from considerations of the symmetry of anisotropic centers and the nature of a uniform elastic deformation of a cubic lattice, it is possible to derive equations which in general depend on several parameters and which determine the shift and splitting of the bands of centers in an elastically deformed lattice.

This calculation is of interest in establishing quantitative laws for the phenomena and in permitting comparison with experiments since such comparison allows one to obtain supplementary information about the centers.

THE ANISOTROPIC CENTER IN AN ELASTICALLY DEFORMED LATTICE

Consider an isolated anisotropic center whose axis N is directed along one of the symmetry axes of the crystal (C_4, C_3, or C_2). Let the system of coordinates xyz, which coincides with the cubic axes, be oriented with respect to the axes of the center N as shown in the Figure. Let the optical transition frequency between levels in the center in the original crystal be ν_0. In the elastically deformed crystal, the frequency of the transition changes to ν.* The problem then is to determine the magnitude of the frequency shift $\Delta = \nu - \nu_0$ as a function of direction or of deformation of the lattice. Let us limit ourselves to the case of relatively small stresses, for which one need only include linear terms in the expression for band displacement as a function of stress.

*Here, just as in ref. 1, we assume that either the levels of isolated centers in the deformed lattice are displaced but not split (i.e., the levels are nondegenerate), or that the splitting caused by the deformation is much smaller than the displacement, so that the splitting can be neglected.

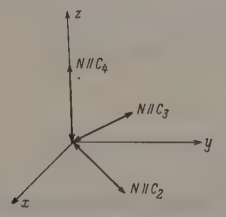

Diagram of the location of the coordinate axes relative to the directions of orientation of the anisotropic centers.

The stress state of the crystal subjected to a uniform deformation can be described with the help of six components of the stress tensor σ_{xx}, σ_{yy}, σ_{zz} (the normal stresses) and σ_{xy}, σ_{yz}, and σ_{zx} (the shear stresses). If it is assumed that the displacement of the levels of the center are linear functions of the stress components in a uniformly deformed lattice, one can write

$$\Delta = A_{xx}\sigma_{xx} + A_{yy}\sigma_{yy} + A_{zz}\sigma_{zz} + A_{xy}\sigma_{xy} + A_{yz}\sigma_{yz} + A_{zx}\sigma_{zx}, \quad (1)$$

where the A_{ik} are constant coefficients which are determined by the actual structure of the center and its interaction with the lattice. Let the tensor $\{\sigma_{ik}\}$ be expressed in the system of coordinates associated with the orientation of the center as shown in the Figure. It can be shown that for various cases of orientation of the centers, symmetry considerations show that some of these coefficients turn out to be equal to each other (or equal to zero).

Let us consider various cases:

1. $N \parallel C_4$. Clearly, the normal stresses σ_{xx} and σ_{yy} make equal contributions to Δ, i.e., $A_{xx} = A_{yy} = A_2^{(4)}$. Symmetry considerations also indicate that the sign of the shear stress is unimportant insofar as Δ is concerned. Hence, it follows that Δ cannot be a first degree function of σ_{xy}, σ_{yz}, and σ_{zx}, i.e., $A_{xy} = A_{yz} = A_{zx} = 0$. Thus, for $N \parallel C_4$

$$\Delta^{(4)} = A_1^{(4)}\sigma_{zz} + A_2^{(4)}(\sigma_{xx} + \sigma_{yy}). \quad (1a)$$

The superscript in parentheses denotes the order of the symmetry axis along which the center is orientated and indicates that the corresponding quantities (Δ, A) belong to the particular orientation of the centers under consideration.

2. $N \parallel C_3$. From considerations completely analogous to the preceding case, it follows that $A_{xx} = A_{yy} = A_{zz} = A_2^{(3)}$ and $A_{xy} = A_{yz} = A_{zx} = A_2^{(3)}$. Hence,

$$\Delta^{(3)} = A_1^{(3)}(\sigma_{xx} + \sigma_{yy} + \sigma_{zz}) + A_2^{(3)}(\sigma_{xy} + \sigma_{yz} + \sigma_{zx}). \quad (1$$

3. $N \parallel C_2$. Similarly, $A_{xx} = A_{yy} = A_2^{(2)}$; $A_{yz} = A_{zx} = 0$; $A_{zz} = A_1^{(2)}$ and $A_{xy} = A_3^{(2)}$, from which

$$\Delta^{(2)} = A_1^{(2)}\sigma_{zz} + A_2^{(2)}(\sigma_{xx} + \sigma_{yy}) + A_3^{(2)}\sigma_{xy}. \quad (1$$

The quantity Δ can also be expressed in terms of the components of the stress tensor in a different coordinate system directly related to the center. For this coordinate system it is essential to choose a set of three orthogonal axes, one coinciding with the axis of the center N and the other two lying in a plane perpendicular to this axis. In terms of crystallographic notation, we choose the following set of cartesian coordinates for the centers: for $N \parallel C_4$ ($\parallel [100]$)—the directions [100], [001], and [010]; for $N \parallel C_3$ ($\parallel [111]$)—[111], [$1\bar{1}0$], and [$11\bar{2}$];* and for $N \parallel C_2$ ($\parallel [110]$)—[110], [001], and [$1\bar{1}0$]. From symmetry considerations it follows that Δ can be a linear function of only the normal stresses in this system of coordinates; these stresses can be denoted by σ with suitable direction indices:

*For the given direction [111] it would be possible to choose three pairs of perpendicular directions of the type [110], [112].

$$\Delta^{(4)} = a_1^{(4)}\sigma_{100} + a_2^{(4)}(\sigma_{010} + \sigma_{001}), \quad (1$$

$$\Delta^{(3)} = a_1^{(3)}\sigma_{111} + a_2^{(3)}(\sigma_{1\bar{1}0} + \sigma_{11\bar{2}}), \quad (1$$

$$\Delta^{(2)} = a_1^{(2)}\sigma_{110} + a_2^{(2)}\sigma_{1\bar{1}0} + a_3^{(2)}\sigma_{001}. \quad (1$$

The new coefficients "a" are related to the old coefficients "A" as follows:

$$a_1^{(4)} = A_1^{(4)}, \quad a_2^{(4)} = A_2^{(4)}, \quad a_1^{(3)} = A_1^{(3)} + A_2^{(3)},$$

$$a_2^{(3)} = A_1^{(3)} - \frac{1}{2}A_2^{(3)}, \quad a_1^{(2)} = A_2^{(2)} + \frac{1}{2}A_3^{(2)},$$

$$a_2^{(2)} = A_2^{(2)} - \frac{1}{2}A_3^{(2)}, \quad a_3^{(2)} = A_1^{(2)};$$

Eqs. (2a), (2b), and (2c) can be looked upon as generalizations of the results of the Johnson-Williams[4] thermodynamic theory for the case of anisotropic centers and arbitrary deformation; in their theory, they considered the effect of hydrostatic compression (i.e., from all directions) on the spectral bands of an isotropic center in a cubic crystal. In the linear approximation of this theory the displacement of the maximum of the band was determined by the expression

$$\Delta\nu = pAx_0,$$

where p is the pressure, A the "effective" surface of the center, and x_0 the difference between the equilibrium configuration coordinates for the two levels of the center. Comparison of this equation with (2a), (2b), and (2c) clarifies the physical meaning of the coefficients "a" in the latter.

In the preceding discussion, we have treated the displacement Δ of the transition frequency in an anisotropic center as a function of the stresses in the basic lattice. In a completely analogous way, Δ can be investigated as a function of the components of the deformation tensor of the crystal lattice. If this tensor is expressed in the s

tem of coordinates shown in the Figure, the components u_{xx}, u_{yy}, and u_{zz} can be described as relative elongations along these axes, and u_{xy}, u_{yz}, and u_{zx} as changes in the angles between them.[3] If the considerations used in deriving Eqs. (1a), (1b), and (1c) are applied, one can write:

$$\Delta^{(4)} = B_1^{(4)} u_{zz} + B_2^{(4)} (u_{xx} + u_{yy}), \quad (3a)$$

$$\Delta^{(3)} = B_1^{(3)} (u_{xx} + u_{yy} + u_{zz}) + B_2^{(3)} (u_{xy} + u_{yz} + u_{zx}), \quad (3b)$$

$$\Delta^{(2)} = B_1^{(2)} u_{zz} + B_2^{(2)} (u_{xx} + u_{yy}) + B_3^{(2)} u_{xy}. \quad (3c)$$

An expression for the coefficients B in terms of the parameters A which appear in Eqs. (1a), (1b), and (1c) can be obtained by applying Hooke's Law:[3]

$$B_1^{(4)} = c_1 A_1^{(4)} + 2c_2 A_2^{(4)}; \quad B_2^{(4)} = c_2 A_1^{(4)} + (c_1 + c_2) A_2^{(4)};$$

$$B_1^{(3)} = (c_1 + 2c_2) A_1^{(3)}; \quad B_2^{(3)} = c_3 A_2^{(3)};$$

$$B_1^{(2)} = c_1 A_1^{(2)} + 2c_2 A_2^{(2)}; \quad B_2^{(2)} = A_1^{(2)} + (c_1 + c_2) A_2^{(2)}; \quad B_3^{(2)} = c_3 A_3^{(2)}.$$

where c_1, c_2, and c_3 are elastic constants of the cubic crystal.

The dependence of Δ on deformation in the set of coordinates chosen in the same way as for (2a), (2b), and (2c) (when Δ was determined by relative extensions along the three axes of the center) takes on the form

$$\Delta^{(4)} = b_1^{(4)} u_{100} + b_2^{(4)} (u_{010} + u_{001}), \quad (4a)$$

$$\Delta^{(3)} = b_1^{(3)} u_{111} + b_2^{(3)} (u_{1\bar{1}0} + u_{\bar{1}\bar{1}2}), \quad (4b)$$

$$\Delta^{(2)} = b_1^{(2)} u_{110} + b_2^{(2)} u_{1\bar{1}0} + b_3^{(2)} u_{001}. \quad (4c)$$

The relations between coefficients b and B are written as follows:

$$b_1^{(4)} = B_1^{(4)}; \quad b_2^{(4)} = B_2^{(4)}; \quad b_1^{(3)} = B_1^{(3)} + 2B_2^{(3)};$$

$$b_2^{(3)} = B_1^{(3)} - B_2^{(3)}; \quad b_1^{(2)} = B_2^{(2)} + B_3^{(2)};$$

$$b_2^{(2)} = B_2^{(2)} - B_3^{(2)}; \quad b_3^{(2)} = B_1^{(2)}.$$

The coefficients b have an obvious physical meaning: they determine the change of energy for an electronic transition in the center when there is a unit relative change of distance in the lattice along the direction of the axis of the center and along the two directions perpendicular to it (it must be remembered that the relative deformations considered here refer to the normal crystal lattice; in the case of perturbations like those of a center which has its own localized elastic properties, the deformations can differ somewhat from the values given above). A knowledge of the coefficients b can be used to determine those displacements in the lattice which have the greatest effect on the levels of the center; also to determine the shape of the potential curves of the ground and excited states of the center and the kind of lattice vibrations with which the center interacts strongly.

Thus the displacement of the bands (and the levels) of an anisotropic center in a cubic lattice caused by an elastic deformation can be expressed as a linear combination of components of the stress tensor or of the deformation tensor containing two (for $N \parallel C_4$ and $N \parallel C_3$) or three (for $N \parallel C_2$) independent coefficients characterizing the interaction between the centers and the lattice. These equations allow one to find the displacement of the spectral lines of the center for various stress states of the crystal—hydrostatic compression, uniaxial compression or tension, shearing stress, etc., if only the stress or deformation tensors of the crystal are known.

Consider a uniaxial compression when the compression axis P in the crystal has the direction cosines n_x, n_y, and n_z in the coordinate system shown in the Figure. In this case the stress components are defined by $\sigma_{ik} = p n_i n_k$ [3] where p is the compressing stress. For convenience we shall henceforth consider unit compressive stress (p = 1) and the "specific" displacement of the bands caused by this stress, which we denote by δ. We shall use Eqs. (1a), (1b), and (1c), where we substitute $\sigma_{ik} = n_i n_k$. In this case

$$\delta^{(4)} = A_1^{(4)} n_z^2 + A_2^{(4)} (n_x^2 + n_y^2), \quad (5a)$$

$$\delta^{(3)} = A_1^{(3)} + A_2^{(3)} (n_x n_y + n_y n_z + n_z n_x), \quad (5b)$$

$$\delta^{(2)} = A_1^{(2)} n_z^2 + A_2^{(2)} (n_x^2 + n_y^2) + A_3^{(2)} n_x n_y. \quad (5c)$$

Equations (5a), (5b), and (5c) show that the shift of the bands of the center for uniaxial compression of crystals depends on the direction cosines of the compression axes P, this relationship being different for centers of different orientations.

SPLITTING OF THE SPECTRAL BANDS OF ANISOTROPIC CENTERS AS A RESULT OF UNIAXIAL STRESS IN A CRYSTAL

Consider next the splitting of the spectral bands of anisotropic centers, oriented along certain equivalent axes of specified order for uniaxial elastic compression of a cubic crystal along its symmetry axes. This splitting is caused, as was already mentioned, by the difference in displacements δ for several groups of centers, oriented along various axes of the same order and arranged in these various ways with respect to the compression axis P. Thus, a solution of the band splitting model requires a calculation of the displacement δ for each of these groups of centers. For this purpose, it is convenient to use Eqs. (5a), (5b), and (5c). Groups of centers of a specific orientation ($N \parallel C_n$) disposed in various ways with respect to P, will have different values for the direction cosines of the compression axes n_x, n_y, and n_z in the coordinate system associated with the center (cf. Figure). The values of these cosines are readily determined from the known orientation of the centers with respect to the axis P. By using them, it is possible to compute the displacement δ for all orientations of the centers ($N \parallel C_4$, $N \parallel C_3$, $N \parallel C_2$) and directions of the compression axes ($P \parallel C_4$, $P \parallel C_3$, $P \parallel C_2$) from Eqs. (5a), (5b), and (5c). The calculated values of δ, which are functions of $A^{(n)}$, are given in the Table. The groups of centers are characterized in this table by the cosines of angle $\angle PN_1$ which the axes of the centers in each group make with the compression axis P; the number of groups m, similarly oriented with respect to P, i.e., having similar angles $\angle PN$, is also given. The values of δ given in the Table (for known coefficients $A^{(n)}$) completely determine the desired magnitudes of the splitting and displacement of lines of anisotropic centers of different orientations for compression of the crystal along its symmetry axis.

Thus, the splitting of spectral bands of anisotropic bands in cubic crystals subjected to deformations are completely determined by two independent "piezospectroscopic" parameters for $N \parallel C_4$ and $N \parallel C_3$ and three in the case of $N \parallel C_2$. In particular, it follows that since the total number of components into which the lines are split for any of the various orientations of the centers with respect to the three directions of uniaxial compression ($P \parallel C_4$, $P \parallel C_3$, $P \parallel C_2$) exceeds the number of corresponding coefficients $A^{(n)}$, then in addition to the dependence on $A^{(n)}$, there exist relations between the displacements of the various components of the splitting when the crystal is subjected to compression along the C_4, C_3, and C_2 axes (3 relations for $N \parallel C_4$ and $N \parallel C_3$, and 4 relations

Nature of the deformation	$N \parallel C_4$: cos ∠ PN	m	$\delta^{(4)}$	$N \parallel C_3$: cos ∠ PN	m	$\delta^{(3)}$	$N \parallel C_2$: cos ∠ PN	m	$\delta^{(2)}$
$P \parallel C_4$	1	1	$A_1^{(4)}$	$\frac{1}{\sqrt{3}}$	4	$A_1^{(3)}$	$\frac{1}{\sqrt{2}}$	4	$A_2^{(2)}$
	0	2	$A_2^{(4)}$				0	2	$A_1^{(2)}$
$P \parallel C_3$	$\frac{1}{\sqrt{3}}$	3	$\frac{1}{3}A_1^{(4)}+\frac{2}{3}A_2^{(4)}$	1	1	$A_1^{(3)}+A_2^{(3)}$	$\sqrt{\frac{2}{3}}$	3	$\frac{1}{3}A_1^{(2)}+\frac{2}{3}A_2^{(2)}+\frac{1}{3}A_3^{(2)}$
				$\frac{1}{3}$	3	$A_1^{(3)}-\frac{1}{3}A_2^{(3)}$	0	3	$\frac{1}{3}A_1^{(2)}+\frac{2}{3}A_2^{(2)}-A_3^{(2)}$
$P \parallel C_2$	$\frac{1}{\sqrt{2}}$	2	$\frac{1}{2}A_1^{(4)}+\frac{1}{2}A_2^{(4)}$	$\sqrt{\frac{2}{3}}$	2	$A_1^{(3)}+\frac{1}{2}A_2^{(3)}$	1	1	$A_3^{(2)}+\frac{1}{2}A_3^{(2)}$
	0	1	$A_2^{(4)}$	0	2	$A_1^{(3)}-\frac{1}{2}A_2^{(3)}$	$\frac{1}{2}$	4	$\frac{1}{2}A_1^{(2)}+\frac{1}{2}A_2^{(2)}$
							0	1	$A_2^{(2)}-\frac{1}{2}A_3^{(2)}$
Hydrostatic compression			$A_1^{(4)}+2A_2^{(4)}$			$3A_1^{(3)}$			$A_1^{(2)}+2A_2^{(2)}$

for $N \parallel C_2$). Furthermore, there is an additional relation for the displacement of the center of gravity of the split components for the different directions of compression. If this displacement is defined for $N \parallel C_n$ and $P \parallel C_k$ as

$$\bar{\delta}_k^{(n)} = \frac{1}{12/n} \sum_i m_i \delta_{k,\cos \angle PN_i}^{(n)},$$

(where the displacements $\delta_{k,\cos \angle PN_i}^{(n)}$ with the weights m_i, which are equal to the number of groups of centers associated with the component, are summed over all components of the lines), then it can be seen from the Table that the quantity $\bar{\delta}_k^{(n)}$ is the same for all three compression axes (C_4, C_3, C_2) and is equal to:

$$\bar{\delta}^{(4)} = \frac{1}{3}(A_1^{(4)} + 2A_2^{(4)}); \quad \bar{\delta}^{(3)} = A_1^{(3)}; \quad \bar{\delta}^{(2)} = \frac{1}{3}(A_1^{(2)} + 2A_2^{(2)}).$$

It can be shown that the displacement of the center of gravity of the split lines is determined entirely by the change of crystal volume when it is subjected to a uniaxial compression $\Delta V/V$; this quantity is independent of the direction of compression.

The Table also includes the magnitudes of the displacements of the lines of anisotropic centers expressed in terms of the $A^{(n)}$ coefficients for the case of a crystal subjected to hydrostatic compression (for unit hydrostatic pressure $p = 1$). These quantities can be obtained from Eqs. (1a), (1b), and (1c) by substituting in them appropriate values of the terms in the stress tensor for hydrostatic compression ($\sigma_{xx} = \sigma_{yy} = \sigma_{zz} = 1$; $\sigma_{xy} = \sigma_{yz} = \sigma_{zx} = 0$). As is shown in the Table, the displacement of lines of an anisotropic center subjected to hydrostatic compression is three times the displacement of the center of gravity of the split lines for uniaxial compression for the same "pressure" ($\Delta V/V$ is three times as large for hydrostatic compression as it is for uniaxial compression). Note also that the magnitude of the line displacement for hydrostatic compression in the case of anisotropic centers, generally speaking, can be considerably smaller than the magnitude of the line splitting for uniaxial compression.

The "piezospectroscopic" parameters of the centers $A^{(n)}$, which determine the behavior of the lines in spectra of elastically deformed crystals, can be found experimentally by comparing the observed values of the displacements for several (depending on the number of coefficients) of the splitting components in spectra of uniaxially stressed crystals with the expressions for $\delta^{(n)}$ in terms of $A^{(n)}$ given in the Table. A given component of splitting can easily be compared with a definite group of centers by starting from the observed state of polarization of the component.* A knowledge of the values of $A^{(n)}$ permits one to predict the behavior of the lines for any crystalline deformation, in particular for hydrostatic compression, uniaxial compression or extension in any direction, shearing stress etc. Furthermore, once the coefficients $a^{(n)}$ and $b^{(n)}$ in Eqs. (2) and (4) are determined from the known values of $A^{(n)}$, one can infer important physical characteristics of the center as regards its interaction with the lattice. (See the Note I note added in proof at the end of the paper.)

*In calculating the polarization of the splitting components,[1] we did not take account of the fact that in a uniaxially stressed crystal, double refraction (which can cause depolarization) may appear as a result of the deformation. It is readily seen, however, that this effect can be ignored for the cases considered in ref. 1, for which $P \parallel C_4$, $P \parallel C_3$, $P \parallel C_2$ and the polarization picture was investigated by transverse observation, with $E \parallel P$ and $E \perp P$ (in these cases the principal axis of the ellipsoid of the polarizability coincides with P). For all other directions of P one must in general consider the possibility of depolarization of the components as a result of photoelasticity.

REMARKS CONCERNING THE SPLITTING OF SPECTRAL LINES IN UNIAXIALLY STRESSED CRYSTALS

1. In this paper, and also in ref. 1, we were concerned with the simplest kind of anisotropic centers in cubic crystals; these centers were oriented along the symmetry axes of the crystal C_n and had a symmetry axis of their own whose order was no lower than that of C_n. This anisotropy of the center, consisting in the presence in it of some preferred axis, could be caused by anisotropy in the structure of the center itself, which could for instance occupy several lattice sites (e.g., multiple vacancies, a system consisting of an impurity ion and an adjacent defect, etc.) or by anisotropy associated with its position, which could result if an otherwise "isotropic" center occpuies a cubic lattice site characterized by preferred directions (e.g., a foreign or nonstoichiometric atom at an interstitial site; an impurity atom or a vacancy on a lattice site which lacks cubic point symmetry etc.) (See Note II added in proof at the end of this paper.)

In cubic crystals, however, it is possible to have even more complicated anisotropic centers: centers which have a symmetry axis of lower order than the axis C_n along which they are oriented; centers oriented in the lattice along crystallographic directions with higher indices than [100], [110], or [111]; complex centers in which it is generally not possible to distinguish preferred direction etc. The oscillatory model for optical transitions in these centers can also be more complicated than the linear and plane oscillators discussed above: oscillators that are not completely anisotropic, various cases of orientation of the oscillators with respect to the centers, etc. For these more complicated cases, it should be noted that if one starts from the same premises as those used for "simple" anisotropic centers, it is possible to generalize the results for the latter, as regards the number and polarization of components as well as the magnitude of the splitting, to the numerous more complex centers described above.

2. Just as was found for localized centers, one ought to expect polarized splitting in uniaxially stressed crystals in the spectra associated with any of the other energy states of cubic crystals which have "orientational" degeneracy similar to that possessed by the anisotropic centers. Here we refer to excited (exciton) states of the normal lattice sites, the symmetry of whose orientation is characterized by the existence of preferred axes, or of band states of electrons and holes in the vicinity of the extremum points where the band has several extrema at equivalent points in k space, corresponding to electrons (holes) with momentum $k_0 \neq 0$ directed along several identical crystallographic directions. Thus a uniaxial compression of the lattice which, for example, gives rise to different displacements of the minima in the conduction band associated with the several directions of k_0 [6] should in principle give rise to a splitting of the red edge of the fundamental absorption band, whose location is determined by the energy required by the electron to make a transition from maxima in the valence band to the bottom of the conduction band. The nature of the splitting of this edge will be different for different directions of compression. If the polarization of the elementary optical transitions between bands is taken into account, then a polarization effect (dichroism) can arise in the absorption edge of a uniaxially stressed cubic crystal. When one considers spectra associated with band-to-band transitions in uniaxially stressed crystals, one finds that to a considerable degree it will be possible to make use of the same considerations as those applied in discussing the spectra of anisotropic centers (this is true for both the number and polarization of the components of the split line in the spectrum and for the quantitative rules for the magnitudes of the splitting). A study of the effect of uniaxial compression of a crystal on the edge of its fundamental absorption band can turn out to be a rich source of information about the structure of the bands and of exciton levels in crystals.

REFERENCES

1. A. A. Kaplyanskii, Opt. i Spektr. 7, 677 (1959), Optics and Spectroscopy 7, 406 (1959).
2. A. A. Kaplyanskii, Opt. i Spektr. 7, 683 (1959), Optics and Spectroscopy 7, 409 (1959).
3. A. Lyav, "Mathematical Theory of Elasticity." Ob'ed. Nauch. i Tekh. Izd., Moscow, 1935.
4. P. Johnson and F. Williams, Phys. Rev. 95, 69 (1954).
5. Ya. Ya. Kirs and A. I. Laisaar, Trudy Inst. Fiz. i Astron., Akad. Nauk. EstonSSR, No. 10, 51 (1959).
6. C. Herring and E. Vogt, Phys. Rev. 101, 944 (1956).

Notes added in proof

I. The rules derived above for determining the magnitudes of the splitting have been confirmed in a study of the effect of uniaxial compression on the spectra of anisotropic centers in the fluorides of Li and Ca [A. A. Kaplyanskii, N. A. Moskvin and A. K. Przhevuskii, Opt. i Spectr. 10, No. 4 (1961), Optics and Spectroscopy 10, No. 4 (1961)].

II. Anisotropy can also appear in the centers as a result of the Jahn-Teller effect [cf. N. N. Kristofel', Trudy Inst. Fiz. i Astron. Akad. Nauk EstonSSR, No. 12, 20 (1960)]. At sufficiently large deformations, the behavior of "isotropic" impurity centers with large radii has much in common with our anisotropic centers when the band corresponding to a carrier bound to the impurities by the coulomb field has several extrema near $\kappa \neq 0$, e.g., "shallow" donors in Ge and Si [P. J. Price, Phys. Rev. 104, 1223 (1956)].

THE COMPLEX NATURE OF THE F-BAND IN KCl CRYSTALS

N. G. Politov (pp. 173-176)

Received 29 December 1959

Experimental data are presented indicating the complex nature of absorption and phosphorescence excitation spectra in colored KCl crystals.

In investigations of colored alkali-halide crystals,[1-3] the F-center band is usually assumed to be simple in structure. Theories on the transformation of color centers are developed on this basis. At the same time, a large body of data has been accumulated indicating the optical absorption in the F-region[4-17] to be complex in nature.

There are several viewpoints concerning the nature of the new bands overlapping the F-band. Van Doorn came to the conclusion that these bands are not associated with F-centers, but are due to transitions in M- and R-centers.[7,8] Bohun suggested that the new types of centers correspond to new bands, such as an F-center, in the vicinity of which is located one of the hole V-centers or a cation vacancy.[9] Varley[10] thinks that the F-band is overlapped by a band which is caused by the excitation of electrons trapped in anion vacancies occupied by neutral atoms of the metal. According to Lambe and Compton, F-centers interact with aggregate centers; the energy absorbed by F-centers is transported first to the R_1 center, then to the M-center. This energy transmission takes place before any radiative transition of the F-center to the ground state. In a later paper,[12] Compton and Klick underline the particular importance of the fact that R-, M-, and N-centers are located close to one another. Only a few authors have succeeded in isolating the bands which overlap the pure F-band. The A- and B-bands observed by Petrov[4] could not be reproduced by other authors.[18]

Some data are communicated in the present paper concerning the complex nature of the absorption and phosphorescence excitation spectra of colored KCl crystals.

Single crystals were grown by the Kyropoulos method from a melt of KCl salt. The technique of obtaining pure samples is described in ref. 19. Irradiation and measurements were made at room temperature.

Absorption spectra were recorded with an SF-2 spectrophotometer (see curves of Figs. 2-4), or measured with an SF-4 (curves of Fig. 1). Excitation spectra (the phosphorescence was investigated) were measured on an SF-4, using an attachment described in ref. 20.

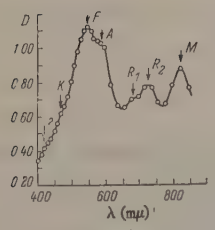

Fig. 1

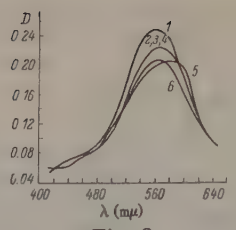

Fig. 2

Fig. 1. Absorption spectrum of an additively colored KCl crystal.

Fig. 2. Absorption spectra of an x-rayed KCl crystal. Curve 1—after coloring; curve 2—after illumination with light of $\lambda = 565$ mμ (1 hr); curve 3—after storage in the dark (1 hr); curve 4—after additional storage in the dark (24 hr); curve 5—after a second illumination with 565 mμ light (1 hr); curve 6—after illumination with 450 mμ light (1 hr).

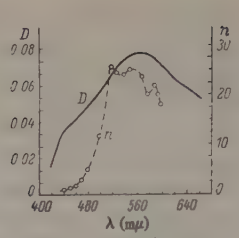

Fig. 3

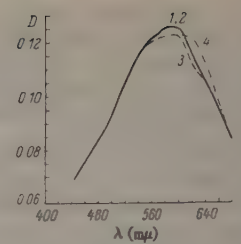

Fig. 4

Fig. 3. Absorption spectrum (curve D) and phosphorescence excitation spectrum (curve n) of an x-rayed KCl crystal.

Fig. 4. Absorption spectra of an additively colored KCl crystal, bleached by a reversal of the direction of the field and then repeatedly colored by irradiation with undecomposed light of a quartz mercury lamp, PRK-4. Curve 1—after holding in the dark (16 days); curve 2—after irradiation with light of $\lambda = 560$ mμ (30 min) (coincides with curve 1); curve 3—after irradiation with light of $\lambda = 580$ mμ (30 min); curve 4—after irradiation with light of $\lambda = 520$ mμ (30 min).

The intensity of phosphorescence was measured five seconds after the excitation of the crystal was terminated. The investigation was made on weakly absorbing crystals with optical density $D < 0.3$. The relative error of the measurements did not exceed 3%. Absorption and excitation spectra were compared for a given sample, or for a series of simultaneously irradiated samples cleaved from the same single crystal.

The data obtained indicate that, in the F-region of the spectrum, bands with maxima at approximately 590 and 520 mμ can be observed in addition to the "pure" F-band near 560 mμ.

A band at 590 mμ is clearly apparent in the absorption spectrum of additively colored crystals (Fig. 1). This band is more difficult to observe in crystals colored by x-rays, but it is well developed after illumination in the F-maximum (Fig. 2, curve 5). It is interesting to note that illumination of the sample with light on the short wavelength flank of the F-band causes a weakening of the band at 590 mμ (Fig. 2, curve 6).

It is known that the spectrophotometric absorption method has limited sensitivity; it is easier to determine the structure of complex bands from the excitation spectra of the crystals. The 590 mμ band appears clearly in phosphorescence excitation spectra of x-rayed crystals. This maximum was observed in many dozens of excitation spectra of x-rayed KCl crystals cleaved out of single crystal slugs of different melts. Control experiments with modified experimental conditions were also set up. Thermoluminescence was investigated along with the absorption and luminescence spectra. The long wavelength band in the F-region can be considered as corresponding to the glow curve peak near 410°K.[21]

When investigating the influence of bleaching by light from the F-band, it is necessary to consider the possibility of formation of Z-bands caused by the presence of such impurities as Ca^{++} and Sr^{++}.[22,23] The experiments indicated that, after irradiation of KCl-Ca crystals in the F-band, a Z_1-band emerges ($\lambda_m \cong 630$ mμ, $\delta \cong 3$ ev, which overlaps the F-absorption band, consequently shifting the maximum of the common band to the red as compared to the location of the F-band maximum.[22] This raises the question of whether the structure of the F-band which we observed could not be explained by the overlapping of a "pure" F-band and a Z_1-band. We do not believe so. As noted above, illumination in the F-band (on its short wavelength slope) caused a weakening of the 590 mμ band. We did not observe any increase in absorption near the Z_1-band—the maximum was displaced toward the blue.

Furthermore, the band at 590 mμ appears in the excitation spectrum without previous illumination in the F band (Fig. 3). This also indicates that we are not dealing with a Z_1-band. Absorption spectra of x-rayed KCl-Ca crystals and the influence of illumination in the F-band were studied at room temperature in the work done by Coufova.[24] If the 590 mμ band which we observed was connected with a Ca impurity, it should appear in the absorption spectrum of KCl-Ca crystals. This was not reported in ref. 24. Let us note that besides the band at 590 mμ, we also observed a band at 520 mμ in the F-region of the spectrum of weakly absorbing crystals.

A series of crystals prepared in the following manner was investigated, along with additively colored and x-rayed crystals: the crystal block was colored by an electrical method (with a potassium electrode) and then bleached by reversing the direction of the field. Samples were cleaved from such a block and then colored by irradiation with ultraviolet light. We observed an additional band in these samples in the 620-680 mμ region. The experiments indicated that the centers responsible for this new band are thermally less stable than F-centers. (The new band was weakened more than the F-band by storage in the dark for one day, which caused a noticeable bleaching of the crystals.) A band with a maximum near 590 mμ (Fig. 4, curve 1) appeared after protracted storage in the dark (15 days), accompanied by pronounced bleaching of the crystals (the optical density at the maximum of the F-band decreased 3 to 4 times). Irradiation with light from the region of the 590 mμ band weakened this band; at the same time a new band was clearly apparent at about 640 mμ (Fig. 4, curve 3.) Irradiation with light from the blue flank of the F-band ($\lambda = 520$ mμ) caused an increase of the intensity of the 640 mμ band (Fig. 4, curve 4).* A similar effect was also observed upon irradiation

*As shown above, illumination with light on the blue flank of the F-band causes a weakening of the band at 590 mμ with light of still shorter wavelength (460 mμ).

It can be concluded from the abovementioned facts that in KCl crystals, bands with maxima near 590 and 520 mμ are superposed on the "pure" F-band with

$\lambda_m \cong 560$ mμ. It should be noted that we succeeded in observing these bands at low F-band intensities inasmuch as they are masked when the F-band is strong.

Some viewpoints were listed above concerning the nature of the new bands in the F-region of the spectrum. It is possible that the bands which we observed are bands predicted in the papers by Deigen and Vinetskii.[25-27] Theoretical investigations indicated that three absorption bands each correspond to F_2^+ and to F_2 color centers. According to calculations, the three bands corresponding to F_2^+ centers are the following: the first is the well-known R_1 band, the second is a weak band on the short wavelength side of the F-band, and the third is the most intense band, located inside the F-band. It is possible that the bands which we observed near 520 and 590 mμ are the predicted second and third bands of F_2^+ centers.[27]

F_2^+ and F_2 centers can probably develop not only upon additive coloration, but also upon coloration with x-rays, although a bleaching action of x-rays undoubtedly takes place as convincingly demonstrated by Lushchik.*

*R-bands were also observed immediately after x-raying in refs. 29 and 30.

The author expresses his gratitude to M. Sh. Getiya for hig help with the work and to E. L. Andronikashvili for discussions.

REFERENCES

1. N. Mott and R. W. Gurney, "Electronnye processy v ionnykh Kristallakh" (Electronic Processes in Ionic Crystals). Izd. Innostrannoi. Lit. 1950; 2nd ed. Oxford Univ. Press, 1948.
2. F. Seitz, Rev. Modern Phys. **26**, 7 (1954).
3. Ch. Lushchik, Trudy Inst. Fiz. i Astron., Akad. Nauk EstonSSR No. 3, 3 (1955).
4. S. Petroff, Z. Physik **127**, 443 (1950).
5. J. D. Konitzer and J. J. Markham, Phys. Rev. **107**, 685 (1957).
6. J. J. Markham and J. D. Konitzer, J. Chem. Phys. **29**, 673 (1958).
7. C. Z. Van Doorn, Philips Research Repts. **12**, 309 (1957).
8. C. Z. Van Doorn and Y. Haven, Phys. Rev. **100**, 753 (1955).
9. A. Bohun, Acta Phys. Acad. Sci. Hung. **8**, 65 (1957).
10. J. H. O. Varley, J. Nuclear Energy **1**, 130 (1954).
11. J. Lambe and W. D. Compton, Phys. Rev. **106**, 684 (1957).
12. W. D. Compton and C. C. Klick, Phys. Rev. **112**, 1620 (1958).
13. R. Casler, P. Pringsheim, and P. Yuster, J. Chem. Phys. **18**, 887 (1950).
14. J. J. Oberly, Phys. Rev. **83**, 228 (1951); Ibid. **84**, 1257 (1951).
15. A. Halperin and A. Braner, Phys. Rev. **98**, 1135 (1955).
16. F. N. Zaitov, Trudy Inst. Fiz. i Astron., Akad. Nauk EstonSSR No. 7, 254 (1958).
17. K. Przibram, "Verfärbung and Lumineszenz" (Coloration and Luminescence). Springer, Wien, 1953.
18. S. Petrov and E. Petrova, Izvestia Bulgat. Akad. Nauk Otdel. Fiz.-Mat. i Tekh. Nauki, Ser. Fiz. **7**, 13 (1958).
19. A. S. Kheinman and K. B. Tolpygo, Sbornik "Zentry okraski v shchelochno-galoidnykh kristallakh" (Color Centers in Alkali-Halide Crystals). Izd. Innostrannoi Lit., Moscow, Leningrad, 1958;
D. Saint-James, J. phys. radium **18**, 260 (1957).
20. N. G. Politov, Trudy Inst. Fiz. Akad. Nauk Gruzin. SSR No. 7, 221 (1960).
21. N. G. Politov, Trudy Inst. Fiz. Akad. Nauk Gruzin. SSR No. 5, 77 (1957).
22. F. N. Zaitov and V. Ya. Kark, Trudy Inst. Fiz. i Astron. Akad. Nauk Eston. SSR No. 6, 82 (1957).
23. G. R. Cole and R. J. Friauf, Phys. Rev. **107**, 387 (1957).
24. P. Coufova, Czechoslov. J. Phys. **9**, 168 (1959).
25. M. F. Deigen, Zhur. Eksptl. i Teoret. Fiz. **21**, 992 (1951); Ibid. **24**, 631 (1953).
26. M. F. Deigen and V. L. Vinetskii, Zhur. Eksptl. i Teoret. Fiz. **32**, 289 (1957), Soviet Phys.-JETP **5**, 226 (1957).
27. V. L. Vinetskii and M. F. Deigen, Opt. i Spektr. **4**, 60 (1958).
28. Ch. B. Lushchik and G. G. Liid'ya, Trudy Inst. Fiz. i Astron., Akad. Nauk EstonSSR No. 7, 193 (1958).
29. W. D. Compton, Phys. Rev. 107, 1271 (1957).
30. H. Yagi, J. Phys. Soc. Japan 11, 430 (1956).

FLASHLIKE RISE OF LUMINESCENCE
II. ZnS-Co and ZnS-Ag,Co Phosphors

N. A. Tolstoi, A. A. Anufriev, P. G. Deineka, L. A. Rusinov, V. A. Sokolov, and A. A. Spartakov (pp. 177-181)

Received 30 March 1960

The properties and rules of the flashlike rise of luminescence of cobalt-activated and silver,cobalt-activated zinc sulfide phosphors are described. The nature of the phenomenon is shown to be connected specifically with the kind of activator present. The experimental results are interpreted from the viewpoint developed in previous papers.

1. Discovery of the flashlike rise of luminescence (FR) of zinc sulfide phosphors activated by manganese[1,2] and nickel,[3,4] naturally raised the question of its occurrence in other phosphors of a similar type. This article describes the properties and rules of FR discovered in zinc sulfide activated by cobalt[5] and by silver and cobalt. ZnS-Co in the wurtzite form and ZnS-Ag,Co in the wurtzite and sphalerite forms were available to us. The characteristics of the three phosphors investigated are presented in the Table.

For the investigation of FR, we constructed an instrument based on the apparatus described in ref. 2. As an additional refinement to the method, we electronically stabilized the luminous flux of the SVDSh-250 mercury-vapor lamp used for exciting the phosphors ($\lambda = 365$ mμ). The circuit of the stabilizer which we constructed differs somewhat from that originally proposed by Shirokov.[6] The stabilizer was simple to adjust and easy to operate (Fig. 1).

The luminescence was measured by an AEG cesium oxide photomultiplier. A glass filter was used to eliminat the 436 mμ mercury line for measurement of the blue luminescence band (Zn and Zn + Ag) and a Schott RG-3 filter was used for measurement of the red band (Co).

2. All of the phosphors listed in the Table have FR in the red luminescence band. The kinetics of rise of the blue band are normal. Curves showing the flash intensity $V = I_{max}/I_{\infty}$ as a function of the dark period between two excitations of certain ZnS-Co phosphors are presented in Fig. 2. A comparison of these functions $V(\log t_0)$ with similar functions for ZnS-Mg and ZnS-Ni, obtained in refs. 2 and 4 respectively, leads to the following conclusions:

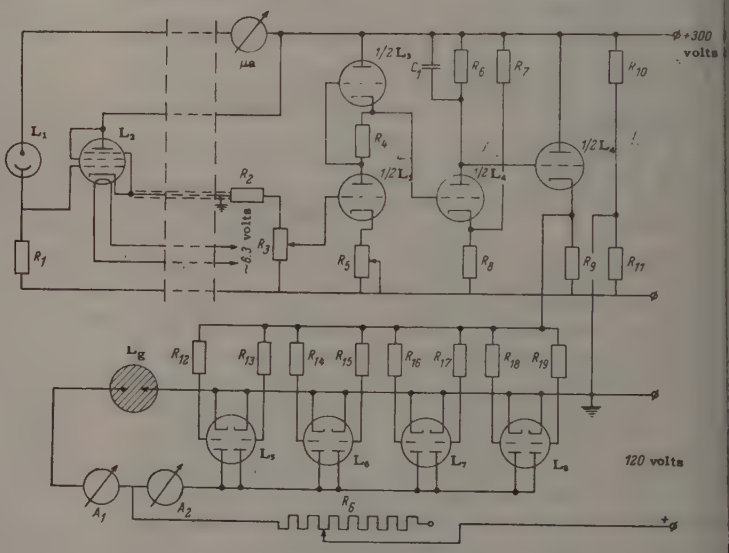

Fig. 1. Schematic of the stabilizer for the luminous flux of the mercury vapor lamp. L_1—STs V-3; L_2—6Zh1B; L_3, L_4—6N1P; L_5, L_6, L_7, L_8—6N5S; L_9—SVDSh-250; μa—100a; A_1—10a; A_1—3a; R_1—430 kohm; R_2—10 kohm; R_3—8.2 kohm; R_1, R_5—10 kohm; R_6—620 kohm; R_1—24 kohm; R_8—5.1 kohm; R_9—130 kohm; R_{10}—24 kohm; R_{14}—30 kohm; R_{12}-R_{19}—100 ohm; R_6—20 ohm; C_1—390 $\mu\mu$f.

Experimental conditions	ZnS-Co				ZnS-Ag, Co								
Calcining temperature	900°	1200°			900°					1200°			
Modification	Sphalerite	Wurzite			Sphalerite					Wurtzite			
Ag content (gm/gm)	—	—			$5 \cdot 10^{-4}$					$5 \cdot 10^{-3}$			
Co content (gm/gm)	10^{-6}	$5 \cdot 10^{-6}$	$5 \cdot 10^{-5}$	10^{-4}	$5 \cdot 10^{-6}$	10^{-5}	$5 \cdot 10^{-5}$	10^{-4}	$2 \cdot 10^{-4}$	$5 \cdot 10^{-6}$	10^{-5}	$5 \cdot 10^{-5}$	10^{-4}
U ripening (ev)	0.5	0.67	0.88	0.83	1.1	0.62	0.58	0.65	0.46	0.63	0.62	0.67	0.94
t_0 ripening at 20° C (sec)	1	1	0.7	0.3	35	15	8	1.5	0.5	35	15	8	1

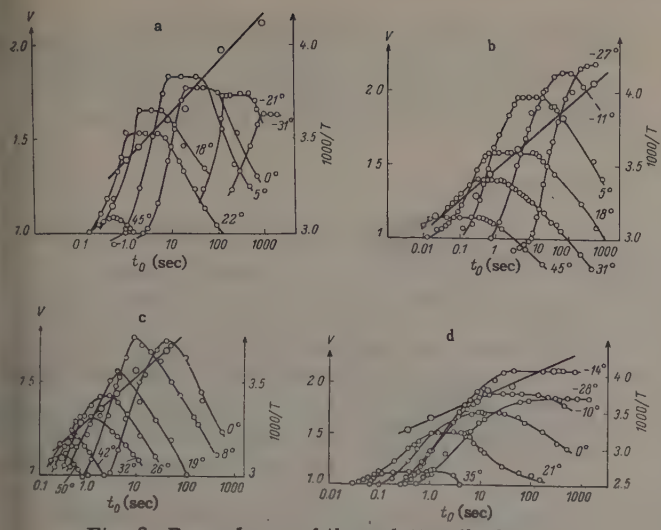

Fig. 2. Dependence of the relative flash V on the logarithm of the times of the dark period t_0 at different temperatures, for a ZnS-Co phosphor. Heavy line—dependence of times t_0, corresponding to the maximum flash ($\bar{t}_0$), on the reciprocal of absolute temperature. Concentration of Co (in gm/gm) and modification; a—5×10^{-6}, wurtzite; b—5×10^{-5}, wurtzite; c—2×10^{-4}, wurtzite; d—10^{-6}, sphalerite.

(a) The "ripening" time to maximum flash $\bar{t}_0$ for phosphors activated by cobalt is usually greater than for ZnS-Mn, but less than for ZnS-Ni (the times $\bar{t}_0$ are compared at room temperature).

(b) The function V(log t_0) for ZnS-Mn does not have a plateau, i.e., overripening takes place as though it occurred immediately after ripening. The function V(log t_0) for ZnS-Ni has a plateau of such long duration that even at temperatures somewhat above room temperature it extends practically to infinity. This means that the overripening process is not observed over any reasonable period of observation (24 hr). Finally, the function V(log t_0) for ZnS-Co is "intermediate" in character, i.e., the well-expressed plateau (Fig. 2) is replaced by the clearly observed overripening process.

Thus, the rule followed by the flashlike rise of luminescence in zinc sulfides activated by Mn, Ni, and Co is specifically connected with the nature of the activator—it is possible to determine which activator was used from the form of the graph V(log t_0). Since the phenomenon of FR, in several instances, is observed at very small concentrations of the long wavelength activator, it is possible to establish a qualitative method for determining small amounts of impurities in zinc sulfide, such as the typical "poisons" nickel, cobalt, and iron.

It is known that for ZnS activated by cobalt, the rate of rise and decay is slow, and "tails" are present on the curves. This well-known fact was always connected either with the green luminescence band of copper (for ZnS-Cu, Co phosphors), or with the blue band of zinc. We discovered that a similar sluggishness is also characteristic of the red luminescence band of ZnS-Co, in which a flashlike rise is observed. A combination of the slow rate of rise and the flashlike character in the case of ZnS-Co and ZnS-Ag,Co produces a characteristic form of flash, which is schematically presented in Fig. 3 (the flash has already occurred and is completed, but the luminescence still continues to increase). It is evident from the figure that for ZnS-Co, flashes with a relative intensity $V = I_{max}/I_\infty$ of less than unity may be observed.

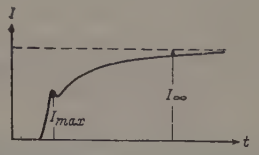

Fig. 3. Form of the curve of the flashlike rise for ZnS-Co at $V < 1$.

3. The effect of a second activator—silver—on the parameters of FR in zinc sulfide activated by cobalt is rather significant. In both the sphalerite and wurtzite forms of ZnS-Ag,Co the presence of silver increases the ripening time $\bar{t}_0$. The lower the concentration of cobalt, the greater the increase in $\bar{t}_0$ (see the Table). At high cobalt concentrations, the value of $\bar{t}_0$ for ZnS-Ag,Co approaches that of ZnS-Co.

This effect of silver on the value $\bar{t}_0$ may be explained in terms of concepts developed in ref. 4. Let us assume that silver, like zinc, forms the first trapping levels (for example, holes); let the probability of a second trapping of holes ejected into the valence band be relatively large for the silver levels and relatively small for the zinc. Then the time during which relocalization of holes from the first to the second levels must occur (i.e., the ripening time) will be greater for ZnS-Ag,Co than for ZnS-Co. Actually, the holes ejected into the band must "make a choice": whether to be relocalized at the first trapping level or to go to the second level. This choice depends on the number and capture cross section of both the first and second trapping levels. A second trapping at the first levels prolongs the ripening process, so that the addition of Ag increases $\bar{t}_0$; a movement of holes to levels at which they are trapped a second time is also a ripening process; consequently, an increase in the concentration of Co directs the flow of holes to centers where they are trapped again, and the value of $\bar{t}_0$ is reduced. Why, in the absence of silver, does the value of $\bar{t}_0$ not depend on the concentration of Co? In terms of the proposed explanation, this phenomenon should be connected with the fact that the first trapping levels of zinc have only a slight ability to recapture. Therefore, an increase in the number of second trapping centers should not accelerate ripening because, in the absence of multiple capture, the rate of relocalization depends only on the rate of ejection of holes into the valence band; i.e., it is determined only by the nature of the first trapping centers; an ejected hole no longer has a "choice" and must proceed to a second trapping level.

The maximum relative intensities of the flash for ZnS-Co and ZnS-Ag,Co were $\bar{V} = 2.3$ and 3.2 respectively.

4. Experiments involving the illumination of ZnS-Co and ZnS-Ag,Co phosphors during the dark period showed that, as in the case of ZnS-Ni and ZnS-Mn, infrared illumination accelerates the ripening process, and greenish-orange illumination accelerates the overripening process. The prolonged action of infrared light may produce some overripening (as in the case of ZnS-Ni). It should be noted that in the case of ZnS-Ag,Co phosphors, greenish-orange illumination does not produce complete overripening even after a very prolonged exposure. Both of these facts seem to indicate that both first and second trapping levels have a certain "energy depth spectrum." The low-energy limit of the spectrum of the second trapping levels is responsible for the ability of infrared radiation to produce some overripening; the high-energy

limit of this spectrum is the cause of the inability of greenish-orange radiation to produce complete over-ripening. Investigations with monochromatic illumination would permit an investigation into the structure of these energy depth spectra, and also an examination of the extent to which second levels overlap first levels on the one hand, and the excitation spectrum on the other.

5. The existence of the red part of the luminescence spectrum of ZnS-Co has been known for some time; however, statements have been made which suggest that this part of the spectrum of phosphors activated by elements of the iron group is only a "tail" of the blue band (see, for example, ref. 7). There are profound differences in the relaxation laws of the blue and red bands of ZnS-Co and ZnS-Ag,Co which completely refute this opinion. Moreover, equally pronounced differences also exist between the stationary properties of the blue and red bands. Actually, the relation of the stationary intensity of luminescence L_∞ to the intensity of excitation light E is supralinear for the blue band (linear in special cases) and the luminescence is quenched with increasing temperature. For the red band, the relation $L_\infty(E)$ is sublinear (linear in special cases) and the luminescence increases on heating (until temperature quenching does occur). Thus, using the old Lenard terminology, one may say that the blue band is "cold" and the red band is "hot". Variations in the form of the stationary relation $L_\infty(E)$ to temperature, for the red band, are described in ref. 8.

REFERENCES

1. N. A. Tolstoi and P. P. Feofilov, Doklady Akad. Nauk SSSR 68, 285 (1949).
2. N. A. Tolstoi, N. N. Tkachuk, M. Ya. Tsenter, Z. S. Mansurova, and A. V. Burlakov, Opt. i Spektr. 1, 719 (1956).
3. N. A. Tolstoi, Opt. i Spektr. 1, 271 (1956).
4. N. A. Tolstoi, A. M. Tkachuk, and N. N. Tkachuk, Opt. i Spektr. 2, 760 (1957).
5. N. A. Tolstoi, Doklady Akad. Nauk SSSR 111, 582 (1956) Soviet Phys.-Doklady 1, 698 (1956).
6. V. I. Shirokov, Izvest. Akad. Nauk SSSR, Ser. Fiz. 20 605 (1956).
7. Gy. Gergely, J. phys. radium (Colloque de Luminescence) 17, 679 (1956).
8. N. A. Tolstoi, Opt. i Spektr. 3, 73 (1957).

FINAL STAGES OF LUMINESCENCE DECAY IN PHOSPHORS WITH LEVELS OF SEVERAL KINDS

V. V. Antonov-Romanovskii (pp. 182-187)

Received 30 March 1960

A calculation is carried out for the later stages of decay when only the deepest traps of either sign are effective. The calculation is carried out on the assumption that the probability of repeated capture far exceeds the probability of recombination.

The initial stages of phosphorescence decay and flare-up were considered in ref. 1. It is a special feature of these stages that under certain definite conditions, which are often satisfied experimentally, they can be described by linear or quasi-linear differential equations. This linearity, however, is limited in time. Nonlinearity must, as a rule, occur in later stages. Another very essential fact is that usually only the smaller portion of the light sum is either emitted or stored in the initial stages. The later stages are therefore at least as interesting as the earlier stages. In this article we shall consider the case of decay.

As indicated in ref. 1, linearity stops as soon as charges from the deepest traps of either or both signs begin to play a part. This means that we must consider the kinetics of phosphorescence in the case where there is only one level of one sign but several levels of the opposite sign.

To pinpoint the problem, let there be one kind of electron trap ($m^- = 1$). Then the number of kinds of hole traps must be no less than two ($m^+ \geqslant 2$). Two cases are possible here: either the probability p^+ of holes leaving the shallowest traps is comparable with p^-, the probability of escape of electrons, or it is much smaller. We shall not consider the case in which it is much larger, since this reduces to the linear problem considered in ref. 1.

The probability (per unit time) p_1^+ of a hole leaving the shallowest traps is determined by the quantity w_1^+, or more precisely (see ref. 1) by the quantity* λ_1^+ written in the form

$$p_1^+ = \lambda_1^+ = w_1^+\left(1-\frac{\sigma_1^+\nu_1^+}{\sum_1^{m^+}\sigma_k^+\nu_k^+}\right) \qquad (1)$$

since part of the liberated electrons may be repeatedly localized on "their own" levels. However, the probability of the electrons leaving their own traps is no longer a constant since such a departure can only be caused by recombination, there being no deeper traps. Hence

$$p^- = w_1^-\frac{\sum_1^{m^+}\sigma_{0k}^-n_k^+}{\sum_1^{m^-}\sigma_k^-\nu_k^-}. \qquad (2)$$

The kinetics are nonlinear just because p^- is variable (due to the variability of n_k^+).

For $m^- = 1$, when inequalities (I, 5) (absence of saturation) and (I, 6) (smallness of recombination) hold, we obtain from Eqs. (I, 1) and (I, 2) the following system of equations:

*The notation is the same as in ref. 1. When referring to formulas of ref. 1, such formulas will be prefixed by the symbol I.

$$\frac{dn_i^+}{dt} = -w_i^+ n_i^+ - \sigma_i^+ v_i^+ \cdot u^+ N^+ - \sigma_{0i}^- n_i^+ \cdot u^- N^-, \quad (3)$$

$$\frac{dn^-}{dt} = -\sum_1^{m^+} \sigma_{0k}^- n_k^+ u^- N^-, \quad (4)$$

where

$$n^+N^+ = \frac{\sum_1^{m^+} w_k^+ n_k^+}{\sum_1^{m^+} \sigma_k^+ v_k^+} \text{ and } n^-N^- \leqq \frac{w^- n^-}{\sigma^- v^-}. \quad (5)$$

This system of equations is difficult to solve in the general case. We may, however, use data from the diffusion theory of phosphorescence.[2] According to this theory, the effective cross section for the recombination of free and localized charges (as long as the latter are not compensated) is not structurally sensitive. In this case we may set all

$$\sigma_{0i}^- = \sigma_0^-. \quad (6)$$

If this is the case, then from Eq. (5) and the fact that

$$\sum_1^{m^+} n_k^+ = n^-,$$

we have, instead of Eqs. (3) and (4),

$$\frac{dn_i^+}{dt} = -w_i^+ n_i^+ + \frac{\sigma_i^+ v_i^+}{\sum_1^{m^+} \sigma_k^+ v_k^+} \sum_1^{m^+} w_k^+ n_k^+ - \frac{\sigma_0^- n_i^+}{\sigma^- v^-} w^- n^-, \quad (7)$$

$$\frac{dn^-}{dt} = -\frac{\sigma_0^- w^-}{\sigma^- v^-} n^{-2}. \quad (8)$$

Integrating Eq. (3), we obtain

$$n^- = \frac{n_0^-}{1 + \frac{\sigma_0^- w^-}{\sigma^- v^-} n_0^- t}, \quad (9)$$

i.e., the quantity n^- decreases as a first degree hyperbola. Such a result is quite understandable: If the effective recombination cross sections are equal, then any redistribution of holes among traps cannot affect the rate of recombination of free electrons.

We can easily show that if we set

$$n_i^+ = \eta_i^+ n \quad (10)$$

and take account of Eq. (8), then the system of equations (7) becomes

$$\frac{d\eta_i^+}{dt} = -w_i^+ \eta_i^+ + \frac{\sigma_i^+ v_i^+}{\sum_1^{m^+} \sigma_k^+ v_k^+} \sum_1^{m^+} w_k^+ \eta_k^+, \quad (11)$$

which is identical with the system of equations whose solution was given in ref. 1. Using the scheme indicated in ref. 1 to determine the η_i^+, we find n_i^+ by means of Eqs. (9) and (10). The only difference here is that recombination losses caused by the encounter of free electrons with localized holes are automatically taken into account by means of the factor n^- in Eq. (10). On the other hand, the losses caused by the recombination of free holes, as previously, are taken into account successively each time as soon as traps of some kind are relieved in turn from an excess of holes.

Since

$$p_1^+ \gg p_2^+ \gg p_3^+ \gg \ldots \quad (12)$$

and since only p_1^+ may be comparable to p^- (as indicated above, the inequality $p_1^+ \gg p^-$ reduces to the case considered in ref. 1), i.e., since

$$p_1^+ \sim p^- \text{ or } p_1^+ \ll p^-, \quad (13)$$

it may seem at first that there is no point in considering the decay at the late stage when the dominant role in the kinetics of holes is played by traps with the subscript i = 2. This is the case since Eqs. (12) and (13) give

$$p_2^+ \ll p^-, \quad (14)$$

All further decay (the whole recombination) is therefore determined by the motion of the holes only. This, however, is not quite correct. The fact is that, according to Eq. (2), p^- is a decreasing quantity. The time may come, therefore (even though the phosphor might by then have emitted almost all of the light sum), when after all (insofar as $p_2^+ = \text{const.}$).

$$p_2^+ \sim p^-. \quad (15)$$

On the basis of this, the investigation which we carried out may be meaningful for later decay stages as well.

Finally, the time will arrive when the hole traps next to the last in depth ($i = m^+ - 1$) will have "done their job." From that instant, only one kind of trap of each sign will remain active. Thus if condition (6) is satisfied the problem may be solved completely.

Let us now consider the intensity of the radiation. Using Eqs. (I, 12) and (9) and the fact that $m^- = 1$, we obtain

$$I_j = q_j \frac{\sigma_{0j}^- n_j^+}{\sigma^- v^-} \frac{w^- n_0'^-}{1 + \frac{\sigma_0^+ w^-}{\sigma^+ v^-} n_0'^- t},$$

$$n_j^+ = n_{j0}^+ e^{-\lambda_j^+ t} + \sum_1^{j-1} \delta_k^+ n_{k0}'^+ \left(e^{-\lambda_j^+ t} - e^{-\lambda_k^+ t} \right), \quad (16)$$

where λ_i^+ is determined from Eq. (I, 23). Only the recombination losses (which are essentially a correction) caused by electron motion are taken into account.

Given a situation which is the converse of that considered above, i.e., where there is only one hole level ($m^+ = 1$) but several electron levels, it would be possible to use Eq. (I, 12) directly. This would be the case because that formula does not give explicitly the form of the function n_i^+, which in our case is nonexponential, and according to Eq. (9) (in which the superscript is changed to +) is hyperbolic. Since $l^- = m^- - 1$, we now obtain (only one band being emitted in this case)

$$I = q\sigma_0^- \frac{n_0^+}{1 + \frac{\sigma_0^+ w^+}{\sigma^+ v^+} n_0^+ t} \sum_1^{m^- - 1} \frac{w_j^-}{S_j^{m^-}} n_{j0}'^- e^{-\lambda_j^- t}. \quad (17)$$

Equations (16) and (17) are no longer valid from the moment that the traps (hole or electron) which are next to the last in depth are "removed from circulation." In this case the decay follows a second degree hyperbola.

The results obtained above (and also in ref. 1) lead to the following conclusion: As long as the traps which are active are not the deepest, and if conditions (I, 5) and (I, 6) are fulfilled, then the fundamental process consists in a redistribution of charges among traps of different depths while the recombination process can be considered merely as a correction.

As a result, the decay kinetics are described by quasi-linear equations and are therefore either exponential or quasi-exponential. They might be called biexponential insofar as the kinetics of charges of both signs are exponential. From the instant of termination of the process of redistribution of charges of either sign among traps, the kinetics become nonlinear with regard to

charges of this sign since a purely recombinatory process begins to predominate. At this state, therefore, the process as a whole may be called exponential-hyperbolic. Finally, the final stage of decay sets in, when the process of redistribution among traps of charges of the opposite sign also dies down. As a result, the kinetics of charges of both signs turn out to be nonlinear and as a whole might be called bihyperbolic.

It should be noted at this point that there is an obstacle to the experimental determination of whether the kinetics are linear or nonlinear: The sum of the exponential decay curves can often be approximated over a large range of brightness by a single hyperbolic function. Other complicating circumstances are also possible. (In particular, we shall show below that the decay can proceed hyperbolically for an entirely different reason.)

We return to the initial equations (3) and (4); this time, however, we shall assume that the σ_{0i}^- may differ, i.e., that relation (6) is no longer satisfied. We shall consider the case when the motion of holes may be neglected as compared with the motion of electrons. Then the system of Eqs. (3) and (4) has approximately the form

$$\frac{dn_i^+}{dt} = -\sigma_{0i}^- n_i^+ \frac{w^- n^-}{\sigma^- \nu^-}, \tag{18}$$

$$\frac{dn^-}{dt} = -\sum_1^{m^+} \sigma_{0i}^- n_i^+ \frac{w^- n^-}{\sigma^- \nu^-}. \tag{19}$$

Multiplying both sides of Eq. (18) by dt/n_i^+ and carrying out the integration, we obtain

$$n_i^+ = n_{i0}^+ e^{-\sigma_{0i}^- z}, \tag{20}$$

where

$$z = \frac{w^-}{\sigma^- \nu^-} \int_0^t n^- dt. \tag{21}$$

Since

$$n^- = \sum_1^{m^+} n_k^+,$$

$$n^- = \sum_1^{m^+} n_{k0}^+ e^{-\sigma_{0k}^- z}. \tag{22}$$

It follows from Eq. (21) that

$$t = \frac{\sigma^- \nu^-}{w^-} \int_0^z \frac{dz}{n^-}. \tag{23}$$

The problem can thus be considered solved, although in parametric form; z is the parameter.

It follows from Eq. (20) that

$$n_j^+ \sim (n_i^+)^\alpha, \quad \alpha = \frac{\sigma_{0j}^-}{\sigma_{0i}^-}. \tag{24}$$

This leads to an interesting result. Due to the difference in the rate of decrease of the quantities n_i^+, an instant t′ must occur in the later stages beyond which the relation

$$n^- \approx n_j^+, \tag{25}$$

will hold. Here n_j^+ is the concentration of the ionized luminescence centers for which σ_j^- has a minimum value. In such a case it is not difficult to show that the quantities n^- and n_j^+ decrease along a first degree hyperbola, i.e.,

$$n^- \approx n_j^+ \approx \frac{n_{j0}'^+}{1 + \frac{\sigma_j^- w^-}{\sigma^- \nu^-} n_{j0}'^+ t}, \tag{26}$$

where $n_j'^+$ has the meaning of an initial concentration.

It follows from relations (20) and (26) that starting at $t = t'$,

$$n_i^+ \approx n_{i0}^+ \left(\frac{n_{j0}'^+}{n_{j0}^+}\right)^{\frac{\sigma_{0i}^-}{\sigma_{0j}^-}} \left(1 + \frac{\sigma_j^- w^-}{\sigma^- \nu^-} n_{j0}'^+ t\right)^{-\frac{\sigma_{0i}^-}{\sigma_{0j}^-}}, \quad (\sigma_{0i}^- > \sigma_{0j}^-), \tag{2}$$

i.e., the quantity n_i^+ decreases along a hyperbola with a exponent $\alpha > 1$.

Since $I_i \sim n^- n_i^+$, it follows from relations (26) and (27) that

$$I_i \sim \left(1 + \frac{\sigma_j^- w^-}{\sigma^- \nu^-} n_{j0}'^+ t\right)^{-\alpha}, \quad \alpha = 1 + \frac{\sigma_{0i}^-}{\sigma_{0j}^-} \geqslant 2. \tag{2}$$

We have $\alpha = 2$ only for $i = j$; i.e., the intensity of luminescence of the j-th band decreases as a second degree hyperbola, while all other bands decay faster.

It should be pointed out that certain changes in the decay may be caused by the redistribution of holes among traps of different kinds, provided this process is exponential in nature and is therefore capable of finally "catching up" with the rate of the hyperbolic process. (The rate of decay in the hyperbolic process differs from that in the exponential process in not being constant, but decreasing monotonically to zero.) This can be easily certified since

$$\frac{e^{-\lambda t}}{t^\alpha} \to 0 \text{ for } t \to \infty. \tag{2}$$

In this connection we shall consider the same system of equations (18) and (19), introducing the distinction however, that there is a noticeable departure of holes from the shallowest traps. This is the case when n_1^+ no longer obeys an equation of type (18) but

$$\frac{dn_1^+}{dt} = \lambda_1^+ w_1^+ n_1^+ - \sigma_{01}^- n_1^+ \frac{w^- n^-}{\sigma^- \nu^-}, \tag{3}$$

where

$$\lambda_1^+ = 1 - \frac{\sigma_1^+ \nu_1^+}{\sum_1^{m^+} \sigma_k^+ \nu_k^+}. \tag{3}$$

It is not difficult to show that in this case

$$n_1^+ = n_{10}^+ e^{-\lambda^- w^- t - \sigma_{01}^- z}, \tag{3}$$

$$n_i^+ = \left\{ n_{i0}^+ + \delta_i^+ w_1^+ n_{10}^+ \int_0^t e^{-\lambda_1^+ w_1^+ t - (\sigma_{0i}^- - \sigma_{01}^-) z} dt \right\} e^{-\sigma_{0i}^- z}, \quad (i \geqslant 2), \tag{3}$$

where

$$\delta_i = \frac{\sigma_i^+ \nu_i^+}{\sum_1^{m^+} \sigma_k^+ \nu_k^+}, \tag{3}$$

while z and t, as before, are determined from Eqs. (21) and (23). Formula (22) is no longer valid for n^-, and we must simply use the expression $n^- = \sum_1^{m^+} n_k^+$. By analogy it is not difficult to write formulas for the time instant when the second level of traps begins to "act," etc.

Thus if the traps are "sharply separated," i.e., if their consecutive action is assured, the problem may be fully solved even for the most general "nonlinear" case when the quantities σ_{01}^- differ among themselves.

Let us note in conclusion that "exotic" cases are possible in nonlinear kinetics as well: for example, traps may differ markedly not only in the values of the probability of a charge being freed from them but also in some other parameters. Conversely, they may differ but little in depth. All this may result in the appearance of special rules, as was shown for one case in ref. 3.

REFERENCES

1. V. V. Antonov-Romanovskii, Opt. i Spektr. 7, 376 (1959), Optics and Spectroscopy 7, 245 (1959).
2. V. V. Antonov-Romanovskii, Opt. i Spektr. 3, 592 (1957).
3. V. V. Antonov-Romanovskii, Opt. i Spektr. 7, 827 (1959), Optics and Spectroscopy 7, 484 (1959).

THE PROCESS RESPONSIBLE FOR THE VOLTAGE DEPENDENCE OF THE MEAN LUMINESCENCE BRIGHTNESS

A. N. Georgobiani and M. V. Fok (pp. 188-193)

Received 11 February 1960

The voltage dependence of the mean luminescence brightness, and also the temperature variation of this dependence, shows that the mean luminescence brightness is determined mainly by a tunnel penetration of electrons through a certain potential barrier. Such a barrier may develop, for example, at the boundary between crystals of zinc sulfide and the surface phase.

It has been shown[1] that the formation of the main peak of wave brightness depends on the release of localized electrons by an electric field, and that a complete destruction of electron traps occurs at a certain field value, which we called critical. The problem concerning the mean brightness was not examined previously. The present article is devoted to the study of the mechanism responsible for the dependence of the mean luminescence brightness on the value of the electric field. The same luminescence condenser is studied in this article as was used in our earlier work.[1]

As is known, the voltage dependence of the mean luminescence brightness is approximated by the formula

$$I \sim \exp\left(-\frac{B}{\sqrt{U_0}}\right), \qquad (1)$$

where U_0 is the amplitude value of the excitation voltage. Relation (1) is applicable over the studied temperature interval (T = 77-413°K) and the voltage range (U_0 = 4.2 × 10^4-3 × 10^5 volts/cm) for sinusoidal and trapezoidal excitation voltages.

Since, according to the Schott model, in the region of field concentration the field is proportional to the square root of the applied voltage, i.e., $E \sim \sqrt{U}$, relation (1) may be rewritten in the form

$$I \sim \exp\left(-\frac{B_1}{E_0}\right). \qquad (2)$$

As before, we used voltages which extend on either side of the critical field. We did not notice any change in the nature of the dependence of the mean luminescence brightness on the magnitude of the electric field, upon changing the field intensity through the critical value. This is evident from Fig. 1, where the dependence of log $\bar{I}$ on $1/\sqrt{U_0}$ for two temperatures (curve I for T = 77°K and curve II for T = 373°K) is represented. The critical voltages for these temperatures are noted by arrows. It is apparent from the figure that the experimental points fall on the same straight line on either side of the arrows. This leads us to believe that the factor which controls the voltage dependence of the mean luminescence brightness remains the same. Hence, it is clear that the processes which are responsible for the voltage dependence of the mean brightness and waveform brightness, are different.

Several authors[2-4] believe that relation (2) may be explained on the basis of the mechanism of impact ionization, if the mean probability of impact ionization is expressed by the Seitz formula[5]

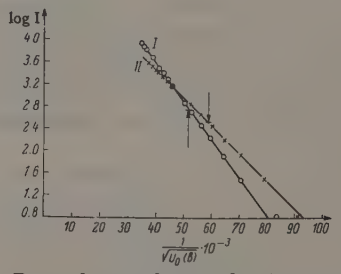

Fig. 1. Dependence of mean luminescence brightness on the amplitude of excitation voltage. Temperature (in °K); curve I—77; curve II—373. Critical voltages for each temperature are indicated by arrows.

$$\bar{W}_i^{im} \sim \exp\left(-\frac{E_1}{E}\right), \qquad (3)$$

where E_1 is a certain characteristic field value. However, the Seitz formula was obtained from a simplified model and is approximate. A more accurate formula for the mean probability of impact ionization may be obtained by solution of the kinetic equation. Examination of this problem by Chuenkov,[6] using the kinetic equation, shows that relation (3) is valid only in the fields

$$E \ll E' \equiv \frac{2P}{el_0}, \qquad (4)$$

where P is the ionization potential, l_0 is the length of free travel of the electron having a kinetic energy equal to the ionization potential, and e is the electron charge. In fields greater than E', the relation takes another form

$$\bar{W}_i^{im} \sim \exp\left(-\frac{E_2^2}{E^2}\right), \qquad (5)$$

where E_2 is once again a certain characteristic field value.

For electrons of thermal energy in ZnS, the length of free travel is of the order of 10^{-6} cm.[3,7] Since the length of free travel in ionic crystals increases proportionally with energy,[8]

$$l_0 = \frac{l_T \cdot P}{kT}, \qquad (6)$$

where l_T is the length of free travel for an electron of thermal energy, k is the Boltzmann constant, and T is the absolute temperature. In this instance, the inequality (4) may be rewritten in the following form

$$E \ll E' \equiv \frac{2kT}{el_T}. \qquad (7)$$

Values of E′, calculated from formula (7) for the appropriate temperatures, are presented in the Table.

T (°K)	E′×10⁻⁴ (volts/cm)
77	1.3
293	5.1
413	7.1

As noted above, we applied to the cell a mean field of $U_0 = 4.2 \times 10^4$-3×10^5 volts/cm. If we consider that field concentration occurs during luminescence, then it becomes apparent that, in our experiment, the conditions of (4) are not fulfilled over almost the whole range of measurement. On the other hand, the experimentally discovered temperature dependence of the characteristic field V also does not conform to the theory. It is apparent from Fig. 2, that the value of V falls with an increase of temperature. According to a theoretical study by Chuenkov[9] and Keldysh,[10] the characteristic field for the process of impact ionization in ionic crystals with a large length of free travel increases with temperature in accordance with the formula

$$E_2 \sim \sqrt{\frac{\exp\left(\frac{h\omega}{kT}\right)+1}{\exp\left(\frac{h\omega}{kT}\right)-1}}, \qquad (8)$$

($h\omega$ is the energy of an optical phonon) in the case of formula (5), but does not depend on temperature in the case of formula (3).

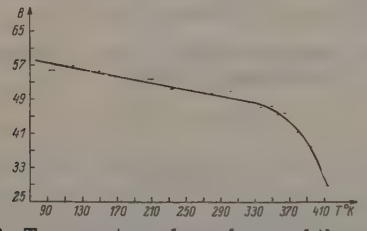

Fig. 2. Temperature dependence of the characteristic field value.

Let us now attempt to compare the experimental relation (2) with field ionization by means of a tunnel release of electrons. According to the theoretical study of Keldysh,[11] the probability of tunnel electron release at a temperature T lying in the range

$$\left(\frac{E}{10^4}\ \text{volts/cm}\right)\ °\text{K} < T < T_D, \qquad (9)$$

where T_D is the Debye temperature, is expressed by the formula

$$W_T^- \sim \exp\left(-\frac{4\sqrt{2m}\Delta^{3/2}}{3heE}+\frac{h\omega_{k_0}}{kT}\right). \qquad (10)$$

where m is the mass of the electron, Δ is the depth of the level, and $h\omega_{k_0}$ is the phonon energy necessary for fulfilling the law of conservation of impulses in the tunnel effect. The probability of tunnel release increases with temperature, because of an increase in the number of phonons with $h\omega_{k_0}$. Moreover, the characteristic field decreases with a temperature increase as a result of a decrease in the depth of the barrier Δ on heating. According to data in the literature[12] the relative change of Δ with temperature is of the order of the coefficient of linear expansion of the lattice.

Thus, the dependence of the mean luminescence brightness on the field and also the temperature variation of this dependence conform with the process of tunnel electron release. The depth of the potential barrier through which tunnel release of electrons may occur (in discharged fields with an intensity of about 10^6 volts/cm must be less than 1 ev if the thickness of this barrier is of the order of the lattice constant.

The levels from which electron release occurs cannot be electron levels of the interior of the ZnS-Cu crystal. This follows from the fact that at low temperatures as was shown previously,[1] release of electrons from local levels in ZnS-Cu occurs mainly by means of impact ionization. Furthermore, these new levels must possess a wider energy spectrum than the bulk levels of the crystal since, otherwise, saturation of the brightness would be observed when the critical field was reached because of complete destruction of levels acting as electron sources.

It is possible that the source of electrons, participating in the process of ionization of luminescence centers in a ZnS-Cu crystal, may be surface levels or levels of a surface phase (for example, copper sulfide deposited on the surface of ZnS-Cu crystals). Washing copper sulfide from the surface of phosphors is known to produce a sharp decrease of electroluminescence.[13] Conversely, formation of a surface phase produces electroluminescence even in nonluminescing phosphors of ZnS-Cu.[14] On the other hand, it was shown in ref. 15 that an accumulation of electrons which participate in the process determines the growth of the mean luminescence brightness after applying the electric field. Also, as previously mentioned, the waveform brightness is determined not by the total number of electrons participating in electroluminescence, but by the migration of these electrons through the crystal during the process.

A zonal scheme for a ZnS-Cu phosphor, with a surface phase of Cu_2S, is presented in Fig. 3. An explanation of it is given in the appendix. The tunnel penetration of electrons from the valence band of Cu_2S into the conduction band of ZnS is indicated by the arrows I. It is apparent from the diagram that for the tunnel effect to occur it is necessary to apply a potential difference of $U \geq 0.3$ volts. This condition is undoubtedly fulfilled in the experiment, because it is necessary to ensure a potential difference of $U > 2.5$ volts for ionization of luminescence centers.

Thus, the main process responsible for the voltage dependence of the mean luminescence brightness is evi

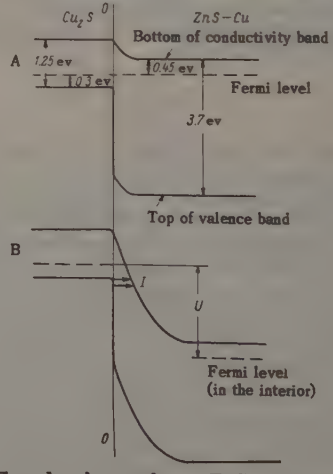

Fig. 3. Zonal scheme for a ZnS-Cu phosphor in contact with a surface phase of Cu_2S. A—in the absence of an external potential difference; B—with a potential difference of U.

dently the penetration of electrons from some surface levels into the conduction band of ZnS through the potential barrier. After applying an alternating electrical field there occurs a gradual accumulation in the interior of the ZnS-Cu crystal of the electrons escaping from these levels, until this process is compensated by a reverse electron flow caused by a charge on ZnS-Cu in relation to Cu_2S. The stationary value of the mean luminescence brightness is then achieved. Furthermore, the electrons penetrating into the ZnS-Cu crystal take part in the process of impact ionization of luminescence centers. The rapid change of brightness observed during the process (wave brightness) is due to the release by the electric field of electrons already accumulated in the crystal, and their migration to a region of the crystal where they can recombine with ionized luminescence centers.

For a complete clarification of the nature of the potential barrier through which electrons leak during the establishment of mean brightness, further experiments are necessary.

Appendix

A POSSIBLE ZONAL SCHEME FOR A ZnS-Cu PHOSPHOR WITH A SURFACE PHASE OF Cu_2S

As noted above, in the preparation of a ZnS-Cu phosphor, a second phase of Cu_2S forms on the surface of the ZnS-Cu crystals.

The width of the forbidden band in Cu_2S may be determined from the absorption edge spectrum, measured in ref. 16. It is approximately 1.25 ev. In ZnS, the width of the forbidden band is approximately 3.7 ev.

The position of the Fermi level relative to the conduction band may be calculated by the formula

$$\Delta_F = kT \ln \frac{N_{\text{eff.}}}{n_0}, \qquad (1')$$

where $N_{eff} = 2.5 \times 10^{19}$ cm^{-3}, and n_0 is the equilibrium concentration of electrons in the conduction band. The value of n_0 is 10^{12} cm^{-3}, according to ref. 1, which was based on data from ref. 17 concerning the conductivity of luminescent monocrystals of ZnS. In this instance, $\Delta_{F\ ZnS-Cu} = 0.45$ ev.

It was shown in ref. 16 that Cu_2S is a semiconductor with P-type conductivity. This means that the Fermi level is located in the lower half of the forbidden band in Cu_2S. We make the least error if we assume that it is situated in the middle of the lower half of the forbidden band (i.e., approximately 0.3 ev above the top of the valence band). At thermodynamic equilibrium, an alignment of Fermi levels occurs along the whole specimen, and this is shown in Fig. 3A.

In precontact regions, as a result of carrier diffusion from one semiconductor to another, a spacial charge forms, creating a field which produces a distortion of zones for these regions. Thus, a contact potential difference arises which, according to ref. 18, is equal to

$$U_k = \frac{kT}{e} \ln \frac{n_n}{n_p}, \qquad (2')$$

where n_n and n_p are equilibrium concentrations of the conductivity electrons in electron and hole-type semiconductors, respectively. Practically the whole contact potential difference is concentrated in the ZnS-Cu crystal, since, according to the data of refs. 16 and 17, the specific resistance of Cu_2S is of the order 10^3 ohm-cm, and of ZnS-Cu is 10^6 ohm-cm.

The difference between the energy corresponding to the bottom of the conductivity band in Cu_2S and that in ZnS, originating at the contact of these two crystals, according to formulas (1′) and (2′) is equal to

$$\Delta = \Delta_{F_{Cu_2S}} - \Delta_{F_{ZnS-Cu}} \approx 0.5 \text{ ev}. \qquad (3')$$

During the "joining" of zones, we have assumed that, at contact, equilibrium is attained by electron diffusion from one crystal to another (thereby "joining" evenly the conductivity bands). During "joining" of valence bands, an additional step occurs as a result of the different crystalline structure of objects in contact (Fig. 3A). If equilibrium is established mainly by diffusion of holes, then the valence bands are evenly "joined" and an additional barrier arises in the conductivity band. An intermediate case can occur, but the precise form of the potential barrier originating in the contact region is not essential for us.

Upon applying an external voltage, practically the whole potential difference is concentrated in the high-resistance part of the specimen—the contact region (Fig. 3B). Then, the bottom of the conductivity band in ZnS may drop below the top of the valence band in Cu_2S and, consequently, result in possible tunnel leakage of electrons from Cu_2S to ZnS, as shown in Fig. 3B, by the arrows I.

REFERENCES

1. A. N. Georgobiani and M. V. Fok, Opt. i Spektr. 9, 775 (1960), Optics and Spectroscopy 9, 407 (1960).
2. G. Destriau and H. F. Ivey, Proc. I.R.E. 43, 1911 (1955).
3. P. Zalm, Philips Research Repts. 11, 353 (1956).
4. W. W. Piper and F. E. Williams, Solid State Phys. 6, 95 (1958).
5. F. Seitz. Phys. Rev., 76, 1376 (1949).
6. V. A. Chuenkov, Soviet Phys.—Solid State 1, 1601 (1960 (1960).
7. F. A. Kröger, Physica 22, 637 (1958).
8. B. I. Davydov and I. M. Shmushkevich, Zhur. Eksptl. i Teoret. Fiz. 10, 1043 (1940).
9. V. A. Chuenkov, Izvest. Akad. Nauk SSSR, Ser. Fiz. 22, 369 (1958).
10. L. V. Keldysh, Zhur. Eksptl. i Teoret. Fiz. 37, 713 (1959), Soviet Phys.-JETP 10, 509 (1960).
11. L. V. Keldysh, Zhur. Eksptl. i Teoret. Fiz. 34, 962 (1958), Soviet Phys.-JETP 7, 665 (1958).
12. H. I. Fan, Repts. Progr. in Phys. 19, 107 (1956).
13. S. Larach and R. E. Shrader, J. Phys. Chem. Solids 3, 159 (1957).
14. I. N. Bowtell and N. S. Bate, Proc. I.R.E. 44, 697 (1956).
15. E. E. Bukke, L. A. Vinokurov, and M. V. Fok, Inzh. Fiz. Zhur. 7, 113 (1958).
16. L. Eisenmann, Ann. Physik 10, 129 (1952).
17. A. Lempicki, D. R. Frankl, and V. A. Brophy, Phys. Rev. 107, 1238 (1957).
18. B. M. Vul, Elektrichestvo 7, 102 (1955).

THE LUMINESCENCE PROPERTIES OF GOLD-ACTIVATED ZINC SELENIDE

L. Ya. Markovskii and R. I. Smirnova (pp. 194-197)

Received 28 April 1960

A description is given of certain luminescence properties of gold-activated zinc selenide under photoexcitation and cathodoexcitation.

Moskvin's book[1] mentions the activation of zinc selenide by gold. It also gives certain brightness characteristics of this phosphor, but no details of its luminescent properties and peculiarities. It should be noted that until recently gold was rarely used as a phosphor activator. Leverenz even asserts in his monograph[2] that gold is a quencher, rather than activator, of zinc sulfide phosphors. Thus Kröger and collaborators[3] used gold as the second activator in their single-component zinc sulfide phosphor, which emits white light. Hoogenstraaten[4] ascribes the 545 mμ maximum in sphalerite and the 528 mμ maximum in wurtzite to gold; these bands are shifted appreciably towards longer wavelengths as compared with the copper emission bands.

In recent years there has been a steadily increasing interest in the use of gold as an activator. A series of papers has appeared[5-7] devoted to gold activation of zinc sulfide and mixed zinc cadmium sulfide phosphors. Henderson and Ranby[7] also briefly considered gold activation of zinc sulfo-selenide phosphors with low selenium contents (up to 30% ZnSe). It has been found that the phosphors thus obtained are very similar in luminescent properties to phosphors of the ZnS-CdS:Au series.

The present paper is devoted to a study of the luminescence properties of gold-activated pure zinc selenide. This activation will be shown to result in a very efficient phosphor with an emission maximum near 700 mμ. The phosphor has relatively low inertia and a highly stabile spectral composition at elevated temperatures.

PROCEDURE USED FOR PREPARATION OF PHOSPHORS

Zinc selenide was obtained by the so-called "wet process" from phosphor-grade zinc sulfide and selenious acid. (H_2SeO_3). The iron content of the raw materials did not exceed 5×10^{-5}%. The zinc selenide obtained after baking at 800°C contained zinc oxide, which was removed by treatment with a $NH_4OH + NH_4Cl$ solution. The iron content of the substance thus obtained amounted to 1×10^{-4}%. In some of the experiments we used a particularly pure zinc selenide obtained by the hydrogen selenide process (Fe, Cu, Co, Ni $< 3 \times 10^{-5}$%), and purified of traces of oxide by reduction in hydrogen at 500°C. Gold chloride was introduced into the mixture for activation.

In all experiments we used NaCl and $MgCl_2$ as fluxes. The baking of the phosphors was carried out in closed quartz crucibles either in air or in an atmosphere of purified nitrogen ($< 0.01\%$ O_2) at 900°C for 30 min. In the latter case, the crucible containing the mixture was placed in a quartz tube filled with nitrogen.

The luminescence characteristics of prepared samples under cathodoexcitation (raster type) were measured in a demountable electron beam tube. A UM-I monochromator with an FEU-22 photomultiplier were used to measure the emission spectra. The characteristics of luminescence under photoexcitation ($\lambda_{max} = 365$ mμ) were obtained using a ZMR-3 monochromator. The FEU-22 photomultiplier was again used as the radiation detector. The duration of phosphorescence was measured oscillographically.

STUDY OF THE LUMINESCENT PROPERTIES OF THE PHOSPHOR UNDER PHOTOEXCITATION

The spectral distribution of light from gold-activated phosphors excited by 365 mμ radiation is shown in Fig. 1 for different gold contents. As a comparison, similar curves are given for nonactivated zinc selenide and a ZnSe:Cu phosphor, both baked under the same conditions (30 min at 900°C). The figure shows that the position of the maxima of the curves for the ZnSe:Au phosphors depends on the concentration of gold and lies between 690 and 720 mμ. The curves show only an inappreciable bulge near 600 mμ.

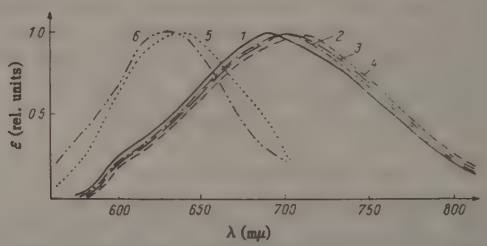

Fig. 1. Spectral distribution curves of light from ZnSe:Au phosphors with different gold contents (curves 1-4), ZnSe:Cu (curve 5), and nonactivated ZnSe (curve 6) under photoexcitation. Gold content (in %): curve 1—5×10^{-3}; curve 2—5×10^{-2}; curve 3—1×10^{-1}; curve 4—5×10^{-1}.

Figure 2 represents the emission spectra of ZnSe:Au phosphors obtained at different temperatures. The figure shows that at low temperatures it is possible to resolve the short wavelength component of the spectral distribution curves whose maximum is near 600 mμ. As the temperature is lowered, this band "flares up" and the emission from the phosphor "yellows." At 100°C the shape of the spectral distribution curves does not change, even though the radiation intensity is lowered due to temperature quenching.

Thus the data obtained allow us to demonstrate that the emission spectrum of photoexcited ZnSe:Au contains both the emission band of nonactivated zinc selenide ($\lambda_{max} = 600$ mμ) and the emission band of gold itself ($\lambda_{max} = 690$-720 mμ). A similar situation is also observed under cathodoexcitation.

STUDY OF THE ZnSe:Au PHOSPHOR UNDER CATHODOEXCITATION

The measurement of the luminescent properties of phosphors with different activator concentrations was

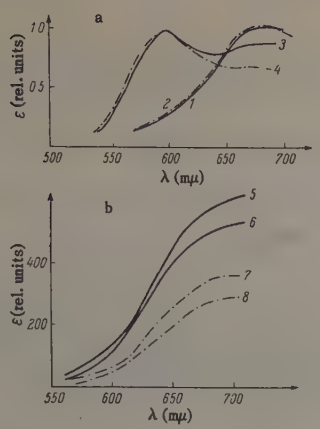

Fig. 2. Spectral distribution curves for light from ZnSe:Au phosphors obtained at different temperatures and gold concentrations using photoexcitation. Gold content (in %) and temperature (in °C): curve 1—5×10^{-1}, +20; curve 2—1×10^{-2}, +20; curve 3—5×10^{-1}, −100, curve 4—1×10^{-2}, −100; curve 5—5×10^{-2}, +20; curve 6—1×10^{-2}, +20; curve 7—5×10^{-2}, +100; curve 8—1×10^{-3}, +100.

carried out at a voltage of 9 kv and a current density of 1 $\mu a/cm^2$. The brightness was measured by comparison with the ZnSe:Cu and $Zn_3(PO_4)_2$:Mn phosphors. The data obtained are shown in the Table and in Fig. 3.

Luminescent Properties of Phosphors as a Function of Gold Concentration

Composition of mixture (%)	Gold concentration (10^{-2} %)	Intensity of emission measured "by reflection" using a selenium photocell (%)		Maximum of spectral distribution curve (mμ)	Duration of afterglow measured to 5% of initial brightness (10^{-5} sec)
		ZnSe:Cu standard	$Zn_3(PO_4)_2$:Mn standard		
ZnSe (100), NaCl (2), $MgCl_2$ (1)	1	85	200	600	2
	5	75	184	600	3
	10	69	169	600 and 680	5
	100	58	143	600 and 680	5
	200	57	139	600 and 680	5
	500	56	140	600 and 680	1

As shown in Fig. 3, two maxima (near 600 and 680 mμ) can already be clearly observed in the spectral distribution curves of the ZnSe:Au phosphors at a gold concentration of 1×10^{-2}%. When the gold concentration is increased, the first maximum becomes weaker and the second one stronger. Concentration quenching of the gold band is observed only when the gold concentration exceeds 5×10^{-2}%. The Table shows that the intensity of the radiation emitted by ZnSe:Au is close to that of ZnSe:Cu. The relatively low inertia of the radiation emitted by ZnSe:Au is a particularly valuable feature of this phosphor.

We should note that the long wavelength band in the emission spectrum of this phosphor is independent of the quality of the zinc selenide used in its preparation. The experimental data indicate that identical spectra are obtained from phosphors prepared from zinc selenide obtained by the interaction of ZnS with H_2SeO_3 and from zinc selenide obtained by the hydrogen selenide process. Special experiments have also shown that the long wavelength band of ZnSe:Au is extinguished after baking in hydrogen and is re-established after a second baking in air.

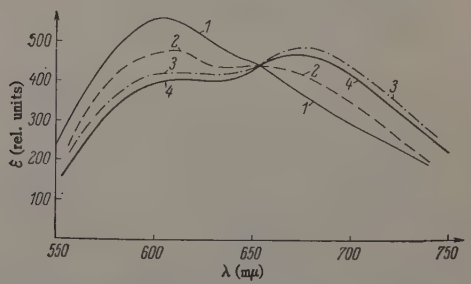

Fig. 3. Spectral distribution curves for the light from ZnSe:Au phosphors under cathodoexcitation. Gold content (in %): curve 1—1×10^{-3}; curve 2—5×10^{-3}; curve 3—5×10^{-2}; curve 4—5×10^{-1}.

In conclusion we wish to thank F. M. Pekerman and O. N. Kazankina for their help in some of the measurements.

REFERENCES

1. A. V. Moskvin, "Katodolyuminestsentsiya" (Cathodoluminescence), Vol. 2. Gosudarst. Tekh. i Teoret. Izd., Moscow, Leningrad, 1949.
2. H. Leverenz, "Luminescence of Solids." Wiley, New York, 1950.
3. F. Kröger, A. Brill, and O. Dickhoff, Philips Research Repts. 7, 241 (1952).
4. W. Hoogenstraaten, Philips Research Repts. 13, 552 (1958).
5. N. Arpiarian, Compt. rend. acad. sci. 240, 1202, 1333 (1955).
6. N. Arpiarian, J. chim. phys. 55, 667 (1958).
7. S. Henderson and P. Ranby, J. Electrochem. Soc. 106, 27 (1959).

REFLECTION OF RADIATION BY AN INFINITE FLAT SURFACE, ILLUMINATED FROM A POINT SOURCE

II. Particular Cases, Important for Practical Applications

B. A. Grigor'ev, A. G. Ershov, and V. A. Uvarov (pp. 198-208)

Received 3 October 1959

Basic particular cases, which are important for practical applications, are examined on the basis of an investigation of the characteristics of the radiation field previously conducted by the authors. The basic equations are derived and are used for the analysis and the numerical calculation of characteristics; values of moduli of reflected illumination are also tabulated for ideally diffused and for specular reflection.

General solutions for the given problem were obtained in a preceding paper by the authors.[1] Retaining all conditions, coordinates, and designations adopted in ref. 1, let us examine the following particular cases, important for practical applications: (1) a reduction of radiation by the medium is not taken into account, the projection of the source on the plane XOY is located on one of the axes or at the origin of the coordinates (simplified problem); (2) the receiver is located near a reflecting surface (low receiver arrangement); (3) the illuminated receiver surface is turned towards the reflecting surface and parallel to it (parallel receiver arrangement); and (4) the illuminated receiver surface is located perpendicular to a direct ray from the source (perpendicular receiver arrangement).

SIMPLIFIED PROBLEM

Let us limit ourselves to a study of the modulus of reflected illumination for an ideally diffused reflection, inasmuch as the calculation, from general solutions, of the remaining values does not present any difficulties. The simplified problem is distinguished by the fact that all Buger criteria are equal to zero, and that the exponential factor, which depends on them, is equal to unity. The expression for M obtained in ref. 1 can therefore be written in the following form:

$$M=\frac{L\left[X_0^2+Y_0^2+(L-1)^2\right]}{\pi}\times\int_B^{+\infty}\int_{-\infty}^{+\infty}\frac{(Y\sin\psi-L\cos\psi)\,dY\,dX}{(X^2+Y^2+L^2)^2\left[(X-X_0)^2+(Y-Y_0)^2+1\right]^{\frac{3}{2}}}. \quad (1)$$

Three cases are possible, depending on the location of the source: $X_0 = 0$, $Y_0 \neq 0$; $X_0 \neq 0$, $Y_0 = 0$; $X_0 = Y_0 = 0$. In all these cases it is possible to make a single analytic integration of Eq. (1) and considerably facilitate the remaining numerical integration. If $X_0 = 0$, $Y_0 \neq 0$ the integration is made with respect to X and

$$M=\frac{L}{2\pi}\left[1+\frac{(L-1)^2}{Y_0^2}\right]\left[\int_B^{Y_r}(Y\sin\psi-L\cos\psi)\,F_1(Y)\,dY+\int_{Y_r}^{+\infty}(Y\sin\psi-L\cos\psi)\,F_2(Y)\,dY\right], \quad (2)$$

where

$$Y_r=\frac{1}{2Y_0}(1+Y_0^2-L^2), \quad (3)$$

$$F_1(Y)=\frac{1}{(Y_r-Y)^2}\left[\frac{1}{(Y_r-Y_0)^2+1}+\frac{1}{2(Y^2+L^2)}\right]-\frac{1.5\,(Y^2+L^2)-Y_0(Y_r-Y)}{2\sqrt{2}\sqrt{Y_0}\,(Y^2+L^2)^{\frac{3}{2}}(Y_r-Y)^{\frac{5}{2}}}\times\left\{\arcsin\left[1-\frac{2(Y^2+L^2)}{(Y-Y_0)^2+1}\right]+\frac{\pi}{2}\right\}, \quad (4)$$

$$F_2(Y)=\frac{1}{(Y-Y_r)^2}\left[\frac{1}{(Y_r-Y_0)^2+1}+\frac{1}{2(Y^2+L^2)}\right]-\frac{1.5\,(Y^2+L^2)+Y_0(Y-Y_r)}{2\sqrt{2}\sqrt{Y_0}\,(Y^2+L^2)^{\frac{3}{2}}(Y-Y_r)^{\frac{5}{2}}}\ln\left|\frac{2(Y^2+L^2)}{(Y-Y_0)^2+1}\times\left[\sqrt{1-\frac{(Y-Y_0)^2+1}{Y^2+L^2}}+1\right]-1\right|. \quad (5)$$

$$F_1(Y_r)=F_2(Y_r)=F(Y_r)=\frac{32\,Y_0^2}{15\,(Y_r^2+L^2)^3}. \quad (6)$$

If $B \geq Y_r$ the first integral in (2) is discarded and the second the lower limit is changed to B.

If $X_0 \neq 0$, $Y_0 = 0$ the integration is made with respect to Y and

$$M=\frac{L\left[X_0^2+(L-1)^2\right]}{\pi}\left[\int_{-\infty}^{X_r}F_1(X)\,dX+\int_{X_r}^{+\infty}F_2(X)\,dX\right]. \quad (7)$$

The expressions for $F_1(X)$ and $F_2(X)$ are not listed because of their bulkiness and for lack of space (they are different for $B \geq 0$ and $B < 0$), but

$$X_r=\frac{1}{2X_0}(1+X_0^2-L^2). \quad (8)$$

If $X_0 = Y_0 = 0$* the integration is made with respect to X and

$$M_0=\frac{2L}{\pi(L+1)^2}\int_B^{+\infty}(Y\sin\psi-L\cos\psi)\,F(Y)\,dY, \quad (9)$$

and for $L = 1$, $M_0 = 0$.

For $L < 1$

$$F(Y)=\left[\frac{1}{Y^2+1}+\frac{1}{2(Y^2+L^2)}\right]-\frac{3(Y^2+L^2)-(1-L^2)}{4\sqrt{1-L^2}\,(Y^2+L^2)^{\frac{3}{2}}}\left\{\arcsin\left[1-\frac{2(Y^2+L^2)}{Y^2+1}\right]+\frac{\pi}{2}\right\}; \quad (10)$$

*$0 < \psi < \pi$; the case $\psi = \pi$ is examined later.

for $L > 1$

$$F(Y)=\left[\frac{1}{Y^2+1}+\frac{1}{2(Y^2+L^2)}\right] \tag{11}$$
$$-\frac{3(Y^2+L^2)+(L^2-1)}{4\sqrt{L^2-1}\,(Y^2+L^2)^{\frac{3}{2}}}\ln\left|\frac{2(Y^2+L^2)}{Y^2+1}\left(\sqrt{1-\frac{Y^2+1}{Y^2+L^2}}+1\right)-1\right|.$$

LOW RECEIVER ARRANGEMENT

If $L \ll 1$ and $R_0 \gg 1$, the radiance of the reflecting surface and the angles ψ_1 in the region S can be considered constant and it can be assumed that $R_1 = R_0$, $\cos\psi = 1/R_0$.

Under these conditions, taking into account that the values of R_2 and L are small, the exponential factor can be set equal to one and it can be approximately obtained that:*

*The integration is made over one half of the plane XOY, because of the symmetry of reflection, and the result is doubled.

$$M\approx\frac{2L}{\pi\sqrt{X_0^2+Y_0^2+(L-1)^2}}\int_B^{+\infty}\int_0^{+\infty}\frac{Y\sin\psi-L\cos\psi}{(X^2+Y^2+L^2)^2}\,dY\,dX$$
$$=\frac{\sin^2\frac{\psi}{2}}{\sqrt{X_0^2+Y_0^2+(L-1)^2}}. \tag{12}$$

PARALLEL RECEIVER ARRANGEMENT

The reflected radiation is gathered on the receiver surface from the entire reflecting surface, but the direct radiation is not always falling on the receiver.

The modulus of reflected illumination $M_{\parallel}$ can be determined with the help of equations obtained in ref. 1, assuming $\psi = \pi$, $\cos\psi_3 = L/R_2$, and $B = -\infty$. With these assumptions,

$$M_{\parallel}=\frac{R_0^2L^2}{\pi}\int_S\frac{\exp\{Bu_0R_0-Bu_2R_2-R_1[Bu_0(1-L)+Bu_2L]\}}{R_1^3R_2^4}\,dS. \tag{13}$$

Changing to Cartesian coordinates and placing the source on the OY axis ($X_0 = 0$, $Y_0 \geq 0$) we obtain:

$$M_{\parallel}=\frac{2L^2\left[Y_0^2+(L-1)^2\right]}{\pi}$$
$$\times\int_{-\infty}^{+\infty}\int_0^{+\infty}\frac{dY\,dX}{(X^2+Y^2+L^2)^2\left[X^2+(Y-Y_0)^2+1\right]^{\frac{3}{2}}} \tag{14}$$
$$\times\exp\left\{Bu_0\sqrt{Y_0^2+(L-1)^2}-Bu_2\sqrt{X^2+Y^2+L^2}\right.$$
$$\left.-\sqrt{X^2+(Y-Y_0)^2+1}\,[Bu_0(1-L)+Bu_2L]\right\}.$$

The angle of incidence of direct radiation is obtained from the equation

$$\cos\psi_0=\frac{(L-1)}{\sqrt{Y_0^2+(L-1)^2}}, \tag{15}$$

from which it follows that direct radiation falls on the receiver surface if $L \geq 1$.

In the case of specular reflection

$$M_{\parallel}^*=\frac{(L+1)\left[Y_0^2+(L-1)^2\right]}{\left[Y_0^2+(L+1)^2\right]^{\frac{3}{2}}}\exp\left\{Bu_0\sqrt{Y_0^2+(L-1)^2}\right.$$
$$\left.-\frac{\sqrt{Y_0^2+(L+1)^2}}{(L+1)}\left[2LBu_2+Bu_0(1-L)\right]\right\}. \tag{16}$$

If the exponential factor in (14) is equal to unity, it is possible to make a single analytic integration with respect to X [according to (2)-(6)], assuming hereby Y $\sin\psi - L\cos\psi = L$.

When the source and the receiver are located on the OZ axis ($X_0 = Y_0 = 0$) it is possible to change to cylindrical coordinates with origin at point 0 and to introduce polar coordinates (R, θ) on the reflecting surface. The area of the surface element is equal in this case to $dS = Rd\theta dR$. It is therefore possible to replace Eqs. (13) and (14) by:

$$M_{\parallel 0}=\frac{L^2(L-1)^2}{\pi}\int_0^{\infty}\int_0^{2\pi}\frac{RdRd\theta}{(R^2+L^2)^2(R^2+1)^{\frac{3}{2}}}$$
$$=2L^2(L-1)^2\int_0^{\infty}\frac{RdR}{(R^2+L^2)^2(R^2+1)^{\frac{3}{2}}}. \tag{17}$$

For $L < 1$

$$M_{\parallel 0}=\frac{2L^2}{(L+1)^2}$$
$$\left\{1+\frac{1}{2L^2}-\frac{3}{4\sqrt{1-L^2}}\ln\left|\frac{2}{L^2}\left[\sqrt{1-L^2}+1\right]-1\right|\right\}; \tag{18}$$

for $L > 1$

$$M_{\parallel 0}=\frac{2L^2}{(L+1)^2}$$
$$\left\{1+\frac{1}{2L^2}-\frac{3}{4\sqrt{L^2-1}}\left[\arcsin\left(1-\frac{2}{L^2}\right)+\frac{\pi}{2}\right]\right\}; \tag{19}*$$

*The last part of the right side of Eq. (19) can be transformed thus:

$$-\frac{3}{4\sqrt{L^2-1}}\left[\arcsin\left(1-\frac{2}{L^2}\right)+\frac{\pi}{2}\right]=\frac{3}{2\sqrt{L^2-1}}\left[\operatorname{arctg}\left(\frac{1}{\sqrt{L^2-1}}\right)-\frac{\pi}{2}\right].$$

and finally for $L = 1$, $M_{\parallel 0} = 0$.

The values of $M_{\parallel 0}$ are listed in Table 1 and in Fig. 1. It is not possible to use the value of $M_{\parallel 0}$ at $L = 0$ because of the shadowing of the reflecting surface by the receiver, and approximate values of $M_{\parallel 0}$ are therefore given in the table for a value of L close to zero ($\ll 1$).

Table 1

L	$M_{\parallel 0}$	L	$M_{\parallel 0}$	L	$M_{\parallel 0}$
$\ll 1$	≈ 1 (< 1)	1.5	0.0677	25	1.6806
0.1	0.7684	2	0.1937	30	1.7300
0.2	0.5551	3	0.4531	35	1.7662
0.3	0.3844	4	0.6806	40	1.7938
0.4	0.2548	5	0.8343	50	1.8333
0.5	0.1598	6	0.9672	60	1.8601
0.6	0.0926	8	1.1609	70	1.8794
0.7	0.0473	10	1.2947	80	1.8940
0.8	0.0193	12	1.3921	90	1.9055
0.9	0.0046	15	1.4968	100	1.9148
1	0	20	1.6091	∞	2

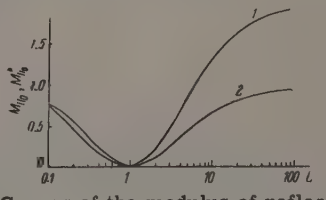

Fig. 1. Curves of the modulus of reflected radiation $M_{\parallel 0}$ as a function of the height of the receiver when the source is located on axis OZ in a parallel arrangement with respect to the receiver. Curve 1—ideally diffused reflection, curve 2—specular reflection.

The illumination moduli have a maximum value for $X_0 = Y_0 = 0$ and $L = \infty$, that is, $M_{max} = 2$ and $N_{max} = 1 + 2\rho$.

If $X_0 = Y_0 = 0$ and the exponential factor is equal to unity, equation (16) can be written

$$M^*_{\parallel 0} = \frac{(L-1)^2}{(L+1)^2}. \qquad (20)$$

Values of $M^*_{\parallel 0}$ are shown in Table 2 and in Fig. 1; because of the shadowing of the direct beam by the receiver, the values of $M^*_{\parallel 0}$ for $L < 1$ must be considered as approximations for small values of the X_0 and Y_0 coordinates, only one of which can be equal to zero.

Table 2

L	$M^*_{\parallel 0}$ (for small X_0, Y_0)	L	$M^*_{\parallel 0}$	L	$M^*_{\parallel 0}$
		1	0	20	0.8186
⩽1	≈1 (<1)	1.5	0.0400	25	0.8521
0.1	0.6694	2	0.1111	30	0.8751
0.2	0.4444	3	0.2500	35	0.8920
0.3	0.2899	4	0.3600	40	0.9048
0.4	0.1837	5	0.4444	50	0.9231
0.5	0.1111	6	0.5102	60	0.9355
0.6	0.0625	8	0.6049	70	0.9475
0.7	0.0311	10	0.6694	80	0.9512
0.8	0.0124	12	0.7160	90	0.9565
0.9	0.0028	15	0.7656	100	0.9608
				∞	1

In the case of specular reflection maximum values of the moduli ($M^*_{max} = 1$ and $N^*_{max} = 1 + \rho$) are also obtained for $X_0 = Y_0 = 0$ and $L = \infty$.

Values of $M_{\parallel}$ and $M^*_{\parallel}$ are shown in Tables 3 and 4 and in Figs. 2 and 3 (with the exponential factor being equal to one) for a large range of Y_0 and L values.* It is easy to see that for $L \leqslant 5$ the functions $M_{\parallel} = f(Y_0)$ have maxima in the region of small values of $Y_0 (\leqslant 3)$, the maxima being smoothed out on both sides of $L = 1$, and that these functions decrease monotonically for $L \ll 1$ and $L > 5$. It should be noted that for $L \leqslant 1$ and $Y_0 \geqslant 12$, $M_{\parallel} \leqslant 0.1$. Changes of $M^*_{\parallel}$ as a function of Y_0 and L are generally similar, the maxima of the function $M^*_{\parallel} = f(Y_0)$ occurring for $L \leqslant 8$ and lying in the region $Y_0 < 6$.

*Calculations of $M_{\parallel}$ values were made by Mamontov and Shishova, under the guidance of Shleining, using the electronic computer "Strela" ("Arrow"); the values of $M^*_{\parallel}$ were calculated by Galushkin.

Table 3

L \ Y_0	0.5	1	2	3	4	5	6	8	10	12	15	20	25
⩽1	0.894	0.707	0.446	0.316	0.242	0.196	0.163	0.124	0.100	0.083	0.066	0.050	0.040
0.5	0.260	0.405	0.430	0.341	0.266	0.214	0.178	0.133	0.105	0.087	0.069	0.051	0.041
1	0.089	0.262	0.434	0.400	0.329	0.266	0.220	0.159	0.123	0.100	0.077	0.056	0.045
2	0.230	0.316	0.475	0.508	0.462	0.396	0.334	0.240	0.182	0.142	0.106	0.072	0.054
3	0.467	0.503	0.585	0.615	0.585	0.526	0.459	0.344	0.260	0.204	0.148	0.098	0.071
4	0.673	0.686	0.718	0.729	0.700	0.646	0.580	0.452	0.351	0.277	0.202	0.131	0.093
5	0.835	0.841	0.846	0.838	0.807	0.755	0.692	0.560	0.446	0.357	0.264	0.170	0.120
6	0.966	0.965	0.962	0.941	0.906	0.855	0.794	0.662	0.540	0.440	0.328	0.215	0.151
8	1.160	1.155	1.140	1.112	1.078	1.026	0.971	0.845	0.717	0.589	0.468	0.315	0.222
10	1.293	1.289	1.271	1.246	1.210	1.166	1.114	0.994	0.873	0.757	0.607	0.424	0.306
12	1.389	1.385	1.372	1.346	1.315	1.276	1.228	1.122	1.008	0.892	0.738	0.535	0.395
15	1.497	1.496	1.485	1.463	1.435	1.402	1.364	1.270	1.170	1.062	0.910	0.695	0.531
20	1.609	1.608	1.602	1.590	1.565	1.540	1.510	1.442	1.363	1.276	1.140	0.930	0.750
25	1.680	1.676	1.668	1.656	1.640	1.622	1.602	1.550	1.490	1.420	1.303	1.112	0.942

Table 4

L \ Y_0	0.5	1	2	3	4	5	6	8	10	12	15	20	25
⩽1	0.894	0.707	0.446	0.316	0.242	0.196	0.163	0.124	0.100	0.083	0.066	0.050	0.040
0.5	0.189	0.320	0.408	0.368	0.312	0.266	0.230	0.179	0.146	0.122	0.099	0.074	0.060
1	0.057	0.179	0.354	0.384	0.358	0.320	0.284	0.228	0.188	0.160	0.130	0.099	0.079
2	0.132	0.190	0.320	0.393	0.408	0.393	0.368	0.313	0.266	0.230	0.189	0.145	0.118
3	0.259	0.285	0.358	0.416	0.442	0.442	0.427	0.380	0.333	0.292	0.245	0.190	0.155
4	0.365	0.379	0.416	0.454	0.480	0.480	0.472	0.434	0.390	0.348	0.290	0.230	0.191
5	0.447	0.453	0.475	0.497	0.512	0.516	0.511	0.480	0.439	0.397	0.342	0.274	0.226
6	0.511	0.515	0.526	0.540	0.548	0.550	0.545	0.519	0.481	0.441	0.386	0.313	0.260
8	0.605	0.605	0.609	0.611	0.613	0.610	0.604	0.583	0.551	0.515	0.461	0.383	0.323
10	0.669	0.669	0.669	0.669	0.667	0.662	0.654	0.634	0.606	0.574	0.523	0.445	0.381
12	0.716	0.716	0.715	0.712	0.708	0.702	0.697	0.677	0.651	0.622	0.575	0.499	0.433
15	0.765	0.765	0.764	0.760	0.756	0.751	0.744	0.727	0.705	0.680	0.639	0.568	0.502
20	0.819	0.818	0.816	0.814	0.810	0.805	0.800	0.787	0.769	0.749	0.716	0.655	0.595
25	0.852	0.852	0.850	0.849	0.845	0.842	0.838	0.827	0.813	0.797	0.770	0.720	0.665
30	0.875	0.875	0.873	0.872	0.870	0.867	0.863	0.855	0.844	0.831	0.810	0.766	0.719
35	0.892	0.892	0.891	0.890	0.888	0.886	0.883	0.876	0.867	0.856	0.838	0.802	0.761
40	0.905	0.905	0.904	0.903	0.901	0.900	0.897	0.892	0.884	0.876	0.860	0.830	0.795

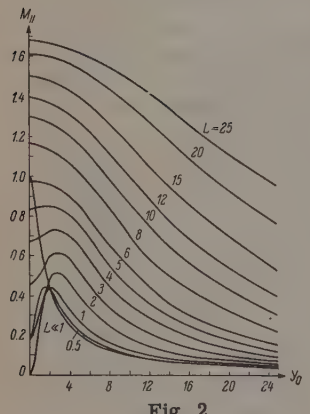

Fig. 2

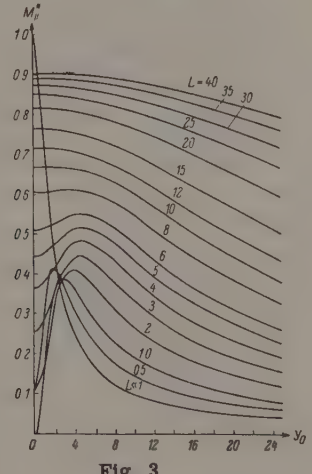

Fig. 3

Fig. 2. Modulus of reflected illumination $M_{\parallel}$ for a parallel arrangement of the receiver as a function of the source coordinate Y_0 and the receiver height L in the case of ideally diffused reflection.

Fig. 3. Modulus of reflected illumination $M^*_{\parallel}$ for a parallel arrangement of the receiver as a function of the source coordinate Y_0 and the receiver height L in the case of specular reflection.

It is also necessary to point out that for equal $L \leqslant 1$ the functions $M_{\parallel} = f(Y_0)$ and $M^*_{\parallel} = f(Y_0)$ are close to each other in value and that for $L \ll 1$ they are identical. Figure 4 shows the influence of the magnitude of the Buger criterion in a homogeneous medium ($Bu = Bu_0 = Bu_1 = Bu_2$) for $Y_0 = 5$ and $L = 10$ to illustrate the influence of

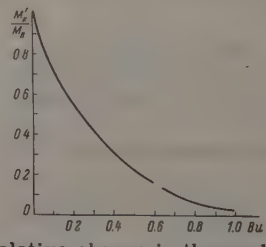

Fig. 4. Relative change in the modulus of reflected illumination $M'_{\parallel}/M_{\parallel}$ as a function of the Buger criterion Bu for $Y_0 = 5$ and $L = 10$.

the decrease in radiation on the modulus of reflected illumination. The curve in Fig. 4 gives the relative change $M_{\perp}/M_{\parallel}$, where $M_{\parallel}$ is the modulus of reflected illumination for Bu = 0 (the exponential factor is equal to one). It follows from the figure that a decrease of $M_{\parallel}$ by 10% is already reached at Bu ≈ 0.027, by 30% at Bu ≈ 0.1 and by 50% at Bu ≈ 0.22. If Bu = 1, $M_{\perp}$ is only 4% of $M_{\parallel}$.

PERPENDICULAR RECEIVER ARRANGEMENT

This arrangement is characterized by the condition $\psi_0 = 0$ and, as a consequence, by a variable value of the angle ψ, which depends on Y_0 and L. The direct radiation always falls on the receiver.

It follows from geometrical relationships that

$$\cos\psi_3 = \frac{R_0^2 + R_2^2 - R_1^2}{2R_0R_2}, \tag{21}$$

and hence

$$M_{\perp} = \frac{R_0 L}{2\pi} \int_S \frac{R_0^2 + R_2^2 - R_1^2}{R_1^3 R_2^4} \times \exp\{Bu_0 R_0 - Bu_2 R_2 - R_1[Bu_0(1-L) + Bu_2 L]\}\, dS. \tag{22}$$

It is easy to satisfy oneself that $\sin\psi = Y_0/R_0$, $\cos\psi = (1 - L)/R_0$ and that, therefore,

$$B = \frac{L(1-L)}{Y_0}, \tag{23}$$

$$Y\sin\psi - L\cos\psi = \frac{Y_0(Y-B)}{\sqrt{Y_0^2 + (L-1)^2}}. \tag{24}$$

The source is located on the OY axis ($X_0 = 0$, $Y_0 \geqslant 0$); the modulus of reflected illumination can be expressed in Cartesian coordinates and, taking (23) and (24) into account, as

$$M_{\perp} = \frac{2Y_0 L}{\pi}\sqrt{Y_0^2 + (L-1)^2} \times \int_B^{+\infty}\int_0^{+\infty} \frac{(Y-B)}{(X^2 + Y^2 + L^2)^2 [X^2 + (Y - Y_0)^2 + 1]^{\frac{3}{2}}} \times \exp\left\{Bu_0\sqrt{Y_0^2 + (L-1)^2} - Bu_2\sqrt{X^2 + Y^2 + L^2} - \sqrt{X^2 + (Y-Y_0)^2 + 1}\,[Bu_0(1-L) + Bu_2 L]\right\} dY\, dX. \tag{25}$$

Table 5

L \ Y_0	0.5	1	2	3	4	5	6	8	10	12	15	20	25
⩽1	0.047	0.103	0.124	0.108	0.092	0.079	0.068	0.054	0.045	0.038	0.031	0.024	0.019
0.25	0.028	0.108	0.230	0.252	0.230	0.200	0.172	0.125	0.100	0.080	0.066	0.053	0.048
0.5	0.015	0.113	0.320	0.360	0.330	0.290	0.255	0.198	0.153	0.122	0.100	0.080	0.070
0.75	0.019	0.127	0.348	0.432	0.415	0.370	0.330	0.256	0.205	0.167	0.133	0.105	0.092
1	0.031	0.150	0.400	0.492	0.485	0.440	0.395	0.313	0.250	0.205	0.170	0.130	0.112
1.5	0.125	0.225	0.460	0.576	0.582	0.545	0.500	0.410	0.340	0.280	0.230	0.180	0.159
2	0.230	0.310	0.530	0.638	0.652	0.630	0.595	0.492	0.412	0.346	0.285	0.222	0.190
3	0.466	0.505	0.650	0.740	0.770	0.770	0.744	0.645	0.545	0.465	0.390	0.303	0.250
4	0.675	0.694	0.770	0.840	0.870	0.867	0.846	0.760	0.650	0.570	0.478	0.372	0.316
5	0.840	0.850	0.880	0.922	0.951	0.953	0.938	0.868	0.755	0.662	0.570	0.451	0.376
6	0.970	0.974	0.988	1.010	1.030	1.030	1.020	0.953	0.850	0.752	0.648	0.517	0.438
8	1.161	1.162	1.167	1.170	1.166	1.157	1.140	1.085	0.997	0.910	0.797	0.650	0.550
10	1.295	1.295	1.292	1.288	1.280	1.267	1.248	1.192	1.122	1.040	0.930	0.773	0.650
12	1.390	1.390	1.388	1.380	1.371	1.356	1.336	1.283	1.227	1.163	1.060	0.892	0.750
15	1.497	1.497	1.496	1.490	1.480	1.467	1.450	1.407	1.357	1.300	1.210	1.046	0.885
20	1.609	1.609	1.608	1.602	1.595	1.585	1.572	1.545	1.510	1.470	1.400	1.250	1.082
25	1.680	1.680	1.676	1.670	1.663	1.656	1.647	1.620	1.590	1.554	1.492	1.368	1.223
30	1.730	1.730	1.730	1.726	1.720	1.710	1.700	1.677	1.648	1.612	1.554	1.450	1.335
35	1.766	1.766	1.762	1.760	1.755	1.749	1.740	1.718	1.691	1.660	1.610	1.518	1.420
40	1.780	1.780	1.780	1.778	1.772	1.766	1.760	1.740	1.715	1.688	1.646	1.570	1.493

Table 6

L \ Y_0	0.5	1	2	3	4	5	6	8	10	12	15	20	25
⩽1	0	0	0.600	0.800	0.882	0.923	0.946	0.969	0.980	0.986	0.991	0.995	0.996
0.25	0	0.019	0.499	0.726	0.833	0.889	0.921	0.955	0.970	0.980	0.987	0.993	0.995
0.5	0	0.048	0.429	0.665	0.787	0.857	0.897	0.940	0.964	0.973	0.982	0.990	0.994
0.75	0	0.071	0.383	0.616	0.750	0.828	0.876	0.926	0.951	0.966	0.978	0.988	0.992
1	0.014	0.089	0.354	0.576	0.716	0.800	0.854	0.913	0.942	0.959	0.974	0.985	0.990
1.5	0.064	0.129	0.330	0.523	0.662	0.755	0.817	0.888	0.926	0.947	0.965	0.980	0.987
2	0.129	0.179	0.334	0.497	0.626	0.720	0.786	0.866	0.910	0.935	0.957	0.976	0.984
3	0.259	0.287	0.379	0.490	0.593	0.677	0.742	0.830	0.882	0.910	0.945	0.968	0.978
4	0.366	0.384	0.439	0.514	0.592	0.660	0.718	0.804	0.859	0.895	0.929	0.957	0.972
5	0.449	0.458	0.496	0.546	0.604	0.658	0.706	0.787	0.843	0.881	0.916	0.952	0.967
6	0.513	0.520	0.545	0.582	0.623	0.667	0.708	0.777	0.830	0.868	0.907	0.945	0.962
8	0.605	0.609	0.622	0.642	0.667	0.693	0.721	0.775	0.819	0.852	0.891	0.930	0.952
10	0.670	0.672	0.680	0.692	0.708	0.723	0.743	0.780	0.814	0.845	0.881	0.920	0.945
12	0.717	0.718	0.723	0.730	0.740	0.751	0.764	0.792	0.819	0.844	0.875	0.914	0.938
15	0.766	0.767	0.770	0.773	0.779	0.787	0.794	0.811	0.830	0.848	0.874	0.907	0.931
20	0.820	0.820	0.821	0.822	0.825	0.828	0.832	0.842	0.852	0.862	0.879	0.904	0.924
25	0.852	0.852	0.853	0.855	0.856	0.857	0.860	0.865	0.871	0.877	0.888	0.909	0.923
30	0.875	0.875	0.876	0.876	0.877	0.879	0.880	0.883	0.887	0.892	0.899	0.911	0.924
35	0.892	0.892	0.892	0.893	0.893	0.894	0.895	0.897	0.900	0.903	0.908	0.917	0.927
40	0.905	0.905	0.905	0.905	0.906	0.906	0.907	0.908	0.910	0.912	0.916	0.922	0.932

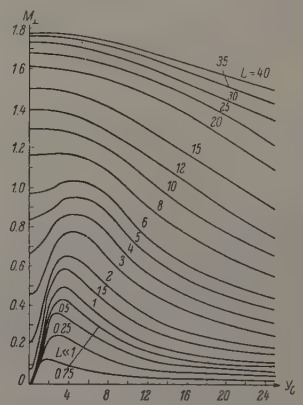

Fig. 5. Modulus of reflected illumination $M_{\perp}$ for a perpendicular receiver arrangement, as a function of the source coordinate Y_0 and the receiver height L for ideally diffused reflection.

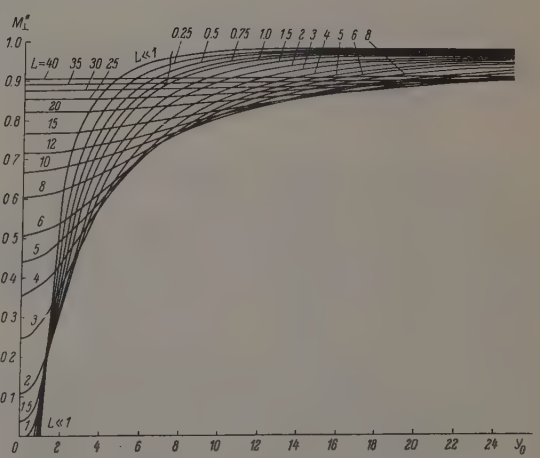

Fig. 6. Modulus of reflected illumination $M_{\perp}^{*}$ for a perpendicular receiver arrangement, as a function of the source coordinate Y_0 and the receiver height L for specular reflection.

In the case of specular reflection

$$\cos\psi_3 = \frac{Y_0^2 + (L^2 - 1)}{\sqrt{Y_0^2 + (L-1)^2}\sqrt{Y_0^2 + (L+1)^2}}. \quad (26)$$

It is possible for the specularly reflected radiation to fall on the receiver surface being illuminated (that is, $0 \leq \psi_3 \leq \pi/2$) if, starting out with the condition $\cot\psi \leq Y_0/(L+1)$, adduced in ref. 1, the condition $Y_0^2 \geq (1 - L^2)$ is fulfilled.

The modulus of the reflected illumination for specularly reflected radiation is

$$M_\perp^* = \frac{[Y_0^2 + (L^2-1)]\sqrt{Y_0^2 + (L-1)^2}}{[Y_0^2 + (L+1)^2]^{\frac{3}{2}}} \exp\left\{ Bu_0 \sqrt{Y_0^2 + (L-1)^2} - \frac{\sqrt{Y_0^2 + (L+1)^2}}{(L+1)} [2LBu_2 + Bu_0(1-L)] \right\}. \quad (27)$$

When the exponential factor in Eq. (25) is equal to one, it is possible, after a single analytical integration with respect to X, to obtain, by means of a transformation of (2),

$$M_\perp = \frac{L}{\pi}\sqrt{\frac{(Y_r - B)}{2Y_0}} \times \left[\int_B^{Y_r} (Y - B) F_1(Y)\, dY + \int_{Y_r}^{+\infty} (Y - B) F_2(Y)\, dY \right] \quad (28)$$

and to use the equations (3) to (6).

If $Y_0 = 0$ and $L \geq 1$, it is obvious that $M_{\perp 0} = M_{\parallel 0}$ and $M^*_{\perp 0} = M^*_{\parallel 0}$, inasmuch as $\psi = \pi$. When $Y_0 = 0$ and $L < 1$, then $M_{\perp 0} = 0$, $\psi = 0$, and the reflected radiation does not fall on the receiver surface being illuminated.

Values of $M_\perp$ and $M_\perp^*$ are listed in the Tables and in Figs. 5 and 6 (for an exponential factor equal to one).* It is easy to see that the general course of the changes of $M_\perp$ as a function of Y_0 and L is the same as the course of the changes of $M_\parallel$ and $M_\parallel^*$. The maxima of the functions $M_\perp = f(Y_0)$ occur for $L \leq 8$ and lie in the region $Y_0 \leq 5$.

*The calculations were made by the persons listed above.

Table 7

Y_0	1	2	3	4	5	6	7
$M_\perp^*$	0	0.330	0.490	0.592	0.658	0.708	0.74
Y_0	8	9	10	12	15	20	25
$M_\perp^*$	0.775	0.798	0.814	0.884	0.874	0.909	0.92

It is important to note that for approximate calculations (with an error of up to 10%) the following relationship can be used for equal Y_0 and for $L > 3$:

$$M_\perp \approx 1.89\, M_\parallel^*. \quad (29)$$

The general course of the changes of $M_\perp^*$ is very much different from the course of the changes of moduli examined above. The functions $M_\perp^* = f(Y_0)$ increase monotonically and approach unity as $Y_0 \to \infty$. A region is thus formed which can be limited at the bottom by the envelope $M_\perp^* = f_1(Y_0)$ and inside of which lie all the functions $M_\perp^* = f(Y_0)$. Coordinates of points on this envelope are listed in Table 7.

It should be noted that for $Y_0 \geq 3.5$, $M_\perp^* \geq 0.5$.

REFERENCE

1. B. A. Grigor'ev, A. G. Ershov, and V. A. Uvarov, Opt. i Spektr. 10, 96 (1961), Optics and Spectroscopy 10, 46, (1961).

POLARIZATION OF PHOSPHORESCENCE IN ORGANOPHOSPHORS

V. A. Pilipovich (pp. 209-213)

Received 29 April 1960

The anisotropy of the afterglow and total luminescence of organophosphors is studied. A variation in the degree of polarization of β-phosphorescence in the emission spectrum was found for all the compounds investigated. The results are discussed from the viewpoint of the hypothesis of the complex structure of a metastable state.

Carelli and Pringsheim[1] showed that the degree of polarization of the α-phosphorescence and the fluorescence of eosin in gelatin films are the same. A similar result was obtained by Vavilov and Levshin[2] for the phosphorescence of rhoduline in sugar. At low temperatures, according to the data of these authors, β-phosphorescence is completely depolarized.

Together with a study of the polarization of the entire luminescence spectrum (either as phosphorescence or total luminescence) Vavilov and Pringsheim[4] studied the degree of polarization of separate spectral regions of both the phosphorescence and the total luminescence. It was found that the degree of polarization of phosphorescence and total luminescence decreases upon passing from the short wavelength to the long wavelength part of the spectrum. The authors explain the change of the degree of fluorescence polarization in the emission spectrum of esculin as the superposition of phosphorescence from the long wavelength phosphorescence band (β-phosphorescence) which is either completely unpolarized or has a negative polarization. The presence of negative polarization in β-phosphorescence was noted by Pringsheim and Vogels[5] for solid solutions of certain dyes at liquid air temperature and by Jablonski[6,7] for adsorbed molecules of dyes. The polarization of β-phosphorescence was studied further in the works of Frölich and Gombay,[8] Sveshnikov and Ermolaev;[9] and in ref. 9 a concentration depolarization of the long wavelength phosphorescence is indicated. The dependence of the degree of polarization on the wavelength of the exciting light obtained in ref. 9 is of particular interest; and on the basis of this, inferences are made about the similarity of the phosphorescent level with the second singlet level.

An investigation of the polarization of α-phosphorescence of dyes in solid solutions was performed by Feofilov.[10-12] It is shown by him that the polarization spec-

tra and the curves for concentration depolarization are practically identical for α-phosphorescence and fluorescence.

Recently, Laffitte[13] investigated the polarization of the phosphorescence of dyes in plexiglass. According to her data, the α-phosphorescence of dyes is always less polarized than the fluorescence, and the β-phosphorescence is always completely depolarized.

For an explanation of the data on the kinetics of the decay of the afterglow of organophosphors in refs. 14-16, the supposition was made that the phosphorescent level is not simple. In searching for additional evidence of this supposition we turned to an investigation of the degree of polarization of β-phosphorescence in different parts of the emission spectrum. Naturally, such polarization measurements might prove to be very useful for explanation of the structure of the metastable state. The experiments were further justified by the fact that until now a universal viewpoint concerning the properties of the polarization of long wavelength phosphorescence is missing from the literature.

Sugar gels activated by esculin, carbazole, auramine, trypaflavine, and acridine yellow, and also boric gels activated by fluorescein and gelatin, and congealed alcohol activated by trypaflavine were the objects of our investigation. The concentrations of the activator for the various compounds were taken from 1×10^{-4} to 1×10^{-5} gm/gm. The apparatus in which the measurements were made was described earlier.[17]

The experiments of Vavilov and Pringsheim[4] were repeated for esculin in a sugar gel. The polarization of the phosphorescence of esculin at room temperature in the long wavelength part of the spectrum is positive and varies in the emission spectrum from 10% to zero in agreement with their data.

Measurements of the polarization of the phosphorescence at liquid air temperature showed that it is negative in nearly the entire spectrum, and the absolute values of the degree of polarization increase in the direction of high frequencies. It is clear from Fig. 1 that the distribution of the phosphorescence spectrum of carbazole in sugar gels does not change its position upon lowering the temperature from +20 to −180°C. Consequently, the afterglow of this phosphor is connected only with the β-process. As is evident from the figure, the degree of polarization of the phosphorescence of carbazole changes in the emission spectrum and increases in absolute value in the direction of high frequencies.

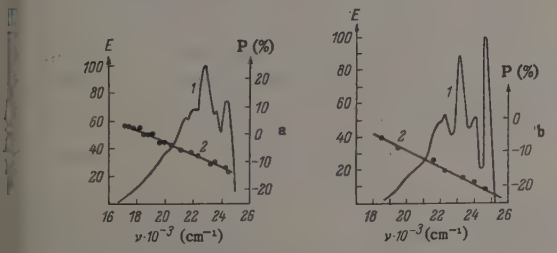

Fig. 1. Phosphorescence spectra of carbazole in a sugar gel (curve 1) and the variation of the degree of polarization of the phosphorescence in the spectrum (curve 2) at room temperature (a) and liquid air temperature (b).

The polarization of acridine yellow phosphorescence remains positive both at room temperature and at liquid air temperature (Fig. 2). At room temperature the polarization in the blue-green part of the spectrum (in the region from 21,200 to 19,000 cm^{-1}) remains constant. Lowering the temperature to liquid air temperature affects not only the magnitude of the polarization but also the character of its change in the phosphorescence spectrum.

The influence of the solvent on the luminescent properties of complex molecules is noted in a series of works. In this connection it is essential to make clear to what extent the surrounding medium affects the polarization of the phosphorescence and its variation in the emission spectrum. Trypaflavine was chosen as the material for investigation and gelatin, congealed alcohol, and sugar gel were chosen as solvents. The results of the measurements of the polarization of β-phosphorescence from trypaflavine in the designated materials are given in Fig. 3 (curves 1 and 2) and Fig. 4 (curve 5). For all three solvents the nature of the change of the degree of phosphorescence polarization in the emission spectrum is the same. The phosphorescence from trypaflavine in gelatin and in a sugar gel is depolarized only in a small part of the long wavelength region of the emission spectrum. In the remainder of the spectrum the degree of polarization of β-phosphorescence increases in absolute value with increasing ν for all three solvents. The same behavior of the polarization was observed for the β-phosphorescence of auramine in a sugar gel (Fig. 5, curve 5).

Together with a study of polarized β-phosphorescence, the degree of polarization of α-phosphorescence and the nature of its change in the emission spectrum were also investigated. The results of the measurements are given in Fig. 4 (for trypaflavine in a sugar gel, curve 4) and Fig. 5 (for auramine in a sugar gel, curve 4).

It is evident from the figures that in the part of the afterglow spectrum which corresponds to α-phosphorescence (coincident with fluorescence) the degree of polarization remains constant. In the part of the spectrum which corresponds to β-phosphorescence, the polarization of the emission is significantly diminished. These observations are in complete agreement with the data of Vavilov and Pringsheim[4] published earlier. Evidently, it is necessary to explain the decrease of polarization in the direction of long wavelengths by the superposition of a β-band, which for these dyes also exists at room temperature, on the α-phosphorescence spectrum.

The change in the degree of polarization of the total emission (fluorescence + phosphorescence) in the emission spectrum of trypaflavine and auramine in sugar gels is shown in Figs. 4 and 5 (curves 3). Curves 3 and 4 of

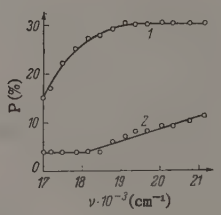

Fig. 2

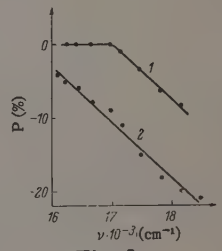

Fig. 3

Fig. 2. Change of the degree of polarization of the phosphorescence of acridine in a sugar gel in the emission spectrum at room temperature (curve 1) and at liquid air temperature (curve 2).

Fig. 3. Change of the degree of polarization of the phosphorescence of trypaflavine in gelatin (curve 1) and in alcohol (curve 2) at liquid air temperature.

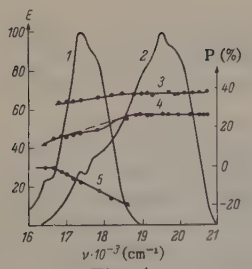

Fig. 4

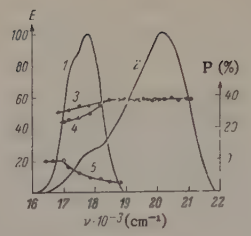

Fig. 5

Fig. 4. Spectra of the phosphorescence of trypaflavine in a sugar gel at room temperature (curve 2) and at liquid air temperature (curve 1), and curves for the change of the degree of polarization in the total emission spectrum (curve 3), α-phosphorescence (curve 4) and β-phosphorescence (curve 5).
Fig. 5. Spectra of the phosphorescence of auramine in a sugar gel at room temperature (curve 2) and at liquid air temperature (curve 1), and curves for the change of the degree of polarization in the total emission spectrum (curve 3), α-phosphorescence (curve 4), and β-phosphorescence (curve 5).

these figures indicate the general nature of the change of polarization of α-phosphorescence and total emission. However, since the amount of β-phosphorescence in the total emission is less than the α-phosphorescence, the decrease of the degree of polarization in the long wavelength part of the total emission spectrum is less.

The change of the degree of polarization of β-phosphorescence (from positive to negative values) during the transition from room temperature to liquid air temperature is unusual from the viewpoint of existing ideas. It is usual to say that the phosphorescence of esculin at all temperatures is caused by a transition from one and the same electronic (metastable) level to the normal state. According to this idea, the degree of polarization of the afterglow would not need to undergo significant changes during a transition from room temperature to −180°C.

From the viewpoint of an oscillator model, a change of sign of the polarization of the phosphorescence means that the oscillators producing the emission at room temperature and at liquid air temperature are different. In view of this it is heardly possible to maintain that at liquid air temperature one electronic level corresponding to a metastable state takes part in the emission. Such a supposition would be justifiable under the condition of constancy of the degree of polarization in the phosphorescence spectrum or, in the extreme case, of a small change in the degree of polarization. The data indicate a very strong change of polarization in the emission spectrum. Evidently one can explain this change if one assumes that not one, but several electronic (metastable) states, each of which has its own degree of polarization,* take part in the emission.

*The dependence of the degree of polarization of fluorescence in the emission spectrum described in refs. 18-20 is explained by the authors as the effect of molecular vibrations. Since the anisotropy of the α-phosphorescence and total emission of the organophosphors investigated in the present work remains constant, it is natural to assume that the influence of molecular vibrations on the polarization of emission is not great in this case. In order to explain by molecular vibrations the observed change of polarization in the long wavelength phosphorescence spectrum, it is necessary to assume that the effe of these vibrations is different in the case of α- and β- processes.

The absence of polarization of long wavelength phos phorescence is indicated in refs. 3 and 13. The data for the anisotropy of β-phosphorescence presented above is evidence that such an opinion is wrong.

The fact that the degree of polarization of the total emission and the α-phosphorescence in that part of the spectrum which corresponds to β-processes is very hig is somewhat unusual. For its explanation, it is necessar to suppose that the spectrum corresponding to transitio from an unstable to a normal level spreads to a signifi- cant extent into the spectral region of β-phosphorescenc

Investigation of the nature of the change in the degr of polarization of α- and β-phosphorescence in the emis sion spectrum and the data for the anisotropy of the tota emission permit one to make certain observations con- cerning a hypothesis about luminescent centers. This hypothesis was proposed by Jablonski[21-24] to explain cer tain questions about fluorescence; in particular, questio about the damping and depolarization of emission. Recently, the author of the hypothesis used a model of luminescent centers for explanation of the nonexponential character of the decay of phosphorescence and its depolarization in the process of decay.[25]

According to the ideas of Jablonski, different luminescent centers have their own probability of deactivation and correspond to differently oriented oscillators. This must express itself not only in the nonexponential character of the decay of the afterglow, but also in the dependence of the rate of decay and degree of polarization of the phosphorescence on the frequency of the radiation, if each center has its own spectrum. Both our experiments[16] and experiments of other authors[26-28] indicate a different rate of decay for different regions of the β-phosphorescence spectrum. Therefore, assuming Jablonski's hypothesis, one must expect changes of the degree of polarization in the spectrum for β- and α- phosphorescence and also for fluorescence if it does not decay exponentially. It is shown above that the degree of polarization of β-phosphorescence is different for differ ent regions of the emission spectrum. At the same time, the degree of polarization both of α-phosphorescence and fluorescence remains constant in the emission spectrum (if one excludes the superposition of luminescence from β-processes) for all the compounds investigated. The different behavior for the polarization of the luminescenc in the first and second cases agrees poorly with Jablonski's hypothesis, since according to his model the luminescent centers in all cases must determine both the deactivation probability of the excited state and the aniso tropy of the emission.

The author sincerely thanks B. Ya. Sveshnikov for the attention he gave the work during its completion.

REFERENCES

1. A. Carelli and P. Pringsheim, Z. Physik 17, 287 (1923).
2. S. I. Vavilov and V. L. Levshin, Z. Physik 35, 290 (1926).
3. S. I. Vavilov and V. L. Levshin, Zhur. Russ. Fiz.-Khim Obshchestva 58, 555 (1926).
4. S. I. Vavilov and P. Pringsheim, Z. Physik 37, 705 (1926).
5. P. Pringsheim and H. Vogels, Acta Phys. Polon. 4, 341 (1935).

6. A. Jablonski, Acta Phys. Polon. 4, 311 (1935).
7. A. Jablonski, Bull. intern. acad. Cracovie 30 (1935).
8. P. Frölich and L. Gombay, Kolloid-Z. 94, 147 (1941).
9. B. Ya. Sveshnikov and V. L. Ermolaev, Doklady Akad. Nauk SSSR 71, 647 (1950).
10. P. P. Feofilov, Doklady Akad. Nauk SSSR 44, 159 (1944).
11. P. P. Feofilov, Kand. Diss., Gosudarst. Opt. Inst. (State Optical Institute), Leningrad, 1943.
12. P. P. Feofilov, "Polyarizovannaya lyuminestsentsiya atomov, molekul i kristallov" (Polarized Luminescence of Atoms, Molecules and Crystals). Gosudarst. Izd. Fiz. Mat. Lit., Moscow, 1959.
13. E. Laffitte, Ann. phys. 10, 71 (1955).
14. V. A. Pilipovich and B. Ya. Sveshnikov, Opt. i Spektr. 4, 116 (1958).
15. V. A. Pilipovich and B. Ya. Sveshnikov, Opt. i Spektr. 4, 541 (1958).
16. V. A. Pilipovich and B. Ya. Sveshnikov, Opt. i Spektr. 5, 290 (1958).
17. V. A. Pilipovich and B. Ya. Sveshnikov, Doklady Akad. Nauk SSSR 119, 59 (1958), Soviet Phys.-Doklady 3, 286 (1958).
18. G. P. Gurinovich and A. N. Sevchenko, Izvest. Akad. Nauk SSSR, Ser. Fiz. 22, 1407 (1958).
19. A. N. Sevchenko, G. P. Gurinovich, and A. M. Sarzhevskii, Doklady Akad. Nauk SSSR 126, 979 (1959), Soviet Phys.-Doklady 4, 644 (1959).
20. A. N. Sevchenko, G. P. Gurinovich, and A. M. Sarzhevskii, Doklady Akad. Nauk SSSR 126, 979 (1959), Soviet Phys.-Doklady 4, 644 (1959).
21. A. Jablonski, Z. Physik 103, 526 (1923).
22. A. Jablonski, Z. Physik 94, 38 (1935); Ibid. 95, 53 (1935).
23. A. Jablonski, Acta Phys. Polon. 14, 295 (1955).
24. A. Jablonski, Acta Phys. Polon. 13, 175 (1954).
25. A. Jablonski, Acta Phys. Polon. 15, 471 (1957).
26. V. V. Bredel', Doklady Akad. Nauk SSSR 109, 787 (1955).
27. M. D. Khalupovskii, Opt. i Spektr. 3, 385 (1957).
28. P. P. Dikun, A. A. Petrov and B. Ya. Sveshnikov, Zhur. Eksptl. i Teoret. Fiz. 21, 150 (1951).

SOME SPECIAL CASES OF LUMINESCENCE KINETICS

V. V. Antonov-Romanovskii (pp. 216-219)

Received 31 March 1960

The case considered is that of decay when two kinds of traps which differ slightly in depth are present. It is shown that the quadratic dependence of the steady-state photoconductivity on the intensity of the exciting light can be explained within the framework of the conventional zone model of a phosphor.

It follows from the study conducted in ref. 1 that if the difference in trap depths is large, the traps act sequentially, i.e., as if they were independent of each other. Such an independence will no longer exist if the probabilities of liberating electrons from them are comparable. For example, we have examined the case in which two adjacent electron levels—the (j – 1)-th and j-th—differ by so little in depth that (for simplicity we will replace the indices j – 1 and j by 1 and 2 in all that follows)

$$\frac{dn_1}{dt} = -w_1 n_1 + \frac{\sigma_1 \nu_1}{\sum_1^m \sigma_k \nu_k}(w_1 n_1 + w_2 n_2),$$
$$\frac{dn_2}{dt} = -w_2 n_2 + \frac{\sigma_2 \nu_2}{\sum_1^m \sigma_k \nu_k}(w_1 n_1 + w_2 n_2). \quad (1)$$

In this case the approximate formulas presented in ref. 1 will be already incorrect.*

*In referring to the formulas of ref. 1 the equation number will be preceded by 1.

The exact solution of Eq. (1.15), which determines the characteristic quantities λ_1 and λ_2 (i.e., λ_{j-1} and λ_j), has the following form (see ref. 1):

$$\lambda_{1,2} = \frac{1}{2}[w_1(1-\delta_1) + w_2(1-\delta_2)] \pm \sqrt{\frac{1}{4}[w_1(1-\delta_1) - w_2(1-\delta_2)]^2 + w_1 w_2 \delta_1 \delta_2}, \quad (2)$$

where

$$\delta_1 = \frac{\sigma_1 \nu_1}{\sum_1^m \sigma_k \nu_k}, \qquad \delta_2 = \frac{\sigma_2 \nu_2}{\sum_1^m \sigma_k \nu_k}. \quad (3)$$

Similarly the exact values of the quantities A_1, B_1, C_2, and A_2 which are used in the determination of the concentrations n_1 and n_2 from (1.17) and (1.18) in which

$$n_1 = A_1 e^{-\lambda_1 t} + B_1 e^{-\lambda_2 t}, \qquad n_2 = C_2 e^{-\lambda_1 t} + A_2 e^{-\lambda_2 t}, \quad (4)$$

will be equal to

$$A_1 = \frac{[w_1(1-\delta_1) - \lambda_2] n_{10} - w_2 \delta_1 n_{20}}{\lambda_1 - \lambda_2},$$
$$C_2 = \frac{-w_1 \delta_2 n_{10} + [w_2(1-\delta_2) - \lambda_2] n_{20}}{\lambda_1 - \lambda_2},$$
$$B_1 = \frac{-[w_1(1-\delta_1) - \lambda_1] n_{10} + w_2 \delta_1 n_{20}}{\lambda_1 - \lambda_2},$$
$$A_2 = \frac{w_1 \delta_2 n_{10} - [w_2(1-\delta_2) - \lambda_1] n_{20}}{\lambda_1 - \lambda_2}. \quad (5)$$

If there is no external quenching the luminescence intensity of any (unquenched) luminescence band will be proportional to the number of liberated electrons, i.e., the quantity $w_1 n_1 + w_2 n_2$. That is why we investigated this quantity, or more reasonably (as it will follow from the subsequent development below) its product with the constant multiplier $1 - \delta_1 - \delta_2$.

Using (4) and (5) this product can be expressed in the form

$$(1-\delta_1-\delta_2)(w_1n_1+w_2n_2)=\lambda_1 n_{0\lambda_1}e^{-\lambda_1 t}+\lambda_2 n_{0\lambda_2}e^{-\lambda_2 t}, \quad (6)$$

where

$$\left.\begin{aligned} n_{0\lambda_1}&=\frac{\lambda_2}{w_2}\frac{\lambda_1-w_2}{\lambda_1-\lambda_2}n_{10}-\frac{\lambda_2}{w_1}\frac{w_1-\lambda_1}{\lambda_1-\lambda_2}n_{20},\\ n_{0\lambda_2}&=\frac{\lambda_1}{w_2}\frac{w_2-\lambda_2}{\lambda_1-\lambda_2}n_{10}+\frac{\lambda_1}{w_1}\frac{w_1-\lambda_2}{\lambda_1-\lambda_2}n_{20}.\end{aligned}\right\} \quad (7)$$

The quantity $(1 - \delta_1 - \delta_2)(w_1n_1 + w_2n_2)$ has a simple meaning—it determines the rate of electron loss from levels of the first and second kinds. In such a case the integral of this value over the total decay time must be equal to $n_{10} + n_{20}$, i.e., the initial number of electrons in traps of the first and second types. Actually it follows from (6) and (7), when (3) is taken into account, that

$$\int_0^\infty (1-\delta_1-\delta_2)(w_1n_1+w_2n_2)\,dt=n_{0\lambda_1}+n_{0\lambda_2}=n_{01}+n_{02}. \quad (8)$$

It follows from the form of the right side of Eq. (6) that the mathematical problem of the decay of a phosphor with two kinds of traps under conditions of repeated capture is equivalent to the problem of decay in the absence of repeated capture. To make this clear it is necessary only to replace the values for the rate of electron ejection from the traps w_1 and w_2 by the quantities λ_1 and λ_2, and the initial concentrations n_{01} and n_{02} by the fictitious concentrations $n_{0\lambda_1}$ and $n_{0\lambda_2}$. The fictitiousness of these concentrations clearly follows from the fact that according to (7) the quantity $n_{0\lambda_1}$ can even take on negative values (see below), though according to (8) the sum of the fictitious concentrations will always equal the sum of the true values.

Formula (3) has the following interesting property. It is easy to show that if

$$w_1-w_2\to 0, \quad (9)$$

such that in the limit $w_1 = w_2 = w$, then

$$\lambda_1\to w \text{ and } \lambda_2\to w(1-\delta_1-\delta_2), \quad (10)$$

i.e., the difference

$$\lambda_1-\lambda_2\to w(\delta_1+\delta_2). \quad (11)$$

Thus this difference, in contrast to the difference $w_1 - w_2$, will not go to zero. If one refers to the fictitious light sums, then it follows from (7) that in addition

$$n_{0\lambda_1}\to 0 \text{ and } n_{0\lambda_2}\to n_{10}+n_{20}. \quad (12)$$

This implies that in (6) the "amplitude" associated with the first exponent goes to zero and thus it follows that one can expect an expression with two exponentials in (6) which degenerates to a single exponential expression. On the other hand this takes place in a very unexpected way since it was "naturally" assumed that this would occur as a result of the values λ_1 and λ_2 drawing closer together (until they coincided). The reason for this peculiar situation is explained by the interaction of levels which depend on the transfer of electrons from levels of one kind to levels of another.

The interaction is most effective when electrons, due to the initial conditions and definite relationship of the constants, are transferred from deeper levels to the shallower ones. This will occur in its purest form when all the electrons are initially present only in the deeper traps, i.e., when

$$n_{10}=0. \quad (13)$$

Then from (7) we obtain

$$n_{0\lambda_1}=-\frac{\lambda_2}{w_1}\frac{w_1-\lambda_1}{\lambda_1-\lambda_2}n_{20} \text{ and } n_{0\lambda_2}=\frac{\lambda_1}{w_1}\frac{w_1-\lambda_2}{\lambda_1-\lambda_2}n_{20}. \quad (14)$$

Since (under the conditions of the assumptions) $w_1 \geq w_2$ and $\lambda_1 \geq \lambda_2$, then it follows from (2) that $w_1 \geq \lambda_1$; moreover, $w_1 \geq \lambda_2$. For this reason $n_{0\lambda_1}$ is always less than 0 and $n_{0\lambda_2} > 0$. The first term on the right side of (6) is therefore negative. This leads to the following interesting possibility—an increase in free electron concentration during the initial stages and as a result growth also in conductivity u^-N^- and intensity I_l of the decay!*

*Translator's note: The author uses the word "decay" in referring to luminescence which accompanies de-excitation.

To prove this it must be shown that the first derivative of the right side of the expression (6) is positive. After differentiating (6) we obtain, on substituting (14),

$$\frac{d}{dt}\left[\lambda_1 n_{0\lambda_1}e^{-\lambda_1 t}+\lambda_2 n_{0\lambda_2}e^{-\lambda_2 t}\right] \quad (15)$$

$$=\frac{\lambda_1\lambda_2 n_{20}}{(\lambda_1-\lambda_2)w_1}\left[\lambda_1(w_1-\lambda_1)e^{-\lambda_1 t}-\lambda_2(w_1-\lambda_2)e^{-\lambda_2 t}\right]>0.$$

Inasmuch as the first term decreases more rapidly than the second, the greatest probability of fulfilling the inequality will occur when $t \approx 0$. If it is taken into account that the multiplier $\lambda_1\lambda_2 n_{20}/(\lambda_1 - \lambda_2)w_1$ is positive, then when $t \approx 0$ we derive a condition from (15) which takes on the following form:

$$w_1\delta_1 > w_2(1-\delta_2). \quad (16)$$

To obtain this result we multiply by $\lambda_1 - \lambda_2 (\lambda_1 > \lambda_2)$ and make use of the fact that according to (2) $\lambda_1 + \lambda_2 = w_1(1 - \delta_1) + w_2(1 - \delta_2)$.

Since $w_1 > w_2$ this condition can be fulfilled. In particular, it is fulfilled automatically if the probability of repeated capture in the traps under consideration is very high, i.e., $\delta_1 + \delta_2 \approx 1$, or, putting it another way, $1 - \delta_2 \ll \delta_1$.

In this way even a transient increase in light output is possible during decay under certain conditions. The necessary conditions for this to occur are that the deeper levels be initially more highly populated than the shallower ones, and that the probability be higher for repeated capture at shallower levels than at the deeper.

We point out that this effect can be quite appreciable. To show this we consider the most favorable case in which

$$\delta_1\sim 1 \text{ and } \delta_2\ll 1. \quad (17)$$

Then we obtain from (2)

$$\lambda_1\approx w_1(1-\delta_1), \quad \lambda_2\approx w_2, \quad (18)$$

after which it follows from (14) that

$$n_{0\lambda_1}\approx -\frac{w_2\delta_1}{w_1(1-\delta_1)-w_2}n_{20}$$

$$\text{and } n_{0\lambda_2}\approx\left[1+\frac{w_2\delta_1}{w_1(1-\delta_1)-w_2}\right]n_{20}. \quad (19)$$

The quantity $n_{0\lambda_1}$ will be almost equal to the negative of $n_{0\lambda_2}$ if the denominator of the fraction is less than the numerator, i.e.,

$$w_1(1-\delta_1)-w_2<w_2\delta_1. \quad (20)$$

Then we deduce from (19) that at the instant $t = 0$

$$p(0)=\lambda_1 n_{0\lambda_1}e^{-\lambda_1 t}+\lambda_2 n_{0\lambda_2}e^{-\lambda_2 t}=\frac{\lambda_1\lambda_2}{w_1}n_{20}, \quad (21)$$

and at $t \sim 1/\lambda_1$, assuming in addition that $e^{-\lambda_1 t} \ll 1$ and $e^{-\lambda_2 t} \sim 1$,

$$p\left(\frac{1}{\lambda_1}\right)=\lambda_1 n_{0\lambda_1}e^{-\lambda_1 t}+\lambda_2 n_{0\lambda_2}e^{-\lambda_2 t}\approx\frac{w_1-\lambda_2}{\lambda_1-\lambda_2}\frac{\lambda_1\lambda_2}{w_1}n_{20}. \quad (22)$$

We show that the ratio

$$\frac{p\left(\frac{1}{\lambda_1}\right)}{p(0)} \approx \frac{w_1 - \lambda_2}{\lambda_1 - \lambda_2} \tag{23}$$

can considerably exceed 1. For example, let us assume that $\delta_1 = 0.9$, $\delta_2 = 0$, and $w_2 = 0.05w_1$. Using Eq. (18) we derive that $\lambda_1 = 0.1w_1$ and $\lambda_2 = 0.5w_1$ (i.e., λ_1 and λ_2 differ by a factor of 2). Then it follows from (23)

$$\frac{p\left(\frac{1}{\lambda_1}\right)}{p(0)} \approx 20. \tag{24}$$

This indicates that the intensity associated with decay can increase many times. However it is not possible to reduce the difference $\lambda_1 - \lambda_2$ to zero in formula (23) because then the exponents in (21) would decay in almost exactly the same way. The result is that the conditions $e^{-\lambda_1 t} \ll 1$ and $e^{-\lambda_2 t} \sim 1/\lambda_1$ at $t \sim 1/\lambda_1$, which are essential for the realization of formula (22), are impracticable.

Thus during the time when $t \sim 1/\lambda_1$, i.e., during a time comparable to the mean lifetime of an electron in the shallow levels, the concentration of free electrons and consequently decay intensity and conductivity can change in very unusual ways, namely, to increase rather than diminish as usual. The anomaly in afterglow can be developed not only at constant temperature but also during the uniform heating of a phosphor. For example, the shape of the thermoluminescence curves can be distorted (the thermoluminescence peaks may become narrower). The results obtained have a different form if the second type of level turns out to be the deeper because the "linearity" of the initial equations then vanishes, however they remain qualitatively similar.

Let us now turn to an examination of another case in which we are dealing with steady excitation. Suppose that in the phosphor there is only one kind of trap of both signs, and that the action of the exciting light results only in transfer of electrons from filled bands to electron levels. Also assume that holes on reaching the activator will not be thermally liberated later on. It then follows from the general formulas (1)-(3) of ref. 2 that this particular case (assuming an absence of saturation and that the probability of repeated capture considerably exceeds the probability of recombination) can be described by the following equations:

$$\sigma_0^- n^+ \cdot u^- N^- = \sigma^+ \nu^+ \cdot u^+ N^+, \tag{25}$$

$$\sigma_{02}^+ n_2^- \cdot u^+ N^+ + w_2^- n_2^- = \sigma_2^- \nu_2^- \cdot u^- N^- + \varkappa_2^- \nu_2^- E, \tag{26}$$

$$u^- N^- = \frac{w_2^- n_2^-}{\sigma_0^- n^+ + \sigma_2^- \nu_2^-}, \tag{27}$$

$$u^+ N^+ = \frac{\varkappa_2^- \nu_2^- E}{\sigma_{02}^+ n_2^- + \sigma^+ \nu^+}. \tag{28}$$

According to the principle of charge compensation $n_2^- = n^+$ so one of the equations (25)-(28) is superfluous. Let it be the most complex equation, i.e., (26). Then taking into account that $\sigma_0^- n^+ \ll \sigma_2^- \nu_2^-$ and $\sigma_{02}^- n_2^- \ll \sigma^+ \nu^+$ we obtain from (25), (27), and (28)

$$n_2^- = n^+ = \sqrt{\frac{\sigma_2^+ \nu_2^+}{w_2^-} \frac{\varkappa_2^- \nu_2^- E}{\sigma_0^-}}, \tag{29}$$

$$u^- N^- = \sqrt{\frac{w_2^-}{\sigma_2^+ \nu_2^+} \frac{\varkappa_2^- \nu_2^- E}{\sigma_0^-}}. \tag{30}$$

If the liberation of localized electrons takes place in a primarily thermal way, i.e., $w = w_T$, then it follows from (29) and (30) that

$$n_2^- = n^+ \sim \sqrt{E}, \quad N^- \sim \sqrt{E}, \quad N^+ \sim E. \tag{31}$$

However if the liberation is mainly accomplished by the exciting light itself, i.e., $w = w_E = \alpha E$, then we get from (29) and (30)

$$n_2^- = n^+ \approx \text{const}, \quad N^- \sim E, \quad N^+ \sim E. \tag{32}$$

Thus the concentration of free electrons and consequently the electronic conductivity can be proportional to both E and $\sqrt{E}$ at a time when the free hole concentration, and, as a result, the hole conductivity, will always be proportional to E.

If there are still shallow traps along with the deep ones, resulting in the concentration of electrons in them being such that $n_1^- \ll n_2^-$, then even this does not appreciably violate the rule set forth above. If in addition the quantity w_1^- is primarily thermal in nature, i.e., $w_1^- \approx w_T^-$, the electron concentration in the shallow levels will be in equilibrium with the filled band and for that reason

$$n_1^- \sim N^-. \tag{33}$$

Consequently, the quantity n_1^- will conform to the same laws as N^-, i.e., it will be as if n_1^- "follows" N^-.

Let us now assume that a small fraction of the electrons in the shallow traps will nevertheless be liberated by the exciting light itself. Then the expression for the total electronic conductivity (steady state) can be written in the form

$$S_\infty^- = S_{\infty T}^- + S_{\infty E}^-, \tag{34}$$

where $S_{\infty T}^-$ is the thermally dependent conductivity, and $S_{\infty E}^-$ is that due to optical electrons. Although the number of optical electrons is appreciably less than the number of thermal ones, it can be shown that their role in conductivity is decisive because of their longer free path and smaller effective mass (for example, in a polaron the effective mass can exceed the electronic[3] mass by two or three orders). In this case it can be shown that

$$S_\infty^- \approx S_{\infty E}^-. \tag{35}$$

Since $S_{\infty E}^- \sim w_{1E}^- n_1^-$, where $w_{1E}^- \sim E$, then

$$S_\infty^- \sim E n^-. \tag{36}$$

According to (31)-(33) this leads to the unusual relationships

$$S_\infty^- \sim E^{3/2} \text{ and } S_\infty^- \sim E^2. \tag{37}$$

The experiment in ref. 4 showed that the dependence of the steady-state photoconductivity S_∞ on E can often be approximated by the formula

$$S_\infty \sim E^p, \quad p \leqslant 2, \tag{38}$$

where p turns out to be a function of temperature T. At first the value of p increases with T, subsequently reaching the value 2, after which it starts to decrease.

The presence of some specific temperature interval in which p = 2 (or 3/2) also follows from our scheme. At low temperatures the liberation of electrons from shallow as well as deep traps is primarily brought about by optical means, but at high temperatures thermal mechanisms dominate. In both these cases the shallow and the deep traps "act" similarly, whereby they disrupt the conditions which lead to the square (or 1.5 power) dependence of S_∞ on E.

The results obtained, along with the results of ref. 5, are of particular interest in view of the fact that in experiment such relationships are not that rare. At one time they even gave rise to the unconventional "two

step'' theory of phosphorescence and conductivity* formulated by Tolstoi[6] because he felt that the usual semiconductor model was not able to explain them.

*One of the unusual features of the ''two step'' kinetics in comparison with the conventional zone scheme is that in it the recombination probability of an electron is assumed to be independent of the concentration of ionized centers.[6]

REFERENCES

1. V. V. Antonov-Romanovskii, Opt. i Spektr. 7, 376 (1959), Optics and Spectroscopy 7, 245 (1959).
2. V. V. Antonov-Romanovskii, Opt. i Spektr. 8, 73 (1960), Optics and Spectroscopy 8, 35 (1960).
3. S. I. Pekar, ''Issledovaniya po elektronnoi teorii kristallov'' (A Study of the Electron Theory of Crystals). Moscow-Leningrad, 1951.
4. V. E. Lashkarev and G. A. Fedorus, Izvest. Akad. Nauk SSSR, Ser. Fiz. 16, 81 (1959);
N. A. Tolstoi, B. T. Kolomiets, O. I. Golikova, and M. Ya. Tsenter, Zhur. Eksptl. i Teoret. Fiz. 30, 575 (1956), Soviet Phys.-JETP 3, 465 (1956);
N. A. Tolstoi, Radiotekh. i Elektron. 1, 1137 (1956);
N. A. Tolstoi and V. A. Sokolov, Opt. i Spektr. 3, 495 (1957);
N. Kallmann and V. Kramer, Phys. Rev. 87, 91 (1956).
5. V. V. Antonov-Romanovskii, Opt. i Spektr. 7, 827 (1959), Optics and Spectroscopy 7, 484 (1959).
6. N. A. Tolstoi, Zhur. Eksptl. i Teoret. Fiz. 30, 109 (1956), Soviet Phys.-JETP 3, 81 (1956);
N. A. Tolstoi and A. V. Shatilov, Opt. i Spektr. 1, 216 (1956); Opt. i Spektr. 5, 596 (1958); Opt. i Spektr. 6, 665 (1959), Optics and Spectroscopy 6, 430 (1959).

FLASHLIKE RISE OF LUMINESCENCE
III. Effect of the Intensity of the Exciting and De-Exciting Light

N. A. Tolstoi, A. M. Tkachuk, and A. I. Ryskin (pp. 220-224)

Received 16 April 1960

The magnitude and area of the flash in the long wavelength luminescence band are shown to be independent of the intensity of the exciting light owing to identical population of the first trapping levels. Data are presented to show that the form of the rising portion of the short-wavelength luminescence band is affected only by the number of electrons or holes involved in the first trapping.

1. In a previously published article[1] devoted to the flashlike rise of luminescence (FR) of ZnS-Ni phosphors, we showed that the absolute value of the flash I_{max} is independent of the intensity of the exciting light E_∞, and as a result of this, concluded that the number of electrons and holes involved in the first trapping is independent of E_∞. I_{max} was found to be independent of the intensity of the exciting light when the latter was varied by a factor of about 25. We presented arguments showing that the independence of the first localization on E_∞ is explained by the de-exciting action of the exciting light (DAEL), which restricts the number of electrons and holes in a practically unlimited number of corresponding local levels. This point of view naturally is opposed to another opinion, according to which a practical limitation of the number of local levels occurs and these levels are completely filled during preliminary excitation. These two alternate viewpoints lead to two alternate ways of interpreting the whole luminescence mechanism of phosphors having FR, and hence, any phosphors of the sulfide type. Actually the viewpoint based on DAEL makes it impossible to use the idea of the complete filling of local levels, or to deal with the resulting difficulties which arise in connection with the recombination of carriers through these levels. The other viewpoint considers several specific effects which become possible only if these levels are filled.

Clarification of the cause of the limitation of the number of trapped electrons is essential. We therefore considered it necessary to make a more thorough study of this question on the basis of recent experiments and ideas.

First of all, let us note that the degree to which the preliminary exciting light E_∞ can be weakened without affecting the value of the flash I_{max} is very different for different phosphors. For ZnS-Ni and ZnS-Ag,Ni, E_∞ can sometimes be varied over a range of 10^4 to 10^5. For all phosphors, this range is rapidly reduced with increasing temperature.

Having established that under ''good'' conditions the variation of E_∞ does not affect I_{max}, we conclude that it is the intensity of the de-exciting light E_d which is responsible for the value of I_{max}. Actually, the experiment shows that I_{max} and E_d are related almost linearly. The small deviations from linearity are connected with the finite rise time of the front of the light impulse E_{lum}. Let us now introduce the concept of the area of the flash S, which is defined as the area enclosed between the rise curve corresponding to FR, and the rise curve obtained after complete overripening, i.e., in the absence of any FR (Fig. 1a). The value of S is proportional to the number of additional quanta emitted by a phosphor in which a flash has developed to some degree, in comparison to a phosphor in which the conditions for its formation are absent.

Experiment shows that the value of S remains constant despite variation of E_d (Fig. 2). This is connected with the fact that the descending part of the upper curve in Fig. 1 acquires a gentler slope (see Fig. 1b) upon reduction of E_d, and therefore the area S, despite the decrease in I_{max}, stays the same. Hence, it follows that one and the same limiting light sum is emitted during the flash; when the light is weaker, this light sum is emitted more slowly. Proof of the existence of a constant light sum is essential for understanding the mechanism of FR. Since a given light sum corresponds to a given number of trapped electrons and holes, we may now connect not only the ripening and overripening processes, but also the FR

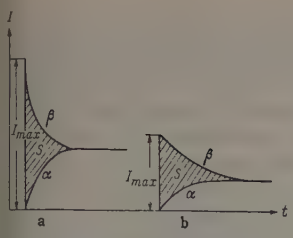

Fig. 1

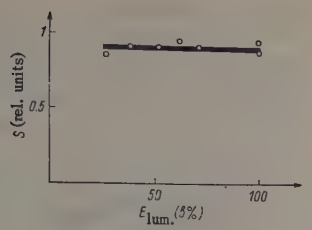

Fig. 2

Fig. 1. Explanation of the concept of the area of flash S. α-rise curve of a phosphor devoid of Fr; β-rise curve of a completely ripened phosphor; S—area of flash (cross-hatched area between the curves α and β). a—$E_d = 2$; b—$E_d = 1$.

Fig. 2. Dependence of the area of the flash S on the intensity of the de-exciting light E_d.

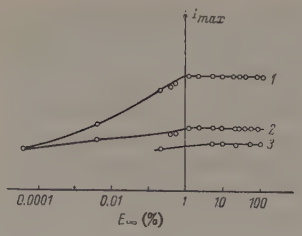

Fig. 3

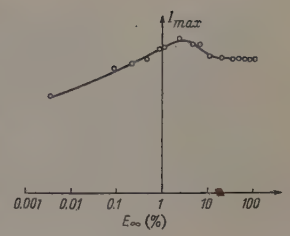

Fig. 4

Fig. 3. Dependence of the absolute value of the flash I_{max} on E_∞ at different temperatures for a ZnS-Ni phosphor—sphalerite ($C_{Ni} = 10^{-4}$ gm/gm). Temperature (in °C): Curve 1—20; curve 2—44; curve 3—70.

Fig. 4. Dependence of the value of I_{max} on E_∞ for a ZnS-Ni phosphor—sphalerite ($C_{Ni} = 5 \times 10^{-5}$ gm/gm).

process, with the concept of localization of carriers.

Thus, the ability to produce a flash is connected with a definite number of carriers being involved in the second trapping, and the area of the flash is a measure of the number of these localized carriers. The absolute magnitude of the flash I_{max} is proportional to S and E_d (in other words, it reflects the interaction of the exciting light with carriers of the second localization). We have not determined the nature of this interaction since it may be diverse.

The dependence of I_{max} on E_∞ indicates the following: Outside of its dependence on the intensity of the preliminary excitation a ripened phosphor can exist in only one particular state, with a given flash-producing capacity. However, this means that the number of electrons or holes involved in the second trapping does not depend on E_∞. Hence, either (1) levels of the second trapping are filled completely (and therefore the number of electrons or holes in them, being the limiting number, remains constant even if there is a sharp decrease in E_∞), or (2) levels of the second trapping are only partially filled, but then the number of electrons or holes in levels of the first localization is independent of E_∞ over a wide range of E_∞ values. In the latter instance, the initial conditions of the ripening process being identical (for different values of E_∞) leads to an identical final condition. In other words, identical first trappings lead to identical second trappings (not forgetting that the process of relocalization occurs in the dark).

In ref. 1 the independence of the flash on E_∞ is explained by the independence of the number of first-trapping carriers on E_∞. This explanation is "sufficient." The present paper shows that it is also "necessary." Actually, the first of the abovementioned assumptions (complete filling of the second trapping levels) may be excluded for the following reasons: (1) I_{max}, being independent of E_∞, may depend on temperature (Fig. 3). (2) As E_∞ decreases, the value of I_{max}, as we will see below, may increase somewhat before it starts to fall (Fig. 4). (3) Neither the ripening time nor even the ripening process depends on E_∞. This independence is illustrated, for example, in Fig. 8 of ref. 2, which depicts parts of the V(log t_0) plots obtained for different ZnS-Mn phosphors at various temperatures and different values of $E_\infty = E_d$ near the maxima of V. In all instances, the positions of the maxima coincide.

As another example, three complete V(log t_0) plots obtained at different intensities $E_\infty = E_d$ and then normalized to the same E_d are presented in Fig. 5. The graphs are compared to a "pure" ZnS, i.e., to a phosphor with an unidentified activator, giving FR. It is apparent from the figure that the normalized curves coincide perfectly. This means that the process of transition of electrons or holes from the first trapping state to the second is the same for different values of E_∞. However, the sameness of the transition process indicates sameness in the first trapping states; the sameness of the second trapping states is inferred as a consequence of this, and is in no way connected with complete filling of levels of the second. Thus, complete filling of the second trapping levels is an explanation of the independence of I_{max} on E_∞ must be discarded.

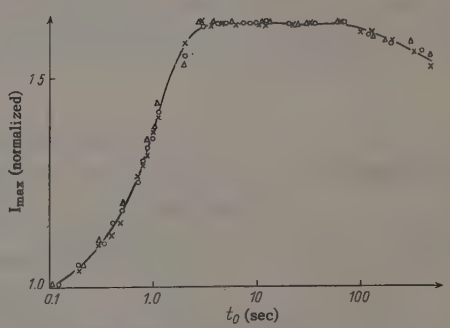

Fig. 5. Standardized ripening curves, obtained for different excitation energies (ZnS phosphor, t = 45°C).

A second explanation remains: equal filling of the first trapping levels for different values of E_∞. Arguments have already been given in ref. 1 which show that this equal filling of the first trapping levels for different values of E_∞ is caused by DAEL, not by the complete filling of these levels. More detailed data concerning this problem will be given in a later publication.

Let us now turn to the correlation between the rise curve of the long wavelength ("red") luminescence band, which has FR, and the rise-curve of the short wavelength ("blue") band, which does not have FR. We have already shown that an increase in the "sluggishness" of rise of the blue band corresponds to ripening of the flash in the red band. For an illustration of this, let us turn to Fig. 6a, which shows the flash in the red band as a function of the dark period t_0 (curve K) for ZnS-Ni. The "sluggishness" of the blue band as a function of t_0 (curve G) is also given in this figure. (The flash is represented on this graph by its area, or more correctly, by the decrease in the value of S for a given rise curve, compared to its value for the "standard" curve, i.e., one completely free

of any flashlike rise. The latter is simply a completely overripened or, what is the same thing, a completely unripened rise curve of the red band.) On the other hand, the "sluggishness" of the blue band is characterized in our graph by an increase in the value L_p in comparison with the value for a completely unripened phosphor. L_p is defined[3] as the area which, when added to the rise curve, makes a rectangle. Both curves are normalized; i.e., the saturation value for each curve is taken as 100%.

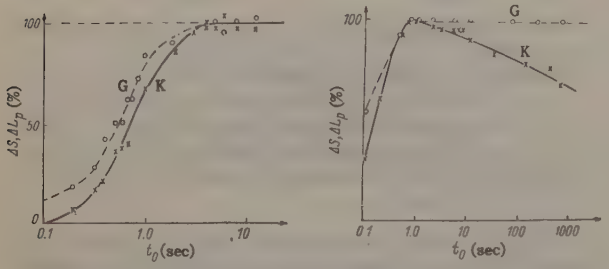

Fig. 6. Parallelism between the effect of the dark period t_0 on the area of the flash S in the red (K) band and on the area L_p, which characterizes the "sluggishness" of the blue (G) band. a—ZnS-Ni phosphor (C_{Ni} = 10^{-6} gm/gm, t = 20°C); b—ZnS-Mn phosphor (C_{Mn} = 10^{-3} gm/gm, t = 20°C).

A difficulty arises in the construction of curve G: in order to express the magnitude of the increase in L_p, it is necessary to know the initial value of L_p, i.e., L_p for the blue band of the completely unripened phosphor. Obviously, this would necessitate making measurements at $t_0 \to 0$, which is impossible. It is practical to start measurements from t_0 = 0.1 sec, assuming L_p at t_0 to be zero by convention, although it actually has a finite value. This leads to a certain error in the initial part of curve G; however, this error becomes smaller as the curve rises. Consequently, the first part of curve G should be shifted downwards. Considering the foregoing, it is evident that there is a complete concurrence of the ripening process of sluggishness in the blue band and the ripening process of the flash in the red band.

Similar curves for a ZnS-Mn phosphor are presented in Fig. 6b. The difference here consists in the fact that curve K indicates overripening, whereas curve G does not. There is a complete parallelism between the ripening processes of the flash and the sluggishness.

From the facts presented and the abovementioned considerations, it is quite obvious that the form of the rise curve of the short wavelength luminescence is affected only by the number of electrons or holes involved in the first trapping. In this connection, it is perfectly clear that the maximum sluggishness in the rise of the blue band attained during the ripening process does not change with further increases in t_0 (it does not "overripen"). Actually, the removal of carriers from the first trapping locations is a final process, since the carriers proceed to positions which are energetically deeper (second trapping).

REFERENCES

1. N. A. Tolstoi, A. M. Tkachuk, and N. N. Tkachuk, Opt. i Spektr. 2, 759 (1957).
2. N. A. Tolstoi, N. N. Tkachuk, M. Ya. Tsenter, Z. S. Mansurova, and A. V. Burlakov, Opt. i Spektr. 1, 719 (1956).
3. N. A. Tolstoi, Doklady Akad. Nauk SSSR 95, 249 (1954).

ROLE OF THE STIMULATING ACTION OF EXCITING LIGHT IN THE KINETICS OF LUMINESCENCE OF ZnS:Cu CRYSTALLINE PHOSPHORS

L. A. Vinokurov and M. V. Fok (pp. 225-231)

Received 21 April 1960

It is shown that when exciting light frees electrons from traps in the ZnS:Cu phosphor, this results in a decrease of electron concentration in deep traps as the intensity of excitation increases. After the excitation stops, the distribution of electrons among traps gradually approaches the equilibrium value. The flash produced by infrared radiation is determined mainly by the freeing of electrons from deep levels. The indicated effects can therefore be found by measuring the magnitude of this flash for different afterglow intensities and at different decay stages.

The stimulating action of the exciting light is known to be due to the following: The exciting light is absorbed by localized electrons and raises them to the conduction band. The existence of this effect has already been shown a long time ago; until recently, however, a few people have taken it into account in their papers. Yet it can play a very important role, particularly for strong excitation.*

*The exciting light can also have a quenching action. (See refs. 1 and 2.)

In the first place, the stimulating action slows down the rate of increase of the stored light sum when the intensity of excitation increases. In the limit it results in a certain constant value of the light sum at large intensities of excitation, even though only a small part of the traps remains filled hereby.

Furthermore, if the crystalline phosphor has a system of electron traps of different depths, the stimulating action results in a sharp departure of the distribution of electrons among traps from its thermal equilibrium value. During the afterglow, when there is no longer any exciting light, the thermal distribution is gradually re-established. This process has a marked effect on the course of luminescence decay.

Finally, the quantum yield of luminescence measured at high luminescence intensities is found to be smaller than at lower intensities. This is due to the fact that some of the quanta are absorbed by electrons in traps[3] rather than by luminescence centers.

Our purpose here is to estimate quantitatively the stimulating action of the exciting light using as an example the luminescence of the ZnS:Cu:Cl crystal. The

same crystal was also used in ref. 4. It has a molar concentration of copper of the order of 10^{-4}. The crystal was excited by light with $\lambda = 365$ mμ, which insured sufficient uniformity of excitation throughout the thickness of the sample. The maximum intensity of excitation taken as 1000 units amounted to

2.2×10^2 erg/cm²/sec or 4×10^{14} quanta/cm²/sec.

Experiments carried out at room temperature and above have shown that electron traps of two types play the leading role in this phosphor. The solution of kinetic equations for this case shows that, in the absence of external quenching, the stored light sum n depends on the excitation intensity E according to

$$n = \sqrt{\frac{aE}{L}}, \tag{1}$$

where

$$L = \frac{\beta w_1 w_2}{\delta_1 w_2 + \delta_2 w_1}. \tag{2}$$

The notation is made clear in Fig. 1. In the calculation we neglected the concentration of free electrons as compared to the concentration of localized ones. We did not neglect the probability of recombination as compared to the capture probability. In the presence of stimulating action, the probabilities of electron release from traps are

$$\left.\begin{aligned} w_1 &= w_{10} + D_1 E, \\ w_2 &= w_{20} + D_2 E. \end{aligned}\right\} \tag{3}$$

It follows from these formulas that when E is sufficiently small, $n \sim \sqrt{E}$, while for E large n is constant. Figure 2 represents the functional relation $n = n(\sqrt{E})$ found experimentally for the ZnS:Cu:Cl crystal at different temperatures. We see that there is a departure from proportionality between n and $\sqrt{E}$ already at relatively low intensities of the order of a few units, i.e., of the order of 10^{12} quanta/cm²/sec. At higher temperatures this departure is less pronounced and appears at higher excitation intensities. This can be explained as follows: The probability of thermal liberation of the electrons increases with increasing temperature; hence the probability of optical liberation becomes comparable to it at high intensities of excitation. At still higher excitation intensities, the light sum no longer depends on the excitation intensity. This means that the probability of optical liberation of electrons from those traps where the main portion of the light sum is concentrated far exceeds the probability of their thermal release from the same traps.

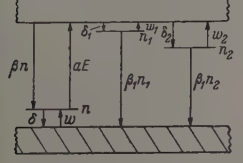

Fig. 1

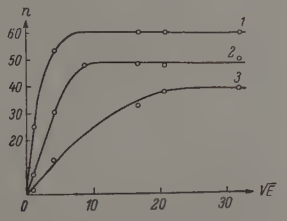

Fig. 2

Fig. 1. Diagram of electronic transitions in a crystalline phosphor with traps of different depth. The letters refer to the probabilities of the corresponding transitions.
Fig. 2. The stored light sum (in relative units) as a function of the square root of the excitation intensity. Temperature of the experiment (in °C): curve 1—25; curve 2—46; curve 3—67.

We shall consider the dependence of the stored light sum on the intensity of excitation. Let

$$w_{20} \gg w_{10}, \tag{4}$$

i.e., let level 1 be appreciably deeper than level 2. If also

$$\frac{\delta_1}{w_1} \gg \frac{\delta_2}{w_2}, \tag{5}$$

then

$$L = L_1 = \frac{\beta w_1}{\delta_1}, \tag{6}$$

and Eq. (1) becomes

$$n = \sqrt{\frac{aE\delta_1}{\beta(w_{10} + D_1 E)}}. \tag{7}$$

If the intensity of excitation is so small that

$$w_{10} \gg D_1 E, \tag{8}$$

then $n \sim \sqrt{E}$. As the intensity of excitation increases, the inequality (8) no longer holds and becomes replaced by its converse. If inequality (5) is still valid here, then in a certain range of values of E, n turns out to be independent of the intensity of excitation. A further increase in the excitation intensity results in a violation of inequality (5). If the relation between the constants is favorable, this inequality can also be replaced by its converse. It is sufficient for this, for example, that

$$\delta_2 \gg \delta_1 \tag{9}$$

and

$$D_1 > D_2. \tag{10}$$

In this case

$$L = L_2 = \frac{\beta w_2}{\delta_2}. \tag{11}$$

If the levels differ so greatly in depth or in the magnitude of the coefficients D that the further inequality

$$w_{20} \gg D_2 E, \tag{12}$$

is satisfied at this intensity, then n will be found again proportional to $\sqrt{E}$. Finally, when this inequality is also replaced by its converse, n is again constant. Thus the magnitude of n must increase in two stages.

It has been shown[4] that this ZnS:Cu:Cl crystal has deep traps with $\varepsilon = 0.66$ ev. It is known, on the other hand, that crystalline ZnS:Cu phosphors have traps with a depth of around 0.33 ev. Hence we deduce that the traps in the ZnS:Cu:Cl crystal must be markedly separated in depth. Even if we assume that they have frequency factors of the same order, then even at the highest temperature used the probabilities of thermal liberation of electrons from these traps will be found to differ by almost five orders of magnitude. We can expect therefore that the stages will be well separated. It is, however, difficult to observe both of these stages since this requires measurements in an extremely wide range of excitation intensities. It is necessary that at minimum illumination the probability of optical liberation of the electrons should be at least one order of magnitude smaller than the probability of their thermal liberation from the deep levels; at maximum excitation intensity it should be an order of magnitude larger than the probability of thermal liberation from the shallow levels. In our case this interval comprises seven orders of magnitude. We could vary the excitation intensity, however, by only three orders.

The question arises in this connection as to which of the two stages we observed experimentally. This can be determined by studying the temperature dependence of

the position of this stage. Indeed, in the first case the value of the stored light sum n is determined by Eq. (7) and in the second case by

$$n=\sqrt{\frac{aE\delta_2}{\beta(w_{20}+D_2E)}}. \qquad (13)$$

These formulas differ only by the subscripts attached to w, δ, and D. Let us therefore consider one of them assuming that the subscript i stands for either 1 or 2. Let us denote by n_∞ the value of n corresponding to the horizontal portion of the stage

$$n_{i\infty}=\sqrt{\frac{a\delta_i}{\beta D_i}}. \qquad (14)$$

Then

$$\frac{n}{n_{i\infty}}\sqrt{\frac{1}{\frac{w_{i0}}{D_iE}+1}}. \qquad (15)$$

We see that this relation depends only on the ratio of the probabilities of thermal and optical liberation of electrons from the given level. If we therefore plot the function n = n(E) on a log-log scale, we shall obtain a curve whose shape does not depend on any parameters and which can be easily determined theoretically. The location of this curve is determined by the scale factors $n_{i\infty}$ and w_{10}/D_1. Therefore, the experimental curves obtained at different temperatures must coincide with different portions of the same theoretical curve.

This curve is shown in Fig. 3 together with the experimental points for the ZnS:Cu:Cl crystal. Circles, squares, and crosses denote data referring to temperatures of 25°, 46°, and 67°C, respectively. We see that all the points fall satisfactorily on the theoretical curve, except for the last two which correspond to the lowest measured values of the light sum. This may possibly be connected with a systematic error in the determination of the light sum, which arises because of the neglect of the later afterglow stages whose brightness is below the sensitivity of the experimental arrangement.

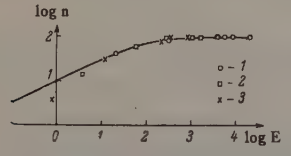

Fig. 3. The logarithm of the stored light sum (in relative units) as a function of the logarithm of the excitation intensity. Solid curve—theoretical; 1—25°C, 2—46°C, 3—67°C.

The depth of the electron traps, as determined from the displacement required to bring the curves into coincidence, was found to be 0.67 ev. This agrees well with results of ref. 4 where the value 0.66 ev was found. We are thus dealing here with the first stage. This means that for low and intermediate values of the excitation intensity used, the main portion of the light sum was concentrated at the deep levels. From these data we may also estimate the magnitude of the stimulating action of the exciting light, i.e., the ratio of the probabilities of optical and thermal liberation of electrons from these levels. For maximum intensity of excitation (4×10^{14} quanta/cm²/sec) at room temperature, the ratio D_1E/w_{10} is about 200.

Such a large stimulating action must, of course, strongly manifest itself in the distribution of electrons among traps of different depths. A calculation actually gives the following values for the concentration of electrons in deep and shallow traps, respectively:

$$\left.\begin{aligned} n_1&=\frac{\delta_1w_2n}{\delta_1w_2+\delta_2w_1}=\sqrt{\frac{aE\delta_1^2w_2}{\beta w_1(\delta_2w_1+\delta_1w_2)}},\\ n_2&=\frac{\delta_2w_1n}{\delta_1w_2+\delta_2w_1}=\sqrt{\frac{aE\delta_2^2w_1}{\beta w_2(\delta_1w_2+\delta_2w_1)}}. \end{aligned}\right\} \qquad (16)$$

These formulas show that when condition (4) holds, there exists an intensity range in which n even decreases with the intensity of excitation.

One of us found experimentally such an effect in the ZnS:Cu:Ni:Cl phosphor.[5] The magnitude of the flash under the action of infrared radiation decreased when the intensity of excitation increased. Since the value of the stored light sum increased hereby, this decrease could only be explained as follows: The infrared liberates electrons from the deep levels while an increase in the intensity of excitation results in a decrease in the concentration of electrons in these levels. At that time, however, theoretical calculations had not yet been carried out. We repeated the same experiments using the ZnS:Cu:Cl crystal and obtained analogous results. On the basis of the calculations performed, more far reaching conclusions may be drawn from these experiments.

We shall compute the brightness of the flash caused by infrared. It is known that the brightness of luminescence is

$$J=\beta nN^-, \qquad (17)$$

where β is a constant and N^- is the concentration of electrons in the conductivity band. It is determined from the concentrations of electrons in different levels and the probabilities of their liberation, and is given by

$$N^-=\frac{aE+w_1n_1+w_2n_2}{\delta_1+\delta_2}. \qquad (18)$$

When infrared is applied, these probabilities change instantaneously, N^- changing with them. At the same time the concentrations of localized electrons and ionized centers decrease gradually rather than abruptly. Therefore, shortly after the application of infrared, the brightness is more stationary and is given by

$$J_{\text{i.r.}}=\beta nN^-_{\text{i.r.}}. \qquad (19)$$

If we assume, in accordance with the above, that infrared liberates electrons from deep levels only, then Eqs. (17) and (19) will differ only in the value of the probability w_1. In the absence of infrared w_1 is determined from Eq. (3) while in the presence of infrared it is given by

$$w_1=w_{10}+D_1E+P_1I, \qquad (20)$$

where P_1 is a constant and I is the infrared intensity. Then the magnitude of the flash will be given by

$$J_{\text{fl.}}=J_{\text{i.r.}}-J=\frac{\beta P_1Innn_1}{\delta_1+\delta_2}. \qquad (21)$$

We see that in order to have a decrease in the flash when the excitation intensity increases, it is insufficient for only n_1 to decrease. It is necessary that the product nn_1 should decrease. Equations (7), (1), and (2) indicate that this product can never decrease. At best it will remain constant but even that will occur only for such a high value of the excitation intensity that the stimulating action of the exciting light would manifest itself even on shallow levels. Thus some other factor has to be taken into consideration to explain the observed effect. The most important limitation which we have introduced in the calculation is the neglect of external quenching, i.e., of the liberation of holes from ionized luminescence centers and of their recombination with localized electrons.

If we take this process into account, we must replace L by L + Q in Eq. (1) where

$$Q=\frac{\beta_1 w}{\delta} \tag{22}$$

(The notation is made clear in Fig. 1.) Equations (16) are then replaced by:

$$\left.\begin{aligned} n_1&=\frac{\delta_1 w_2+\delta_1 Qn}{\delta_1 w_2+\delta_2 w_1+(\delta_1+\delta_2)\,Qn}\,n,\\ n_2&=\frac{\delta_2 w_1+\delta_2 Qn}{\delta_1 w_2+\delta_2 w_1+(\delta_1+\delta_2)\,Qn}\,n. \end{aligned}\right\} \tag{23}$$

This solution is valid only in the case when the probabilities of recombination of electrons and holes are small as compared with the capture probability.

The addition of Q is by itself insufficient to cause nn_1 to decrease with an increase in E. If we assume, however, that external quenching occurs also partly at the expense of the exciting light, i.e., that

$$w=w_0+DE, \tag{24}$$

we find that there may be a range of excitation intensity in which nn_1 decreases. It is sufficient for this that

$$\left.\begin{aligned} &w_0\ll DE,\\ &Qn\ll w_2,\\ &Qn\delta_2\gg\delta_1 w_2+\delta_2 w_1. \end{aligned}\right\} \tag{25}$$

These inequalities are compatible due to the inequalities (14) and (10). The fact that the exciting light liberates holes from the ionized centers of the green luminescence of the ZnS:Cu phosphor has been confirmed by data obtained by one of us.[6] In that paper it was also found that the blue luminescence of ZnS:Cu arises also when the exciting light is absorbed by the green luminescence centers at a low temperature, when the thermal liberation of holes from the "green" centers is impossible.

Let us consider now how the stimulating action of the exciting light will affect afterglow. Obviously, since the exciting light is not acting during the period of the afterglow, such an effect can be only indirect. This does not mean, however, that it is insignificant. As stated above, the stimulating action manifests itself in the decrease in the relative concentration of electrons in deep traps as compared with the thermal equilibrium value. After excitation stops, the electrons move from shallow to deep traps. This manifests itself as follows: When infrared is switched on during the afterglow, the flash is the larger for the more time which elapses between the switching off of the exciting light and the switching on of the infrared. The flash begins to decrease only at the end of the decay. This is seen clearly in Fig. 4, which shows data for the same ZnS:Cu:Cl crystal. One curve refers to +25°C, the other to +46°C.

Figure 4 shows that the maximum of the flash is reached earlier when the temperature is increased. Since a small portion of the stored light sum can be released

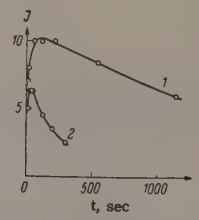

Fig. 4. Magnitude of flash as a function of decay time. Temperature of the ZnS:Cu:Cl single crystal (in °C): curve 1—25; curve 2—46.

during this time, the time required to reach the maximum may be considered to be approximately proportional to the lifetime of the electrons in shallow levels. The depth of these levels can be estimated from the variation of this time with temperature. Such an estimate is, of course, highly inaccurate. On the one hand in the experiment it is necessary to observe such a flash against the background of the decreasing brightness of the afterglow. On the other hand it is clear from theoretical considerations that the time interval for reaching the maximum of the flash should not be exactly proportional to the lifetime of the electrons in the traps, for example, because of the change in the concentration of ionized luminescence centers. In the two series of experiments which we performed with the same ZnS:Cu:Cl crystal, we obtained values for the depth of 0.30 and 0.37 ev. The average of 0.34 ev agrees well with the known value of the depth of the level in the ZnS:Cu phosphor. At the same time the spread in the results is seen to be rather large

We should note that the flash under the action of the infrared is not proportional to the afterglow intensity even if the infrared is turned on at the later afterglow stages, for example half an hour after cessation of excitation. This means that the distribution of electrons among traps of different depths in the ZnS:Cu phosphor practically never assumes its thermal equilibrium value, except possibly in the very latest stages of afterglow which are accessible to observation. Hence the stimulating action of the exciting light must be taken into account not only in the study of the steady state but also in the decay of luminescence of crystalline phosphors.

REFERENCES

1. V. V. Antonov-Romanovskii, Izvest. Akad. Nauk SSSR, Ser. Fiz. 13, 91 (1949).
2. V. V. Antonov-Romanovskii, Izvest. Akad. Nauk SSSR, Ser. Fiz. 15, 637 (1951).
3. L. I. Anikina, Doklady Akad. Nauk SSSR 88, 41 (1953).
4. L. A. Vinokurov and M. V. Fok, Opt. i Spektr. 10, no. 3 (1961), Optics and Spectroscopy 10 (1961), in press.
5. L. A. Vinokurov, Opt. i Spektr. 1, 901 (1956).
6. M. V. Fok, Opt. i Spektr. 2, 475 (1957).

CERTAIN PROBLEMS IN THE THEORY OF THE SCATTERING OF ELECTROMAGNETIC RADIATION BY SUBMICROSCOPIC NONSPHERICAL PARTICLES

A. I. Slutsker and V. A. Marikhin (pp. 232-239)

Received 27 April 1960

The scattering of electromagnetic radiation by particles whose refractive index does not differ greatly from that of the medium is considered. The influence of the nonspherical shape of the particles on the character of the angular dependence of the scattering intensity (the scattering indicatrices) is explained. Two cases of practical importance are analyzed and compared—the scattering of visible light and of x-rays by submicroscopic particles (linear dimensions of order 10-1000 A).

1. At the present time, physical methods based on the phenomena of scattering of electromagnetic radiation in a submicroscopically heterogeneous medium are widely used for the study of diverse subjects: colloidal particles, solutions of large molecules (particularly albumins), crystallites in polymers, two-phase solid systems (alloys) and solutions, atmospheric clouds, discontinuities in solid and liquid substances, etc.

The complete and exact theory of electromagnetic radiation scattering—the theory of Mie[1]—leads to results that are expressed in an extremely awkward and inconvenient form for the analysis and treatment of experimental data (infinite, sometimes slowly converging series). The expressions become particularly complicated for nonspherical particles.[2] Hence it becomes desirable to develop approximate methods for the scattering calculations. The works of Debye, Shifrin, and others[3-6] greatly facilitate the application of scattering theory to experiment, and at the same time extend the possibilities of utilizing scattering in the study of numerous phenomena.

For the experimental study of systems containing submicroscopic heterogeneities (particles), the methods of electromagnetic radiation scattering are used, as a rule, in two spectral regions: visible light (wavelength of the order of 1000 A) and x-rays (wavelength about 1 A). Because of strong absorption, it is extremely difficult to work in the spectral region lying between the limits indicated (i.e., from ~10 A to ~2500-3000 A). But since it is a question of studying submicroscopic particles (with dimensions from 10 A to 1000 A), for which the most complete information can be obtained under conditions such that the wavelength of the applied radiation is not very far from the linear dimension of the particles, the use of the spectral regions directly adjoining the "closed" part becomes necessary.

The case considered in this paper, in which the refractive index of the particulate substance does not differ greatly from the refractive index of the medium, is quite widespread and occurs in practically all the cases enumerated above as well as in a number of others. Actually, for x-rays this condition is always realized, since the refractive index of all substances in the region $\lambda \sim 1$ A differs very little from unity. And in the case of visible light the condition given is also fulfilled quite often, if we take as the media gases, visually transparent liquids, glasses, crystals, and polymers; the heterogeneities appear as inclusions of the very same substances. The absolute values of the refractive indexes for visible light of the substances indicated (m_a) (not near an absorption band) lie in the range from 1 to ~2, and, consequently, the difference in the magnitudes of the refractive indexes is small ($|\Delta m| = |m_i - m_a| \lesssim 1$, where m_i is the absolute refractive index of the particulate substance), and the value of the relative refractive index ($m = m_i/m_a \simeq \frac{1}{2}-2$) likewise is small.

The smallness of the magnitude of the relative refractive index allows one to carry out an approximate calculation of the scattering indicatrix. Shifrin obtained approximate expressions based on general electrodynamic considerations of the problem of the emergence of the secondary (scattered) waves upon excitation by the incident wave of vibrations in the particle, taking into account that for small m it is possible to take the effective field in the particle equal to that in the medium. It is convenient to carry out the scattering calculation for spheres by Shifrin's method; however, for nonspherical particles considered as ellipsoids of revolution cumbersome expressions are obtained, even in this case.

The small value of m permits the computation of the scattering indicatrix if one calculates the result of the interference at a point some distance from the particle of waves that are scattered once and independently from different (small) portions of the particle. Such a method of calculation is applied in the case of x-radiation (e.g., in ref. 7). In the present work it is shown that the use of this method allows the computation of scattering both for visible light and for x-rays. Moreover the method presented turns out to be extremely convenient for the calculation of scattering from nonspherical particles.

2. Using the scheme shown in Fig. 1, we obtain for the intensity of monochromatic unpolarized radiation scattered by a single particle into solid angle $d\omega$, at an angle φ, the following expression:

$$dI = I_0 \frac{9\pi^2}{\lambda^4}\left(\frac{m^2-1}{m^2+2}\right)^2 \cdot \frac{1+\cos^2\varphi}{2} \cdot \left|\int_V e^{i\bar{h}\bar{r}}\,dv\right|^2 \cdot d\omega, \qquad (1)$$

where I_0 is the intensity density of the incident radiation, m is the relative refractive index, λ is the wavelength in the medium, V is the volume of the particle, $\bar{h} = (2\pi/\lambda)(\bar{s} - \bar{s}_0)$ ($\bar{s}_0$ and $\bar{s}$ are unit vectors of the incident wave and the wave scattered at angle φ), and $\bar{r}$ is the radius vector of the volume element (dv) of the particle relative to an arbitrary center (O).

Thus, the form of the angular dependence of the in-

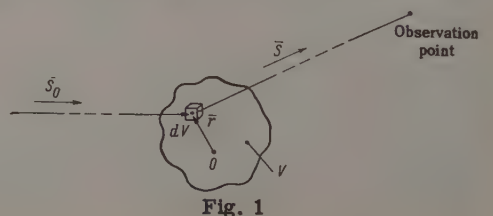

Fig. 1

tensity of the scattered radiation is determined by the integral in Eq. (1) and depends on the geometric characteristics of the particle (its dimensions and shape), and also on its orientation relative to the wave vector of the incident radiation.

Not pausing for a consideration of the scattering from spherical particles, which leads to the well known angular dependence formula

$$\Phi\left(\frac{R}{\lambda}, \varphi\right)=\left\{\frac{4\pi R^3}{3}\left[\frac{3(\cos q - q\sin q)}{q^3}\right]\right\}^2,$$

where R is the radius of the particle, and $q = 4\pi(R/\lambda)\sin(\varphi/2)$, we shall proceed to the nonspherical particles.

We shall approximate the shape anisotropy of the particle by a rectangular parallelepiped and consider the scattering for a particle so situated that one of its sides is perpendicular to the wave vector of the incident radiation, with the plane of observation (the plane passing through the incident and scattered rays) parallel to one of the other two sides (Fig. 2). In this case the calculation of the integral in a rectangular coordinate system becomes simplified, and the following expression is obtained:

$$\Phi\left(\frac{H_x}{\lambda}, \frac{H_y}{\lambda}, \frac{H_z}{\lambda}, \varphi\right)=(8H_xH_yH_z)^2\left(\frac{\sin q_x}{q_x}\right)^2\cdot\left(\frac{\sin q_z}{q_z}\right)^2, \quad (2)$$

where H_x is the half-width of the particle along the incident ray (the "ray" dimension), H_z is the half-width of the particle perpendicular to H_x and lying in the observation plane, H_y is the half-width of the particle in the third dimension, and

$$q_x=4\pi\frac{H_x}{\lambda}\sin^2\frac{\varphi}{2}; \qquad q_z=2\pi\frac{H_z}{\lambda}\sin\varphi. \quad (3)$$

An essential feature of Eq. (2) is that with its help it is easy to trace the influence of the different dimensions of the particle on the form of the indicatrix. Actually, one's attention is drawn to the unusual "separation of variables," i.e., each of the factors that determine the angular dependence contains only one of the particle dimensions. According to the form of the functions $(\sin q/q)^2$ and their angular dependence [Eq. (3)], it can be concluded that the magnitude of H_x/λ determines the forward "elongation" of the indicatrix (the so-called "Mie effect"), which grows with increasing H_x/λ, and the magnitude of H_z/λ determines the "squashing" of the indicatrix, increasing with increasing H_z/λ.

The third dimension (H_y) has no influence on the form of the angular dependence but enters only into the expression for the absolute value of the scattering intensity.

3. We shall now consider the characteristics of the scattering of light and x-rays from submicroscopic particles.

For light, the expression for the scattering indicatrix retains the form

$$dI=I_0\frac{9\pi^2}{\lambda^4}\left(\frac{m^2-1}{m^2+2}\right)^2\cdot\frac{1+\cos^2\varphi}{2}\cdot(8H_xH_yH_z)^2\left[\frac{\sin\left(4\pi\frac{H_x}{\lambda}\sin^2\frac{\varphi}{2}\right)}{4\pi\frac{H_x}{\lambda}\sin^2\frac{\varphi}{2}}\right]^2\times\left[\frac{\sin\left(2\pi\frac{H_z}{\lambda}\sin\varphi\right)}{2\pi\frac{H_z}{\lambda}\sin\varphi}\right]^2\cdot d\omega. \quad (4)$$

Taking $\lambda \approx 5000$ A and having in mind particles of submicroscopic dimensions ($H \gtrsim 1000$ A, i.e., linear dimensions of the particles are less than the radiation wavelength), we obtain $q \gtrsim 2$. Consequently the scattering indicatrix retains appreciable values for all scattering angles down to 180 deg.

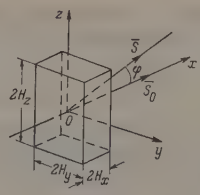

Fig. 2

As an illustration, the scattering indicatrices of a particle having the form of a parallelepiped are shown in Fig. 3 for various orientations of the particle relative to the incident ray and observation plane. It is easily seen that the form of the indicatrix is most sensitive to changes in the "ray" dimension H_x (note the difference between curves 1 and 2); the dependence on H_z is noticeably weaker (see the separation of curves 2 and 3).

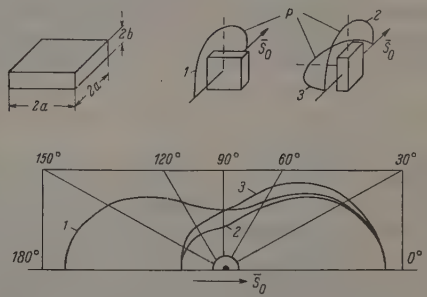

Fig. 3. P—plane of observation; a = 750; b = 150 A; λ = 5000 A. The numbers next to the curves correspond to the orientation number of the particle relative to the primary ray and the plane of observation.

For x-radiation the picture changes substantially, because of the short wavelength of the x-rays (which we take to be about 1 A) in comparison to the linear dimensions of the particles ($H \simeq 10$-1000 A). For values of $H/\lambda \simeq 10$-1000 the basic part of the scattering intensity (~95 percent), which is centered at the zero-point maxima of the functions $(\sin q/q)^2$, lies in the region of extremely small scattering angles (from a few minutes to several degrees). This permits a simplification of the expressions for q, using the condition $\sin\psi \to \psi$ for small ψ. Then we obtain

$$q_x\simeq\pi\frac{H_x}{\lambda}\varphi^2; \quad q_z\simeq 2\pi\frac{H_z}{\lambda}\varphi. \quad (5)$$

Considering further that in the region of a zero-point maximum the function $(\sin q/q)^2$ is approximated quite well by a gaussian dependence of the form $\exp(-q^2/3)$, we get yet another simplification. (A comparison of the functions $(\sin q/q)^2$ and $\exp(-q^2/3)$ is shown in Fig. 4.) Of course, the smooth gaussian curve does not give the secondary maxima characteristic of the function $(\sin q/q)^2$. However, when we realize the smallness of these side maxima in comparison to the zero-point maximum, and also the fact that in the overwhelming majority of experimental studies of x-ray scattering from submicroscopic particles these side maxima have not been successfully observed, it is expedient to use this simple and convenient approximation which describes the basic part of the scattering rather well.

The centering of the scattering in the small-angle region allows one to take the polarization factor (1 +

$\cos^2\varphi)/2$ as equal to 1. Besides this, we shall use the expression for the relative refractive index for x-rays

$$m = 1 - \frac{1}{2}\left(\frac{e^2}{m_e c^2}\right)\cdot\frac{\lambda^2}{\pi}(n_i - n_a), \qquad (6)$$

where e and m_e are the electronic charge and mass, respectively, c is the velocity of light, and n_i and n_a are the electron densities in the particle and in the medium, respectively.

Finally, from Eqs. (1) and (2), taking into account Eqs. (3), (5), and(6), and also using the gaussian approximation, we obtain for the x-ray scattering intensity the expression

$$dI = I_0\left(\frac{e^2}{m_e c^2}\right)^2 (n_i - n_a)^2 (8H_xH_yH_z)^2\, e^{-\frac{\pi^2}{3}\left(\frac{H_x}{\lambda}\right)^2\varphi^4} e^{-\frac{4\pi^2}{3}\left(\frac{H_z}{\lambda}\right)^2\bar{\varphi}^2} d\omega. \qquad (7)$$

The form of the exponential factors in Eq. (7) shows that the first of them (because of its dependence on φ^4) falls in the small angle region considerably more slowly than the second, if $H_x/H_z \gtrsim 50$. Hence we can take the first exponential factor equal to 1 in the neighborhood of the zero-point maximum of the second. Noticing also that $8H_xH_yH_z = V$ (the volume of the particle), we obtain finally

$$dI = I_0\left(\frac{e^2}{m_e c^2}\right)^2 (n_i - n_a)^2 V^2 e^{-\frac{4\pi^2}{3}\left(\frac{H_z}{\lambda}\right)^2\bar{\varphi}^2} d\omega. \qquad (8)$$

It follows from Eq. (8) that the form of the angular dependence of x-ray scattering intensity actually depends only on one linear dimension of the particle (perpendicular to the incident ray and lying in the plane of observation). The latter is illustrated in Fig. 5, from which it is seen that a change in orientation of the particle, while keeping H_z constant, does not influence the angular dependence of the scattering intensity, whereas with a change in H_z, the sharpness of the drop in intensity with angle changes drastically.

Thus we can state the essential difference between visible light and x-rays with respect to the sensitivity of the form of the indicatrix to a change in the linear dimensions of submicroscopic particles: The indicatrix for light scattering depends principally on the "ray" dimension of the particle; the indicatrix for x-ray scattering on the other hand is determined by the dimension perpendicular to the ray and lying in the plane of observation. It seems to us that the rules just stated reflect general properties of the scattering of radiation in the sense that if the wavelength is greater than the linear dimension of the scattering object, then the "ray" dimension (the "lightlike" case) determines the form of the indicatrix, but if the wavelength is less than the size of the object, then the scattering properties are analogous to the case of x-ray scattering from submicroscopic particles.

This unusual property of the "supplementarity" of wavelengths larger and smaller than the dimensions of the scattering particles can create, it seems to us, interesting possibilities for the use of different radiations for studying the same objects, not only with the aim of simply doubling the data, but also for combining radiations in order to obtain more complete and accurate information about particles that are anisotropic in form.

Of course, in real cases we do not have to deal with "angular" particles since, as a rule, they have smooth surfaces and generally approach an ellipsoidal shape. Hence it is necessary to satisfy oneself that the scattering indicatrix calculation for the parallelepiped does not deviate too greatly from the indicatrix for a "round" particle. Besides this, it is necessary to ascertain how correct the method of calculating the interference of the secondary waves emanating from separate parts of the particle is in itself.

In Fig. 6 are presented the scattering indicatrices for light, calculated for a sphere according to the exact theory of Mie (curve 1), for the same sphere according to Eq. (1), and for a cube of the same volume as the sphere, according to Eq. (4).

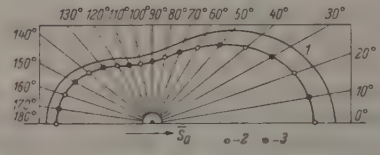

Fig. 6. λ = 5000 A; m = 1.25; curve 1—calculated from Mie's theory for a sphere of R = 600 A; curve 2—calculated from Eq. (1) for the same sphere; curve 3—calculated for a cube having the same volume as the sphere.

The closeness of the two curves for the sphere is evidence that the method of calculating scattering which we have used is quite suitable—the forms of the indicatrices practically coincide (indeed, a knowledge of the indicatrix shape is required, as will be seen later, for the determination of particle dimensions). Moreover, the absolute values of the scattering intensity also do not differ much. And the closeness of the curves for the sphere and cube indicates that the "angularity" of the particle model does not introduce substantial changes in the shape of the calculated indicatrix. Hence, the impression is gained that even nonspherical particles (ellipsoids) can be represented rather well by right-angled "blocks" with unequal edges.

It follows from Fig. 7 that just the same kind of coincidence (for the cases of the sphere and a cube of equal volume) is observed in the comparison of the angular dependences of x-ray scattering.

It seems to us, therefore, that the illustrations presented give credence to the acceptability of the approximations we have used and the suitability of the formulas obtained for application to the analysis of experimental data.

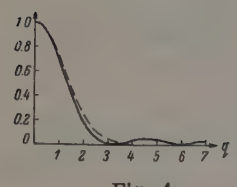

Fig. 4

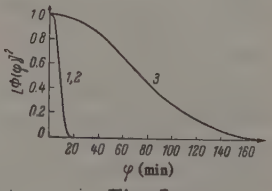

Fig. 5

Fig. 4. Continuous curve—$(\sin q/q)^2$; dashed curve—$\exp(-q^2/3)$.

Fig. 5. The symbols and orientation numbers of the particle are the same as in Fig. 3. a = 100 A; b = 10 A; λ = 1 A.

4. In the experimental study of scattering we always have to deal with extremely large aggregates of submicroscopic particles. In order that we might use the formulas obtained for a single particle in the analysis of the results of the measurement of scattering from groups of particles, the system of particles should satisfy a number of conditions.

In particular, a so-called "loose" packing of the particles must exist, so that the optical density of the system should not be too great. (For more details of these and other conditions see ref. 4.)

The expressions derived in this paper can be applied to a system of loosely-packed, monodispersed, nonspherical, oriented particles. To this end it is recommended that experimental scattering data be treated in the following fashion:

(a) For light scattering. From the degree of forward elongation of the indicatrix, i.e., from the ratio of the scattering intensity in the forward and backward angles, the "ray" dimension of the heterogeneities is determined. For this the relation

$$\frac{I(\varphi)}{I(180^\circ - \varphi)} = f(H_x, \lambda, \varphi),$$

calculated from Eq. (4), can be used. For example, for scattering angles from 20 to 160° we obtain

$$\frac{I(20^\circ)}{I(160^\circ)} = 1024\left[\frac{\sin\left(0.382\frac{H_x}{\lambda}\right)}{\sin\left(12.20\frac{H_x}{\lambda}\right)}\right]^2.$$

The graph of this function is plotted against H_x/λ in Fig. 8.

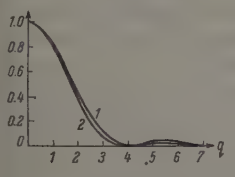

Fig. 7

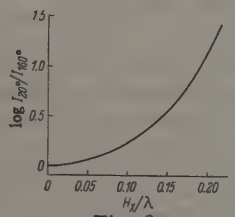

Fig. 8

Fig. 7. Curve 1—calculated for a sphere; curve 2—calculated for a cube having the same volume as the sphere.

(b) For x-ray scattering. From the steepness of the drop in scattering intensity with angle the H_z dimension of the heterogeneities is determined. For this purpose log I is plotted as a function of φ^2 and from the slope of the straight line for a given λ, H_z is calculated.

In order to find the dimensions of the particles in different directions it is necessary to perform a series of measurements of the indicatrix, orienting the system of particles differently relative to the incident ray and plane of observation.

Examples of similar experiments and results of particle shape determinations are to be found in ref. 8.

The authors express their sincere thanks to S. N. Zhurkov for his guidance in and attention to the present work, and also to K. S. Shifrin for his interest in the work and discussion of the results.

REFERENCES

1. G. Mie, Ann. Physik 25, 377 (1908).
2. F. Möglich, Ann. Physik 83, 609 (1927).
3. P. Debye and B. Bueche, J. Appl. Phys. 20, 518 (1949).
4. K. S. Shifrin, "Rasseyanie sveta v mutnoi srede" (The Scattering of Light in a Turbid Medium). Gosudarst. Izd. Tekh. i Teoret. Lit., Moscow-Leningard, 1951.
5. J. Keane and R. Stein, J. Polym. Sci. 20, 327 (1956).
6. I. Ya. Slonim, Opt. i Spektr. 8, 98 (1960), Optics and Spectroscopy 8, 48 (1960).
7. R. James, "Optical Principles of X-Ray Diffraction." Izd. Inostrannoi Lit., Moscow, 1948.
8. S. N. Zhurkov, A. I. Slutsker, and V. A. Marikhin, Fiz. Tver. Tela 1, 1752 (1959), Soviet Phys.—Solid State 1, 1601 (1960).

RAYLEIGH SCATTERING OF LIGHT BY SOLUTIONS OF NITROBENZENE IN HEXANE

D. K. Beridze and M. I. Shakhparonov (pp. 240-248)

Received 10 February 1960

A photoelectric method is described for investigating the intensity I and the degree of depolarization Δ of light scattered through 90°. The i and Δ values of the light scattered by solutions of nitrobenzene in normal hexane are investigated between 10 and 45°C. The scattering intensities are calculated on the basis of fluctuations of the anisotropy, concentration, and density. It is shown that the anomalies in the dependence of I and Δ on temperature and wavelength of the light which are observed in the region of critical opalescence depend on the dimensions and form of the cell and are clearly connected with multiple scattering. It is concluded that to obtain reliable data on the properties of singly scattered Rayleigh radiation close to the critical point, methods of investigation are necessary which allow one to take account of the influence of multiple scattering. It is established that the anisotropic scattering calculated according to the formulas valid for liquids and gases not having an oriented arrangement of the molecules, agrees with experiment within the concentration interval $x_2 \lesssim 0.5$. This indicates that there is no orientation of nitrobenzene molecules in pure nitrobenzene or its solutions in normal hexane.

Investigations of light scattering in the critical region of phase separation of solutions show that deviations from Rayleigh's law are observed close to the point of separation; that is, the intensity of the scattered light I is not proportional to λ^{-4}.[1-3] When the temperature decreases to approximately the critical point, the degree of depolarization of unpolarized light, Δ, and the degree of depolarization of light whose electric vector vibrates in the vertical plane, Δ_v, pass through a minimum, after which they increase sharply.[4,5] There is also a dispersion of the quantities Δ and Δ_v.

These effects have received little attention up to the present time. However a systematic study of the details of light scattering close to the critical region of phase separation is of great interest, because in principle it should allow one to clarify the laws of growth and development of the nuclei of new phases in a homogeneous medium and to understand the nature of critical phenomena.

We have investigated the scattering of light in mixtures of nitrobenzene and hexane from 5 to 45°C, over a wide range of concentrations. Nitrobenzene-hexane mix-

tures have a critical point at 20.3°C and 43.15 mole % nitrobenzene.

METHOD OF INVESTIGATION

The photoelectric method was used to measure the intensity and degree of depolarization of the scattered light.

The experimental apparatus was an improved version of the apparatus described in ref. 14, and permits one to measure the relative intensity I and degree of depolarization Δ of monochromatic radiation scattered by liquids over a broad range of temperatures. The schematic of the apparatus is given in Fig. 1. Light from a SVDSh-250-3(1) mercury lamp passes through condenser K_1(f = 50 mm) and long focus lens L_2(f = 200 mm) and is focused on the cross-shaped cell C, which is filled with the liquid being investigated. Diaphragms d_1, d_2, d_3, and d_4 are used to define a uniform beam of light. An iris diaphragm between lens L_2 and the cell makes it possible to vary the half-aperture angle from 3 to 1°. The lamp, condenser K_1, the diaphragms, and lens L_2 are mounted on an OSK-1 optical bench. The cell is enclosed in a thermostat T. The accuracy of the thermostatic control is ±0.005°. The position of the cell in the thermostat is rigidly fixed with the help of supports.

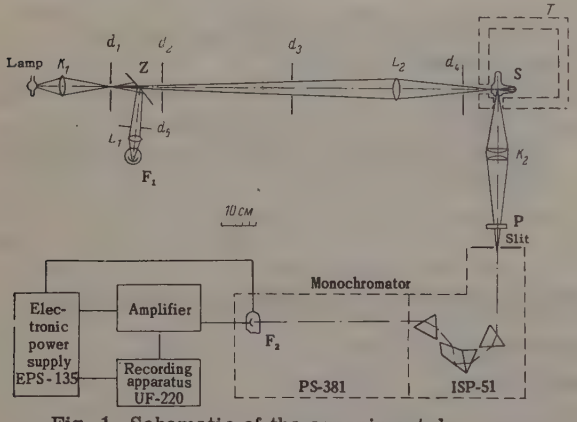

Fig. 1. Schematic of the experimental apparatus.

The light scattered through 90° with respect to the direction of the incident beam passes through the window of the cell, a thin layer of the thermostating liquid (water or alcohol), the glass window of the thermostat, and then, by means of condenser K_2(f = 94 mm), is focused on the slit of an ISP-51 spectrograph (condenser K_2 is diaphragmed down to an aperture of 50 mm). Polaroids are located at P, between K_2 and the spectrograph; the slit-width of the spectrograph is 0.4 mm. To avoid parasitic light in the region between window of the thermostat T, lens K_2, and the slits of the cell, the beam of scattered light was enclosed within a tube.

After passage through the optical system of the spectrograph the spectrum of the scattered light is recorded with the help of a PS-381 photoelectric apparatus. In our apparatus, the ISP-51 spectrograph and the PS-381 exit collimator fulfill the functions of a monochromator. An FEU-17 photomultiplier is located behind the slit of the exit collimator. Our FEU-17 had an integral photocathode sensitivity of 80 μa/lumen and a dark current of 10^{-10} μa for a voltage of 800 volts. The photocurrent was then fed to a dc amplifier. The signal from the amplifier went to a mirror galvonometer, which was part of a UF-220 photorecording apparatus. The power for the photomultiplier, the amplifier, and the recording apparatus comes from the EPS-135 electronic power supply included with the PS-3 A detailed description of the PS-381 photoelectric attachment is given in ref. 7.

A barretter is included to stabilize the lamp. The lamp normally operates at 4a and 74 volts. The lamp is located inside a large jacket and is air-cooled.

To exclude the influence of the fluctuations of the intensity of the light beam, produced by a change of the position of the light spot between the lamp's electrodes or by other causes, we used optical feedback.[7] A mirror z, with an opening, was placed in the light beam at an angle of 45°. The main part of the light beam passes through the mirror in the direction of the cell; a small fraction, reflected by the mirror, was focused by the le L_1 on the photoelement F_1 (Fig. 1) which, through a variable resistor, is connected between the second and fourt dynodes of photomultiplier F_2. The resistor and the aperture of diaphragm d_3 are chosen so that a change o voltage on the lamp electrodes of 5 to 7 volts has only a insignificant influence on the galvanometer reading in th recording apparatus.

The measurement of the relative intensity of the scattered light was carried out in the following manner:

It is known that the photocurrent of the photomultiplier depends not only on the intensity of the scattered light, but also on its state of polarization. The polarization of the light incident on the photocathode is changed on passing through the apparatus. In order to exclude th influence of polarization, we used two Polaroids perpendicular to the optic axis of the apparatus in front of the slit of the spectrograph. Both Polaroids were mounted a special holder and could be rotated around the optic axis. The positions of the Polaroids could be read with an accuracy of ±0.1°.

In measuring the relative intensity of the scattered light, the principle planes of both polaroids were located parallel to one another at an angle of 45° to the vertical. The beam of light transmitted through the Polaroids in this case is always plane polarized at an angle of 45°. I intensity equals

$$I' = \frac{k_1 k_2}{2} I, \qquad (1$$

where k_1 and k_2 are the absorption coefficients respectively of the first and second Polaroids, and I is the light intensity scattered by the liquid.

Thus, to determine the relative intensity of the scattered light it is sufficient to observe the ratio between th galvanometer readings for the liquid being investigated and a standard liquid. Benzene was used as the standard liquid. The intensity of light scattered by benzene at 25° at a given wavelength λ was taken as unity. Each measurement was repeated 3 to 5 or more times. The control measurements of the scattering intensity of benzene were carried out each time at the beginning and end of the experiments.

Measurements of the degree of depolarization were carried out in the following fashion: The Polaroid closest to the spectrograph was fixed securely so that its principle plane formed an angle of 45° with the vertical. The second Polaroid was rotated about its optical axis. In the initial position, the principle plane of the second Polaroid was set parallel to the first. Then the second Polaroid was turned 45° to the right or to the left. The light which entered the spectrograph then had an intensity equal respectively to

$$I_1 = \frac{k_1 k_2}{2} I_s \text{ and } I_2 = \frac{k_1 k_2}{2} I_s. \qquad (2$$

Since when the second Polaroid is rotated 45° to the right or to the left, the light beam in both cases is plane polarized at an angle of 45°, the fluxes I_1 and I_2 experience identical losses by reflection in the spectral apparatus. Thus, the degree of depolarization is determined as the ratio of the readings of the apparatus for the two positions of the Polaroid:

$$\Delta = \frac{I_x}{I_z} = \frac{I_1}{I_2}.$$

Each measurement of Δ was repeated no fewer than five times.

In the calculating the values of I and Δ, it was assumed that the photocurrent depends linearly on the intensity of the light. To verify the linearity of the photomultiplier we used a system of three Polaroids contained in a special holder. The outside Polaroids are held rigidly fixed and the middle one is rotated around the optic axis of the apparatus, and the angle of rotation is read off. In the initial position the principle planes of all three Polaroids are parallel. On rotation of the middle Polaroid through an angle α, the light flux transmitted through the polaroids varies as $\cos^4 \alpha$. The first Polaroid guarantees the independence of the result of the measurement on the state of polarization of the light beam incident on it. The last Polaroid, as has already been stated, avoids the necessity of taking account of changes in polarization of the light introduced by the apparatus and of the sensitivity characteristics of the photocathode. We used a photomultiplier which deviated less than 1.5% from linearity. The correction for the finiteness of the aperture was made according to the Gans formulas. The correction for the refraction index C_n was calculated according to the formula

$$\sqrt{C_n} = \frac{n_i\left(1 - \frac{a_i}{r}\right)}{n_{st.}\left(1 - \frac{a_{st.}}{r}\right)}, \qquad (3)$$

where

$$a_i = r_1 \frac{n_i - n_1}{n_i} + \left(r_1 \frac{n_1}{n_i} + r_2\right)\frac{n_1 - n_2}{n_1}$$

$$+ \left[\left(r_1 \frac{n_1}{n_i} + r_2\right)\frac{n_2}{n_1} + r_3\right]\frac{n_2 - n_3}{n_2}. \qquad (4)$$

The meaning of the symbols r, r_1, r_2, and r_3 is clear from Fig. 2; n_i is the refractive index of the liquid investigated, n_{st} is the refractive index of the standard liquid (benzene), n_1, n_2, n_3 correspond to the refractive indices of the thermostat liquid, the glass, and air. The value of a_{st} is computed from (4) by substituting n_{st} for n_i.

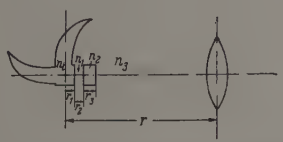

Fig. 2. The meaning of the parameters of Eqs. (3) and (4).

In our experiments $r_1 = 20.0$ mm, $r_2 = 5.0$ mm, $r_3 = 30.0$ mm, $r = 155$ mm, $n_1 = 1.340$; $n_2 = 1.524$.

The correction C_n varied from 1.025 in the experiments with nitrobenzene to 0.820 in the experiments with normal hexane. The correction for the active volume of the liquid C_v was not taken into account, since under the conditions of the experiments $C_v = 1$ with sufficient accuracy.

The cell, the method of preparation, and the removal of dust from the liquid were the same as in ref. 8. After chemical purification and multiple distillation, the nitrobenzene and normal hexane had the following properties: nitrobenzene—boiling point (at 760 mm Hg) 210°C, $n_D^{20} = 1.5525$, freezing point = +5.75°C; hexane—boiling point (at 760 mm Hg) 68.7°C, $n_D^{20} = 1.3748$.

The accuracy of the measurements for I and Δ, after all corrections have been made, is estimated at ±2%. In the immediate vicinity of the critical point, where small changes of temperature result in large changes in scattering intensity, the accuracy decreases to ±5 percent.

RESULTS AND DISCUSSION

Tables 1 and 2 and Figs. 3 and 4 give values of the intensity I and the degree of depolarization Δ of the light scattered by individual liquids and solutions. These values were obtained by interpolation from graphs constructed from the experimental data. For each liquid sample, the scattering was investigated for two wavelengths of the incident radiation—yellow ($\lambda = 5780$ A) and green ($\lambda = 5460$ A). In those cases where the values measured for the lines 5460 and 5780 A are the same within the limits of experimental error, the results presented are for $\lambda = 5780$ A.

Table 1. The Relative Intensity I* and the Degree of Depolarization Δ of Light ($\lambda = 5780$ A), Scattered by Nitrobenzene and Hexane at Different Temperatures

t (°C)	n.-C_6H_{14}		$C_6H_5NO_2$	
	I	$\Delta \cdot 100$	I	$\Delta \cdot 100$
+5	0.25	10.7	—	—
10	0.27	10.1	3.17	73.0
15	0.28	9.6	3.18	72.5
20	0.29	9.2	3.19	72.0
25	0.30	8.8	3.19	71.5
30	0.31	8.4	3.20	71.0
35	0.32	8.0	3.20	70.5
40	0.34	7.7	3.21	70.0
45	0.35	7.4	3.21	69.5
50	0.36	7.0	3.22	69.0

*The intensity of light scattering ($\lambda = 5780$ A) by benzene at 25°C is taken as 1.

According to ref. 9, at 20° and $\lambda = 5890$ A, I = 0.36 and $\Delta \times 10^2 = 9.0$ for hexane. For nitrobenzene,[6] I = 3.30, $\Delta \times 10^2 = 72.0$. Comparison of these values with the data in Table 1 shows that very good agreement is observed (only the values of I are somewhat lower than those given in refs. 6 and 9; this disagreement may be explained by the fact that the correction for the refractive index was not taken into account in the previous measurements).

In solutions close to the phase separation point, an increase in Δ is observed over a rather broad range of concentrations. In the region of critical opalescence, Δ increases very strongly. Dispersion of Δ and significant deviations from the $I \sim \lambda^{-4}$ law are observed simultaneously, and the intensity of the scattered light passes through a maximum. Similar maxima in $I = f(t)$ curves were observed previously by Drickamer and Cataldi[10] in the liquid-vapor critical region of ethylene and ethane.

Out supplementary investigations of I and Δ for light scattered by a solution in the region of critical opalescence in cells of different dimensions and forms showed that the effects observed depend strongly on both the dimensions and form of the cell. In particular, the appearance of maxima in the $I = f(t)$ curves, and also the growth and dispersion of Δ, are connected with multiple scattering, which is particularly important near the

Table 2. The Relative Intensity I* and the Degree of Depolarization Δ of Light Scattered by Nitrobenzene-Hexane Mixtures**

$x_2 = 0.380$; λ = 5780 Å			$x_2 = 0.489$; λ = 5780 Å			$x_2 = 0.588$					$x_2 = 0.686$					$x_2 = 0.683$; λ = 5780 Å			$x_2 = 0.8512$; λ = 5780 Å		
							λ = 5780 Å		λ = 5460 Å			λ = 5780 Å		λ = 5460 Å								
t (° C)	I	Δ · 100	t (° C)	I	Δ · 100	t (° C)	I	Δ · 100	I	Δ · 100	t (° C)	I	Δ · 100	I	Δ · 100	t (° C)	I	Δ · 100	t (° C)	I	Δ · 100
14.0	12.80	5.2	19.4	141.0	1.36	20.01	525.0	28.6	390.0	38.6	19.6	422.0	1.86	422.0	2.09	19.2	63.3	0.47	5.7	2.40	3.68
15.0	12.04	5.9	19.5	123.0	1.00	20.06	615.0	17.9	495.0	30.3	19.7	387.0	1.58	387.0	1.80	19.5	56.8	0.50	6.0	2.35	3.70
20.0	8.60	8.4	19.6	110.0	0.96	20.1	705.0	13.6	584.0	20.6	19.8	353.0	1.51	365.0	1.57	20.0	52.5	0.53	8.0	2.13	3.77
25.0	6.30	10.4	19.7	99.0	1.00	20.2	581.0	8.70	581.0	11.2	19.9	323.0	1.29	332.0	1.41	21.0	43.5	0.62	10.0	1.92	3.85
30.0	4.64	12.1	19.8	89.0	1.04	20.3	510.0	6.00	510.0	7.7	20.0	293.0	1.19	301.0	1.31	22.0	32.0	0.72	15.0	1.46	4.04
35.0	4.36	13.7	20.0	77.0	1.12	20.4	459.0	4.50	459.0	5.80	20.5	143.0	0.89	147.0	0.97	23.0	25.7	0.85	20.0	1.09	4.24
40.0	4.04	15.1	21.0	49.0	1.32	20.5	412.0	3.50	412.0	4.50	21.0	81.0	0.78	83.0	0.86	25.0	17.4	1.36	25.0	0.85	4.43
45.0	3.78	16.3	22.0	38.0	1.52	20.6	370.0	2.80	370.0	3.60	22.0	60.0	0.79	62.0	0.86	30.0	8.50	2.56	30.0	0.73	4.63
—	—	—	25.0	21.0	2.16	20.7	329.0	2.40	329.0	2.90	23.0	44.0	0.80	45.0	0.86	35.0	5.90	3.51	35.0	0.65	4.86
—	—	—	30.0	12.6	3.36	20.8	294.0	2.05	294.0	2.45	24.0	34.4	0.89	35.0	0.99	40.0	5.20	4.20	40.0	0.61	5.11
—	—	—	35.0	9.7	4.74	21.0	230.0	1.60	230.0	2.00	25.0	28.0	1.12	28.0	1.13	45.0	4.90	4.93	45.0	0.59	5.39
—	—	—	40.0	7.7	6.08	22.0	116.0	1.00	116.0	1.17	30.0	14.1	2.40	14.1	2.41	—	—	—	—	—	—
—	—	—	45.0	6.4	7.52	23.0	73.0	0.90	73.0	0.96	35.0	10.0	2.68	10.1	2.69	—	—	—	—	—	—
—	—	—	—	—	—	25.0	42.0	1.13	42.0	1.16	40.0	8.25	3.96	8.30	3.97	—	—	—	—	—	—
—	—	—	—	—	—	30.0	19.3	1.86	19.3	1.86	45.0	7.00	5.20	7.10	5.21	—	—	—	—	—	—
—	—	—	—	—	—	35.0	12.5	2.46	12.5	2.47	—	—	—	—	—	—	—	—	—	—	—
—	—	—	—	—	—	40.0	9.4	3.26	9.4	3.27	—	—	—	—	—	—	—	—	—	—	—
—	—	—	—	—	—	45.0	7.0	4.60	7.0	4.60	—	—	—	—	—	—	—	—	—	—	—

*cf. note to Table 1.
*x_2 is the mole fraction of n-C_6H_{14} in the mixture.

critical point. Multiple scattering in the region of critical opalescence has a particularly great influence on the results of measurements of I in large cells. If the total path length of the incident and scattered light in the cell is decreased to 5-7 mm, multiple scattering in the critical region decreases, but remains significant. On approaching the temperature of phase separation the increase in the intensity of scattering I is accompanied by an increase of secondary parasitic scattered light from the walls of the cell. This has a particularly strong effect on the results of the measurement of the degree of depolarization, leading to an increase in the values of Δ.

As the dimensions of the cell decrease, the parasitic scattering from the walls of the cell shows a relative increase.

A satisfactory correction for parasitic scattering is very difficult to make. Methods of correcting for multiple scattering have not been discovered as yet.[11] Our experiments therefore lead to the conclusion that our data on the scattering of light in the region of critical opalescence, as well as other data in the literature, (see, for example, ref. 3) cannot be used as a reliable basis for an analysis of the molecular structure of solutions in the region of critical opalescence, i.e., in the region in which deviations from Rayleigh's law are apparently observed. It is necessary to work out new methods for investigating I and Δ in the critical region which permit one to take account of the effects of multiple scattering. Only then can reliable data be obtained on the properties of singly scattered light in the critical region.

Using the formulas

$$I = I_{an.} + I_d + I_c, \quad (5)$$

$$I_{an.} = \frac{13}{6} I \frac{\Delta}{1+\Delta}, \quad (6)$$

$$I_d = \sum_i x_i I_d^i \quad (7)$$

we calculated the scattering intensities of light due to fluctuations of the density I_d, the anisotropy I_{an}, and the concentration I_c. In formula (7), I_d^i denotes the scattering intensity of light due to fluctuations in the density of the individual liquid component i (x_i is the mole fraction of this component in the solution).

The calculations according to (5)-(7) were carried out only in the temperature range in which the initial assumptions of the Smoluchowski-Einstein light scattering theory are applicable, i.e., (a) the scattering by concentration fluctuations can be considered completely polarized and (b) it is possible to neglect correlations of the fluctuations in adjacent volume elements, and multiple scattering.

Let us examine separately the cases of the individual liquids and solutions.

Individual liquids. Out data on the dependence of I_d of hexane and nitrobenzene on temperature agree with the measurements of Vuks and his co-workers.[6,9] The anisotropic scattering of nitrobenzene, in disagreement with

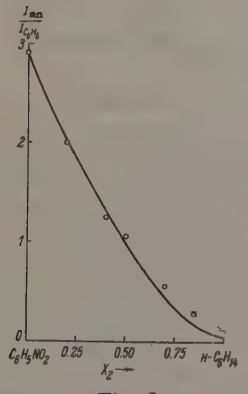

Fig. 3

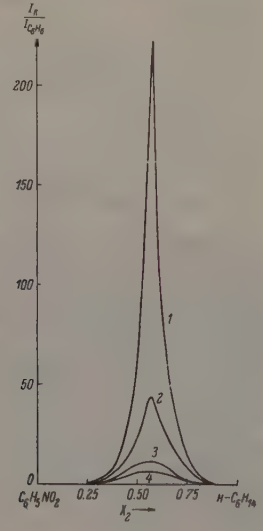

Fig. 4

Fig. 3. Dependence of the intensity of the anisotropic scattering of light I_{an} on concentration in nitrobenzene-hexane mixtures at 25° C. Solid line—experiment (from the data of Table 2); points—calculated from formula (9), cf. note to Table 1.

Fig. 4. Isotherms of the Intensity of light scattering on fluctuations of the concentration I_R for different temperatures. Temperature (in °C): curve 1—21; curve 2—25; curve 3—35; curve 4—45, cf. note to Table 1.

ref. 6, remains constant between 10 and 50°C. If we use the values of the principle semiaxes (a_1, a_2, and a_3) of the polarizability ellipsoid of nitrobenzene found in ref. 12 (the values given in the studies of Stewart and Folkman[13] are not correct), then the theoretical calculation of the values of I_{an} of nitrobenzene for $\lambda = 5460$ A, according to the formula not taking account of the orientational ordering of the molecules, is

$$I_{an} = \frac{13}{45} \frac{8\pi^4}{R_{C_6H_6}\lambda^4} \left(\frac{n^2+2}{3}\right)^4 N_1\gamma^2, \qquad (8)$$

where n is the refractive index, $R_{C_6H_6}$ is the scattering coefficient of benzene for $\lambda = 5460$ A and 25°C, N_1 is the number of molecules in 1 cm³, and

$$\gamma^2 = \frac{1}{2}[(a_1-a_2)^2 + (a_1-a_3)^2 + (a_2-a_3)^2],$$

leads to the value $I_{an} = 2.90$, which agrees with the I_{an} value calculated from the experimental data of Table 1. In ref. 14 it was shown that expression (8) should contain the factor $[(n^2+2)/3]^4$, and not $[(n^2+2)/3]^2$ as follows from the conclusions of Rokar, which we believe to be erroneous. (Refer, for example, to ref. 15, p. 230.) For the scattering coefficient of benzene at 25°C and $\lambda = 5460$ A we took the "high" value $R_{C_6H_6} = 16.3 \times 10^{-6}$. The "low $R_{C_6H_6}$ values in the literature[16] are erroneous because they have not been corrected for the refractive index.[17]

Thus, the calculations made with the aid of (8) indicate the absence of any orientational regularity of the molecules in liquid nitrobenzene. This conclusion is confirmed by data on the dielectric strength of nitrobenzene in static fields. As is known, the dipole moment of a molecule of liquid nitrobenzene μ_1, calculated from Onsager's formula, is equal to μ_g—the dipole moment of a nitrobenzene molecule in the gas phase.[18]

The literature contains assertions[19,20] that molecular complexes with antiparallel dipoles exist in liquid nitrobenzene. This however, would lead to Onsager μ_1 values which are lower than the μ_g values; this also has not been confirmed.

Solutions. Figure 3 shows an isotherm of the anisotropic scattering in solutions of nitrobenzene-hexane at 25°C. The anisotropic scattering of light remains constant over the temperature interval studied and depends only on concentration. The calculation of the values of I_{an} according to the formula

$$I_{an} = \frac{13}{45} \frac{8\pi^4}{R_{C_6H_6}\lambda^4} \left(\frac{n^2+2}{3}\right)^4 N_1 \sum x_i\gamma_i^2 \qquad (9)$$

with the use of an effective value of $\gamma^2_{C_6H_{14}}$ for hexane calculated with the aid of (8), starting from the value of $I_{an} = 0.054$ (on the basis of the data of Table 1), leads to excellent agreement with experiment (Fig. 3) within the concentration interval $x_2 \leq 0.5$. This indicates that in solutions of nitrobenzene-hexane the molecules of nitrobenzene are randomly oriented. Deviations from (9) for $x_2 > 0.5$ can be attributed to orientation of the hexane.

Figure 4 represents the intensity of scattered light as a function of the fluctuations of the concentration I_c from the composition of the solution at 21, 25, 35, and 45 C. Our data qualitatively agree with the measurements of Roshchina, and essentially complement them in the concentration region from x = 0.4 to 0.7 where the dependence of I_c on concentration and temperature present by far the greatest interest. A quantitative comparison of the results of ref. 21 with our data could not be carried out since in ref. 21 the units of measurement of the quantity I are not shown.

REFERENCES

1. R. Fürth, Sitzungsber, Akad. Wiss. Wien **124**, 577 (1915); Proc. Roy. Soc. **A224**, 119 (1954).
2. L. S. Ornstein and F. Zernike, Proc. Acad. Sci. Amsterdam **17**, 793 (1914); Physik Z. **19**, 137 (1918); Ibid. **27**, 761 (1926).
3. Ch. Quantie, Proc. Roy. Soc. **A224**, 90 (1954).
4. A. Rousset, Ann. phys. **5**, 9 (1936).
5. R. S. Krishnan, Proc. Indian Acad. Sci. **5**, 577 (1937).
6. M. F. Vuks and I. I. Bilenko. Zhur. Eksptl. i Teoret. Fiz. **23**, 105 (1952).
7. N. O. Chechik, S. M. Fainshtein, and T. M. Lifshitz, "Elektronnye Umnezhiteli" (Electron Multipliers). Gosudarst. Tekh. Izd., Moscow-Leningrad, 1957.
8. M. I. Shakhparonov and N. G. Shlenkina, Zhur. Fiz. Khim **28**, 1950 (1954).
9. M. F. Vuks and M. I. Dadenkova, Sb. "Stroenie i Fizicheskie Svoistva Veshestva v Zhidkom Sostoyanii," (The Structure and Physical Properties of Substances in the Liquid State) p. 185. Izd. Kiev. Gosudarst. Univ., Kiev, 1954.
10. H. A. Cataldi and H. G. Drickamer, J. Chem. Phys. **18**, 650 (1950).
11. G. V. Rozenberg, Uspekhi Fiz. Nauk **69**, 57 (1959), Soviet Phys.—Uspekhi **2**, 666 (1959).
12. C. LeFévre and R. LeFévre, J. Chem. Soc. 1577 (1954).
13. Landolt-Börnstein, Zahlenwerte und Funktionen, Bd. 1, T. 3, p. 511. Berlin, 1951.
14. L. P. Zatsepina and M. I. Shakhparonov, Vestnik Moskov. Univ. No. 4, 9 (1960).
15. M. V. Vol'kenshtein, "Molekulyarnaya Optika" (Molecular Optics). Gosudarst. Tekh. Izd., Moscow-Leningrad, 1951.
16. G. Vaucouleurs, Ann. phys. **6**, 213 (1951).
17. C. I. Carr and B. H. Zimm, J. Chem. Phys. **18**, 1616 (1950).
18. C. Böttcher, "Theory of Electric Polarisation." (Elsevier), Van Nostrand, New York, 1952.
19. A. Pekar, Izvest. Akad. Nauk SSSR, Ser. Fiz. **24**, 18 (1960).
20. V. Hückel, "Teoreticheskie Osnovy Organicheskoi Khimii" (Theoretical Principles of Organic Chemistry), Vol. 2, p. 229. Izd. Inostrannoi Lit., Moscow, 1958.
21. G. P. Roshchina, Sb. "Termodinamika i Stroenie Rastvorov" (Thermodynamics and the Structure of Solutions), p. 233, Izd. Akad. Nauk SSSR, Moscow, 1959.

IMAGING OF SEPARATE LINEAR OBJECTS OF DIFFERENT WIDTH AND CONTRAST WITH SURROUNDING FIELD BY A COMBINATION OF AN OPTICAL SYSTEM AND A GRANULAR LAYER

L. P. Moroz (pp. 249-256)

Received 25 January 1960

Equations are obtained which enable one to solve the problem of finding the required (threshold) values for the parameters which characterize the optical system of the instrument, the granular layer (image receiver), and the object, and also the problem of compensation of changes in one group of parameters by changes in another group of parameters. A method is proposed to characterize the quality of instruments which operate on the basis of optical imaging.

LIGHT DISTRIBUTION IN THE DIFFRACTION IMAGE OF A BLACK STRIP OR A BRIGHT SLIT

Consider an optical system imaging a black strip of width δ situated in a bright field. Let the contrast of the strip with thebackground(i.e.,the ratio of the difference between the bright and dark over the bright) be $K = 1$. If β is the linear magnification of the optical system, the width of the geometrical image will be $\delta' = \beta\delta$. Furthermore, if the optical system satisfies the sine conditions, then $\beta = \delta'/\delta = A/A'$, where A is the numerical aperture of the system seen from the object side and A′ is the numerical aperture seen from the image side. The field in which the strip is situated can be considered as composed of a multitude of self-luminous slits all of which are parallel to the strip.

Let E be the illumination intensity of the geometrical images of the slits. Because of its finite aperture the optical system images each of the self-luminous slits into a diffused band with a certain intensity distribution. The (diffraction) image of a black strip by an optical system will therefore represent a certain intensity distribution $\mathcal{E}(x')$ which is obtained by superposition of the light intensities of the multitude of the diffused bands. The x′ axis is perpendicular to the strip and we assume that the origin of the x′ coordinate coincides with the intersection of the x′ axis with the axis of the strip image.

We normalize the intensity $\mathcal{E}(x')$ and set $\mathcal{E}(x')/E = \varkappa_T(x')$. In order to find the form of the function $\varkappa_{OT} = \varkappa_T(\delta', x' = 0)$, that is, the relation between the relative intensity of the axial points of the image of a black strip and the strip width. Starting out from the well known light distribution in the diffraction image of a bright line it is possible, by means of graphical integration, to obtain a plot of $\varkappa_{OT}$ as a function of δ'. This function can be closely approximated by

$$\varkappa_{OT} = \varkappa_T(\delta',\ x' = 0) = 10^{-\frac{\delta'}{c_i'}}, \qquad (1)$$

where $c_i' = 1.14\lambda/A'$ and λ is the wavelength of the light.[1,2] If we split the function $\varkappa_{OT}$ into two sections, a more convenient approximation is obtained for each of them. For values $0.28 \leqslant \delta'/c_i' \leqslant \infty$ (the corresponding range of the function is $0.5 \geqslant \varkappa_{OT} \geqslant \infty$) we obtain

$$\varkappa_{OT} = \varkappa_T(\delta',\ x' = 0) = \frac{0.14}{\frac{\delta'}{c_i'}}. \qquad (2)$$

For values $0 \leqslant \delta'/c_i' \leqslant 0.28$ (the corresponding range of the function is $1.0 \geqslant \varkappa_{OT} \geqslant 0.5$) the approximation becomes

$$\varkappa_{OT} = \varkappa_T(\delta',\ x' = 0) = 1 - 1.79\frac{\delta'}{c_i'}. \qquad (3)$$

$\varkappa_{OT}$ \ $\frac{\delta'}{c_i'}$	0.0	0.056	0.112	0.140	0.280	0.420	0.560	0.840	1.400	2.520	∞
By direct integration	1.00	0.89	0.78	0.74	0.50	0.33	0.22	0.13	0.09	0.05	0.00
From Eq. (1)	1.00	0.88	0.77	0.73	0.52	0.38	0.28	0.14	0.04	0.00	0.00
From Eq. (2)	—	—	—	—	0.50	0.33	0.25	0.17	0.10	0.05	0.00
From Eq. (3)	1.00	0.90	0.80	0.75	0.50	—	—	—	—	—	—

In the accompanying Table the values of the function $\varkappa_{OT} = \varkappa_T(\delta', x' = 0)$ obtained by direct integration are compared with the values obtained from the approximation formulas (1), (2), and (3).

It can be readily shown that the relation between the relative intensity $\varkappa_{OC} = \varkappa_C(\delta', x' = 0)$ of the axial points of the image of a bright strip in a dark background and the width of the geometrical image of the strip is given by

$$\varkappa_{OC} = \varkappa_C(\delta',\ x' = 0) = 1 - \varkappa_T(\delta',\ x' = 0). \qquad (4)$$

The function $\varkappa_{OT} = \varkappa_T(\delta', x' = 0)$ gives the relation between the relative intensity of the axial points of the actual image of a black strip in a bright background and the width δ' of the geometrical image of this strip. Starting out from this function one can obtain the function $\varkappa_T(\delta' = \text{const.}, x')$ which gives the relative intensity distribution of the actual image of the black strip in a bright background for any given width δ' of the geometrical image.

It can be readily shown that for points located within the geometrical image of the black strip (i.e., $x' \leqslant \delta'/2$), we have

$$\varkappa_T(\delta' = \text{const},\ x')\Big|_{x' \leqslant \frac{\delta'}{2}} = \frac{1}{2}\varkappa_{OT}\left(2\left(\frac{\delta'}{2} - x'\right)\right) + \frac{1}{2}\varkappa_{OT}\left(2\left(\frac{\delta'}{2} + x'\right)\right), \qquad (5)$$

whereas for points outside the geometrical image (i.e., $x' \geqslant \delta'/2$), we have

$$\varkappa_T(\delta' = \text{const},\ x')\Big|_{x' \geqslant \frac{\delta'}{2}} = \frac{1}{2} + \frac{1}{2}\varkappa_{OC}\left(2\left(x' - \frac{\delta'}{2}\right)\right) + \frac{1}{2}\varkappa_{OT}\left(2\left(x' + \frac{\delta'}{2}\right)\right),$$

or, using Eq. (4),

$$\varkappa_T(\delta' = \text{const},\ x')\Big|_{x' \geqslant \frac{\delta'}{2}} = 1 - \frac{1}{2}\varkappa_{OT}(2x' - \delta') + \frac{1}{2}\varkappa_{OT}(2x' + \delta'). \qquad (6)$$

Equations (5) and (6) are of general character; they apply to any device which is capable of transforming a

luminous line into a diffuse band with a certain intensity distribution (as for example, an optical system with image aberrations, a granular screen, etc.).

In the case of images of bright strips (slits) in a dark background, the transition from the relation giving the intensity of the axial points of the actual images of strips of different widths as a function of the strip width to the relation giving the intensity distribution for a strip of given width is accomplished with the help of the relation

$$\varkappa_c(\delta' = \text{const},\ x')\Big|_{x' \leqslant \frac{\delta'}{2}} = \frac{1}{2}\varkappa_{oc}\left(2\left(\frac{\delta'}{2}+x'\right)\right)+\frac{1}{2}\varkappa_{oc}\left(2\left(\frac{\delta'}{2}-x'\right)\right),$$

or, using Eq. (4),

$$\varkappa_c(\delta' = \text{const},\ x')\Big|_{x' \leqslant \frac{\delta'}{2}} = 1-\left(\frac{1}{2}\varkappa_{oT}(\delta'+2x')+\frac{1}{2}\varkappa_{oT}(\delta'-2x')\right)$$

$$= 1-\varkappa_T(\delta' = \text{const},\ x')\Big|_{x' \leqslant \frac{\delta'}{2}}. \qquad (7)$$

Similarly,

$$\varkappa_c(\delta' = \text{const},\ x')\Big|_{x' \geqslant \frac{\delta'}{2}} = \frac{1}{2}\varkappa_{oT}\left(2\left(x'-\frac{\delta'}{2}\right)\right)-\frac{1}{2}\varkappa_{oT}\left(2\left(x'+\frac{\delta'}{2}\right)\right)$$

$$= 1-\varkappa_T(\delta' = \text{const},\ x')\Big|_{x' \geqslant \frac{\delta'}{2}}. \qquad (8)$$

Thus, knowing the dependence $\kappa_{OT} = \kappa_T(\delta',\ x' = 0)$ of the relative intensity of the axial points of the image of a black strip on the width of the strip, one can obtain the relative intensity distribution of the image of a black strip in a bright background or of a bright slit in a dark background for any given strip or slit widths.

The same problem can obviously also be solved [using relation (4)] if the relation is known between the relative intensity of the axial points of the image of a bright slit and the slit width.

The relative intensity distribution $\kappa_T(\delta' = \text{const.},\ x')$ of the diffraction image of a black strip in a bright background can be obtained by substituting into Eqs. (5) and (6) the values of κ_{OT} obtained either from a graph (plotted from the tabulated values) or from the analytical approximations given by Eq. (1) or by Eqs. (2) and (3). Using Eqs. (7) and (8), one can in a similar way obtain the relative intensity distribution $\kappa_C(\delta' = \text{const.},\ x')$ of the diffraction image of a bright slit.

Using the approximation formula (1) the relative intensity distribution is found to be given by

$$\varkappa_T\Big|_{\frac{x'}{\delta'} \leqslant \frac{1}{2}} = \frac{1}{2}\left(10^{-\frac{\delta'}{c_i'}\left(1+\frac{2x'}{\delta'}\right)}+10^{-\frac{\delta'}{c_i'}\left(1-\frac{2x'}{\delta'}\right)}\right),$$

$$\varkappa_T\Big|_{\frac{x'}{\delta'} \geqslant \frac{1}{2}} = 1+\frac{1}{2}\left(10^{-\frac{\delta'}{c_i'}\left(1+\frac{2x'}{\delta'}\right)}-10^{-\frac{\delta'}{c_i'}\left(\frac{2x'}{\delta'}-1\right)}\right). \qquad (9)$$

From Eqs. (9) is it seen that

$$\varkappa_T = \varkappa_T\left(\frac{\delta'}{c_i'},\ \frac{x'}{\delta'}\right).$$

If the optical system satisfies the sine condition, that is, $\delta'A' = \delta A$, then κ_T can also be expressed in terms of the width δ of the imaged strip, the numerical aperture A seen from the object side, and the corresponding coordinate x, by means of Eqs. (9), provided we put

$$\frac{\delta}{c_i} = \frac{\delta'}{c_i'},\quad \frac{x}{\delta} = \frac{x'}{\delta'},$$

where

$$c_i = \frac{1.14\lambda}{A}.$$

or, more explicitly,

$$\frac{\delta'}{c_i'} = \frac{\delta'}{\frac{1.14\lambda}{A'}} = \frac{\delta}{\frac{1.14\lambda}{A}} = \frac{\delta}{c_i}.$$

In using the approximations (2) and (3), Eq. (2) should be substituted into Eqs. (5) and (6) for values of the argument of κ_{OT} greater than or equal to $0.28c_i'$ (δ' being given in units of c_i'); for argument values less than $0.28c_i'$, Eq. (3) should be used.

A comparison of the results of the calculations shows that Eqs. (9) can be actually applied to describe the relative intensity distribution of the diffraction image of a black strip (and consequently also of a bright slit) of arbitrary width. Also the approximate equations (2) and (3) can be used and in some cases give even better approximations. However, approximation (1), used to derive Eqs. (9), is found more convenient in further investigations in connection with the properties of a granular screen.

BRIGHTNESS ON THE AXIAL POINTS OF THE DIFFRACTION IMAGE OF A STRIP (OR, SLIT) PROJECTED ONTO AN IMAGE RECEIVER

Let us assume that the real image of the black strip is projected onto an image receiver with scattering properties (for example, a granular screen: photographic layer, television screen, etc.). As a result of the scattering properties the screen will transform every luminous line (i.e., narrow luminous slit of width dx') into a diffuse band with a certain intensity distribution. To find the intensity of the axial points of the projected image we consider the field surrounding these points as a multitude of luminous lines parallel to the axis. It is then possible to find the intensity $\mathcal{E}_{s\,OT}$ of the axial points as a superposition of the intensities $d\mathcal{E}_s$ resulting from the individual luminous lines.

In a previous paper[3] we investigated the reproduction by a granular screen (photosensitive layer) of the details of a series of gray strips (i.e., darker strips surrounded by brighter strips) projected directly onto the screen. In this paper we will investigate the case where the intensity distribution that is projected onto the screen is the diffraction image of a black strip (or of a strip of arbitrary grayness) formed by an aberrationless optical system with a circular aperture.

The intensity $\mathcal{E}_{s\,OT}$ at an axial point of the image of a black strip after transformation by the dispersing screen is given by

$$\mathcal{E}_{s\,OT} = 2\int_0^\infty \varkappa_T(x')\,d\mathcal{E}_s, \qquad (10)$$

where $\kappa_T(x')$ is the relative intensity of the optical image of the black strip (δ' = const.) projected onto the screen as a function of the distance x' from the axis of this image ($\kappa_T(x') = \mathcal{E}(x')/E$, where $\mathcal{E}(x')$ is the intensity at a point x' and E is the intensity of a point in the surroundings of the image of the black strip and sufficiently far removed from it).

In the case where the diffraction image of the black strip is formed by an aberrationless optical system of circular aperture the function $\kappa_T(x')$ is given by the ap-

proximate expressions (9); $d\mathcal{E}_s(x')$ is the intensity of a point of the diffuse band, into which the granular screen transforms a narrow bright slit of width dx′, at a distance x′ from the slit.

Frieser[5] investigated the intensity distribution $d\mathcal{E}_s$ for the specific case where the granular screen is a photographic layer and found that

$$d\mathcal{E}_s = \frac{2.3}{c_s} E\, 10^{-\frac{2x'}{c_s}} dx'. \qquad (11)$$

where E is the intensity of the projected bright slit (and coincides with the E introduced previously) and c_s is a constant characteristic of the layer. This constant, the so-called effective constant of the granular layer, has the dimension of a length and can be easily determined experimentally.[3,4]

On substituting into Eq. (10) the values of $\kappa_T(x')$ and dE_s obtained from Eqs. (9) and (11) an expression is obtained for the relative intensity on a granular screen of the axial points of the diffraction image of a black strip formed by an aberrationless optical system with circular aperture projected onto the dispersing screen.

Using simple transformations one obtains

$$\kappa_{s\,OT} = \frac{\mathcal{E}_{s\,OT}}{E} = \frac{2}{E}\int_0^\infty \kappa_T(x')\, d\mathcal{E}_s = \frac{2.3}{c_s}\left(\int_0^\infty 10^{-\frac{\delta'+2x'}{c_i'}-\frac{2x'}{c_s}} dx' + \int_0^{\frac{\delta'}{2}} 10^{-\frac{\delta'-2x'}{c_i'}-\frac{2x'}{c_s}} dx' - \int_{\frac{\delta'}{2}}^\infty 10^{-\frac{2x'-\delta'}{c_i'}-\frac{2x'}{c_s}} dx' + 2\int_{\frac{\delta'}{2}}^\infty 10^{-\frac{2x'}{c_s}} dx'\right) = \frac{10^{-\frac{\delta'}{c_i'}} - \frac{c_s^2}{c_i'^2} 10^{-\frac{\delta'}{c_s}}}{1-\frac{c_s^2}{c_i'^2}}. \qquad (12)$$

We recall that $\delta'/c_i' = \delta/c_i$ and $c_i' = \beta c_i$, where $c_i = 1.14\lambda/A$. Equation (12) can therefore be rewritten as

$$\kappa_{s\,OT} = \frac{\mathcal{E}_{s\,OT}}{E} = \frac{10^{-\frac{\delta}{c_i}} - \frac{c_s^2}{\beta^2 c_i^2} 10^{-\frac{\delta/c_i}{c_s/\beta c_i}}}{1-\frac{c_s^2}{\beta^2 c_i^2}} = f\left(\frac{\delta}{c_i}, \frac{c_s}{\beta c_i}\right). \qquad (12')$$

The contrast between an axial point of an image of a black strip formed by a combination of an aberrationless optical system with a circular aperture and a dispersing screen, and a point of the field at a sufficiently large distance from the image is given by

$$K_{s\,OT} = 1 - \frac{\mathcal{E}_{s\,OT}}{E} = 1 - \frac{10^{-\frac{\delta}{c_i}} - \frac{c_s^2}{\beta^2 c_i^2} 10^{-\frac{\delta/c_i}{c_s/\beta c_i}}}{1-\frac{c_s^2}{\beta^2 c_i^2}} = 1 - f\left(\frac{\delta}{c_i}, \frac{c_s}{\beta c_i}\right). \qquad (13)$$

For convenience we will repeat the meaning of the symbols in Eqs. (12), (12′), and (13): δ is the width of the imaged black strip, β is the linear image-to-object magnification, $\delta' = \beta\delta$ is the width of the geometrical image of the strip, $c_i = 1.14\lambda/A$ is a constant of the optical system, λ is the wavelength of the image-forming light, A is the numerical aperture of the system seen from the object side, $c_i' = 1.14\lambda/A' = \beta c_i$, A′ is the numerical aperture of the system seen from the image side, and c_s is a characteristic constant of the granular layer which is determined experimentally (for photographic layers this constant can be, for example, of the order of 10-30μ, or it can be larger or smaller).

The contrast $K_{s\,OT} = 1 - \kappa_{s\,OT}$ given by Eq. (13) represents at the same time the relative intensity $\kappa_{s\,OC} = \mathcal{E}_{s\,OC}/E$ of an axial point of the image of a bright strip (slit) on a dark background formed by the combination of an optical system and a granular screen [see Eqs. (4)-(8)], that is,

$$K_{s\,OT} = 1 - \kappa_{s\,OT} = \kappa_{s\,OC}. \qquad (13')$$

In this case E represents the intensity of the slit image in the absence of diffraction and the scattering properties of the screen or, in the presence of these effects, for a sufficiently wide slit.

In the limiting cases Eq. (12) reduces to

$$\kappa_{s\,OT}\Big|_{\substack{\frac{c_s}{c_i'}\to 0}} = 10^{-\frac{\delta'}{c_i'}}, \qquad (14a)$$

$$\kappa_{s\,OT}\Big|_{\substack{\frac{\delta'}{c_i'}\to\infty \\ \frac{c_s}{c_i'}\to\infty}} = \frac{-\frac{c_s^2}{c_i'^2} 10^{-\frac{\delta'}{c_s}}}{1-\frac{c_s^2}{c_i'^2}} = 10^{-\frac{\delta'}{c_s}}. \qquad (14b)$$

We note that $c_i' = 1.14\lambda/A'$. Corresponding to the limiting case $c_i' \to 0$ is thus $\lambda \to 0$, that is, the case where diffraction by the optical system can be neglected.

Expressions (12) and (13) can be used to determine experimentally the effective constant c_s of the granular layer. All one has to do is to perform the experiment under conditions which exclude or make negligible the effect of diffraction by the aberrationless optical system which is used to project the strip or slit onto the granular layer. Indeed, measuring, by means of microphotogrammetry, the value of $\kappa_{s\,OT}$ (or, of $\kappa_{s\,OC} = 1 - \kappa_{s\,OT}$) for a given $\delta' = \text{const.}$ we can, using Eq. (12), determine graphically the value of c_s corresponding to the measured value $\kappa_{s\,OT}$. Repeating the experiment for different values of $\delta' = \text{const.}$, it is possible to find the best effective value of the constant c_s of the granular layer for a given range of values of δ′ for layers for which the constant varies with the width δ′.

REPRODUCTION OF GRAY STRIPS (STRIPS DARKER OR BRIGHTER THAN THEIR BACKGROUND) BY THE COMBINATION OF OPTICAL SYSTEM AND RECEIVER

The combination of optical system and image receiver—the granular screen—reduces in the final image the contrast between the strip and its surrounding field (as contrast between two points we define[1] the ratio $(B_1 - B_d)/B_1$). In the case of a black strip in a bright background the object contrast is K = 1 and the contrast between an axial point of the final image of the strip and the surrounding field becomes $K_{s\,OT}$.

We have shown previously[1] that the relation between the contrast $K_{s\,T}$ of the final image of a gray object in a brighter field and the contrast $K_{s\,OT}$ of the final image of a black object is always given by

$$K_{s\,T} = KK_{s\,OT}, \qquad (15)$$

so that the quantity

$$\frac{1}{K_{s\,OT}}=\frac{K}{K_{s\,T}} \qquad (15')$$

is a measure of the contrast reduction by the instrument.

When a gray object is in a field darker than the object and has a contrast K with the field, the contrast $K_{s\,C}$ of the final image is given by

$$K_{s\,C}=\frac{KK_{s\,OT}}{KK_{s\,OT}+(1-K)}=\frac{K_{s\,T}}{K_{s\,T}+(1-K)}, \qquad (16)$$

so that,

$$\frac{K_{s\,T}}{K_{s\,C}}=K_{s\,T}+(1-K)=1-K(1-K_{s\,OT}), \qquad (16')$$

that is, for a given contrast K between object and field, the contrast $K_{s\,C}$ in the final image of a gray object which is brighter than the surrounding field is always greater than the contrast $K_{s\,T}$ in the final image for the case when the object is darker than the surrounding field.

Equations (15)-(16′) apply also for the specific case when the object is a gray strip. For the case of an aberrationless optical system of circular aperture and an image receiver in the form of a granular screen, the contrast $K_{s\,OT}$ is given by Eq. (13). Using Eqs. (13), (13′), (15), and (16) we obtain

$$K_{s\,OT}=1-\varkappa_{s\,OT}=\varkappa_{s\,OC}=\frac{K_{s\,T}}{K}=\frac{\frac{1}{K}-1}{\frac{1}{K_{s\,C}}-1}$$

$$=1-\frac{\frac{c_s^2}{\beta^2c_i^2}10^{-\frac{\delta}{c_i}}-10^{-\frac{\delta}{c_i}}}{\frac{c_s^2}{\beta^2c_i^2}-1}=f\left(\frac{c_s}{\beta c_i},\ \frac{\delta}{c_i}\right). \qquad (17)$$

Equation (17) enables one to solve the problem of finding the necessary (threshold) values for each of the quantities appearing in it, if all the other parameters are given. It also permits the solving of the problem of compensation of changes of one group of parameters by changes in another group.

One part of Eq. (17), namely,

$$K_{s\,OT}=1-\varkappa_{s\,OT}=\varkappa_{s\,OC}=\frac{K_{s\,T}}{K}=\frac{\frac{1}{K}-1}{\frac{1}{K_{s\,C}}-1} \qquad (17')$$

is of general character, that is, it applies also to an instrument in which the optical system has arbitrary image aberrations and the image receiver is of arbitrary dispersing properties. They also apply to the case when the instrument is imaging a number of different objects of arbitrary shape, provided that in the final image the contrast is determined between an object point and a point of the surrounding field about which there is an area of constant intensity of dimensions, which are at least of the order of magnitude of the effective diffusion disc into which a point source is imaged by the instrument. It is therefore convenient to characterize the instrument (that is, the combination of optical system and image receiver) by the experimentally obtained graph of κ_s or $\kappa_{s\,OC}$ for a given object point as a function of a parameter which is characteristic of the dimensions of the object. In particular, for an object in the form of a strip or slit it is convenient to characterize the instrument by a graph of the experimentally obtained function $\kappa_{s\,OT}(\delta'=\beta\delta)$ or $\kappa_{s\,OC}(\delta'=\beta\delta)$. Using Eq. (17) it is then possible to use this graph for finding the necessary (threshold) values of parameters which characterize the instrument and object.

When the objects are at a large distance from the instrument the variables which determine $K_{s\,OT}$ assume the following form. If f is the focal length of the optical system, D is the diameter of its entrance pupil, and h is the object distance, then

$$\beta=\frac{f}{h};\quad A=\frac{D}{2h};\quad C_i=\frac{1.14\lambda}{A}=\frac{2.28h\lambda}{D}$$

and

$$\frac{c_s}{\beta c_i}=0.44\frac{D}{f}\frac{c_s}{\lambda}; \qquad (18a)$$

$$\frac{\delta}{c_i}=\frac{0.44\cdot D\cdot\delta}{\lambda\cdot h}. \qquad (18b)$$

In the accompanying Figure a graph is shown of the function $K_{s\,OT}(\delta/c_i)$ calculated from Eq. (17) for different values of $c_s/\beta c_i$ = const.

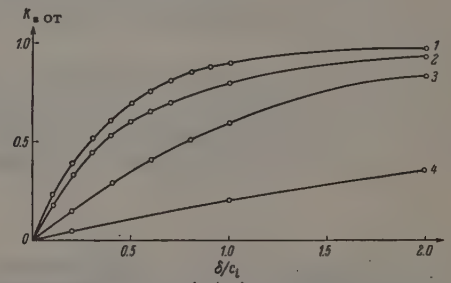

The function $K_{s\,OT}(\delta/c_i)$ for different values of $c_s/\beta c_i$ = const. Values of $c_s/\beta c_i$: curve 1—0; curve 2—1.0; curve 3—2.0; curve 4—10.0.

REFERENCES

1. L. P. Moroz, Opt. i Spektr. 5, 692 (1958).
2. L. P. Moroz, Zhur. Nauch. i Priklad. Fot. i Kinematografii 3, 443 (1958).
3. L. P. Moroz, Zhur. Nauch. i Priklad. Fot. i Kinematografii 4, 81 (1959).
4. L. P. Moroz, Zhur. Nauch. i Priklad. Fot. i Kinematografii 4, 367 (1959).
5. H. Frieser, Phot. Korr. 92, 52 (1956).

AN ANALYSIS OF METHODS OF ALIGNING MAGNETIC ELECTRON MICROSCOPES

Yu. V. Vorob'ev (pp. 257-264)

Received 25 March 1960

A method is proposed for the direct measurement of the distance by which the magnetic fields of dispersion of the lenses deflect the axis of the objective. An appropriate expression has been derived. It has been shown that magnetic alignment of the objective can be employed only within restricted limits and that with this method of alignment additional chromatic aberration appears.

The imperfect production of magnetic electron lenses and also the presence of various heterogeneities in the materials used lead to a displacement of the axes of the objective and the projection lenses relative to each other, which sharply impairs the quality of the image in magnetic electron microscopes.

Similar effects also are elicited by magnetic fields of dispersion that arise in the space between the objective and the projection lenses as a result of imperfect magnetic shielding of the microscope.

Various methods have been proposed for the detection of nonuniaxialities of the electron lenses of a microscope and their correction, the majority of which are based on the observation of the movement of the image on the screen when the current in the lenses is changed and when the accelerating voltage is varied. By this same means it is also possible to determine the inclination of the condenser relative to the axis of the objective lens of the microscope.

In the present work a theoretical analysis is made of these methods. It is shown how it is possible to detect and evaluate in terms of the movement of the image both nonuniaxiality of the optic elements and optical effects produced by magnetic deflecting fields in the column of the microscope.

MOVEMENT OF THE IMAGE IN A NONUNIAXIAL TWO-LENS SYSTEM IN THE PRESENCE OF MAGNETIC DEFLECTING FIELDS

In the present discussion we shall use the following basic parameters of the magnetic lenses. Let us consider the paraxial trajectory of an electron U(z), which in front of the lens is parallel to the optic axis and at unit distance from it (see Fig. 1, where f_0 and f_1 are the focal lengths, and z_0 and z_1 are the abscissas of the two principal planes). Together with the paraxial trajectory U(z) we shall use the value of V(z), its mirror image relative to the plane of symmetry of the lens.

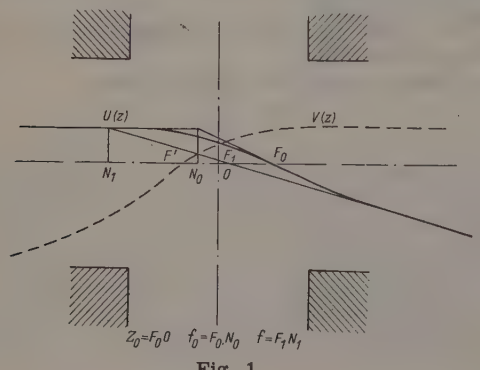

Fig. 1

Let us introduce a stationary system of rectangular coordinates XYz, the origin of which we shall place at the center of the objective lens and the z axis of which we shall direct along its optic axis. Along with the stationary system let us employ a movable system of coordinates xyz, which rotates with the electrons around the z axis. In addition,

$$X = x\cos\theta - y\sin\theta,$$
$$Y = x\sin\theta + y\cos\theta,$$

where θ is the angle of rotation of the electrons around the optic axis.

Let us now place an object in the forward focal plane of the objective ($z = -z_0$) and assume that the illuminating beam is parallel to and directed at an angle to the optic axis of the objective, such that the tangents of the angles of inclination of the trajectories before entering the objective are determined by the values of X_0' and Y_0'. Let us consider an arbitrary point on the object with the coordinates X_a and Y_a, the movement of the image of which we shall study. The equation for the trajectory passing through this point can be written in the form

$$\left.\begin{aligned} x &= C_1U(z) + C_2V(z);\\ y &= H_1U(z) + H_2V(z);\\ C_1 &= \frac{f_1}{f_0}(X_a\cos\theta_a + Y_a\sin\theta_a); \quad C_2 = f_1X_0';\\ H_1 &= \frac{f_1}{f_0}(-X_a\sin\theta_a + Y_a\cos\theta_a); \quad H_2 = f_1Y_0'. \end{aligned}\right\} \qquad (1)$$

Here θ_a is the angle of rotation of the trajectory by the field of the objective up to the object. On leaving the objective the trajectory becomes linear and the equation for it has the form

$$x = -\frac{C_1}{f_1}(z - z_1) + f_1X_0'; \quad y = -\frac{H_1}{f_1}(z - z_1) + f_1Y_0'.$$

or in the stationary system of coordinates

$$X = x\cos\theta_0 - y\sin\theta_0,$$
$$Y = x\sin\theta_0 + y\cos\theta_0,$$

where θ_0 is the angle by which the field of the objective rotates the trajectory.

In the space between the objective and the projector there may be deflecting magnetic fields arising either as a result of imperfect magnetic shielding of the column of the microscope (fields of dispersion) or as a result of special magnetic coils used to align the microscope. The deflecting fields change the trajectory, the equation for which takes on the form

$$X = x\cos\theta_0 - y\sin\theta_0 + e_{X(z)},$$
$$Y = x\sin\theta_0 + y\cos\theta_0 + e_{Y(z)},$$

where e_X and e_Y are the deflection in the directions of the X and Y axes.

Let us now pass to the projector. Let the center of the projection lens be at a distance H from the center of the objective. Let us introduce a stationary system of coordinates $\bar{X}\bar{Y}\bar{z}$ associated with the projector, with the z axis directed along the axis of the projector (Fig. 2).

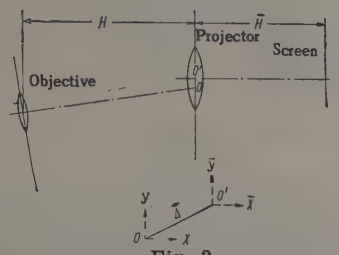

Fig. 2

Then when z = H we have

$$X = X + \Delta_x; \quad Y = Y + \Delta_y; \quad X' = X' + \gamma_x; \quad Y' = Y' + \gamma_y,$$

where Δ_x, Δ_y are the projections of the shift in the axis of the projector relative to the axis of the objective, and γ_x and γ_y are the corresponding angles of inclination of the axes of the projector and the objective.

The equation of the trajectory that we are considering can be written in the form

$$\bar{x} = \bar{C}_1 U_1 + \bar{C}_2 \bar{V}; \quad \bar{y} = \bar{H}_1 U + \bar{H}_2 \bar{V},$$

where $\bar{U}(\bar{z})$ and $\bar{V}(\bar{z})$ are fundamental solutions for the projection lens determined similarly to the solutions U and V.

The condition of continuity of the trajectory and its slope permit calculation of the constants $\bar{C}_1$, $\bar{C}_2$, $\bar{H}_1$, and $\bar{H}_2$, which for large distances between the objective and the projector in comparison with the focal length have the form

$$\left.\begin{aligned}
\bar{C}_1 &= -\cos\theta_0 \frac{C_1}{f_1} H + \sin\theta_0 \frac{H_1}{f_1} H + e_X(H) + \Delta_x;\\
\bar{H}_1 &= -\sin\theta_0 \frac{C_1}{f_1} H - \cos\theta_0 \frac{H_1}{f_1} H + e_Y(H) + \Delta_y;\\
\frac{\bar{C}_2}{f_1} &= -\cos\theta_0 \frac{C_1}{f_1} + \sin\theta_0 \frac{H_1}{f_1} + e'_X(H) + \gamma_x;\\
\frac{\bar{H}_2}{f_1} &= -\sin\theta_0 \frac{C_1}{f_1} - \cos\theta_0 \frac{H_1}{f_1} + e'_Y(H) + \gamma_y.
\end{aligned}\right\} \quad (2)$$

Assuming now that the screen is at a distance H from the center of the projection lens, we find the position of the image of the point on the object that is under consideration. We obtain

$$\left.\begin{aligned}
X &= -\cos\theta_p \frac{\bar{C}_1 H}{f_1} + \sin\theta_p \frac{\bar{H}_1 H}{f_1},\\
Y &= -\sin\theta_p \frac{\bar{C}_1 H}{f_1} - \cos\theta_p \frac{\bar{H}_1 H}{f_1},
\end{aligned}\right\}$$

where θ_p is the angle of rotation of the trajectory by the field of the projector. In deriving formula (3) we also assumed that the distance of the screen from the center of the projector was large in comparison with its focal length.

We shall now investigate the question of how the image of the point on the object that is under consideration moves when the accelerating voltage changes.

When the accelerating voltage changes from V to $V^1 = V + \Delta V$, there naturally is also a change in all the optic constants of the lenses, which we shall designate in the further discussion by the superscript (1). The equation for the new main trajectory of the electrons passing through the same point on the object with the coordinates X_a and Y_a is written in the form

$$x^{(1)} = C_1^{(1)} U^{(1)} + C_2^{(1)} V^{(1)}; \quad y^{(1)} = H_1^{(1)} U^{(1)} + H_2^{(1)} V^{(1)}. \quad (4)$$

Let us return to the initial conditions. Assuming that the inclination of the illuminating beam is constant, we find that $C_2^{(1)} = X'_0 f_1^{(1)}$ and $H_2^{(1)} = Y'_0 f_1^{(1)}$

Further, in the plane of the object we have

$$\left.\begin{aligned}
X_a &= x_a^{(1)} \cos\theta_a^{(1)} - y_a^{(1)} \sin\theta_a^{(1)};\\
Y_a &= x_a^{(1)} \sin\theta_a^{(1)} + y_a^{(1)} \cos\theta_a^{(1)}.
\end{aligned}\right\} \quad (5)$$

As we have already noted above, the object is located in the forward focal plane, where $V(-z_0) = 0$, $V'(-z_0) = 1/f_0$. Furthermore, from the Wronskian we have that $U(-z_0) = f_0/f_1$. Thus we can write

$$U_a^{(1)} = U^{(1)}(-z_0) = U^{(1)}(-z_0^{(1)}) + U^{(1)'}(-z_0^{(1)})(-z_0 + z_0^{(1)})$$

$$= \frac{f_0^{(1)}}{f_1^{(1)}} + U'(-z_0)\,\Delta z_0; \qquad V_a^{(1)} = V^{(1)}(-z_0) = \frac{\Delta z_0}{f_0}.$$

Substituting (4) now in (5) and assuming that

$$C_1^{(1)} = C_1 + \Delta C_1; \quad H_1^{(1)} = H_1 + \Delta H_1; \quad f_0^{(1)} = f_0 + \Delta f_0;$$

$$f_1^{(1)} = f_1 + \Delta f_1; \quad \theta_a^{(1)} = \theta_a + \Delta\theta_a,$$

after several transformations we obtain

$$\left.\begin{aligned}
\Delta C_1 &= -C_1\left(\frac{\Delta f_0}{f_0} - \frac{\Delta f_1}{f_1} + \frac{f_1}{f_0} U^{(1)}(-z_0)\,\Delta z_0\right) - X'_0 \frac{f_1^2}{f_0^2}\Delta z_0 + H_1 \Delta\theta_a;\\
\Delta H_1 &= -H_1\left(\frac{\Delta f_0}{f_0} - \frac{\Delta f_1}{f_1} + \frac{f_1}{f_0} U'(-z_0)\,\Delta z_0\right) - Y'_0 \frac{f_1^2}{f_0^2}\Delta z_0 - C_1 \Delta\theta_a.
\end{aligned}\right\} \quad (6)$$

Differentiating now Eqs. (2) we have

$$\left.\begin{aligned}
\Delta\bar{C}_1 &= \frac{H}{f_1}\left[(\sin\theta_0 C_1 + \cos\theta_0 H_1)\,\Delta\theta_0 - \cos\theta_0\left(\Delta C_1 - C_1\frac{\Delta f_1}{f_1}\right)\right.\\
&\qquad \left. + \sin\theta_0\left(\Delta H_1 - H_1\frac{\Delta f_1}{f_1}\right)\right] + \Delta e_X(H);\\
\Delta\bar{H}_1 &= \frac{H}{f_1}\left[(-\cos\theta_0 C_1 + \sin\theta_0 H_1)\,\Delta\theta_0 - \sin\theta_0\left(\Delta C_1 - C_1\frac{\Delta f_1}{f_1}\right)\right.\\
&\qquad \left. - \cos\theta_0\left(\Delta H_1 - H_1\frac{\Delta f_1}{f_1}\right)\right] + \Delta e_Y(H).
\end{aligned}\right\} \quad (7)$$

Differentiating Eqs. (3) now and eliminating from the equations obtained the values C_1, H_1, $\bar{C}_1$, $\bar{H}_1$, ΔC_1, ΔH_1, $\Delta\bar{C}_1$, and $\Delta\bar{H}_1$ with the aid of (1)-(3), (6), and (7), we obtain the following expressions for the projections on the coordinate axes of the distance by which the image is shifted:

$$\left.\begin{aligned}
\Delta X &= \frac{\Delta m}{m} X - \Delta\theta Y + A,\\
\Delta Y &= \Delta\theta X + \frac{\Delta m}{m} Y + B,
\end{aligned}\right\} \quad (8)$$

where

$$A = m_p\left\{-\cos\theta_p\left[\Delta\theta_a(e_Y(H) + \Delta_y) - \frac{\Delta m_0}{m_0}(e_X(H) + \Delta_x)\right.\right.$$

$$\left. + \left(\cos\theta_0 X'_0 \frac{f_1^2}{f_0^2}\Delta z_0 - \sin\theta_0 Y'_0 \frac{f_1^2}{f_0^2}\Delta z_0\right) m_0 + \Delta e_X(H)\right]$$

$$+ \sin\theta_p\left[-\Delta\theta_a(e_X(H) + \Delta_x) - \frac{\Delta m_0}{m_0}(e_Y(H) + \Delta_y)\right.$$

$$\left.\left. + \left(\sin\theta_0 X'_0 \frac{f_1^2}{f_0^2}\Delta z_0 + \cos\theta_0 Y'_0 \frac{f_1^2}{f_0^2}\Delta z_0\right) m_0 + \Delta e_Y(H)\right]\right\},$$

$$B = m_p\left\{-\sin\theta_p\left[\Delta\theta_a(e_Y(H) + \Delta_y) - \frac{\Delta m_0}{m_0}(e_X(H) + \Delta_x)\right.\right.$$

$$+\left(\cos\theta_0 X_0'\frac{f_1^2}{f_0^2}\Delta z_0-\sin\theta_0 Y_0'\frac{f_1^2}{f_0^2}\Delta z_0\right)m_0+\Delta e_X(H)\Bigg]$$

$$-\cos\theta_p\left[-\Delta\theta_e(e_X(H)+\Delta_X)-\frac{\Delta m_0}{m_0}(e_Y(H)+\Delta_Y)\right.$$

$$\left.+\left(\sin\theta_0 X_0'\frac{f_1^2}{f_0^2}\Delta z_0+\cos\theta_0 Y_0'\frac{f_1^2}{f_0^2}\Delta z_0\right)m_0+\Delta e_Y(H)\right]\Bigg\}.$$

In this process the following designations are used: $\theta_e = \theta_0 - \theta_a$ is the angle of rotation of the image by the objective, $m_0 = H/\bar{I}_0$ is the magnification of the objective, $m_p = \bar{H}/\bar{I}_1$ is the magnification of the projector,

$$\frac{\Delta m_0}{m_0}=\frac{\Delta f_0}{f_0}+\frac{f_1}{f_0}U'(-z_0)\,\Delta z_0$$

is the relative change in magnification of the objective, $\Delta m_p/m_p = \Delta\bar{I}_1/\bar{I}_1$ is the relative change in magnification of the projector, $\theta = \theta_p + \theta_e$ is the total angle of rotation of the image,

$$\frac{\Delta m}{m}=\frac{\Delta m_0}{m_0}+\frac{\Delta m_p}{m_p}$$

is the relative change in the total magnification.

It is well known that

$$\frac{\Delta m}{m}=C_m\frac{\Delta V}{V},\quad \Delta\theta=C_\theta\frac{\Delta V}{V},$$

where C_m and C_θ are the coefficients of the chromatic field aberrations of magnification and rotation. Furthermore, the value z_0 depends only on the parameter of excitation of the objective $k = NI_0/\sqrt{V}$ and consequently $\Delta z_0 = (k/2)z_0'(\Delta V/V)$. Using these relationships, we can rewrite formulas (8) in the form

$$\left.\begin{aligned}\Delta X&=\frac{\Delta V}{V}[C_mX-C_\theta Y+\bar{A}],\\ \Delta Y&=\frac{\Delta V}{V}[C_\theta X+C_mY+\bar{B}],\end{aligned}\right\}\qquad(9)$$

where

$$\bar{A}=m_p\Bigg\{-\cos\theta_p\Bigg[C_{\theta_e}(e_Y(H)+\Delta_Y)-C_{m_0}(e_X(H)+\Delta_X)$$

$$+\left(\cos\theta_0 X_0'\frac{f_1^2}{f_0^2}\frac{k}{2}z_0'-\sin\theta_0 Y_0'\frac{f_1^2}{f_0^2}\frac{k}{2}z_0'\right)m_0+\frac{de_x(H)}{dV}V\Bigg]$$

$$+\sin\theta_p\Bigg[-C_{\theta_e}(e_X(H)+\Delta_X)-C_{m_0}(e_Y(H)+\Delta_Y)$$

$$+\left(\sin\theta_0 X_0'\frac{f_1^2}{f_0^2}\frac{k}{2}z_0'+\cos\theta_0 Y_0'\frac{f_1^2}{f_0^2}z_0'\right)m_0+\frac{de_Y(H)}{dV}V\Bigg]\Bigg\};$$

$$\bar{B}=m_p\Bigg\{-\sin\theta_p\Bigg[C_{\theta_e}(e_Y(H)+\Delta_y)-C_{m_0}(e_X(H)+\Delta_X)$$

$$+\left(\cos\theta_0 X_0'\frac{f_1^2}{f_0^2}\frac{k}{2}z_0'-\sin\theta_0 Y_0'\frac{f_1^2}{f_0^2}\frac{u}{2}z_0'\right)m_0\Bigg]$$

$$\times\cos\theta_p\Bigg[-C_{\theta_e}(e_X(H)+\Delta_X)-C_{m_0}(e_Y(H)+\Delta_y)$$

$$+\left(\sin\theta_0 X_0'\frac{f_1^2}{f_0^2}\frac{k}{2}z_0'+\cos\theta_0 Y_0'\frac{f_1^2}{f_0^2}\frac{k}{2}z_0'\right)m_0+\frac{de_y(H)}{dV}V\Bigg]\Bigg\}.$$

STATIONARY POINTS. MEASUREMENT OF THE DEFLECTING EFFECT OF FIELDS OF DISPERSION

Let us recall some definitions. The point of intersection of the plane of the image (the plane of the screen) with the axis of the projection lens is called the image center. In our symbols the coordinates $\bar{X} = \bar{Y} = 0$ correspond to this point. Let us now change the current in the projection lens by the amount ΔI_p. Then, according to formulas (9), the image of each point on the screen is shifted by the amount

$$\left.\begin{aligned}\Delta X&=-2\frac{\Delta I_p}{I_p}(C_{m_p}X-C_{\theta_p}Y),\\ \Delta Y&=-2\frac{\Delta I_p}{I_p}(C_{\theta_p}X+C_{m_p}Y),\end{aligned}\right\}\qquad(10)$$

C_{m_p} and C_{θ_p} are the coefficients of the chromatic aberrations of magnification and rotation of the projection lens. Since $C_{m_p}^2 + C_{\theta_p}^2 \neq 0$, the only point that remains stationary with variations of the current in the projector must be located at the origin of the coordinates. In other words, the image center is that point which remains stationary with variations in the current in the projection lens. Now let the accelerating voltage and the current in the projection lens remain constant, but let the current in the objective change. Then if we assume that the magnetic deflecting fields do not change with small variations in the current in the objective, the shift of the points in the image will be determined by the formulas

$$\left.\begin{aligned}\Delta X&=-2\frac{\Delta I_0}{I_0}[C_{m_0}X-C_{\theta_e}Y+\bar{A}_m],\\ \Delta Y&=-2\frac{\Delta I_0}{I_0}[C_{\theta_e}X+C_{m_0}Y+\bar{B}_m],\end{aligned}\right\}\qquad(11)$$

where

$$\bar{A}_m=m_p\Bigg\{-\cos\theta_p\Bigg[C_{\theta_e}(e_Y(H)+\Delta_Y)-C_{m_0}(e_x(H)+\Delta_x)$$

$$+m_0\left(\cos\theta_0 X_0'\frac{f_1^2}{f_0^2}\frac{k}{2}z_0'-\sin\theta_0 Y_0'\frac{f_1^2}{f_0^2}\frac{k}{2}z_0'\right)\Bigg]$$

$$+\sin\theta_p\Bigg[-C_{\theta_e}(e_x(H)+\Delta_x)-C_{m_0}(e_Y(H)+\Delta_Y)$$

$$+m_0\left(\sin\theta_0 X_0'\frac{f_1^2}{f_0^2}\frac{k}{2}z_0'+\cos\theta_0 Y_0'\frac{f_1^2}{f_0^2}\frac{k}{2}z_0'\right)\Bigg]\Bigg\};$$

$$\bar{B}_m=m_p\Bigg\{-\sin\theta_p\Bigg[C_{\theta_e}(e_Y(H)+\Delta_Y)-C_{m_0}(e_X(H)+\Delta_X)$$

$$+m_0\left(\cos\theta_0 X_0'\frac{f_1^2}{f_0^2}\frac{kz_0'}{2}-\sin\theta_0 Y_0'\frac{f_1^2}{f_0^2}\frac{k}{2}z_0'\right)\Bigg]$$

$$-\cos\theta_p\Bigg[-C_{\theta_e}(e_X(H)+\Delta_X)-C_{m_0}(e_Y(H)+\Delta_Y)$$

$$+m_0\left(\sin\theta_0 X_0'\frac{f_1^2}{f_0^2}\frac{k}{2}z_0'+\cos\theta_0 Y_0'\frac{f_1^2}{f_0^2}\frac{k}{2}z_0'\right)\Bigg]\Bigg\}.$$

That point in the image which remains stationary with small variations of the current in the objective is called the magnetic center. The coordinates of the magnetic center $\bar{X}_m$ and $\bar{Y}_m$ are found from Eqs. (11) with $\Delta\bar{X} = \Delta\bar{Y} = 0$:

$$X_m=-\frac{\bar{A}_mC_{m_0}+\bar{B}_mC_{\theta_e}}{C_{m_0}^2+C_{\theta_e}^2};\quad Y_m=-\frac{C_{m_0}\bar{B}_m-C_{\theta_e}\bar{A}_m}{C_{m_0}^2+C_{\theta_e}^2}.\qquad(12)$$

The distance R_m from the magnetic center to the enter of the image is

$$R_m = \sqrt{X_m^2 + Y_m^2} = \frac{\sqrt{\bar{A}_m^2 + \bar{B}_m^2}}{\sqrt{C_{m_0}^2 + C_{\theta_e}^2}}. \quad (13)$$

Finally, the point in the image which remains stationary with variations in the accelerating voltage is alled the voltaic center. The coordinates of this point X_V and $\bar{Y}_V$ and its distance from the center of the image re found directly from formulas (9):

$$X_V = -\frac{\bar{A}C_m + \bar{B}C_\theta}{C_m^2 + C_\theta^2}; \quad Y_V = -\frac{C_m\bar{B} - C_\theta\bar{A}}{C_m^2 + C_\theta^2}; \quad (14)$$

$$R_V = \frac{\sqrt{\bar{A}^2 + \bar{B}^2}}{\sqrt{C_m^2 + C_\theta^2}}. \quad (15)$$

We shall now show how we can determine the magitude and the direction of the distance by which the dected fields between the projector and the objective hift the axis of the objective. This distance is calcuted, naturally, in the plane of symmetry of the projion lens.

First of all, as is well known, the vector by which e magnetic field deflects the trajectory of the electrons determined by the formula

$$e(H) = \sqrt{\frac{e}{m}} \int_0^H \frac{B(\zeta)}{2V} (\zeta - H)\, d\zeta,$$

where **B** is the induction of the deflecting magnetic field.

From this we obtain directly

$$\frac{de(H)}{dV} = -\frac{e(H)}{V}. \quad (16)$$

Let us now assume that we have by some means nclination of the illuminating beam or movement of the bjective) brought the magnetic center to the image cenr. In this case it follows from (12) that $\bar{A}_m = B_m = 0$. comparison of the expressions for $\bar{A}_m$, $\bar{B}_m$, and $\bar{A}$, $\bar{B}$ hows, however, that

$$\bar{A} = \bar{A}_m + m_p\left\{-\cos\theta_p \frac{de_x(H)}{dV} V + \sin\theta_p \frac{de_Y(H)}{dV} V\right\};$$

$$\bar{B} = \bar{B}_m + m_p\left\{-\sin\theta_p \frac{de_X(H)}{dV} V - \cos\theta_p \frac{de_y(H)}{dV} V\right\}.$$

In the case that we are considering we have

$$\bar{A} = m_p[\cos\theta_p e_x(H) - \sin\theta_p e_y(H)];$$
$$\bar{B} = m_p[\sin\theta_p e_X(H) + \cos\theta_p e_Y(H)].$$

From formulas (14) we find the coordinates of the voltaic center

$$X_V = -\frac{m_p}{\sqrt{C_m^2 + C_\theta^2}}[e_X(H)\cos(\lambda - \theta_p) + e_Y(H)\sin(\lambda - \theta_p)];$$

$$Y_V = -\frac{m_p}{\sqrt{C_m^2 + C_\theta^2}}[-e_X(H)\sin(\lambda - \theta_p) + e_y(H)\cos(\lambda - \theta_p)],$$

where

$$\cos\lambda = \frac{C_m}{\sqrt{C_m^2 + C_\theta^2}}; \quad \sin\lambda = \frac{C_\theta}{\sqrt{C_m^2 + C_\theta^2}}.$$

The distance of the voltaic center from the center of the image, where the magnetic center is located, is

$$R_V = \frac{m_p}{\sqrt{C_m^2 + C_\theta^2}} |e(H)|.$$

From this we easily find the value of the distance |e(H)| by which the magnetic field deflects the axis of the objective

$$|e(H)| = \frac{R_V}{m_p}\sqrt{C_m^2 + C_\theta^2} \quad (17)$$

and the plane in which the deflection occurs. The latter is turned relative to the meridional plane passing through the voltaic center by the angle $\lambda - \theta_p$.

MAGNETIC ALIGNMENT OF ELECTRON MICROSCOPES

In recent years magnetic coils have come into use in the precise alignment of electron microscopes. Such coils are employed in particular for the alignment of the axis of the objective relative to the axis of the projector.

Let us consider how this sort of alignment should be standardized. We shall assume as before that the deflecting magnetic fields do not depend on the direction and strength of the current in the objective lens.

According to the method of Heine, the first stage of alignment is the selection of currents in the aligning coils such that the image of a point located in the center of the screen will not be shifted when the direction of the current in the objective is reversed.

If the image of a point falls at the image center ($\bar{X} = \bar{Y} = 0$), then according to formulas (1)-(3) its coordinates in the object are associated with a shift in the axis of the objective by the relationships

$$\left.\begin{aligned} e_X(H) + \Delta_x &= m_0(X_a\cos\theta_e - Y_a\sin\theta_e); \\ e_Y(H) + \Delta_y &= m_0(X_a\sin\theta_e + Y_a\cos\theta_e). \end{aligned}\right\} \quad (18)$$

If the image of this point is not shifted when the current in the objective is reversed, then Eqs. (18) remain valid also when θ_e is changed to $-\theta_e$. This can be so only in case $e_X(H) + A_x = e_Y(H) + \Delta_y = X_a = Y_a = 0$. Thus, as a result of the first stage of alignment, the axis of the objective lens falls at the center of the projector.

In the second stage of alignment the magnetic center must be brought to the image center by inclination of the illuminating beam. When this is done, according to formula (13), $\bar{A}_m^2 + \bar{B}_m^2 = 0$, or since $e_X(H) + \Delta_x = e_Y(H) + \Delta_y$,

$$(\cos\theta_0 X_0' - \sin\theta_0 Y_0')^2 + (\sin\theta_0 X_0' + \cos\theta_0 Y_0')^2 = X_0'^2 + Y_0'^2 = 0.$$

Thus as a result of the second stage of alignment the axis of the condenser coincides with the axis of the objective, with which the alignment is completed.

Let us note that the presence of magnetic deflecting fields leads to the result that the voltaic center is not brought to the image center and therefore the chromatic field aberration remains uncorrected and equals

$$\Delta r = \sqrt{\Delta X^2 + \Delta Y^2} = m_p \frac{\Delta V}{V} |e(H)| \quad (19)$$

or, according to formula (17)

$$\Delta r = R_V\sqrt{C_m^2 + C_\theta^2}\,\frac{\Delta V}{V}.$$

Thus, because of the chromatic aberration the magnetic alignment of the objective can be used only within restricted limits. The question arises what these limits are. The axis of the objective falls at the center of the projection lens if $-\bar{\Delta} = \bar{e}(H)$. Then, according to formula (19), the length of the lateral chromatic aberration imparted to the objective will be

$$\delta = \frac{\Delta r}{m} = \frac{\Delta V}{V} \times \frac{\Delta}{m_0}.$$

Hence, taking the permissible value of the chromatic aberration as δ, we can find the value of Δ/m_0 which indicates the necessary accuracy of the preliminary alignment of the objective without the use of deflecting fields.

In conclusion, it should be noted that a similar consideration, in principle, can be carried out also in the case where there is a deflecting field between the lenses that is associated with the field of dispersion of the objective lens and which changes noticeably with a change in the current in the objective. It is true that such a consideration is greatly hindered because of the lack of clarity in the rules for the change in such fields, but it must be noted that even with the simplest assumptions we obtain such a complex method of alignment, based on the measurement of the coordinates of the stationary points of the image, that it can scarcely be used practically. Therefore, in finding such relationships it is necessary to increase the magnetic shielding of the objective lens.

SHORT COMMUNICATIONS

THE USE OF PRESSED DISCS OF KCl IN ULTRAVIOLET SPECTROPHOTOMETRY

V. A. Shlyapochnikov and V. I. Slovetskii (p. 265)

Received 8 March 1960

There are difficulties in obtaining the ultraviolet absorption spectra of certain solid compounds due to the difficulty of growing single crystals of thickness of the order of 0.001 mm or less, insolubility in suitable solvents, etc. We have therefore tried to apply to ultraviolet spectroscopy the method of pressed discs similar to that used in the infrared.

Of several salts (NaF, LiF, KBr, NaCl, and KCl) KCl was found to be the most suitable for this purpose. The Table gives the results of measurements of the optical density of a KCl "glass" of thickness 0.92 mm.

λ (mμ)	220	230	240	250	260	270	280	290	300	310	[illegible]
D	0.205	0.185	0.172	0.163	0.152	0.144	0.136	0.130	0.125	0.120	0.113

Since the intrinsic absorption of the "glass" is relatively low, we hoped to obtain the spectra desired.

The Figure shows absorption spectra of n-nitrotoluol (I) and n-nitroaniline (II) compacted with KCl (solid line) and dissolved in 95% ethyl alcohol (broken line).

We see that the spectra obtained by the two methods are in good agreement. The results can be regarded as semi-qualitative. It must be noted that the absorption in the "glass" was a half to a quarter of the corresponding absorption in the solution.

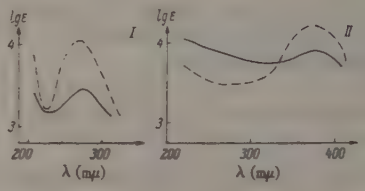

The experimental method was as follows. Chemically pure KCl was precipitated from aqueous solution with acetone and dried at t ~ 150°C for 10-12 hr. It was then heated in a lagged oven at 550-650°C for 3-5 hr, cooled in a vacuum dessicator, and carefully pulverized in an agate or jasper mortar. The required amount of the specimen to be studied is weighed out and placed in a mortar and ground, after which KCl is added to it, in small doses, up to the required amount, the whole mixture being stirred and ground meanwhile. The mixture is compacted under a low vacuum (~1 mm Hg) at a pressure of $8.5\text{-}9 \times 10^3$ kg/cm² (compacting time 10-20 min). The "glass" has dimensions d = 25 mm, thickness 0.8-1.5 mm. Special precautions must be taken with the pressing surfaces—they must be finished mirror-smooth.

DETERMINATION OF THE OPTICAL CONSTANTS OF Ge AND CdTe BY THE REFLECTION METHOD

N. K. Kiseleva and N. N. Pribytkova (pp. 266-268)

Received 21 July 1960

The optical constants of absorbing media—the refractive index n and the absorption coefficient κ—may be determined either by combined measurements of transmission and reflection[1,2] or by measurement of reflection alone. In measuring the transmission of vacuum evaporated films, errors may arise from departure from stoichiometric composition. With monocrystals or ingots it is difficult to obtain thin specimens, and transmission measurements are limited to the region near the intrinsic absorption edge and the region of low absorption. For these reasons, we restrict our interest to the method of determination of optical constants by reflection measurement only.

Certain methods of determining optical constants by reflection measurements have been used for several semiconductors: PbS, PbTe, PbSe,[3] Ge,[4,5] BaO.[6] In the work reported in this paper, the optical constants n and κ of Ge and CdTe monocrystals were determined by Kravits' method,* developed for thick dye films,[7] and later

*The principle of the method is explained by Orsel'.[9]

applied to metals.[8] This method of measuring n and κ requires that the reflectance be measured at the interface between the substance under study and a transparent medium for at least two media.

The chief requirement of the method is optical contact between the semiconductor and a transparent medium of known refractive index, which is ensured by immersing the specimen in a liquid. The following liquids were used: alcohol, toluol, α-chlornaphthaline, and paraffin oil.* Measurement of the reflectance of a given substance

*T. A. Alekseeva measured the refractive index of the liquids.

in air and in these liquids permitted calculations to be made for several combinations of air/liquid and liquid/liquid media.

For the measurements, the specimen under study was fixed in a special frame and a reflectance standard was placed in the same plane. The frame was immersed in the liquid in a cell. The measurements were made with a Beckman spectrophotometer with a special attachment for measuring specular reflectance at normal incidence. The special construction of the cell (Fig. 1a) provided separation in the plane of the photocell of the beams reflected at the glass/air, glass/liquid, and liquid/specimen interfaces, and the photocell recorded only the reflection at the liquid/specimen interface. It can be shown that the absolute value of the reflectance is given by the equation:

$$R = R_s \frac{a}{b},$$

where R_s is the absolute value of the reflectance of the standard in the given medium and a and b are the indications on the transmission scale of the photometer with reflection from the specimen and the standard respectively.

Choice of a standard was difficult. Since errors in relative measurements decrease with reduction of the

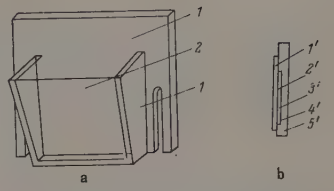

Fig. 1. Construction of the cell and the reflectance standard. 1—Metal body; 2—fused quartz plate. 1'—K-8 glass; 2'—layer of thoria; 3'—air gap; 4'—layer of soot; 5'—metal plate.

difference between the quantities compared (other things being equal), in our case a standard with reflectance 15-20% was desired. A standard with this reflectance across almost the whole spectral range used was prepared by using a plate (wedge) of K-8 glass with a layer of thoria.*

*The thoria layer was deposited by R. S. Sokolova.

Figure 1b shows the construction of the standard. The standard was calibrated in air by reflection from a wedge of K-8 glass. The reflectance of the standard in liquid is given by the equations:

$$R = R_s \left(\frac{1-R_1'}{1-R_1}\right)^2$$

for a wedge and

$$R = (R_s - R_1)\left(\frac{1-R_1'}{1-R_1}\right)^2 + R_1'$$

for a plane-parallel plate.

Here R_s is the reflectance of the standard in air, R_1 is the reflectance at the glass/air interface, and R_1' is the reflectance at the glass/liquid interface. The sources of error in determining the absolute value of R are: (1) the specimen itself (surface imperfections) and (2) the measuring technique (errors in setting the specimen perpendicular to the incident light beam, inaccuracies in aligning the light spot on the same region of the photosensitive surface of the photoelement throughout the measurement, etc.).

The magnitude of the error in measuring the reflectance was estimated by comparing the values of the reflectance of two glasses (K-8 and F-2), calculated from the known values of the refractive indices. The error was found to be about 0.5%. The error in determining the reflectance of the specimen was therefore ~1% since it results from the error of two measurements (calibrating the standard and comparing the standard with the specimen). For a given error in measuring the reflectance, the fractional errors dn/n and $d\kappa/\kappa$ depend on the magnitudes of n and κ. In particular, dn/n is proportional to n and $d\kappa/\kappa$ is proportional to n and inversely proportional to κ^2. At $\lambda = 500$ mμ, for Ge, $dn/n \sim 20\%$ and $d\kappa/\kappa \sim 30\%$; for CdTe the values were 6% and 30% respectively.

The measurements were made on specimens prepared

from Ge and CdTe monocrystals.* The specimen dimensions were not less than 7×7 mm^2. Ge was chosen as one of the specimens because it was possible to compare the results obtained by the method described above with data obtained by other workers using different methods. The measurements gave a spectral variation of reflectance for Ge in air no different from that given in refs. 4 and 5. Figure 2 shows the spectral variation of the refractive index and the absorption coefficient calculated for the range 400-700 mμ. It is easily seen that the curves are qualitatively similar to those given in refs. 4 and 5. The differences in absolute values lie within the limits of experimental error.

*The specimens were polished and figured by T. F. Sorokina.

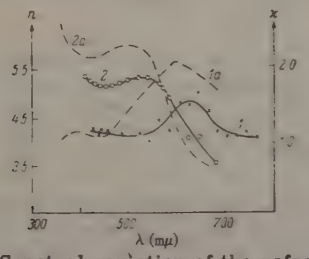

Fig. 2. Spectral variation of the refractive index n (curves 1 and 1a) and the absorption coefficient κ (curves 2 and 2a) for a Ge monocrystal. Solid curve—data of the present work; broken curve—data from ref. 4.

The optical properties of CdTe are known only in the region of the intrinsic absorption edge[10] and also on the long wavelength side of the intrinsic absorption edge.[11] We determined the optical constants of CdTe in the spectral region lying on the short wavelength side of the intrinsic absorption edge. The reflectance was measured for several CdTe specimens in the range 330-960 mμ. Figure 3a gives the spectral variation of the reflectance for one of the specimens. The curve shows a noticeable reflectance maximum in the 390 mμ region and a small step at about 860 mμ. The values of n and κ were calculated with the following results (Fig. 3b): the refractive index is approximately constant at about 2.6 in the range 500-900 mμ, and increases considerably in the short wavelength region (with a maximum at 400 mμ); the absorption coefficient showed two regions of sharp change, at 850 and 400 mμ. The first region corresponds to the well known intrinsic absorption edge,[10] while the second lies in the short wavelength range far beyond the intrinsic absorption edge. A sharp increase in κ in the short wavelength region has also been detected for Ge,[4] PbS, PbTe, PbSe,[3] CdS, and ZnS.[12]

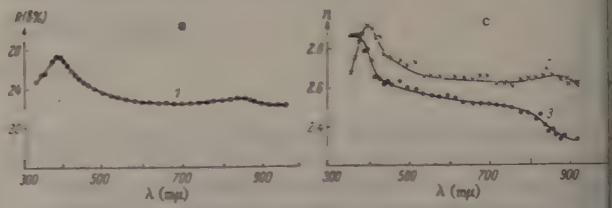

Fig. 3. Spectral variation of reflectance R (curve 1), refractive index n (curve 2), absorption coefficient κ (curve 3) for a CdTe monocrystal.

Finally, the authors express their gratitude to B. T. Kolomiets and M. V. Savost'yanova for their interest in the work and appraisal of the results.

REFERENCES

1. F. Oswald and R. Shade, Z. Naturforsch. **9a**, 611 (1954).
2. F. Lukes, Czechoslov. J. Phys. **7**, 371 (1957).
3. D. G. Avery, Proc. Phys. Soc. **B65**, 425 (1952); Ibid. **B66**, 134 (1953).
4. R. J. Archer, Phys. Rev. **110**, 354 (1958).
5. H. R. Philipp and S. A. Taft, Phys. Ref. **113**, 1002 (1959).
6. F. C. Jahoda, Phys. Rev. **107**, 1261 (1957).
7. N. N. Pribytkova, Opt. i Spektr. **2**, 623 (1957); N. N. Pribytkova and L. S. Agroskin, Opt. i Spektr. **2**, 628 (1957).
8. G. P. Skornyakov and M. M. Kirillova, Opt. i Spektr. **6**, 248 (1959), Optics and Spectroscopy **6**, 159 (1959).
9. Sbornik Metodicheskikh rabot po mikroskopicheskom issledovaniyu rud v otrazhennom svete (Collection of Papers: Work on Methods of Microscopic Ore Study by Reflected Light). Ob'ed. Nauch.-Tekh. Izd., Narodnyi Komissariat Tyazheloi Promyshlennost SSSR, Moscow, 1936.
10. T. S. Moss, "Optical Properties of Semiconductors. Academic Press, New York and London, 1959.
11. D. de Nobel, Philips Research Repts. **14**, 398 (1959).
12. J. F. Hall, J. Opt. Soc. Am. **46**, 1013 (1956).

MEASUREMENT OF THE OPTICAL DENSITY OF THE BLACKENING OF SPECTRAL LINES USING INTERFERENCE MICROSCOPY METHODS

V. P. Koronkevich and E. B. Kolesova (pp. 268-270)

Received 4 July 1960

A method of measuring the blackening of spectral lines, which employs two-beam interference microscopes, was described in works which were devoted to the improvement of the accuracy of the photographic method of determination of the displacement of interference fringes.[1-4] The principle of the method is as follows. During the processing of the photographic material the exposed grains of the emulsion in the photosensitive layer are transformed into metallic silver and the unexposed grains are washed out during the fixing and washing processes. This causes mechanical changes in the microprofile of the photographic material. In the cross section of a plate bearing a photograph of a spectrum the spectral lines will lie somewhat higher than the unblackened parts of the background. The difference in the level of the microprofile depends on the amount of light which illuminated that portion of the photographic plate and for this reason it may serve as the basis of a new method for the determination of the blackening.

In practice the variation of the microprofile of the photographic material is conveniently measured with an interference microscope, using for this purpose fringes of equal thickness. Since it is important for the measuring of the blackening to determine the deflection of the interference fringes accurately it seemed natural to us to employ a multiple beam interference microscope for this purpose.

Figure 1a represents a photograph of part of the iron spectrum observed in the multiple-beam interference microscope "Multimi," made by the firm Johansson, with a x50 magnification (type 1 spectral plates were used; the spectra were photographed on a ISP-28 spectrograph; a spark light source was employed; Agfa-Atomal developer was used. The interference patterns were photographed with a FED-2 camera on "Izopankhrom" film whose sensitivity was 90 GOST units).

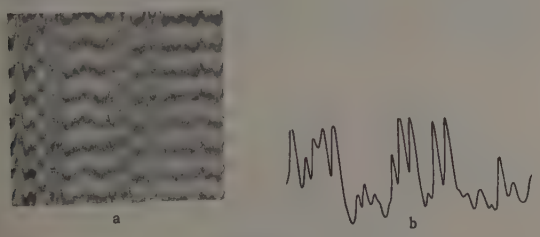

Fig. 1

For comparison Fig. 1b shows the curve obtained when the same part of the spectrum was measured photometrically on the microphotometer type MF-4. It can be seen by comparing Figs. 1a and b that the interference pattern gives a graphic and true representation of the magnitude of the blackening of the lines. Unlike the microphotometer it makes it possible to study the behavior of the blackening in two dimensions, since the interference fringes cross the spectral lines in several places. Furthermore, with a microphotometer one can measure blackenings up to S = 2, whereas with the interference method one can estimate higher values of the blackening (at least up to S = 4).

In order to be able to estimate the magnitude of the absolute blackening, investigations were carried out on the dependence of the deflection of the interference fringes on the illumination, the type of film, and the processing conditions of the photographic material. The best results were obtained with photographs taken on type 1 spectral plates which were processed with Agfa-Atomal developer. One can deduce the relative magnitude of the blackening by measuring the deflection in the fringe sections corresponding to the lines.

To enable an estimation of the possibilities of the new method to be made, photographs of a part of the iron spectrum taken through a stepped absorbing wedge are shown in Fig. 2a. Microphotometer traces made on the MF-4 microphotometer are shown for comparison in the same figure (Fig. 2b). It can be seen from the figures that the microphotometer has a greater accuracy and is more sensitive for smaller blackenings than the proposed method. However, the method can be successfully applied in the region of high blackenings and in a series of problems in which a high accuracy of the determination of the blackening is not necessary.

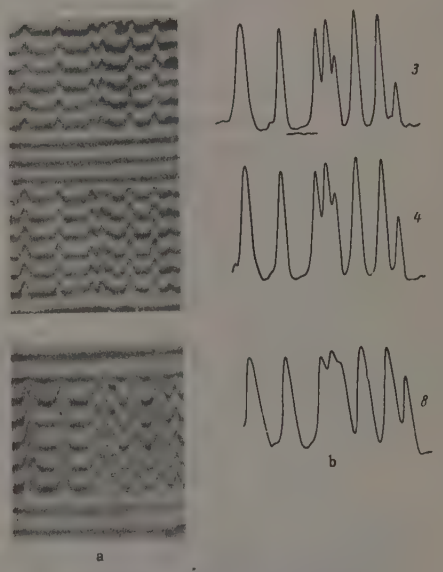

Fig. 2. The numbers at the right are the numbers of the steps of the absorbing wedge.

It should also be mentioned that the whole setup for measuring the blackening may consist of an ordinary microscope of small magnification with a glass plate carrying a partially reflecting silver layer placed in the object space. A partially reflecting layer is deposited onto that part of the photographic plate which is to be measured photometrically. The interference of light rays reflected from the surface of the gelatin layer of the object and

the partially reflecting layer of the glass plate is observed through the microscope. A standard eyepiece micrometer is used for the measurement of the deflection of the fringes.

The enumerated properties of the method raise hopes that it might be applied for the rapid estimation of the density of the blackening of spectral lines.

REFERENCES

1. E. Lau and W. Krug, "Die Äquidensitometrie." Akad Verlag, Berlin, 1957.
2. E. Lau, E. G. Kind, and G. Roose, Optik **15**, 162 (195
3. W. Krug, Arch. tech. Messen **434**, 227 (1959).
4. H. Schmidt, Optik **16**, 538 (1959).

ON THE EFFECTIVE VIBRATIONAL TEMPERATURE OF THE ACETYLENE-AIR FLAME

F. S. Ortenberg and N. A. Nesterko (pp. 270-272)

Received 13 July 1960

Recently, much attention has been paid[1-3] to the study of the energy distribution in reacting systems and to the associated question of temperature measurement. Interest in this problem has been aroused by the fact that chemical reactions taking place in a flame lead in many cases to a nonequilibrium distribution over the energy levels for the initial, intermediate, and final reaction components. The aim of the present work is to study the energy distribution over the vibrational levels of various radicals in a flame. In practice, this problem reduces to the study of the intensity distribution over the vibrational bands in the spectrum of the flame and to the comparison of the established effective vibrational temperature with this distribution. Such a quantitative treatment of the spectral results is possible only when sufficiently reliable data on the values of the transition probabilities are at hand. In view of the fact that progress in the matter of finding these probabilities has been achieved only very recently,[4] investigations analogous to ours are very few.[5,6]

We have studied the intensity distribution over the vibrational bands of the electronic-vibrational band systems of the C_2 and BaO molecules in the inner and outer cones, respectively, of a premixed acetylene-air flame, burning at atmospheric pressure with 11% of C_2H_2 in the mixture. The BaO bands were obtained by introducing a tenth-molar solution of the salt $BaCl_2$ into the flame with the help of an atomizer. A medium-dispersion Zeiss glass spectrograph was used to observe the flame spectrum (Fig. 1). The slit width of the spectrograph equaled 0.03 mm. The spectrograms were taken on isochrome photographic plates of sensitivity 65 state national standard units. The exposure time was so chosen that the BaO and C_2 band heads under study fell into the normal blackening region. The spectrograms were treated by the usual methods of spectrophotometry, with allowance for the dependence of the sensitivity of the plates on the wavelength. The desired band intensity was evaluated from the maximum intensity of the band head by subtracting from the latter the intensity produced by the continuous background and by other bands near the head.

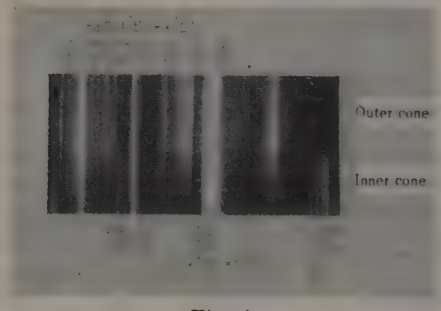

Fig. 1

In determining the effective vibrational temperature we started from the well-known formula for the intensity of a vibrational emission band[7]

$$I = \frac{CP_{v'v''}}{\lambda^4} e^{-\frac{E(v')}{kT_{\text{vib.}}}},$$

where C is some constant which is the same for all bands of a given electronic-vibrational system; $P_{v'v''}$ is the relative transition probability; λ is the wavelength of the transition; $E(v')$ is the energy of the upper vibrational term; $T_{\text{vib.}}$ is the desired vibrational temperature. On setting up the dependence of $\log I - \log (P_{v'v''}/\lambda^4)$ on $E(v')$, we should obtain—so long as a Boltzmann or pseudo-Boltzmann energy distribution over the vibrational levels exists—a straight line, the slope of which determines the temperature. The relative values of the vibrational transition probabilities, $P_{v'v''}$, for the Swan band system (the $A^3\Pi_g \rightarrow X^3\Pi_u$ transition) which we used in the calculation were taken from ref. 8, and those for the band system of the BaO molecule corresponding to the $A^1\Sigma \rightarrow X^1\Sigma$ transition were taken from ref. 9. The straight lines, from the slope of which the temperature was determined, were drawn by the method of least squares. Typical results of our treatment are represented in Fig. 2 for the bands of BaO (lower line) and C_2 (upper line). We note that the scatter of the points for the lower line is considerably less than for the upper.

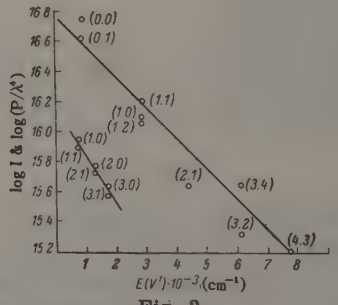

Fig. 2

The average temperature determined from the vibrational structure of the BaO bands amounts to 2200°K and is equal to the temperature of the flame which we studied as measured by the method of reversal of the Na resonance line.[10] The agreement of these temperatures and

the small scatter of the points relative to the line indicates the existence of conditions of thermodynamic equilibrium in the region of the outer cone, located at a distance of roughly 0.5 cm above the reaction zone of the flame. The measurement of the flame temperature on the basis of the BaO bands in a region of the flame which includes the tip of the inner cone leads to a somewhat lower temperature value; however, the deviation of the experimental points from a straight line increases, which indicates the presence of deviations from equilibrium in this part of the flame.

The effective vibrational temperature corresponding to the observed intensity distribution over the C_2 bands amounts on the average to 3000°K. Thus, as also in the case of the Bunsen flame,[1] too high a temperature value is obtained when the temperature is determined on the basis of the C_2 vibrational bands in the reaction zone of the acetylene-air flame. We note that the effective rotational temperature (3600°K)[1] determined on the basis of the C_2 rotational structure exceeds the adiabatic temperature by an even wider margin for a stoichiometric mixture in the acetylene-air flame. This is one more indication of the absence of complete thermal equilibrium in the reaction zone of a flame.

The authors thank V. S. Rossikhin for his interest in the work.

REFERENCES

1. A. Gaydon, "Spectroscopy of Flames." Chapman-Hall, London, 1957. (Izd. Inostrannoi Lit., Moscow, 1959.)
2. Collection "Opticheskaya pirometriya plazmy" (Optical Pyrometry of a Plasma) Izd. Inostrannoi Lit., Moscow, 1960.
3. Natl. Bur. Standards (U.S.) Tech. New Bull. **42**, 131 (1958).
4. V. N. Kolesnikov and L. V. Leskov, Uspekhi fiz. nauk **65**, 3 (1958).
5. H. P. Broida, J. Chem. Phys. **21**, 340 (1953).
6. H. P. Broida and K. E. Shuler, J. Chem. Phys. **20**, 168 (1952).
7. L. V. Leskov, Opt. i Spektr. **4**, 168 (1958).
8. R. W. Nicholls, Proc. Phys. Soc. **A69**, 741 (1956).
9. F. S. Ortenberg, Opt. i Spektr. **9**, 151 (1960), Optics and Spectroscopy **9**, 82 (1960).
10. V. S. Rossikhin and N. A. Nesterko, Zhur. Fiz. Khim. **33**, 3, 665 (1959).

SPECTRAL INVESTIGATION OF THE INFLUENCE OF THE SOLVENT ON THE AGGREGATION OF ORGANIC DYES

Kh. L. Arvan and N. E. Zaitseva (pp. 272-276)

Received 22 July 1960

Regardless of the numerous investigations devoted to the process of aggregation of organic dyes in solution, the nature of this phenomenon is insufficiently clear even at the present time. In particular, there is no common view on the role of the solvent. The point is that the strongest aggregation usually takes place in aqueous solutions, as is well known. In organic solvents, aggregation is observed only with cyanine dyes which aggregate especially readily.[1] Dyes of other classes are aggregated in organic solvents only when considerably cooled.[2,3]

Sheppard[4] and Scheibe[5] turn their attention to the different character of the solubility of organic dyes in water and in organic solvents, as a consequence of the close kinship of the organic molecules to the dye molecule. On the other hand, certain authors[6,7] ascribe the unique role of water to the high value of its dielectric constant, which brings about a weakening of the Coulombic repulsion of ions of the same sign. Derkacheva[7] considers from this point of view the fact, established by her, of the presence of some aggregation of pseudoisocyanine in glycerol and its absence in alcohol.

In the present work, the dependence of the absorption spectra of dyes on their concentration in different solvents has been investigated. We have considered dyes whose absorption spectra reflect the state of aggregation most strongly (methylene blue, rhodamine 6G, pinacyanol iodide). The degree of aggregation was estimated to a first approximation, on the basis of the ratio between the absorption values in the long- and short-wavelength maxima of the curve. In order to increase the choice of solvents with various dielectric constant values, we have used mixtures of two solvents.

The absorption curves of solutions of rhodamine 6G in solvents with different dielectric constant values are presented in Fig. 1. The maximum dye concentration in all solutions was the same ($C = 1.74 \times 10^{-3}$ moles/liter). It can be seen from the figure that, in water, the aggregation of this dye is very considerable. In formamide, which has a greater value of the dielectric constant than water ($\varepsilon_w = 81$, $\varepsilon_f = 109$), the change in the absorption spectra in the concentration interval which we have considered is insignificant. One's attention is also drawn to the fact that, in mixtures of water with glycerol and of water with acetone which have the same dielectric constant value ($\varepsilon = 70$), the state of aggregation is different.

Analogous results have also been obtained for other dyes. The absorption curves of methylene blue solutions of one and the same concentration ($C = 1.07 \times 10^{-3}$ moles/liter) in four solvents with one and the same value of the dielectric constant ($\varepsilon = 60$) are presented in Fig. 2. As in the rhodamine 6G solutions, a lesser aggregation is observed in mixtures containing acetone than in mixtures with glycerol. Ethylene glycol differs insignificantly from glycerol. The alcohol occupies an intermediate position.

A certain intensification of the aggregating action of ethylene glycol in comparison with acetone and acetonitrile can be seen in Fig. 3a, where the absorption curves of pinacyanol iodide in media with dielectric constants of 35.5 to 35.7 are presented. A still greater difference in the state of aggregation of pinacyanol iodide is observed

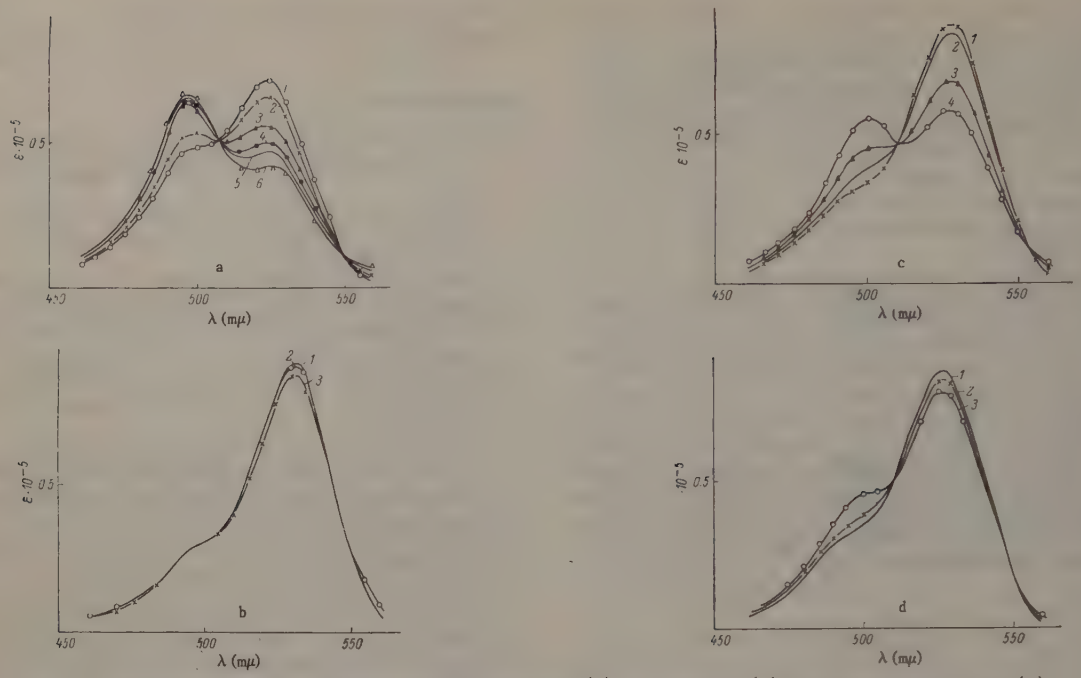

Fig. 1. Absorption spectra of rhodamine 6G in water (a), formamide (b), and water-glycerine (c) and water-acetone (d) mixtures at different dye concentrations. Concentration (moles/liter): a: curve 1—9.3×10^{-5}, curve 2—1.74×10^{-4}, curve 3—4.65×10^{-4}, curve 5—9.3×10^{-4}, curve 6—1.74×10^{-3}; b: curve 1—1.74×10^{-3}, curve 2—5.8×10^{-4}, curve 3—1.16×10^{-6}; c: curve 1—1.16×10^{-5}, curve 2—1.10×10^{-4}, curve 3—5.80×10^{-4}, curve 4—1.74×10^{-3}; d: curve 1—1.16×10^{-4}, curve 2—5.8×10^{-4}, curve 3—1.74×10^{-3}

in the case of glycerol and a water-acetone mixture with a corresponding dielectric constant value (ε = 41.5). In glycerol, the short-wavelength maximum predominates, while in the water-acetone mixture it is significantly less than the long-wavelength one (Fig. 3b).

Thus it appears that the chemical nature of the solvent is of substantial importance for the possibility of aggregation of organic dyes in solution. The value of the dielectric constant must not be considered as decisive.

We note also that the presence of water in the composition of the solvent does not always result in an improvement in the conditions of aggregation. Actually, pinacyanol aggregates more strongly in anhydrous glycerol than in a water-acetone mixture. In the solutions which we have considered of rhodamine in water-acetone and water-ethylene glycol mixtures, the relative mole fraction of water amounts to 94 and 86% respectively. Nevertheless, the degree of aggregation of the dye is greater in the second mixture.

In all the organic solvents which we have considered

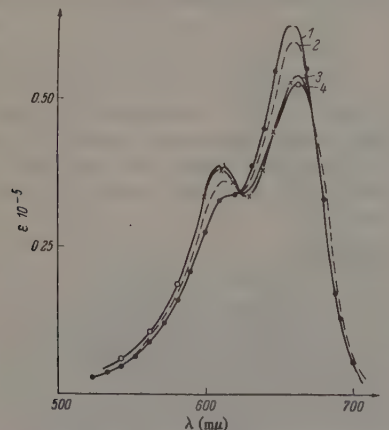

Fig. 2. Absorption spectra of methylene blue ($C = 1.07 \times 10^{-3}$ moles/liter) in different solvents (ε = 60). Solvents (mixtures): curve 1—water-acetone; curve 2—water-isopropyl alcohol; curve 3—water-glycerol; curve 4—water-ethylene glycol.

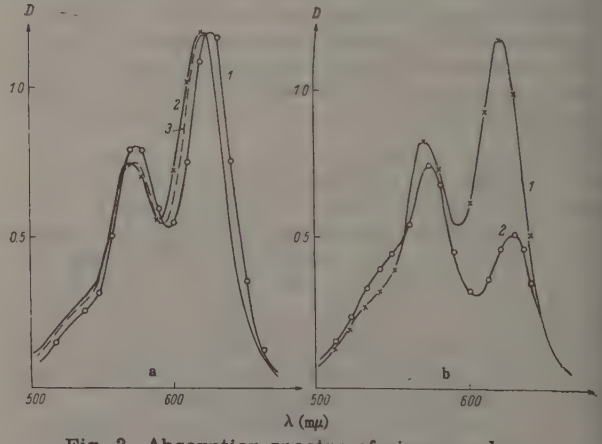

Fig. 3. Absorption spectra of pinacyanol iodide in different solvents at concentrations of 2.5×10^{-3} moles/liter (a) and 2.2×10^{-3} moles/liter (b). Solvents: a (ε = 35.5-35.7): curve 1—ethylene glycol, curve 2—acetonitrile, curve 3—water-acetone mixture; b (ε = 41.5): curve 1—water-acetone mixture, curve 2—glycerol.

(under otherwise equal conditions), the greatest aggregation is observed in glycerol and in ethylene glycol; it is less in acetonitrile, formamide, and acetone (the latter produces a significant deaggregation of the dye even in the presence of a predominant quantity of water.)* In this series, the alcohols occupy an intermediate position.

Apparently a substantial role with respect to the aggregation of a dissolved dye must be ascribed to the hydroxyl groups of the solvent molecule. Without denying the unique role of water in consequence of its lesser kinship to the organic dye molecules, we consider it possible to extend this concept with regard to a comparison of different organic solvents with one another. Hydroxyl-containing organic solvents occupy an intermediate position between water and the remaining organic (polar) solvents with respect to the aggregation of organic dyes.

The presence of dye aggregation in nonpolar and some slightly polar solvents—i.e., in media with very low dielectric constant values—is to be especially noted. We are considering this question separately.

*The deaggregation of dyes in aqueous solutions when certain organic solvents are introduced into them has been observed by us previously.[8] However, at that time the change in the value of the dielectric constant of the solvents was not taken into account, in consequence of which the comparison of the activities of different organic compounds in this respect requires some refinement.

REFERENCES

1. H. Ecker, Kolloid-Z. 92, 35 (1940).
2. G. N. Lewis, J. Am. Chem. Soc. 65, 1150 (1943).
3. V. Zanker, Z. physik. Chem. 200, 250 (1950).
4. S. E. Sheppard and A. L. Geddes, J. Am. Chem. Soc. 66, 1995 (1944).
5. G. Scheibe, Naturwissenschaften 25, 75 (1937).
6. T. H. Förster and E. König, Z. Elektrochem. 61, 344 (1957).
7. L. D. Derkacheva, Izvest. Akad. Nauk SSSR 20, 410 (1956).
8. Kh. L. Arvan, Izvest. Akad. Nauk SSSR 20, 443 (1956).

DISPERSION FORMULA FOR THE ELECTRON IN A POTENTIAL BOX OF FINITE DEPTH AND THE OPTICAL POLARIZABILITY OF MOLECULES

M. N. Adamov, V. K. Kagan, and B. I. Orlov (pp. 276-279)

Received 22 July 1960

The calculation of optical polarizability of the electron moving in an one-dimensional potential box belongs to the few quantum-mechanical problems for which an exact solution in a closed form can be obtained. The solution of this problem for an infinitely deep potential box, which leads to a corresponding dispersion formula, was given earlier.[1] The solution becomes very cumbersome for the case of a potential box of finite depth.[2] It is possible, however, to achieve a substantial simplification of calculations and of the final formulas if one considers separately the states of different symmetries relative to the reflection of the electron coordinate in the center of inversion, the latter being the middle of the bottom of the potential box. The unperturbed wave function $\psi^{(0)}$, and the correction function $\psi^{(1)}$ which corresponds to it in the first approximation, must have opposite parities with respect to the mentioned symmetry operation.

We shall express the discrete energy levels E of the unperturbed system through the parameter β by means of the formula

$$E = \frac{1}{2}\beta^2. \tag{1}$$

The spectrum of the permissible values of β is determined by the equation

$$\lg \beta l = \frac{\gamma}{\beta} \tag{2}$$

for the symmetric states, and by the equation

$$\lg \beta l = -\frac{\beta}{\gamma} \tag{3}$$

for the antisymmetric ones, where $\gamma = \sqrt{2U - \beta^2}$, l is the halfwidth of the potential box, and U is its depth.

The optical polarizability $\alpha(\omega)$ of the electron which occupies one of the discrete levels is found by the method described in detail in ref. 1. As a result of comparatively simple calculations, the following dispersion formulas are obtained: for the symmetric states

$$\alpha_g(\omega) = \alpha_{1g}(\omega) + \alpha_{2g}(\omega), \tag{4}$$

where

$$\alpha_{1g}(\omega) = \frac{A^2}{\omega^2}\left(l\cos 2\beta l - \frac{\sin 2\beta l}{2\beta}\right) + 2AB_1\cos\beta l\left[\frac{\beta_1\gamma\cos\beta_1 l - \beta^2\sin\beta_1 l}{\omega^2} + \frac{l(\gamma\sin\beta_1 l + \beta_1\cos\beta_1 l) - \sin\beta_1 l}{\omega}\right] + 2AB_2\cos\beta l\left[\frac{\beta_2\gamma\cos\beta_2 l - \beta^2\sin\beta_2 l}{\omega^2} - \frac{l(\gamma\sin\beta_2 l + \beta_2\cos\beta_2 l) - \sin\beta_2 l}{\omega}\right];$$

$$\alpha_{2g}(\omega) = -\frac{A^2\cos^2\beta l}{\gamma\omega^2}(2\gamma l + 1) - \frac{4AB_1\cos\beta l\cdot\sin\beta_1 l}{(\gamma+\gamma_1)^2}[(\gamma+\gamma_1)l + 1] - \frac{4AB_2\cos\beta l\cdot\sin\beta_2 l}{(\gamma+\gamma_2)^2}[(\gamma+\gamma_2)l + 1];$$

for the antisymmetric states

$$\alpha_u(\omega) = \alpha_{1u}(\omega) + \alpha_{2u}(\omega), \tag{5}$$

where

$$\alpha_{1u}(\omega) = \frac{A_2}{\omega^2}\left(\frac{\sin 2\beta l}{2\beta} - l\cos 2\beta l\right) - 2AC_1\sin\beta l\left[\frac{\beta_1\gamma\sin\beta_1 l + \beta_1^2\cos\beta_1 l}{\omega^2} + \frac{l(\beta_1\sin\beta_1 l - \gamma\cos\beta_1 l) - \cos\beta_1 l}{\omega}\right] - 2AC_2\sin\beta l\left[\frac{\beta_2\gamma\sin\beta_2 l + \beta_2^2\cos\beta_2 l}{\omega^2} - \frac{l(\beta_2\sin\beta_2 l - \gamma\cos\beta_2 l) - \cos\beta_2 l}{\omega}\right];$$

$$\alpha_{2u}(\omega) = -\frac{A^2\sin^2\beta l}{\gamma\omega^2}(2\gamma l + 1) - \frac{4AC_1\sin\beta l\cdot\cos\beta_1 l}{(\gamma+\gamma_1)^2}[(\gamma+\gamma_1)l + 1] - \frac{4AC_2\sin\beta l\cdot\cos\beta_2 l}{(\gamma+\gamma_2)^2}[(\gamma+\gamma_2)l + 1].$$

ω is here the cyclic frequency of the alternating electric field,

$$A=\left(l+\frac{1}{\gamma}\right)^{-\frac{1}{2}};$$

$$\beta_1=\sqrt{\beta^2+2\omega};\quad \beta_2=\sqrt{\beta^2-2\omega};$$

$$\gamma_1=\sqrt{\gamma^2-2\omega};\quad \gamma_2=\sqrt{\gamma^2+\beta\omega};$$

$$B_1=-\frac{AU\cos\beta l}{\omega^2(\gamma_1\sin\beta_1 l+\beta_1\cos\beta_1 l)};\quad C_1=\frac{AU\sin\beta l}{\omega^2(\beta_1\sin\beta_1 l-\gamma_1\cos\beta_1 l)}.$$

The constants B_2 and C_2 are obtained from B_1 and C_1 through the substitution of β_1, γ_1, by β_2, γ_2, respectively. Inasmuch as finding the limit for $\alpha(\omega)$ at $\omega \to 0$ in the above formulas turned out to be quite laborious, the static polarizability was calculated independently, whereby the following formulas were obtained: for the symmetric states

$$\alpha_g(0)=\alpha_{1g}(0)+\alpha_{2g}(0), \tag{6}$$

where

$$\alpha_{1g}(0)=-\frac{A^2}{2\beta^2}\left[\frac{5l}{2\beta^2}\cos 2\beta l+\frac{2}{3}l^3\right];$$

$$\alpha_{2g}(0)=\frac{A^2}{2\beta^2}\operatorname{cotan}\beta l\left[\frac{2l^2}{\beta}(\operatorname{cotan}^2\beta l-1)\right.$$

$$+\frac{l}{\beta^2}\operatorname{cotan}\beta l(3-5\cos^2\beta l+4\operatorname{cotan}^2\beta l)$$

$$\left.+\frac{1}{2\beta^3}(5-3\operatorname{cotan}^2\beta l+5\operatorname{cotan}^4\beta l)\right];$$

for the antisymmetric states

$$\alpha_u(0)=\alpha_{1u}(0)+\alpha_{2u}(0), \tag{7}$$

where

$$\alpha_{1u}(0)=\frac{A^2}{2\beta^2}\left[\frac{5l}{2\beta^2}\cos 2\beta l-\frac{2}{3}l^3\right];$$

$$\alpha_{2u}(0)=\frac{A^2}{2\beta^2}\tan\beta l\left[\frac{2l^2}{\beta}(1-\tan^2\beta l)+\frac{l}{\beta^2}\tan\beta l(3-5\sin^2\beta l+4\tan^2\beta l)\right.$$

$$\left.-\frac{1}{2\beta^3}(5-3\tan^2\beta l+5\tan^4\beta l)\right].$$

One may use the model of the potential box of finite depth U and width $2l = 13$ for the description of the motion of π-electrons in the molecule of butadiene.

For such a model, the longitudinal polarizability of the π-electrons is expressed, according to ref. 1, by the formula

$$\alpha(\omega)=\frac{3}{2}[\alpha_g(\omega)+\alpha_u(\omega)], \tag{8}$$

where $\alpha_g(\omega)$ and $\alpha_u(\omega)$ are the contributions to $\alpha(\omega)$ of the electron which is in the ground and in the first excited states, respectively.

As an example, we have calculated the optical polarizability with the formulas (4), (5), and (8) for the frequency $\omega = \omega_D = 0.077$, which corresponds to the D-line of sodium, assuming U = 10 ev (the order of magnitude of the ionization potential). It was found that

$$\alpha(\omega_D)=710.$$

This result practically coincides with that obtained with the usual formula of the perturbation theory, if the sum of terms is used that takes into consideration only the transitions to the discrete states. It follows that the contribution of the integral, which takes into account the transitions to the states of the continuous spectrum, is in our example negligibly small. The depth of the potential box substantially affects the polarizability. For $U \to \infty$, the optical polarizability $\alpha(\omega_0) = 188$, which is almost four times smaller than that for U = 10 ev. The dependence of the static polarizability decreases about three times when U increases from 10 ev to infinity.

Dependence of Static Polarizability on the Depth of the Potential Box

U (ev.)	5	10	15	20	∞
$\alpha(0)$ (a.v.)	466	324	246	222	105

REFERENCES

1. M. N. Adamov and I. S. Milevskaya, Opt. i Spektr. 2, 399 (1957).
2. Yu. N. Zhivlyuk, Opt. i Spektr. 8, 421 (1960), Optics and Spectroscopy 8, 220 (1960).

CERTAIN REGULARITIES IN THE NATURE OF YIELD VERSUS FLUORESCENCE BAND POSITION FUNCTIONS FOR A NUMBER OF ORGANIC COMPOUNDS

E. N. Viktorova (pp. 279-281)

Received 1 August 1960

Zelinskii, Kolobkov, and Pikulik[1] have described the relationship between the quantum fluorescence yield ($Y_{fl.}^{qu.}$) and the fluorescence band position ($\nu_{fl.}^{max.}$) for solutions of certain phthalimide derivatives in suitable solvents. In the general case, this curve has two branches: (1) one in which an increase in the value of the quantum yield is accompanied by a shift of the fluorescence spectrum to the blue (branch A); and (2) one in which the quantum yield decreases upon further shifting of the fluorescence spectrum to the blue (branch B). A similar relationship was recently discovered for several substances belonging to a different class of organic compounds.[2-4] The above-mentioned references showed how the yield of a compound changes with a change in the solvent. However, no attention was paid to changes which might have occurred in the nature of the regularities observed in different compounds.

The object of the present investigation was to study any changes in the shape of branch A on going from one compound to another. To do this, we compared the fluorescence yields of solutions with the fluorescence band position for compounds studied previously, and also measured the fluorescence quantum yields of several new compounds.

The results of the investigation and comparison of the branches are presented in the Figure. Analysis of the data obtained indicates that, for related compounds the A-branches are in adjacent spectral regions, although for substances of different classes these locations may differ markedly. For example, for related substances II and III, branch A is located entirely in the 16,400-17,800 cm^{-1} and 16,400-17,500 cm^{-1} regions, respectively, but for compounds XI and XII, which belong to another class but are also related to each other, branch A runs

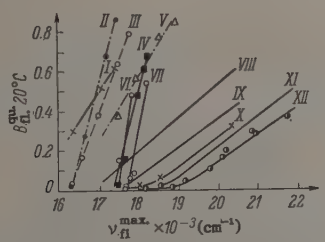

Comparison of A-branches of the relation of fluorescence yield to the position of the maximum of the fluorescence band for different compounds. I—Dimethylnaphtherhodine;[4] II—3-dimethylamino-6-methylamino-N-methylphthalimide; III—3,6-tetramethyldiamino-N-methylphthalimide; IV—3-dimethylamino-6-amino-N-methylphthalimide; V—3,6-diamino-N-methylphthalimide; VI—ethyl ether of the ethyl ester of fluorescein; VII—ethyl ester of fluorescein; VIII—4-amino-N-methylphthalimide (according to ref. 1); IX—2-aminoacridine (according to ref. 4); X—4-methoxy-N-methylphthalimide; XI—cyclohexylaminomaleinimide (according to ref. 4); XII—aminochloromaleinimide.

Compound	$\Delta_{Stokes,\ mean}$ (cm^{-1}) / $\nu_{fl.}^{max.}$ (cm^{-1})
Dimethylnaphtheirhodine	4000 / 17500
3-dimethylamino-6-monomethylamino-N-methylphthalimide	3800 / 17500
3,5-tetramethyldiamino-N-methylphthalimide	4200 / 17850
3,6-diamino-N-methylphthalimide	5400 / 18800
4-amino-N-methylphthalimide	7900 / 20400
Aminochloromaleinimide	8500 / 21900

from 18,500 to 22,000 cm^{-1} and from 18,000 to 21,900 cm^{-1} for XI and XII, respectively.

For some compounds, a pronounced change in the fluorescence yield, on changing solvents, is accompanied by a relatively small shift in the fluorescence spectrum, i.e., the dependence of $Y_{fl.}^{qu.}$ on $\nu_{fl.}^{max.}$ is very marked. Thus, the yield from 3-dimethylamino-6-monomethylamino-N-methylphthalimide in water at $\nu_{fl.}^{max.} = 16,400$ cm^{-1} is only 3%, but in benzene at $\nu_{fl.}^{max.} = 17,500$ cm^{-1} the yield is almost 90%; i.e., the yield changed by a factor of almost thirty for this small change in the position of the fluorescence maximum (1100 cm^{-1}). A much smaller increase in fluorescence yield, over a wider spectral range, occurs for another group of compounds. Thus, a change in yield by a factor of about ten occurs in aminochloromaleinimide for a shift of 2900 cm^{-1} (from 4% in ethyl acetate at $\nu_{fl.}^{max.} = 19,000$ cm^{-1} to 39% in carbon tetrachloride at $\nu_{fl.}^{max.} = 21,900$ cm^{-1}).

Let us note yet another factor which is significant in comparing the nature of the relation of $Y_{fl.}^{qu.}$ to $\nu_{fl.}^{max.}$ for different compounds, namely: The slopes of the A-branches are greater for those located at longer wavelengths. For compounds which have A-branches located in the short wavelength region, slope is much smaller.

Compounds whose A-branches have a low slope show large Stokes shifts. Conversely, those compounds whose A-branches have high slopes exhibit small Stokes shifts. This is evident from the Table, which presents the mean values of the Stokes shifts for several of the compounds studied; these mean values are related to the frequency $\nu_{fl.}^{max.}$ at which the maximum value of the fluorescence yield is attained for a given compound.

In refs. 1, 2, and 5 it was shown that the connection between the fluorescence yield and the spectral characteristics of a compound leads to the hypothesis that deactivation processes are determined by the relative position of potential surfaces of fundamental and excited electronic bonds in the fluorescing molecule. In this connection, some explanation of the regularities observed may be obtained by making use of potential curves.

In conclusion, I would like to thank V. V. Zelinskii for suggesting the problem and for guidance, and also I. E. Obyknovenovaya for help in preparing this article.

REFERENCES

1. V. V. Zelinskii, V. P. Kolobkov, and L. G. Pikulik, Opt. i Spektr. 1, 161 (1956).
2. V. V. Zelinskii, V. P. Kolobkov, and N. D. Krasnitskaya, Opt. i Spektr. 6, 417 (1959), Optics and Spectroscopy 6, 261 (1959).
3. A. S. Kochemirovskii and I. I. Reznikova, Opt. i Spektr. 8, 399 (1960), Optics and Spectroscopy 8, 206 (1960).
4. E. N. Viktorova, A. S. Kochemirovskii, N. D. Krasnitskaya, and I. I. Reznikova, Opt. i Spektr. 9, 544 (1960), Optics and Spectroscopy 9, 288 (1960).
5. V. V. Zelinskii, V. P. Kolobkov, and L. G. Pikulik, Opt. i Spektr. 2, 405 (1957).

THE INFLUENCE OF THE MOLECULAR VOLUME OF A SOLUTE ON THE SUSCEPTIBILITY OF ITS ELECTRONIC SPECTRA TO SOLVENT EFFECTS

I. A. Zhmyreva and I. I. Reznikova (pp. 281-284)

Received 1 August 1960

Onsager's theory of the influence of solvents on spectra, which is based on the macroscopic characteristics of the solvent, assumes that the molecule in question can be replaced by a sphere of a certain radius with a point dipole at the center. The radius of this sphere coincides approximately with the radius of the luminescing molecule. According to the formulas obtained from this model, the effect of the solvent on the spectrum should decrease sharply with increasing molecular volume. In the work of Bakhshiev[1] which was based on these formulas, the volumes of molecules were determined on the basis of the susceptibility of their spectra to solvent effects. The relative dimensions of the molecules calculated by him agree well with the results obtained from structural models.

However, Zelinskii, Kolobkov, and Reznikova concluded rather definitely that the spectra of organic substances in solution were not affected by changes in the molecular volume of the solvent. This same point was discussed in our previous paper,[3] although without particular emphasis. A solution of the question of the effect of the solvent on fluorescence and absorption spectra as a function of the size of the solute molecule would help to clarify the mechanism of the interaction of solvent and solute compounds.

The present study gives a series of examples indicating that a change in the size of the solute molecule does not influence the susceptibility of the spectra to solvent effects.

As objects of investigation we used related derivatives of phthalimide whose molecules differ in the groups replacing hydrogen in the amine group and on the imide nitrogen: 4-amino-M-methylphthalimide and 4-amino-N-cyclohexylphthalimide; 3-amino-N-methylphthalimide and 3-amino-N-phenylphthalimide; 4-formylamino-N-methylphthalimide; 4-acetylamino-N-methylphthalimide and 4-benzoylamino-N-cyclohexylphthalimide. For solvents we chose benzene, acetone, ethyl alcohol, propyl alcohol, and trichloroacetic acid.

Figures 1 and 2 show the fluorescence and absorption spectra of the abovementioned phthalimide derivatives in different solvents. The fluorescence (Fig. 1A) and absorption (Fig. 2A) spectra of 4-amino-N-methylphthalimide and 4-amino-N-cyclohexylphthalimide were measured in benzene, acetone, and ethyl alcohol. The molecular volumes of these compounds differ by a factor of 1.5. As can be seen from the figures, the fluorescence and absorption spectra of 4-amino-N-methylphthalimide and 4-amino-N-cyclohexylphthalimide measured in the solvents indicated coincide, although the fluorescence spectra show a general shift of approximately 4000 cm^{-1} on changing from benzene to ethyl alcohol. The fluorescence (Fig. 1B) and absorption (Fig. 2B) spectra of 3-amino-N-methylphthalimide and 3-amino-N-phenylphthalimide measured in benzene and propyl alcohol also coin-

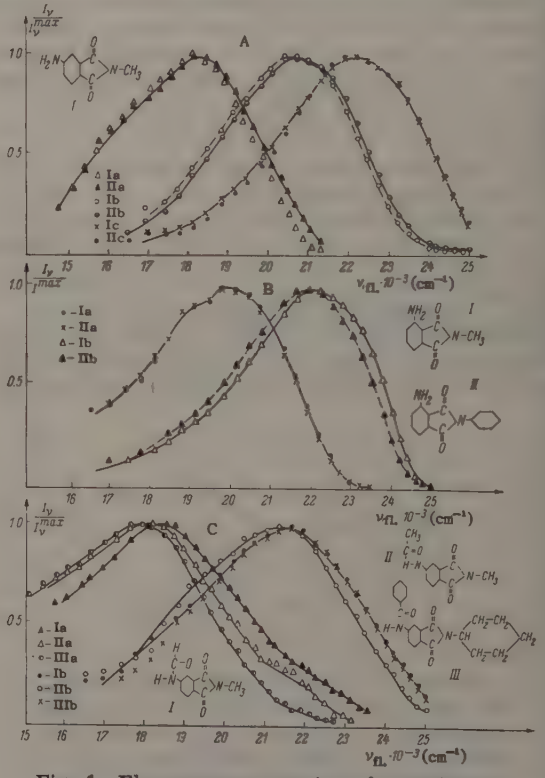

Fig. 1. Fluorescence spectra of a series of N-methylphthalimide derivatives. A: I—4-amino-N-methylphthalimide; II—4-amino-N-cyclohexylphthalimide. Solvents: a—ethyl alcohol; b—acetone; c—benzene. B: I—3-amino-N-methylphthalimide; II—3-amino-N-phenylphthalimide. Solvents: a—propyl alcohol; b—benzene. C: I—4-formylamino-N-methylphthalimide; II—4-acetylamino-N-methylphthalimide; III—4-benzoylamino-N-cyclohexylphthalimide. Solvents: a—trichloroacetic acid; b—ethyl alcohol.

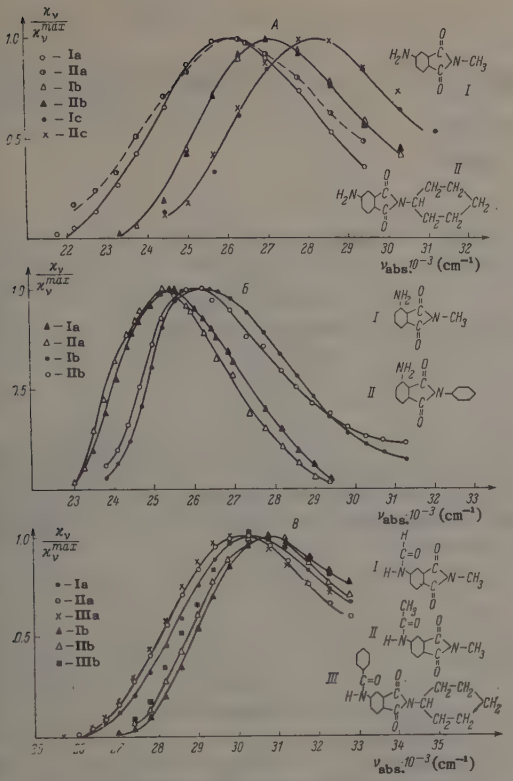

Fig. 2. Absorption spectra of a series of derivatives of N-methylphthalimide. A: I—4-amino-N-methylphthalimide; II—4-amino-N-cyclohexylphthalimide. Solvents: a—ethyl alcohol; b—acetone; c—benzene. B: I—3-amino-N-methylphthalimide; II—3-amino-N-phenylphthalimide. Solvents: a—propyl alcohol; b—benzene. C: I—4-formylamino-N-methylphthalimide; II—4-acetylamino-N-methylphthalimide; III—4-benzoylamino-N-cyclohexylphthalimide. Solvents: a—ethyl alcohol; b—benzene.

cide within the limits of error of the measurements, although the latter molecule is 1 1/2 times larger than the former.

Bakhshiev, in his study, used substances in which the dimensions of the molecule changed only as a result of the introduction of substituents on the amino group. In this case, not only the volume of the molecule was changed, but also the character of the compound itself. In several cases we changed only the volume of the molecule without changing its chemical character. In the case of the molecules of the acylated compounds, where the molecular dimensions are changed due to changing the size of the substituent in the amino group, we further increased the volume by replacing the hydrogen on the imide nitrogen. Thus the chemical character of the compound is not changed.

For 4-formylamino-N-methylphthalimide and 4-benzoylamino-N-cyclohexylphthalimide, one of which is twice as large as the other, the fluorescence spectra (Fig. 1C) measured in ethyl alcohol coincide in position. The fluorescence spectrum of 4-acetylamino-N-methylphthalimide, whose molecular volume is intermediate between 4-formylamino-N-methylphthalimide and 4-benzoylamino-N-cyclohexylphthalimide, shifts somewhat towards the red. The fluorescence spectra of these substances in trichloroacetic acid are slightly shifted to the red relative to one another in proportion to the molecular volume. The absorption spectra (Fig. 2C) of these three compounds measured in ethyl alcohol and benzene coincide within the limits of error of the measurements.

As has already been pointed out, Bakhshiev used substances whose molecular volumes differed relatively little (not more than 30%). We used substances with volumes differing by factors of 1.5 to 2. However, as shown by the abovementioned data, even such pronounced changes in molecular dimensions do not change the susceptibility of the spectra to solvent action. Moreover, in those particular cases where some shift of the spectra occurred, this shift was toward the red with increasing volume (for 4-formylamino-N-methylphthalimide, 4-acetylamino-N-methylphthalimide, and 4-benzoylamino-N-cyclohexylphthalimide). These facts contradict the abovementioned theory of the inverse dependence of the susceptibility of spectra to solvent effects on molecular radius.

This investigation thus shows molecular volume is not one of the factors determining the effect of solvents on absorption spectra. This must be considered as a serious objection against using any theory based on the Onsager model to explain the mechanism of solvent effects on electronic spectra.

In conclusion, we consider it an honor to express our appreciation to V. V. Zelinskii, under whose direct supervision the present work was carried out.

REFERENCES

1. N. G. Bakhshiev, Izvest. Akad. Nauk SSSR, Ser. Fiz. 22, 1387 (1958).
2. V. V. Zelinskii, V. P. Kolobkov, and I. I. Reznikova, Tr. Soveshch. po Termodinamike i Stroeniyu Rastvorov (Proceedings of the Conference on the Thermodynamics and Structure of Solutions). Izd. Akad. Nauk SSSR, Moscow, 1959.
3. I. A. Zhmyreva, V. V. Zelinskii, V. P. Kolobkov, A. S. Kochemirovskii, and I. I. Reznikova, Opt. i Spektr. 8, 412 (1960), Optics and Spectroscopy 8, 214 (1960).

ON APODIZATING DIAPHRAGMS AND DIAPHRAGMS INCREASING RESOLVING POWER

L. M Tuvikene (pp. 284-287)

Received 18 August 1960

INTRODUCTION

The use of filters in the entrance pupil of optical systems in order (1) to reduce the width of the central maximum and thus to increase the resolving power, and (2) to weaken the secondary maxima of the diffraction pattern of a light source, i.e., to achieve apodization, is widely discussed in the literature. However, very little discussion is found on the use of diaphragms of appropriate contours (and uniform light transmission through the diaphragm aperture) to achieve the same result. There is only one paper[1] on an experimental investigation of a rectangular diaphragm used for apodization, and one theoretical paper[2] with calculations on the shape of the diaphragm contour. In the present paper, using the theory developed in ref. 2, some diaphragms—apodizating ones as well as diaphragms increasing the resolving power—are investigated.

METHOD AND RESULTS OF THE CALCULATION

In the previous paper[2] it is shown that in a rectangular cartesian coordinate system the contour of a uniformly transmitting diaphragm is determined by the nonlinear integral equation,

$$\int_{-a}^{+a} \frac{\sin[w\eta(\xi)]}{w} e^{iv\xi} d\xi = \frac{1}{2} u(v, w), \tag{1}$$

where u(v,w) is the predetermined amplitude distribution in the focal plane of the objective (more exactly, along a line w = const., of the diffraction image), $v = (2\pi/\lambda)\alpha$, $w = (2\pi/\lambda)\beta$, α and β are the coordinates of the diffraction image, and ξ is the abscissa of an aperture point of the diaphragm ($|\xi| \leq a$), where the v-axis in the image plane is parallel to the ξ-axis in the diaphragm plane.

Solving Eq. (1) directly,* we find that

*In ref. 2 is given also a second method for solving Eq. (1) (linearization method).

$$\eta(\xi) = \frac{1}{w} \arcsin[w \cdot \psi(\xi, w)], \tag{2}$$

where $\psi(\xi,w)$ is the Fourier transform of $\frac{1}{2}u(v,w)$, that is

$$\psi(\xi, w) = \frac{1}{2\pi} \int_{-\infty}^{+\infty} \frac{1}{2} u(v, w) e^{-iv\xi} dv. \tag{3}$$

We note that $\psi(\xi,w)$ must also satisfy the condition

$$\psi(\xi, w) = \begin{cases} \dfrac{\sin[w \cdot \eta(\xi)]}{w} & \text{where } |\xi| \leq a, \\ 0 & \text{where } |\xi| > a. \end{cases}$$

Let us now consider the case when the amplitude distribution in the central cross section (w = 0) of the diffraction image is given in the form

$$\frac{u(v)}{2\pi} = b_1 \frac{J_1(v)}{v} + b_2 \frac{J_2(v)}{v^2} + b_3 \frac{J_3(v)}{v^3} + \ldots, \tag{4}$$

where J_1, J_2, J_3, ... are Bessel functions of the first kind of order 1, 2, 3, ... respectively, and b_1, b_2, b_3, ... are constants which are determined from the conditions

$$u(v = 0) = 2\pi u_0 \tag{5}$$

that is, by the amplitude in the focal point, and

$$\left.\begin{aligned} u(v = v_1) &= 0, \\ u(v = v_2) &= 0, \\ &\vdots \quad \vdots \end{aligned}\right\}. \tag{6}$$

As an example, let us consider the diffraction pattern of a point source formed by a circular aperture of radius unity. The amplitude distribution in this case is given by the first term of the expansion (4), and the energy distribution is given by

$$I_0 = \left[\frac{J_1(v)}{v}\right]^2$$

and has its first minimum at v = 3.8 and secondary maxima at $v_I = 5.14$, $v_{II} = 8.42$, etc. Thus, if the points, v_1, v_2 ... are chosen in the interval $0 < v < 3.8$ then conditions (6) express the narrowing of the central maximum. If, on the other hand, we let $v_1 = v_I$, $v_2 = v_{II}$, ... then conditions (6) express the weakening of the secondary maxima.*

*Conditions in the form of (6) are used in ref. 3 to calculate amplitude filters for decreasing the secondary maxima.

It can be shown[4] that the conditions (6) can also be replaced by conditions for minimum energy I in the (v′, v″) zone of the diffraction pattern, i.e.,

$$\int_{v'}^{v''} I(v)\, v dv = \min. \tag{7}$$

Using Eqs. (2), (3), and (4) it is found that the dia-

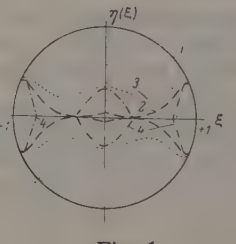

Fig. 1

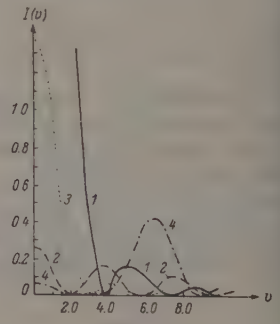

Fig. 2

Fig. 1. Contours of diaphragms which increase the resolving power. The contours 2, 3, and 4 correspond to the energy distribution curves 2, 3, and 4 shown in Fig. 2. All contours coincide as they approach the unit circle 1 (in the neighborhood of the points $\xi = \pm 1$).

Fig. 2. Energy distribution with a narrowing of the central maximum relative to the distribution 1 for the case of a circular aperture (see Fig. 1).

hragm contour for the central cross section, w = 0, is iven by*

*Tables of Fourier transforms have been used to calcuate values of $\eta(\xi)$.

$$\eta_1(\xi) = b_1(1-\xi^2)^{1/2} + \frac{1}{3}b_2(1-\xi^2)^{3/2} + \frac{1}{15}b_3(1-\xi^2)^{5/2} + \ldots \text{ (where } |\xi| \leq 1). \quad (8)$$

Diaphragm contours calculated from this equation or given concrete conditions (5) and (6), or (5) and (7), re shown in Figs. 1 and 3, and the corresponding energy istributions are shown in Figs. 2 and 4. Since the contants b_1, b_2, b_3, ... are given by the conditions (5) and 6), or (5) and (7), in terms of u_0, the value of u_0 was in ach case chosen such that the contour of the correspondng diaphragm would fit within a circle of radius unity.

The contour of the apodizating diaphragm 3 shown in ig. 3 is very close to the rectangular diaphragm which as used in the experimental investigation[1] mentioned reviously

Calculations show that in solving apodization probems conditions (6) and (7) lead to approximately the ame results. However, for diaphragms increasing the esolving power it is found more convenient to use conitions (6).

ONCLUSIONS.

1. With diaphragms of proper contour it is possible ither to increase the resolving power, or to achieve apoization along a straight line (in one cross section of the iffraction pattern).

2. The narrowing of the central maximum together with the elimination of light from a broad zone about the entral maximum requires a diaphragm of a complex ontour (with a number of openings, as shown in Fig. 1, iaphragm 4). However, filters used for this purpose are lso complex.[5,6] Apodizating diaphragms and filters are onsiderably simpler.

3. The relation between the increase in the resolving power and apodization is generally the same for diaphragms as it is for amplitude filters,[5,6] that is, an increase in the resolving power brings with it a worsening of the apodization and vice versa.

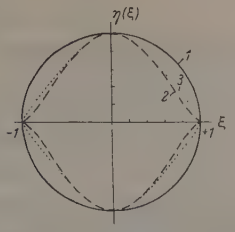

Fig. 3

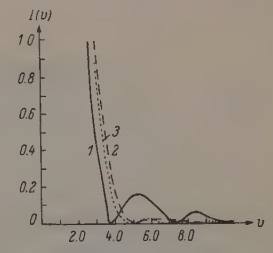

Fig. 4

Fig. 3. Contours of apodizating diaphragms. The contours 2 and 3 correspond to the energy distribution curves 2 and 3 shown in Fig. 4.

Fig. 4. Apodizated energy distribution relative to the distribution 1 for a circular aperture (see Fig. 3).

REFERENCES

1. A. Couder and P. Jacquinot, Comptes rend. **208**, 1639 (1939).
2. L. M. Tuvikene, Uchenye Zapiski Tartusk. Univ. **62**, 197 (1958).
3. G. Lansraux, Rev. Opt. **32**, 73 (1953).
4. R. Straubel, "Pieter Zeeman Verhandlingen" (1935 Pieter Zeeman Proceedings), p. 302. Martinus Nijhoff, 1935.
5. G. G. Slyusarev and N. I. Kulikovskaya, Opt. i Spektr. **4**, 486 (1958).
6. L. M. Tuvikene, Uchenye Zapiski Tartusk. Univ. **62** 192 (1958).
7. I. M. Ryzhik and I. S. Gradshtein, "Tablitsy integralov, summ, ryadov i proizvedenii" (Tables of Integrals, Sums, Series, and Products). Gosudarst. Izd. Tekh.-Teoret. Lit., Moscow-Leningrad, 1951.

THE ORIENTATION PHOTODICHROISM OF VISCOUS SOLUTIONS

B. S. Neporent and O. V. Stolbova (pp. 287-288)

Received 2 September 1960

In 1957, while working with a polarizing microscope, Teitel[1] noticed that preparations stained with congo red and benzopurpurine and illuminated with linearly polarized light become dichroic when dried out. He suggested[1] that this phenomenon is caused by the mechanical action of the polarized light on the absorbing molecules.

In order to explain the anomalously large photodichroism of colored glass, Albrecht[2] has also suggested that light has an orienting effect on absorbing molecules. The theory put forward in ref. 2 considers the rotational diffusion of molecules associated with local heating of the molecules after absorption of a light quantum. Studying solid solutions, Albrecht neglected the thermal disorientation of the molecules which restores the initial isotropy of the specimen.

We believed that a study of photodichroism could give important information on the properties of the electronic levels of molecules (for example, the orientation of the virtual dipoles corresponding to the absorption bands) and on the characteristics of solution and solvent (viscosity, orientation relaxation time of the molecules, etc.). We therefore undertook some studies of the phenomenon discovered by Teitel.*

*The authors are grateful to A. Teitel for kindly communicating information about his work.

We studied films obtained by evaporating an aqueous solution of congo red illuminated by polarized light. When illuminated with light from the mercury 546 mμ line, which is situated in the region of the first absorption band of the dye (450-550 mμ) the film became dichroic; light polarized in the same direction as the orienting beam was absorbed less when the sample was illuminated than when it was not, while light polarized in a perpendicular direction was absorbed more. This confirms Teitel's and Albrecht's views on the orienting effect of light on molecules in solution. Apparently the effect cannot be explained as resulting from photochemical processes[3] or from transition of the molecules into a metastable state.[4]

In the second absorption band (300-400 mμ) the dichroism changes sign, which is easily explained by considering the mutual orientation of the corresponding virtual dipoles. In fact, illuminating the drying film with light of this wavelength range induces the corresponding inverted effect in the first absorption band.

The study of inverse orientation dichroism is particularly important; its appearance is apparently related to the possibility of thermal disorientation of the molecules. In this case, the dichroism obtained under the conditions of the experiment depends on the equilibrium between photo-orientation and thermal disorientation processes in the molecules.* In fact, inverse photodichroism

*Strictly speaking, the action of light is "photodisorientation" of some of the molecules, the virtual dipoles of which have a component parallel to the E vector of the orienting light. Nevertheless, the term photo-orientation, applied to the specimen as a whole, is more convenient.

is observed only over a small range of solvent viscosities, since with low orientation relaxation times the degree of dichroism reached is very low and with high relaxation times the phenomenon is almost completely irreversible.

We succeeded in obtaining inverse photodichroism by illuminating a solution of congo red in polyvinyl alcohol. When this film is heated to a certain temperature switching the orienting light on and off is accompanied by the appearance and disappearance of orientation photodichroism (see the Figure).

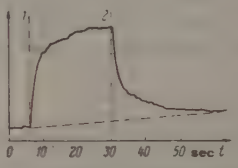

Example of a record of inverse orientation dichroism made with the photoelectric apparatus. 1—Switching-on time; 2—switching-off time of the orienting light beam.

The experiments were performed with a specially selected photoelectric recorder which was capable of measuring dichroism down to 10^{-3}. Mercury 546 mμ radiation was used for illumination.

The dichroism decay curve was close to exponential. Using the approximation $d = d_0 e^{-t/\tau}$ to represent the function d(t), where τ is the orientation relaxation time, we obtained a value of the order of tens of seconds for τ.

Preliminary treatment of the phenomenon, including consideration of thermal disorientation of the molecules in the solution, enabled us to obtain an expression connecting orientation dichroism with the parameters of the dissolved molecules, the properties of the medium, and the intensity of the orienting light. A more detailed description and analysis of our studies will be published later.

There is no doubt that the study of orientation dichroism can yield valuable information on the properties of molecules and solutions.

REFERENCES

1. A. Teitel, Naturwissenschaften **44**, 370 (1957).
2. A. C. Albrecht, J. Chem. Phys. **27**, 1413 (1957).
3. S. Nikitine, Thesis, L'Université de Paris, 1941.
4. S. V. Cherdynstev, Zhur. Eksptl. i Teoret. Fiz. **18**, 332, 360 (1948).

APPLIED OPTICS

INFORMATION FOR CONTRIBUTORS

cope: Papers are welcomed in the broad areas of applied optics, in isciplines related to optics and employing optical techniques. Papers ould be sent to The Editor, APPLIED OPTICS, 1155 Sixteenth St., N. W. ashington 6, D. C. Manuscripts may be submitted in English, French, erman or Russian, and the presentation should be as succinct as compre-ension will permit. One original and one carbon of the manuscript, with wo sets of all illustrations, must be sent. Manuscripts should be typed ouble or triple spaced on one side of 8 1/2 x 11 inch paper, leaving a 1/2 inch margin all round. A small photograph of the author should be ncluded with the manuscript.

n abstract, adequate as an index and summary, of not more than 100 words hould appear at the beginning of the paper after the title, author's ame, affiliation and address. In the case of papers in a non-English anguage, they must be accompanied by an abstract in English as well as ne in the language of the paper.

igures suitable for printer's use should be sent, and they must be wider han they are high. Bear in mind that illustrations will normally be educed to column width (3 5/16 inches - 20 picas). Halftones: two sets f glossy prints are needed, which should be mailed flat, with any pro-ortion or framing indicated on a working copy. Line drawings should be uitable for reproduction and be not larger than 8 1/2 x 11 inches. aptions should be listed on a separate sheet in addition to each caption ppearing on each illustration.

ables should be typed on separate sheets and the data therein be intel-igible, by title, without reference to the text. Tables should contain a inimum of vertical ruling.

eferences must be typed on a separate sheet, be numbered consecutively n the order of their appearance in the text, and follow this form:

1. F. C. Brown, Phys. Rev. 28, 825 (1921)
2. J. Culpeper, Space Optics (Georgetown Institute of Technology Press, Washington, D. C., 1961) pp. 298, 345

A list of abbreviations for the names of journals is published in the American Institute of Physics Style Manual. To make for uniformity of presentation generally, the Style Manual, second edition, should be used.

No galley proofs will be sent to authors; all proof reading will be done in house. Therefore, author will not see his paper from the time it is accepted and any alterations agreed between Editor and Author, until it appears in print two months later.

Letters to the Editor should follow the above suggestions, but no abstract is required.

There will be no page charge in APPLIED OPTICS for the time being.

FILLER MATERIAL - NOT IN RUSSIAN ORIGINAL

IMPORTANT NOTICE TO ALL READERS OF OPTICS AND SPECTROSCOPY

OiS CLUB SCHEME

The Optical Society of America has been translating Optika i Spektroskopiya and distributing this monthly journal free - thanks to an NSF grant - to all OSA members and subscribers to the Journal of the Optical Society of America. This free distribution was an experiment for three years, so that the individual reader might become accustomed to reading a translation journal not as an oddity but as a publication that is looked for each month in the same manner as is J. Chem. Phys., J. Am. Chem. Soc., etc. In December of this year the NSF grant ends, but the interest in Optics and Spectroscopy is now too lively for OSA to discontinue the translation, so they have evolved the OiS CLUB SCHEME.

Put simply, this is a special subscription rate for members of those societies who wish to take part in the OiS CLUB SCHEME, viz:

To OSA members ---------- $ 7.50
To members of the OiS Club ------- $11.00
To non-members ---------- $15.00

OSA is emphatic that if a translation journal is to be of real use (as is the case with any scientific journal) it should be read widely by all the people working in the field, and that these research results should be made available in the shortest possible time. OPTICS AND SPECTROSCOPY is published in English translation within three months of the Russian edition coming out e.g. the March 1961 issue will be published in English on June 10th. OSA is making this special offer to members of some sixty scientific societies across the English speaking world, and it asks the members of those Societies to write to their Society or directly to the Assistant Secretary, OSA, 1155 16th St., N.W., Washington 6, D.C. for further details or to send in their order. (see below)

ALL SUBSCRIBERS PLEASE NOTE that your subscriptions will start with the January 1962 issue which is published in English in March/April 1962 -- so don't start worrying when the January 1962 issue does not appear in that month!

ORDER FORM

To: OPTICS AND SPECTROSCOPY
Optical Society of America
1155 Sixteenth St., N.W.
Washington 6, D.C.

Please enter my/our subscription to OPTICS AND SPECTROSCOPY for one year commencing with the January 1962 issue (which will be published in April), at:

/_/ Special OSA member rate $ 7.50

/_/ Special rate to members of Societies cooperating in OiS Club Scheme $11.00

Name of your Society _____

/_/ Non-members $15.00

/_/ Please send OSA membership information

Membership no. _____

Name _____

Address _____

_____

FILLER MATERIAL - NOT IN RUSSIAN ORIGINAL

Dispersion Formula for the Electron in a Potential Box of Finite Depth and the Optical Polarizability of Molecules . . . . . M. N. Adamov, V. K. Kagan, and B. I. Orlov 139 (276)
Certain Regularities in the Nature of Yield Versus Fluorescence Band Position Functions for a Number of Organic Compounds . . . . . E. N. Viktorova 141 (279)
The Influence of the Molecular Volume of a Solute on the Susceptibility of its Electronic Spectra to Solvent Effects . . . . . I. A. Zhmyreva and I. I. Reznikova 142 (281)
On Apodizating Diaphragms and Diaphragms Increasing Resolving Power . . . . . L. M. Tuvikene 144 (284)
The Orientation Photodichroism of Viscous Solutions . . . . . B. S. Neporent and O. V. Stolbova 146 (287)

EDITOR'S NOTE

Comments on the scientific content of the translated Russian articles published in OPTICS AND SPECTROSCOPY are invited. They should be addressed as a Letter to the Editor of the Journal of the Optical Society of America and forwarded to the Editor of that journal, Dr. D. B. Judd, National Bureau of Standards, Washington 25, D. C.

UNIVERSITY OF ILLINOIS 3
LIBRARY
UNDERGRADUATE DIV
NAVY PIER GRAND AVE
CHICAGO 11 ILL

VOL. X, NO. 2 OPTICS AND SPECTROSCOPY FEBRUARY 1961

CONTENTS

(Numbers in parentheses are original Russian page numbers.
These Russian page numbers are also quoted at the head of each paper.)

Effect of Free Rotation in Molecules on the Normal Vibration Frequencies . . . . . B. L. Livshits 73 (145)
The Theory of the Intensities of Infrared Spectra of Polyatomic Molecules in the Zero and First Approximation of the Generalized Valence-Optical Scheme . . . . . L. M. Sverdlov 76 (152)
Temperature Dependence of the Vibrational Absorption Bands of Crystalline Chloroform and Bromoform . . . . . M. P. Lisitsa and Yu. P. Tsyashchenko 79 (157)
Band-Splitting in the Spectra of Cubic Crystals Subjected to Oriented Deformation . . . . . A. A. Kaplyanskii 83 (165)
The Complex Nature of the F-Band in KCl Crystals . . . . . N. G. Politov 87 (173)
Flashlike Rise of Luminescence II. ZnS-Co and ZnS-Ag,Co Phosphors . . . . . N. A. Tolstoi, A. A. Anufriev, P. G. Deineka, L. A. Rusinov, V. A. Sokolov, and A. A. Spartakov 90 (177)
Final Stages of Luminescence Decay in Phosphors with Levels of Several Kinds . . . . . V. V. Antonov-Romanovskii 92 (182)
The Process Responsible for the Voltage Dependence of the Mean Luminescence Brightness . . . . . A. N Georgobiani and M. V. Fok 95 (188)
The Luminescence Properties of Gold-Activated Zinc Selenide . . . . . L. Ya. Markovskii and R. I. Smirnova 98 (194)
Reflection of Radiation by an Infinite Flat Surface, Illuminated From a Point Source. II. Particular Cases, Important for Practical Applications . . . B. A. Grigor'ev, A. G. Ershov, and V. A. Uvarov 100 (198)
Polarization of Phosphorescence in Organophosphors . . . . . V. A. Pilipovich 104 (209)
Some Special Cases of Luminescence Kinetics . . . . . V. V. Antonov-Romanovskii 107 (214)
Flashlike Rise of Luminescence. III. Effect of the Intensity of the Exciting and De-exciting Light . . . . . N. A Tolstoi, A. M. Tkachuk, and A. I. Ryskin 110 (220)
Role of the Stimulating Action of Exciting Light in the Kinetics of Luminescence of ZnS:Cu Crystalline Phosphors . . . . . L. A. Vinokurov and M. V. Fok 112 (225)
Certain Problems in the Theory of the Scattering of Electromagnetic Radiation by Submicroscopic Nonspherical Particles . . . . . A. I. Slutsker and V. A. Marikhin 116 (232)
Rayleigh Scattering of Light by Solutions of Nitrobenzene in Hexane . . . . . D. K. Beridze and M. I. Shakhparonov 119 (240)
Imaging of Separate Linear Objects of Different Width and Contrast with Surrounding Field by a Combination of an Optical System and a Granular Layer . . . . . L. P. Moroz 124 (249)
An Analysis of Methods of Aligning Magnetic Electron Microscopes . . . . . Yu. V. Vorob'ev 128 (257)

SHORT COMMUNICATIONS

The Use of Pressed Discs of KCl in Ultraviolet Spectrophotometry . . . . . V. A. Shlyapochnikov and V. I. Slovetskii 132 (265)
Determination of the Optical Constants of Ge and CdTe By the Reflection Method . . . . . N. K. Kiseleva and N. N. Pribytkova 133 (266)
Measurement of the Optical Density of the Blackening of Spectral Lines using Interference Microscopy Methods . . . . . V. P. Koronkevich and E. B. Kolesova 135 (268)
On the Effective Vibrational Temperature of the Acetylene-Air Flame . . . . . F. S Ortenberg and N. A. Nesterko 136 (270)
Spectral Investigation of the Influence of the Solvent on the Aggregation of Organic Dyes . . . . . Kh. L. Arvan and N. E. Zaitseva 137 (272)

(Contents continued on inside back cover)